FLORIDA POWER CORPORATION
CRYSTAL RIVER UNIT 3
NUCLEAR GENERATING PLANT

DOCKET NO. 50-302

LICENSE NO. DPR-72

STARTUP REPORT

JULY 27, 1977

8003120 824

A B S T R A C T

Crystal River Unit 3 is a 2452 MWt, Babcock and Wilcox PWR with an 855 MWe Westinghouse tandem compound turbine-generator. It is located on the Gulf Coast of Florida with a saltwater cooled condenser. This report covers fuel loading and startup testing. Important chronology was:

USNRC License DPR-72 Issued	December 3, 1976
Fuel Loading	December 4-7, 1976
Initial Criticality	January 14, 1977
Initial Nuclear Electric Power	January 30, 1977
15% Full Power Reached	February 1, 1977
40% Full Power Reached	February 27, 1977
Unit Declared Commercial	March 13, 1977
75% Full Power Reached	March 14, 1977
100% Full Power Reached	April 1, 1977
All Testing Successfully Completed	April 26, 1977

Based on evaluation of unit startup and power escalation testing, the report comes to the conclusion that the unit is operating as designed and may be safely operated at full rated power.

TABLE OF CONTENTS

TABLE OF CONTENTS (CONT'D)

TABLE OF CONTENTS (CONT'D)

1.0 INTRODUCTION AND SUMMARY

1.1 INTRODUCTION

Florida Power Corporation Crystal River Unit 3 was issued facility operating license DPR-72 by the Nuclear Regulatory Commission on December 3, 1976 for operational modes 5 and 6 (i.e. cold shutdown and refueling). The first fuel assembly was inserted into the core on December 4, 1976 and initial fuel loading was completed on December 7, 1976. This license was later extended to a full power license on December 30, 1976 with an upper power limitation of 5% full power initially imposed.

Zero Power Physics Test commenced with initial criticality on January 14, 1977 and continued 5 days until a severe electrical shortage due to cold weather caused it to be interrupted. Testing resumed on January 27, 1977 and was successfully completed on January 29, 1977. This program was conducted at one isothermal reactor coolant temperature of 532°F.

Following the completion of zero power physics testing, initial power level escalation was started on January 29, 1977, and further power level escalations occurred as required testing was satisfactorily completed. Major power levels, as defined by the power escalation testing sequence, were initially achieved as follows:

Power Level (Percent of Full Power - %FP)	Date Achieved
15	February 1, 1977
40	February 27, 1977
75	March 14, 1977
100	April 1, 1977

The zero power physics and power escalation test programs were done to comply with the requirements of section 13.4 of Crystal River Unit 3 Final Safety Analysis Report (FSAR). These test programs were designed to provide adequate assurance that the unit could be operated in a safe and efficient manner. Throughout these programs, detailed written procedures specifying the sequence of tests, the parameters to be measured, and the conditions under which each test was to be performed were followed. These procedures have provided the data necessary for the analyses made and conclusions drawn in this report.

This report is prepared and submitted in accordance with Technical Specification 6.9.1 and addresses unit startup and power escalation testing through 2400 hours on April 26, 1977. At this time, all scheduled power escalation testing has been successfully completed.

1.2 SUMMARY

Crystal River Unit 3 was declared to be in commercial operation on March 13, 1977 at the completion of 40% full power testing. The nuclear steam supply system was designed by the Babcock and Wilcox Company and was the seventh in this series of systems to be placed into service. The tandem compound turbine generator was supplied by the Westinghouse Electric Company.

During the test program, the unit was operated at power levels up to and including 100% full power. The performance of the unit has been acceptable. Testing and operation of the nuclear steam supply system has revealed few items which were other than predicted, and none which adversely affect unit safety. The deficiencies encountered have been of a nature that would be expected during the initial startup of a unit of this size and, based on an evaluation of unit startup and power escalation test, it has been demonstrated that the unit may be safely operated at full power.

The startup and power escalation testing, as addressed by the various major sections of this report, is summarized below.

1.2.1 INITIAL FUEL LOADING

Initial fuel loading began on December 4, 1976 and was completed on December 7, 1976. Loading of the core was accomplished under semi-dry conditions with the reactor vessel water level maintained above the fuel at the upper mid plane of the reactor vessel hot leg. A total elapsed time of 95.1 hours were required to complete fuel loading with less than 65.5 hours actually utilized to transfer the fuel assemblies. The delays experienced were primarily contributed to adjustment or repairs to fuel handling equipment. Overall, fuel loading was conducted in a safe and orderly manner with a significant increase in the fuel assembly loading rate experienced as crew familiarization and equipment reliability improved.

1.2.2 TESTING PRIOR TO POWER ESCALATION

Following initial fuel loading of Crystal River Unit 3, certain testing was conducted prior to power escalation. This testing was conducted in January 1977 and included the Reactor Coolant Pump Flow and Flow Coastdown Test, the Control Rod Drive Drop Time Test, the Pressurizer Test, and the Zero Power Physics Test. A brief summary of each of these tests follows:

REACTOR COOLANT FLOW AND FLOW COASTDOWN TEST

The measured reactor coolant flow rate during this test for four pump operation was approximately 109.9 percent of the design value. This flow provides adequate margin to both the maximum and minimum allowable flow rates. A later flow determination (110.0%) is given in Section 1.?.3, NSSS Heat Balance Test.

The measured reactor coolant flow rate versus time during the loss of four reactor coolant pumps was above the minimum allowable flow coastdown curve.

An acceptable snubber position for the reactor coolant flow signal was established at position (4). This position results in delay times well within the acceptance criteria limits of 1.00 seconds for multi-pump trips and 1.25 seconds for single pump trips.

CONTROL ROD DRIVE DROP TIME TEST

The rod drop time at 532°F and full flow conditions averaged abouc 1.249 seconds which is well below the acceptance criteria value of 1.660 seconds as stated in section 3.1.3.4 of Technical Specifications. Also, as would be expected, all drop times under no-flow conditions were shorter than full-flow conditions.

PRESSURIZER TEST

The pressurizer spray flow was set at 190.15 gpm which is within the acceptance criteria limit of 190 +19/-6 gpm. The pressurizer spray bypass flow was set at 1.56 gpm which is within the acceptance criteria limit of 1.00 +2.00/-0.25 gpm.

ZERO POWER PHYSICS TEST

Zero power physics testing on Crystal River Unit 3 commenced with initial criticality on January 14, 1977. Part way through the testing, the FPC system load was impacted by a severe cold spell. The license was at that time restricted to 5.0% full power. The decision was therefore made to interrupt testing to save the approximate 30 MWe required to run the reactor coolant pumps and other plant equipment. Testing was finally concluded after the aforementioned eight day delay on January 29, 1977. The program which was intended to verify the nuclear design parameters of the core prior to escalation into the power range was performed at 532°F and 2155 Psig. In general, the Zero Power Physics Test was conducted with favorable agreement between measured and predicted results A summary of each measurement performed is given in Section 3.4, Table 3.4-13.

1.2.3 POWER ESCALATION TESTS

Following the completion of zero power physics testing, initial power escalation commenced on January 29, 1977 with the first nuclear electrical power produced at 1800 on January 30, 1977. The power escalation test program was conducted at four major test plateaus of 15, 40, 75, and 100% full power with minor testing performed at intermediate power levels as required by the controlling procedure for power escalation.

Test results review was performed concurrently with testing. This allowed immediate review and approval by the Test Working Group (TWG) and Plant Review Committee (PRC). Escalation to a new power level always followed promptly behind completion of testing. A brief summary of each of these tests follows:

NUCLEAR INSTRUMENTATION CALIBRATION AT POWER TEST

The power range channels were calibrated to indicate within 2.0% full power of the heat balance and to within ± 3.5% offset of the full incore system several times during the startup program. (These calibrations were required due to variations in reactor coolant system boron concentration, cold leg temperature, control rod configuration and xenon buildin and burnout). Early in the power escalation test program some difficulties were experienced until procedural errors were resolved and instrumentation personnel experience increased. Also near the completion of the 40% full power plateau, the procedural method was modified from an on-line to off-line technique to assist in removing time dependent drift. In spite of these difficulties, the acceptance criteria were met in all calibrations required by the power escalation procedure.

BIOLOGICAL SHIELD SURVEY TEST

Upon completion of the Biological Shield Survey Test, the following conclusions were reached:

(1) Radiation and high radiation areas have been identified and posted.

(2) Radiation levels at various points around the nuclear unit have been established for future reference and comparison.

(3) Areas in which radiation levels exceed their design values are undergoing further design evaluation. In the meantine, they have been appropriately identified and marked.

REACTIVITY COEFFICIENTS AT POWER TEST

The measured results at 40, 75, and 100% full power indicate that the moderator coefficient of reactivity will always be negative during power operation above 95% full power. Comparison between predicated and measured temperature coefficients of reactivity showed favorable agreement.

Analyzed data for the power Doppler coefficient versus power level indicates that the least negative coefficient is $-1.02 \times 10^{-4} \Delta k/k/\%FP$ which is sufficiently more negative than the acceptance criteria of $-0.55 \times 10^{-4} \Delta k/k/\%FP$. The total power Doppler deficit from this measured data is projected at $-1.10\% \Delta k/k$.

CORE POWER DISTRIBUTION TEST

Four normal operating equilibrium xenon core power distributions taken at 15, 40, 75, and 100 percent full power were examined. The maximum radial peaking factors were not more than 5.0% greater than predicted by PDQ-7. The maximum total peaking factors were not more than 7.5% greater than predicted by PDQ-7.

Comparisons between measured and predicted radial and total core power distritutions as expressed in peaking factors on a 1/8 core power distribution showed favorable agreement at all core locations.

The worst case minimum DNBR and maximum LHR measured as part of this test were subject to various types of analysis. On the bases of this study, the following were determined:

(1) A worst case minimum DNBR of 3.03 and maximum LHR of 12.7 kW/ft was measured at 100% full power. This is within their respective acceptance criteria limits of 1.30 and 18.00 kW/ft.

(2) Acceptable core conditions at the trip setpoint of the next power level of escalation were verified prior to escalating reactor power.

(3) Margin analysis on the minimum DNBR and maximum LHR values at the LOCA and design overpower limits resulted in substantial margins.

The results of the quadrant tilt and axial power imbalance calculations for a variety of different core power distributions taken during the power escalation test program yield the following conclusions:

(1) All maximum quadrant power tilts determined during normal power operation were well within the Technical Specifications Limit of 4%. A typical value observed was around +1.80%.

(2) The reactor protection system will provide sufficient protection against exceeding DNBR and LHR limits when the delta flux amplifier has a gain factor of 3.90.

UNIT LOSS OF ELECTRICAL LOAD TEST

Upon completion of the Unit Loss Of Electrical Load Test at 100% full power, the following conclusions were reached:

(1) The unit successfully sustained a net load loss at 100% full power without any fuel or equipment damage.

(2) Unit response to the load loss indicates that the integrated control system successfully ran reactor power back to 15% full power at an average ramp rate 16.8% FP/min with large margins to RPS trip setpoints.

(3) Turbine speed and frequency oscillations were experienced after the runback to 15% full power, thus causing the acceptance criteria on frequency control to be exceeded. Further investigation revealed that since the oscillation magnitude observed was small it did not represent a hazard to the operating equipment on the unit.

TURBINE/REACTOR TRIP TEST

Upon completion of the reactor and turbine trip portions of Turbine/Reactor Trip Test at 40, 75, and 100% full power, the following conclusions were reached:

(1) Analysis of the unit parameters during the reactor and turbine trip transients indicate that all acceptance criteria were met.

(2) Unit response during the turbine trip portions demonstrated that the integrated control system can successfully run reactor power back to 15% full power with large margins to RPS trip setpoints.

(3) The reactor trip caused the turbine to trip which ensures that cooldown rates less than 100°F/hr can be maintained following reactor trips at power.

(4) After adjustments, the feedwater block valves closure times were approximately 28 seconds. This is required to be less than 30 seconds by the procedural acceptance criteria.

INCORE DETECTOR TEST

Upon completion of Incore Detector Testing at 40 and 75% full power, the following was concluded:

(1) The incore monitoring system has performed as expected during the startup period. Verification of flux shapes on symmetric grouping and incore detector response has been excellent.

(2) Computer corrections to the uncorrected detector signals were found to be consistent with hand calculations.

(3) The ability of the computer to determine the radial core power distribution was demonstrated.

(4) Comparison of computer and hand calculated worst case LHR indicates that the computer is slightly in error. No change to the computer is planned since the error is overshadowed by the 24 percent conservatism presently applied.

POWER IMBALANCE DETECTOR CORRELATION TEST

Upon completion of power imbalance detector correlation testing at 40 and 75% full power, the following were concluded:

(1) The measured offset correlation function between the full incore system and each out-of-core detector was determined to be a linear relationship. The average correlation slope measured was 1.08.

(2) A gain factor of 3.90 on each out-of-core power range detector difference amplifier will yield an acceptable slope relationship to the full incore system.

(3) The power/imbalance/flow envelope as set in the reactor protection system will protect the reactor from exceeding minimum DNBR and maximum LHR thermal limits, when a gain factor of 3.90 is utilized.

(4) The backup recorder can provide an acceptable measurement of core imbalance. A measured correlation slope of approximately 1.00 was observed.

NSSS HEAT BALANCE TEST

All primary and secondary heat balance calculations met their respective acceptance criteria of being within $\pm$ 2% full power of the hand calculated value.

The primary reactor coolant system flow rate on Crystal River Unit 3 was set at 110.0 percent of design flow, which is within the minimum and maximum allowable flow values of 105.0 and 115.3 percent of design.

UNIT LOAD STEADY STATE TEST

The average of the measured unit parameters during the test period fell within their respective minimum/maximum limits, except for OTSG outlet steam pressure which was indicating 20 Psig high and therefore controlling low. This was corrected by recalibrating the pressure transmitter controlling steam header pressure.

Analysis of unit parameter stability indicates that all variables are relatively stable. The maximum variation in unit parameters was experienced around 70% full power.

UNIT LOAD TRANSIENT TEST

All transients were performed without exceeding the limits of the Crystal River Unit 3 Technical Specifications and Sections 1 and 2 of Plant Limits And Precautions. In addition, each was completed without causing the reactor protection system to actuate.

The ability of the Integrated Control System to control unit parameters (i.e. power, unit average temperature, loop temperature mismatch, and turbine header pressure) during each transient was excellent.

SHUTDOWN FROM OUTSIDE CONTROL ROOM TEST

The test proved that the reactor can be brought to and maintained in a safe hot standby condition from locations outside the control room by the normal shift complement.

PSEUDO CONTROL ROD EJECTION TEST

The measured worth of the most reactive control rod was found to be 0.20%Δk/k which is less than the acceptance criterion of 0.65%Δk/k.

Analyzed core power distribution and thermal hydraulic data indicated a large perturbation to the steady state core power distribution, as was expected. No core limits were exceeded.

DROPPED CONTROL ROD TEST

Upon analysis of the Dropped Control Rod Test data, the following conclusions were deduced:

(1) Analyzed core power distribution and thermal hydraulic data provided results indicating sufficient margin to minimum DNBR and maximum linear heat rate limiting criteria. The perturbation to the steady state power distribution was as expected with a maximum quadrant power tilt of +13.48%.

(2) The measured worth of the control rod which is calculated to produce the most adverse thermal effects in the core, if it is inadvertently dropped, was found to be -0.12%Δk/k.

(3) The integrated control system accurately detected the asymmetric control rod with appropriate alarms and initiated reactor runback. The power level was below 60.0% full power in 36.7 seconds.

(4) The control rod withdrawal inhibit was shown to limit power to less than 60% full power when an asymmetric control rod condition exists.

LOSS OF OFFSITE POWER TEST

The test proved the plant's ability to sustain a loss of offsite power. A problem in steam generator level control during the transient is still under study. In the meantime, the emergency procedure for loss of offsite power has the operator monitor steam generator water levels and maintains balanced feedflow between steam generators.

2.0 INITIAL FUEL LOADING

Fuel loading was initiated with the insertion of fuel assembly 3C04 into the core on December 4, 1976 and was completed with the loading of 3C53 on December 7, 1976. A total elapsed time of 95.1 hours was required to complete fuel loading. However, less than 65.5 hours were actually utilized to transfer the fuel assemblies with the remaining time required primarily to adjust or repair fuel handling equipment. Figure 2.0-1 depicts the final configuration of the core at the conclusion of initial fuel loading. Table 2.0-1 provides the initial sequence for Crystal River Unit 3.

Neutron count rate was monitored throughout the fuel loading sequence utilizing the unit's two nuclear instrumentation source range channels NI-1 and NI-2, and two temporary incore BF_3 proportional counting systems furnished by Babcock and Wilcox. Prior to their use, each detector system was calibrated and source checked to ensure proper response. During fuel loading independent plots of inverse neutron count rate ratios versus the number of fuel assemblies loaded were maintained from the output of these detectors as each fuel assembly was loaded -- see Figures 2.0-2 through 2.0-5. New base count rates were established for a detector whenever a detector or neutron startup source was moved. When fuel assemblies are being loaded in the vicinity of a detector, geometric effects (i.e. neutron transmission vice multiplication) create large changes in count rate on the affected detector. Whenever this occurred, the procedure allowed the next two most conservative detectors to be used to predict the number of fuel assemblies to criticality. Using this technique, no partial fuel assembly insertions were required during Crystal River Unit 3 initial fuel loading.

Initial fuel loading at Crystal River Unit 3 was a semi-dry operation with the reactor vessel water level maintained above the fuel at the upper mid plane of the reactor vessel hot leg. The semi-dry loading improved visibility of the fuel assemblies during manipulations and provided accessability to the vessel flange area when repositioning the temporary detectors. Radiation levels were not overly restrictive due to the lower water level in the fuel transfer and spent fuel pool canals. The maximum radiation level measured was 10 mRem/hr (n^o) and 1 mRem/hr ($\beta + \gamma$) at the fuel handling bridge during the transfer of the fuel assemblies containing the neutron startup sources.

Several minor problems were encountered during the initial fuel loading. A discussion of these problems and their resolution is given in Table 2.0-2. The effects of these problems in some cases resulted in delaying the fuel loading process. Figure 2.0-6 shows these delays as a function of time into fuel loading with each delay noted. From this Figure, it is seen that there were no major delays which stopped fuel loading for a prolonged period.

In spite of the above problems and delays, the fuel assembly loading rate increased significantly during the loading operation as crew familiarization and equipment reliability improved. Figure 2.0-7 is a plot of the frequency distribution of the fuel assemblies loading time intervals. As can be seen, the mean loading time per assembly was 22.1 minutes.

In summary, initial fuel loading at Florida Power Corporation Crystal River Unit 3 was completed in 95.1 hours, and except for the minor problems and delays noted, fuel loading proceeded in an orderly and smooth manner.

Fuel Assembly Loading Sequence

CRA = Control Rod Assembly
APSRA = Axial Power Shaping Rod Assembly
ORA = Orifice Rod Assembly
BPRA = Burnable Poison Rod Assembly

	ASSEMBLY				Core	
Step	Type	ID#	Feature	ID#	Position	Action
0-1	Support		Detector A		14-H	Insert
0-2	Support		Detector B		10-P	Insert
1	Fuel	3C04	Neutron Source	110	14-N	Insert
2	Fuel	3C20	Neutron Source	111	2-D	Insert
3	Fuel	3C55	ORA	168	13-O	Insert
4	Fuel	3C37	BPRA	B47	13-N	Insert
5	Fuel	3C35	BPRA	B52	12-O	Insert
6	Fuel	3C48	ORA	170	14-M	Insert
7	Fuel	3A04	CRA	C54	12-N	Insert
8	Fuel	3A27	CRA	C51	13-M	Insert
9	Fuel	3B05	BPRA	B66	12-M	Insert
10	Fuel	3B39	BPRA	B42	13-L	Insert
11	Fuel	3B28	BPRA	B68	11-N	Insert
12	Fuel	3A42	APSRA	A06	12-L	Insert
13	Fuel	3A21	CRA	C50	11-M	Insert
14	Fuel	3B50	BPRA	B62	11-L	Insert
15	Fuel	3B41	BPRA	B40	12-K	Insert
16	Fuel	3B15	BPRA	B65	10-M	Insert
17	Fuel	3A44	CRA	C44	10-L	Insert
18	Fuel	3A20	CRA	C39	11-K	Insert
19	Fuel	3B25	BPRA	B15	10-K	Insert
20	Fuel	3B33	BPRA	B18	9-L	Insert
21	Fuel	3B02	BPRA	B37	11-H	Insert
22	Fuel	3A48	APSRA	A08	10-N	Insert
23	Fuel	3A01	CRA	C49	9-M	Insert
24	Fuel	3B23	BPRA	B46	9-N	Insert
25	Fuel	3B61	BPRA	B43	8-M	Insert
25-1	Support		Detector B		10-P	Remove
25-2	Support		Detector B		7-M	Insert
26	Fuel	3A34	CRA	C58	11-O	Insert
27	Fuel	3B21	BPRA	B51	10-O	Insert
28	Fuel	3C29	ORA	112	12-P	Insert
29	Fuel	3C33	ORA	171	11-P	Insert
30	Fuel	3A33	CRA	C40	9-K	Insert
31	Fuel	3A47	CRA	C43	8-L	Insert
32	Fuel	3A54	CRA	C32	10-H	Insert
33	Fuel	3B59	BPRA	B14	8-K	Insert
34	Fuel	3B55	BPRA	B11	9-H	Insert
35	Fuel	3B37	CRA	C31	8-H	Insert
36	Fuel	3B32	BPRA	B17	7-L	Insert
37	Fuel	3B51	BPRA	B08	10-G	Insert
38	Fuel	3A45	CRA	C37	7-K	Insert
39	Fuel	3A39	CRA	C25	9-G	Insert
40	Fuel	3B58	BPRA	B10	7-H	Insert

Table 2.0-1

Fuel Assembly Loading Sequence

Step	ASSEMBLY Type	ID#	Feature	ID#	Core Position	Action
41	Fuel	3B57	BPRA	B07	8-G	Insert
42	Fuel	3A26	CRA	C24	7-G	Insert
43	Fuel	3B48	BPRA	B13	6-K	Insert
44	Fuel	3B20	BPRA	B04	9-F	Insert
45	Fuel	3A56	CRA	C30	6-H	Insert
46	Fuel	3A30	CRA	C19	8-F	Insert
46-1	Support		Detector A		14-H	Remove
46-2	Support		Detector A		10-F	Insert
47	Fuel	3B10	BPRA	B06	6-G	Insert
48	Fuel	3B18	BPRA	B03	7-F	Insert
49	Fuel	3A38	CRA	C18	6-F	Insert
50	Fuel	3B01	BPRA	B36	5-H	Insert
51	Fuel	3L[illegible]	BPRA	B30	8-E	Insert
52	Fuel	3A16	CRA	C23	5-G	Insert
53	Fuel	3A12	CRA	C13	7-E	Insert
54	Fuel	3B13	BPRA	B59	5-F	Insert
55	Fuel	3B49	BPRA	B56	6-E	Insert
56	Fuel	3A23	CRA	C12	5-E	Insert
57	Fuel	3B07	BPRA	B33	4-G	Insert
58	Fuel	3B53	BPRA	B27	7-D	Insert
59	Fuel	3A09	APSRA	A03	4-F	Insert
60	Fuel	3A06	APSRA	A01	6-D	Insert
61	Fuel	3B30	BPRA	B55	4-E	Insert
62	Fuel	3B03	BPRA	B53	5-D	Insert
63	Fuel	3A53	CRA	C08	4-D	Insert
64	Fuel	3B11	BPRA	B31	3-F	Insert
65	Fuel	3B26	BPRA	B22	6-C	Insert
66	Fuel	3A11	CRA	C11	3-E	Insert
67	Fuel	3C28	BPRA	B26	3-D	Insert
68	Fuel	3C14	ORA	173	2-E	Insert
69	Fuel	3A28	CRA	C04	5-C	Insert
70	Fuel	3C11	BPRA	B21	4-C	Insert
71	Fuel	3C52	ORA	175	3-C	Insert
72	Fuel	3C40	ORA	109	4-B	Insert
73	Fuel	3C46	ORA	176	5-B	Insert
74	Fuel	3A50	CRA	C42	6-L	Insert
75	Fuel	3A41	CRA	C36	5-K	Insert
76	Fuel	3B43	BPRA	B61	5-L	Insert
77	Fuel	3A03	CRA	C29	4-H	Insert
78	Fuel	3B36	BPRA	B39	4-K	Insert
79	Fuel	3A07	APSRA	A05	4-L	Insert
80	Fuel	3A25	CRA	C22	3-G	Insert
81	Fuel	3B24	BPRA	B35	3-H	Insert
82	Fuel	3A08	CRA	C35	3-K	Insert
83	Fuel	3B42	BPRA	B41	3-L	Insert
84	Fuel	3C16	CRA	C17	2-F	Insert
85	Fuel	3B60	BPRA	B05	2-G	Insert
86	Fuel	3C43	CRA	C28	2-H	Insert
87	Fuel	3B54	BPRA	B12	2-K	Insert
88	Fuel	3C15	CRA	C41	2-L	Insert
89	Fuel	3C41	ORA	177	1-F	Insert

Table 2.0-1 (Continued)

Fuel Assembly Loading Sequence

Step	Type	ID#	Feature	ID#	Core Position	Action
	ASSEMBLY					
90	Fuel	3C08	ORA	183	1-G	Insert
91	Fuel	3C19	ORA	188	1-H	Insert
92	Fuel	3C10	ORA	189	1-K	Insert
92-1	Support		Detector B		7-M	Remove
92-2	Support		Detector B		1-L	Insert
93	Fuel	3C05	CRA	C61	10-P	Insert
94	Fuel	3C54	ORA	190	10-R	Insert
95	Fuel	3A51	CRA	C57	9-O	Insert
96	Fuel	3B27	BPRA	B20	9-P	Insert
97	Fuel	3C21	ORA	192	9-R	Insert
98	Fuel	3A40	CRA	C53	8-N	Insert
99	Fuel	3B34	BPRA	B50	8-O	Insert
100	Fuel	3C18	CRA	C60	8-P	Insert
101	Fuel	3C07	ORA	193	8-R	Insert
102	Fuel	3A17	CRA	C48	7-M	Insert
103	Fuel	3B46	BPRA	B45	7-N	Insert
104	Fuel	3A02	CRA	C56	7-O	Insert
105	Fuel	3B45	BPRA	B19	7-P	Insert
106	Fuel	3C27	ORA	196	7-R	Insert
107	Fuel	3B08	BPRA	B64	6-M	Insert
108	Fuel	3A10	APSRA	A07	6-N	Insert
109	Fuel	3B47	BPRA	B49	6-O	Insert
110	Fuel	3C02	CRA	C59	6-P	Insert
111	Fuel	3C56	ORA	200	6-R	Insert
112	Fuel	3A18	CRA	C47	5-M	Insert
113	Fuel	3B09	BPRA	B67	5-N	Insert
114	Fuel	3A31	CRA	C55	5-O	Insert
115	Fuel	3C26	ORA	201	5-P	Insert
116	Fuel	3B29	BPRA	B63	4-M	Insert
117	Fuel	3A05	CRA	C52	4-N	Insert
118	Fuel	3C22	BPRA	B48	4-O	Insert
119	Fuel	3A55	CRA	C46	3-M	Insert
120	Fuel	3C09	BPRA	B44	3-N	Insert
121	Fuel	3C59	ORA	203	3-O	Insert
122	Fuel	3C03	ORA	204	2-M	Insert
123	Fuel	3C51	ORA	206	2-N	Insert
124	Fuel	3A13	CRA	C26	11-G	Insert
125	Fuel	3B14	BPRA	B60	11-F	Insert
126	Fuel	3A36	CRA	C33	12-H	Insert
127	Fuel	3B19	BPRA	B34	12-G	Insert
128	Fuel	3A49	APSRA	A04	12-F	Insert
129	Fuel	3A46	CRA	C38	13-K	Insert
130	Fuel	3B31	BPRA	B38	13-H	Insert
131	Fuel	3A35	CRA	C27	13-G	Insert
132	Fuel	3B44	BPRA	B32	13-F	Insert
133	Fuel	3C32	CRA	C45	14-L	Insert
134	Fuel	3B56	BPRA	B16	14-K	Insert
135	Fuel	3C45	CRA	C34	14-H	Insert
136	Fuel	3B38	BPRA	B09	14-G	Insert
137	Fuel	3C31	CRA	C21	14-F	Insert
138	Fuel	3C57	ORA	207	15-L	Insert

Table 2.0-1 (Continued)

Fuel Assembly Loading Sequence

Step	Type	ID#	Feature	ID#	Core Position	Action
	ASSEMBLY					
139	Fuel	3C13	ORA	209	15-K	Insert
140	Fuel	3C06	CRA	213	15-H	Insert
141	Fuel	3C12	ORA	214	15-G	Insert
141-1	Support		Detector A		10-F	Remove
141-2	Support		Detector A		15-F	Insert
142	Fuel	3A29	CRA	C20	10-F	Insert
143	Fuel	3C24	CRA	C01	6-B	Insert
144	Fuel	3C42	ORA	217	6-A	Insert
145	Fuel	3A15	CRA	C05	7-C	Insert
146	Fuel	3B04	BPRA	B01	7-B	Insert
147	Fuel	3C44	ORA	220	7-A	Insert
148	Fuel	3A19	CRA	C09	8-D	Insert
149	Fuel	3B35	BPRA	B23	8-C	Insert
150	Fuel	3C17	CRA	C02	8-B	Insert
151	Fuel	3C01	ORA	221	8-A	Insert
152	Fuel	3A24	CRA	C14	9-E	Insert
153	Fuel	3B22	BPRA	B28	9-D	Insert
154	Fuel	3A52	CRA	C06	9-C	Insert
155	Fuel	3B40	BPRA	B02	9-B	Insert
156	Fuel	3C36	ORA	222	9-A	Insert
157	Fuel	3B16	BPRA	B57	10-E	Insert
158	Fuel	3A37	APSRA	A02	10-D	Insert
159	Fuel	3B17	BPRA	B24	10-C	Insert
160	Fuel	3C25	CRA	C03	10-B	Insert
161	Fuel	3C38	ORA	224	10-A	Insert
162	Fuel	3A14	CRA	C15	11-E	Insert
163	Fuel	3B12	BPRA	B54	11-D	Insert
164	Fuel	3A22	CRA	C07	11-C	Insert
165	Fuel	3C23	ORA	225	11-B	Insert
166	Fuel	3B06	BPRA	B58	12-E	Insert
167	Fuel	3A32	CRA	C10	12-D	Insert
168	Fuel	3C49	BPRA	B25	12-C	Insert
169	Fuel	3A43	CRA	C16	13-E	Insert
170	Fuel	3C50	BPRA	B29	13-D	Insert
171	Fuel	3C60	ORA	227	13-C	Insert
172	Fuel	3C47	ORA	229	14-E	Insert
173	Fuel	3C39	ORA	230	14-D	Insert
174	Fuel	3C04	ORA	110	14-N	Remove
174-1	Fuel	3C04	ORA	110	4-P	Insert
175	Fuel	3C30	ORA	231	14-N	Insert
176	Fuel	3C20	ORA	111	2-D	Remove
176-1	Fuel	3C20	ORA	111	12-B	Insert
177	Fuel	3C34	ORA	232	2-D	Insert
178	Support		Detector B		1-L	Remove
178-1	Fuel	3C58	ORA	233	1-L	Insert
179	Support		Detector B		15-F	Remove
179-1	Fuel	3C53	ORA	234	15-F	Insert

Table 2.0-1 (Continued)

Table 2.0-2

Summary Of Problems Experienced During Initial Fuel Loading

Problem Number	Problem Type	Description Of Problems Encountered And Corrective Actions
1	NI-2 Scaler Timer	During the loading of the first four fuel assemblies, the count rate observed by the scaler timer on NI-2 did not produce the expected increase in count rate. It was taken out of service and replaced with a spare while the fifth fuel assembly was being loaded. The problem was the result of an improper gain adjustment.
2	TYGON Tubing Leak	The auxiliary neutron monitoring cables are pressurized to 20 psig to prevent moisture damage during fuel loading. Gas leaks were found at the TYGON tubing connection to the auxiliary detector (A) (minor leak) and at the TYGON tubing connection to the electronics of auxiliary detector (A) (major leak). The major leak was patched with tape and caulking compound.
3	Loading Assemblies Into Core	During the loading of 3C32 into core location L-14 the assembly would not seat. The assembly was removed from the core, inspected, and found to be okay. The decay heat pump was stopped and after cable manipulation the assembly seated. Fuel assembly 3A43 did not seat on the initial try. The second attempt, however, seated the assembly without any problems.
4	Spent Fuel Bridge	(KEY) The keys which hold the drive wheels on the drive shaft fell out of the keyways. There is a coupling on each end of the bridge. It was felt that one key fell out prior to fuel loading and only one wheel was driving the bridge. When the second key fell out the bridge came to a halt. The problem was resolved by replacing and staking the keys in the keyways.

Table 2.0-2 (Cont'd)

Summary Of Problems Experienced During Initial Fuel Loading

Problem Number	Problem Type	Description Of Problems Encountered And Corrective Actions
4	Spent Fuel Bridge	(SET SCREW) The set screw in the motor coupling loosened twice during fuel loading. Each time the set screw was retightened.
5	Main Fuel Bridge	(HOIST MOTOR) The Main Fuel Bridge hoist motor overheated and stopped operating. This was corrected by installing a fan for cooling.
		(CABLE) The Main Fuel Bridge cable takeup caused problems and required the operators to make sure the cable did not get run over by the main bridge.
		(HYDRAULIC TELESCOPE CYLINDER) The Main Fuel Bridge stopped operation when the hydraulic telescopic cylinder drifted causing the control rod test light to come on and activate an interlock. The rod grapple reset switch was depressed to remove the interlock.
6	Fuel Transfer Mechanisms	(MOTOR COUPLING SET SCREW) The failure of a set screw on the Y upender between the motor coupling and the shaft allowed the shaft to turn freely. The set screw was removed, two holes were drilled and tapped and two set screws installed to secure the coupling on the shaft.
		(HYDRAULIC TUBE) The hydraulic tube for the Y transfer carriage became entangled on the takeup reel twice during fuel loading.
		(HYDRAULIC AIR LEAK) A hydraulic air leak on the Y transfer carriage took this system out of service before the last scheduled move. Loading was completed using the X carriage.
7	Auxiliary Fuel Bridge	There was some trouble latching on to the auxiliary neutron detector. The decay heat pump was secured and movement of the hoist was guided by visually observing the operation with binoculars.

Table 2.0-2 (Cont'd)

Summary Of Problems Experienced During Initial Fuel Loading

Problem Number	Problem Type	Description Of Problems Encountered And Corrective Actions
8	Observable Countrate	During the loading of the last fuel assembly, difficulty was experienced in obtaining a detectable countrate on auxiliary detector A. After trying several positions at the top of the core, the detector was removed and held over the edge of the reactor vessel, thereby providing an adequate countrate.

Final Fuel Loading Distribution For Crystal River Unit 3

	1	2	3	4	5	6	7	8	9	10	11	12	13	14	15
A						3C42 0217	3C44 0220	3C01 0221	3C36 0222	3C38 0224					
B				3C40 0109	3C46 0176	3C24 C001	3B04 B001	3C17 C002	3B40 B002	3C25 C002	3C23 0225	3C20 0111			
C			3C52 0175	3C11 B021	3A28 C004	3B26 B022	3A15 C005	3B35 B023	3A52 C006	3B17 B024	3A22 C007	3C49 B025	3C60 0227		
D		3C34 0232	3C28 B026	3A53 C008	3B03 B053	3A06 A001	3B53 B027	3A19 C009	3B22 B028	3A37 A002	3B12 B054	3A32 C010	3C50 B029	3C39 0230	
E		3C14 0173	3A11 C011	3B30 B055	3A23 C012	3B49 B056	3A12 C013	3B52 B030	3A24 C014	3B16 B057	3A14 C015	3B06 B058	3A43 C016	3C47 0229	
F	3C41 0177	3C16 C017	3B11 B031	3A09 A003	3B13 B059	3A38 C018	3B18 B003	3A[illegible]0 C019	3B20 B004	3A29 C020	3B14 B060	3A49 A004	3B44 B032	3C31 C021	3C33 0234
G	3C08 0183	3B60 B005	3A25 C022	3B07 B033	3A16 C023	3B10 B006	3A26 C024	3B57 B007	3A39 C025	3B51 B008	3A13 C026	3B19 B034	3A35 C027	3B38 B009	3C12 0214
H	3C19 0188	3C43 C028	3B24 B035	3A03 C029	3B01 [illegible]036	3A56 C030	3B58 B010	3B37 C031	3B55 B011	3A54 C032	3B02 B037	3A36 C033	3B31 B038	3C45 C034	3C06 0213
K	3C10 0189	3B54 C012	3A08 C035	3B36 B039	3[illegible]1 C0[illegible]6	3B48 B013	3A45 C037	3B59 B014	3A33 C040	3B25 B015	3A20 C039	3B41 B040	3A46 C038	3B56 B016	3C13 0209
L	3C58 0233	3C15 C041	3B42 B041	3A07 A005	3B43 B061	3A50 C042	3B32 B017	3A47 C043	3B33 B018	3A44 C044	3B50 B062	3A42 A006	3B39 B042	3C32 C045	3C57 0207
M		3C03 0204	3A55 C046	3B29 B063	3A18 C047	3B08 B064	3A17 C048	3B61 B043	3A01 C049	3B15 B065	3A21 C050	3B05 B066	3A27 C051	3C48 0170	
N		3C51 0206	3C09 B044	3A05 C052	3B09 B067	3A10 A007	3B46 B045	3A40 C053	3B23 B046	3A48 A008	3B28 B068	3A04 C054	3C37 B047	3C30 0231	
O			3C59 0203	3C22 B048	3A11 C055	3B47 B049	3A02 C056	3B34 B050	3A51 C057	3B21 B051	3A34 C058	3C35 B052	3C55 0168		
P				3C04 0110	3C26 0201	3C02 C059	3B45 B019	3C18 C060	3B27 B020	3C05 C061	3C33 0171	3C29 0112			
R						3C56 0200	3C27 0196	3C07 0193	3C21 0192	3C54 0190					

3A01 through 3A56 = 1.93 wt % Fuel Assemblies
3B01 through 3B61 = 2.54 wt % Fuel Assemblies
3C01 through 3C60 - 2.83 wt % Fuel Assemblies
B001 through B020 - 1.34 wt % Burnable Poison Assemblies
B021 through B052 = 1.18 wt % Burnable Poison Assemblies
B053 through B068 = 1.01 wt % Burnable Poison Assemblies
C001 through C061 = Control Rod Assemblies
A001 through A008 = Axial Power Shaping Rod Assemblies
0109 through 0234 = Orifice Rod Assemblies

Figure 2.0-1

Inverse Multiplication Versus Number Of Fuel Assemblies Loaded
For Auxiliary Neutron Detector (A)

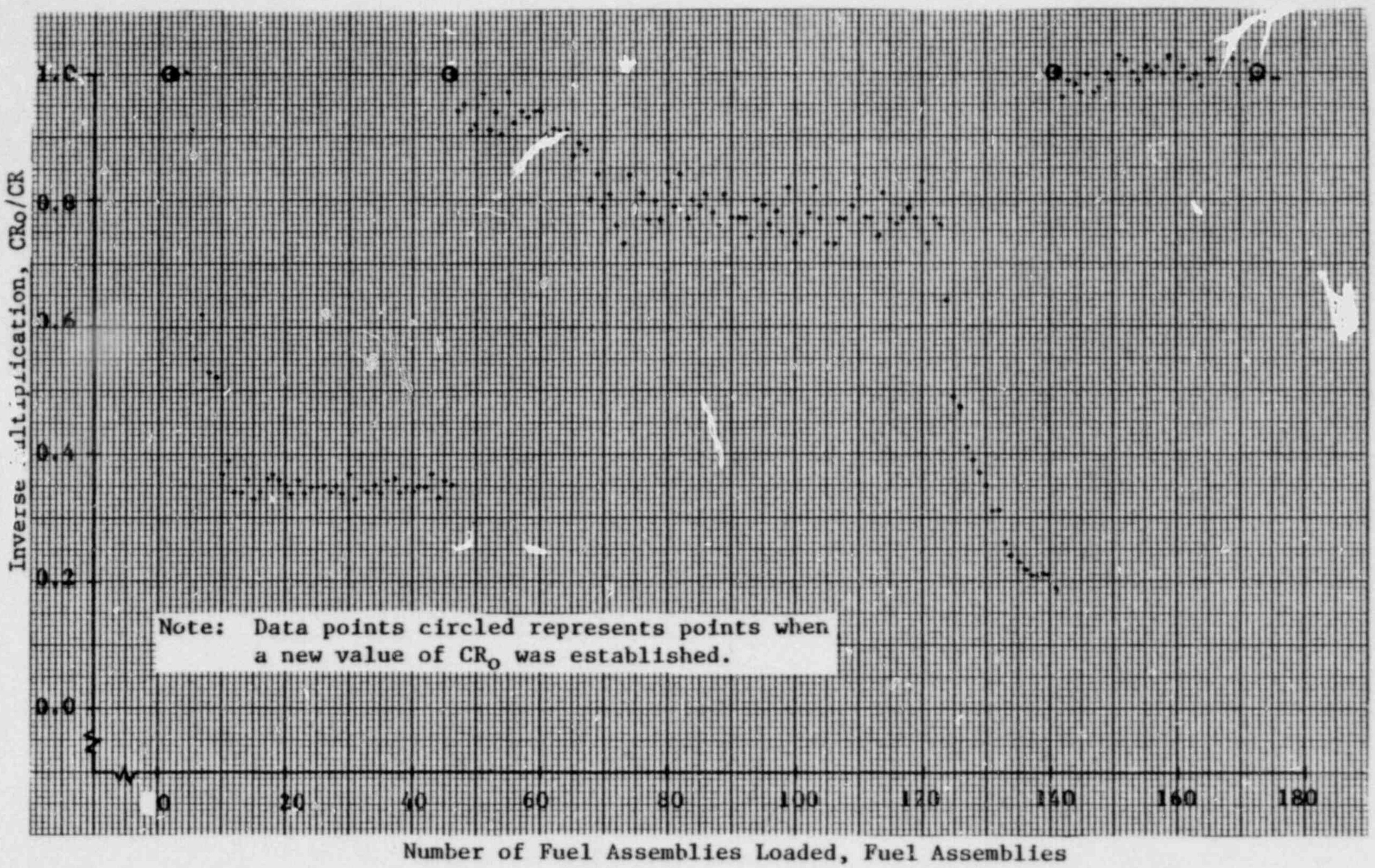

Figure 2.0-2

Inverse Multiplication Versus Number Of Fuel Assemblies Loaded
For Auxiliary Neutron Detector (B)

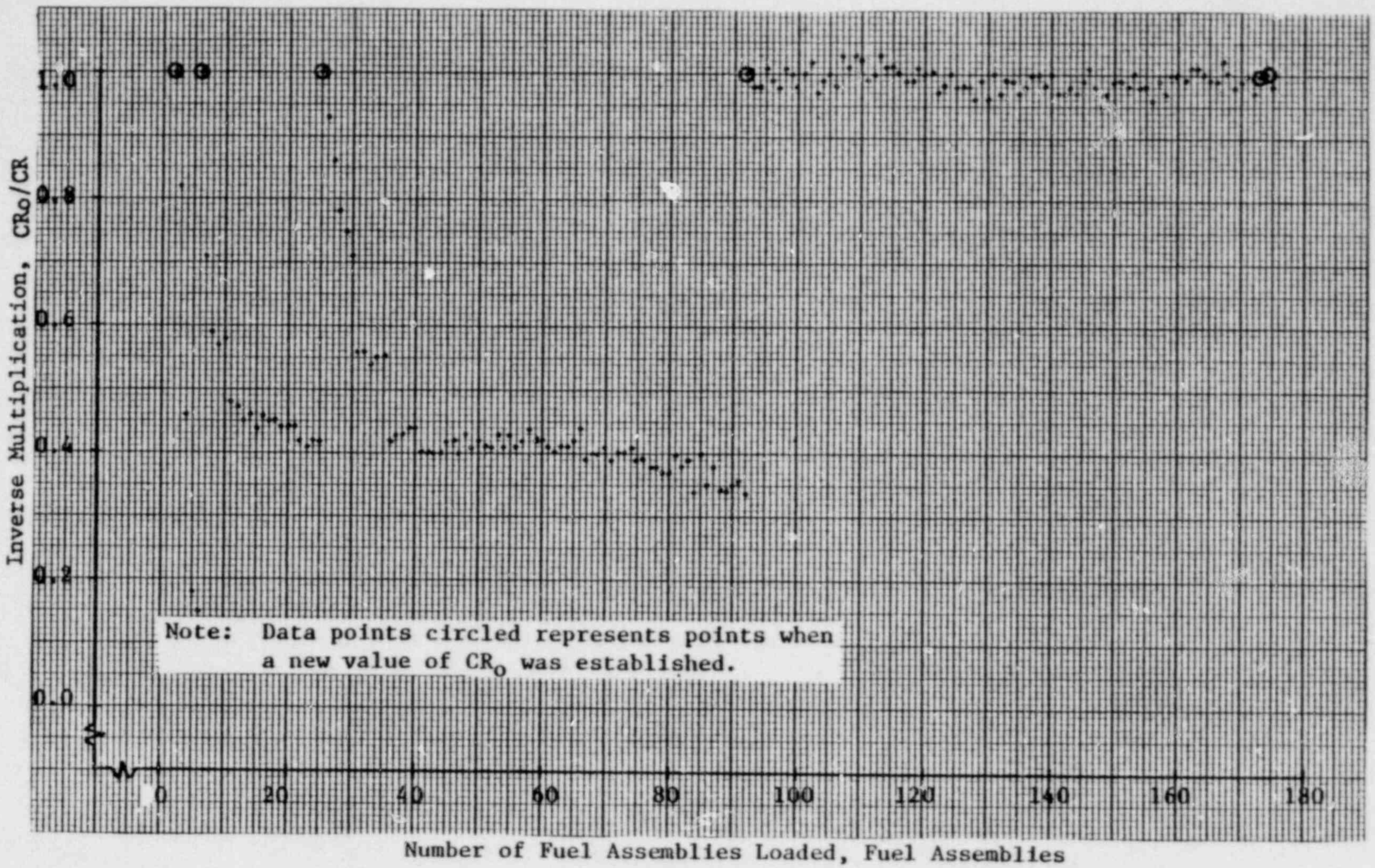

Figure 2.0-3

Inverse Multiplication Versus Number Of Fuel Assemblies Loaded
For Source Range Nuclear Instrumentation Channel NI-1.

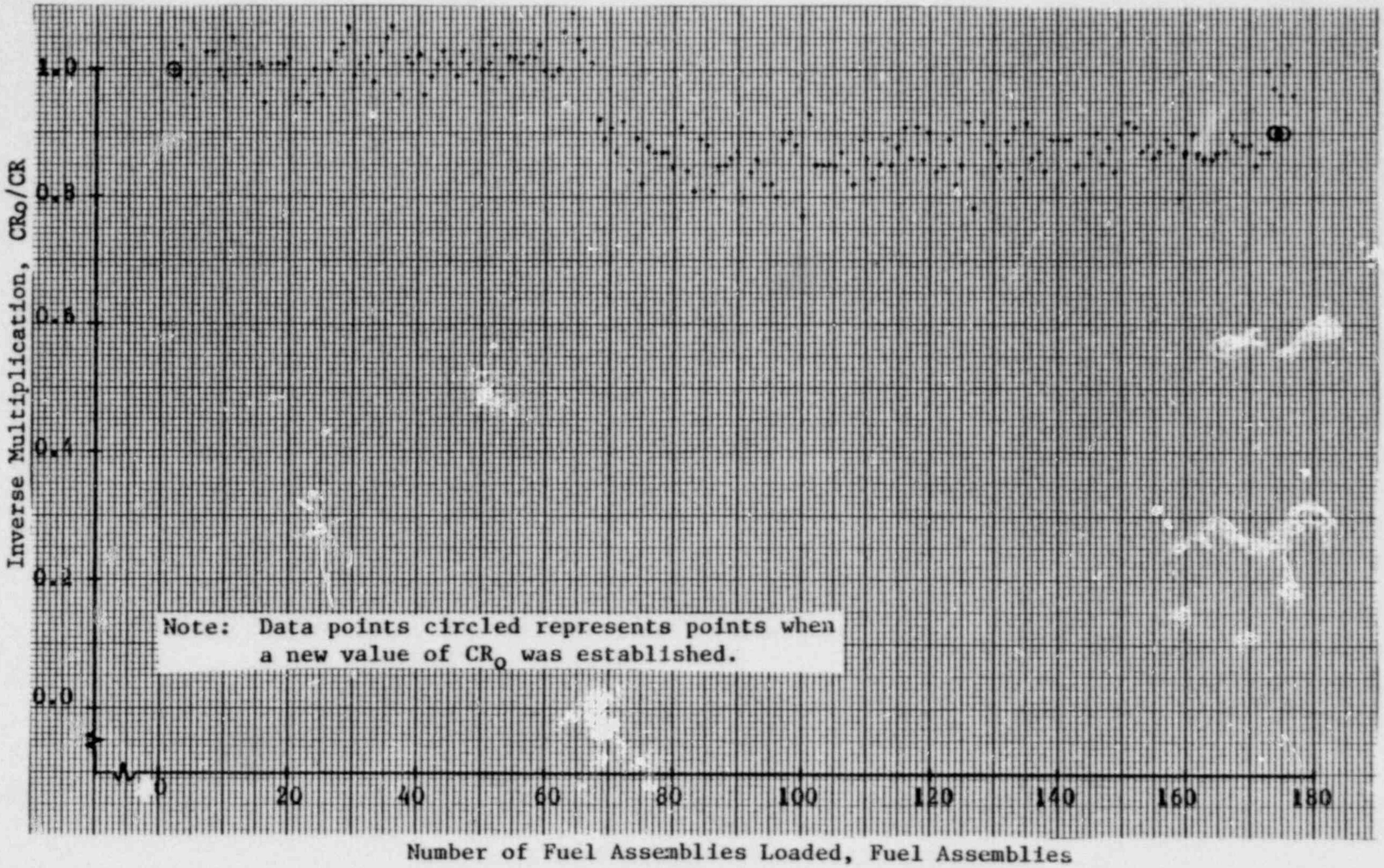

Figure 2.0-4

Inverse Multiplication Versus Number Of Fuel Assemblies Loaded
For Source Range Nuclear Instrumentation Channel NI-2.

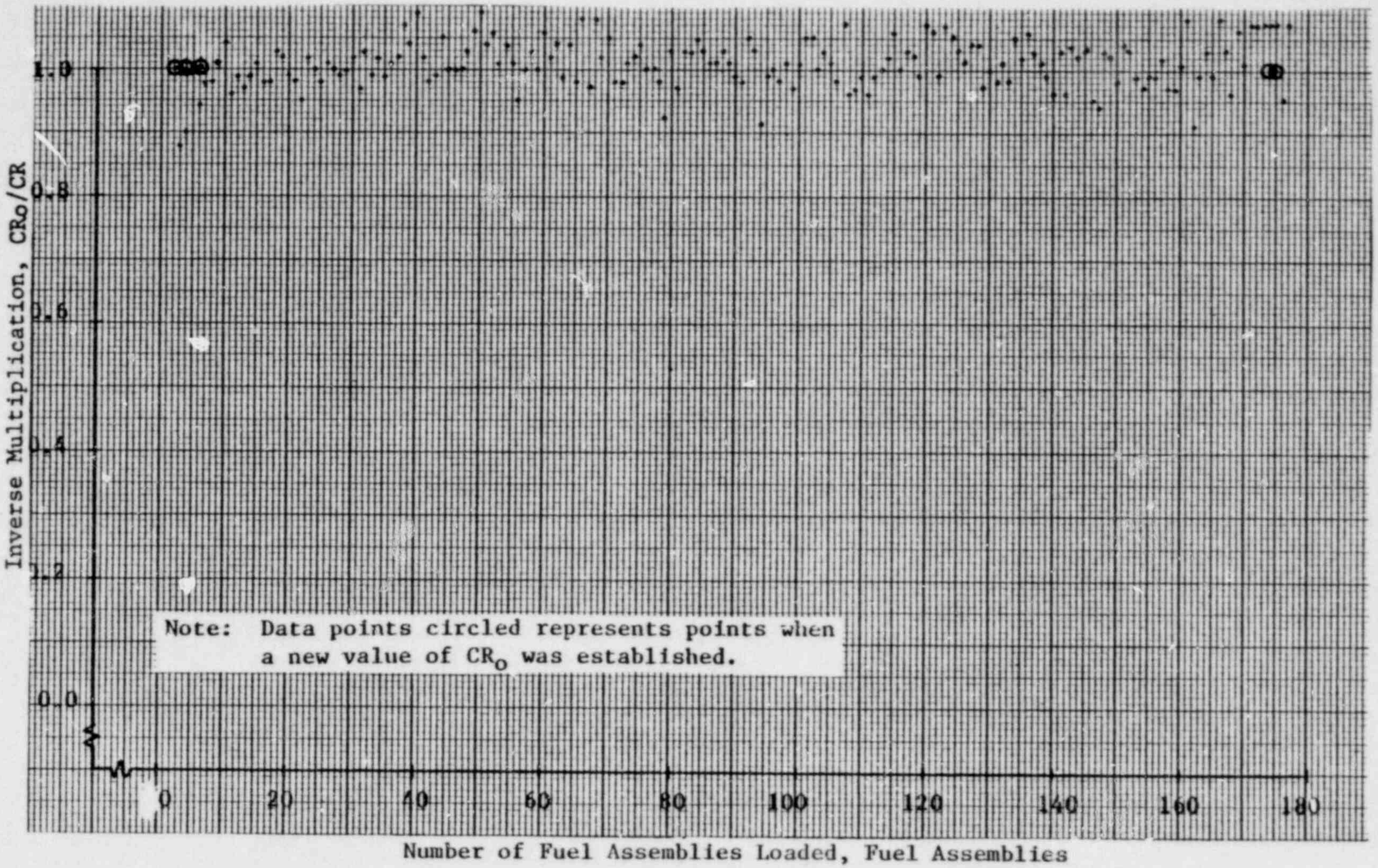

Figure 2.0-5

Fuel Assemblies Loaded Versus Time Into Fuel Loading After Loading The First Assembly

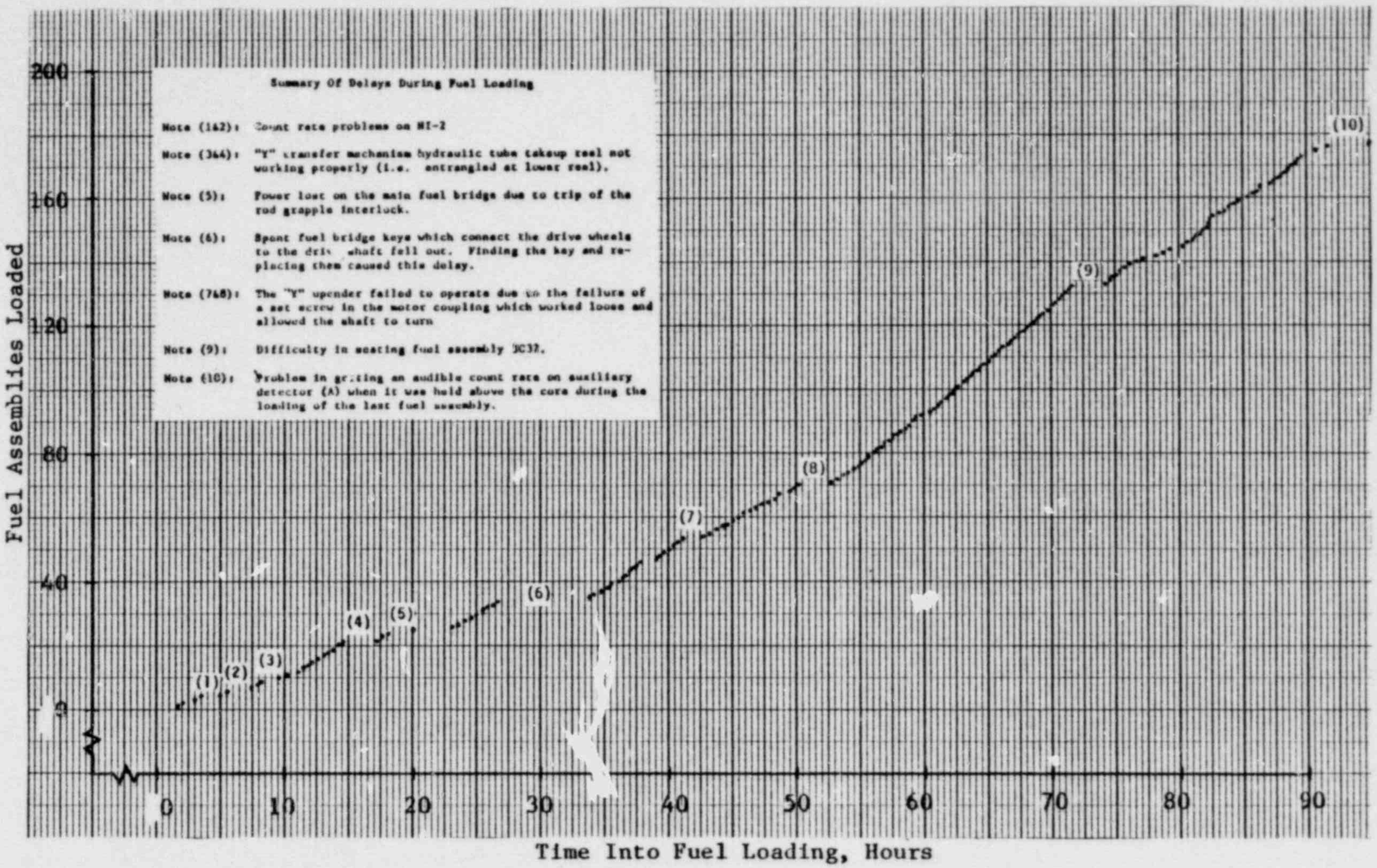

Figure 2.0-6

Frequency Distribution Of Loading Time Intervals During Initial Fuel Loading

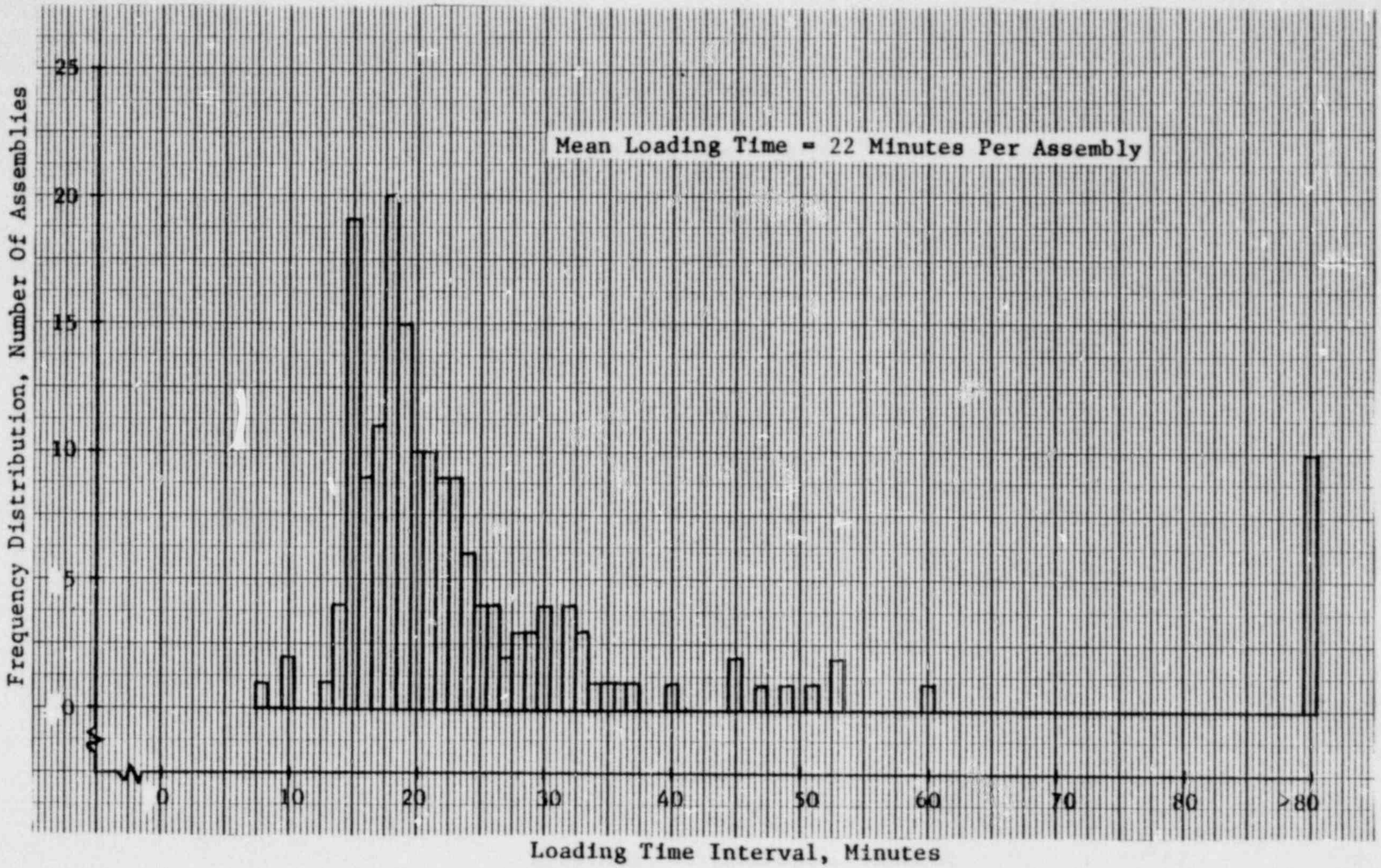

Figure 2.0-7

3.0 TESTING PRIOR TO POWER ESCALATION

Following initial fuel loading of Crystal River Unit 3, certain testing was conducted prior to power escalation. This testing was conducted in January 1977 and included the Reactor Coolant Pump Flow and Flow Coastdown Test, the Control Rod Drive Drop Time Test, the Pressurizer Test, and the Zero Power Physics Test. This section of the report presents the results of these tests. In all cases, all applicable Technical Specifications requirements were met.

3.1 REACTOR COOLANT FLOW AND FLOW COASTDOWN TEST

Prior to Power Escalation, the reactor coolant pump flow and flow coastdown test was performed to ensure the functional capabilities of the reactor coolant system and the reactor coolant pumps during steady state flow and flow coastdown conditions.

This test was conducted at hot conditions of 532°F and 2155 Psig with the core installed. The intent was to measure the normal flow rate with four reactor coolant pumps operating and the minimum flow rate with two and three reactor coolant pumps operating. In addition it also measured the flow coastdown and time delay characteristics for the loss of four, two and one reactor coolant pumps from the normal operating conditions.

3.1.1 PURPOSE

The purpose of the reactor coolant flow and flow coastdown test are listed below:

(a) To measure the reactor coolant flow and flow coastdown characteristics for selected pump combinations at 532°F and 2155 Psig with the core installed.

(b) To compare reactor coolant flow with design calculations and to verify adequate core flow.

(c) To verify that the reactor coolant system flow instrumentation response time is within acceptable limits.

Four acceptance criteria are specified for the reactor coolant flow and flow coastdown test as listed below:

(1) Steady state total reactor coolant system flow with the core and orifice rods installed when corrected to 532°F and 2155 Psig shall be within the limits specified in Table 3.1-2.

(2) The delay time between the snubbered and unsnubbered flow response after a flow reduction equivalent to the flux to flow ratio of 1.044 must be less than 1.25 seconds for the loss of one reactor coolant pump and 1.00 seconds for the loss of two and four reactor coolant pumps from four pump initial conditions at 532°F and 2155 Psig.

(3) The reactor coolant system flow when corrected to 532°F and 2155 Psig, must be greater than or equal to the flow versus time relationship in Figure 3.1-1.

(4) During the operation of four reactor coolant pumps, steady state loop flows shall be within 2 percent of each other.

3.1.2 TEST METHOD

Reactor coolant steady state flows were determined by means of the unit computer which calculated the coolant flow from the loop flow meter ΔP cells as follows:

$$Fm = C_f (\Delta P_m/V_m)^{1/2} \qquad \text{EQ. (3.1-1)}$$

Where: Fm = Flow Rate At Measured Conditions, MPPH

C_f = Flow Meter Coefficient, 407030 *

ΔP_m = Measured Delta Pressure, Psig

V_m = Specific Volume At Measured Conditions, Ft^3/lb.

For each pump operating combination given in Table 3.1-1 ten sets of steady state data was taken on the unit computer and the values averaged to determine the coolant flow rates. These results were then corrected to reference conditions of 532°F and 2155 Psig by using the equation below:

$$Fr = Fm\,(Vm/Vr) \qquad \text{EQ. (3.1-2)}$$

Where: Fr = Flow Rate At Reference Conditions, MPPH

Fm = Flow Rate At Measured Conditions, MPPH

Vr = Specific Volume At Reference Conditions (532°F), Ft^3/lb.

Vm = Specific Volume At Measured Conditions, Ft^3/lb.

The measured flow rates corrected to the reference conditions were then compared to their respective acceptance criteria.

Reactor coolant flow coastdown versus time was determined from temperature compensated square root extractor which solved equation 3.1-1. For each pump trip combination given in Table 3.1-1, steady state data was obtained. Subsequently, all or a portion of the operating pumps were tripped and data was recorded during the ensuing reactor coolant flow transient. Steady state data was again taken following the flow transient. The measured reactor coolant flows at various times during the coastdown transients were then normalized to their initial value, plotted versus time, and compared to the acceptance criteria.

Delay time analysis between unsnubbered and snubbered flow signal response was done for each reactor coolant flow coastdown. For each pump trip combination given in Table 3.1-1, data was collected for snubbered positions 3 and 4, and the time delay relative to the unsnubbered flow signal was calculated versus time. The time delay at a flow reduction of the flux to flow ratio (1.044) was then determined and compared to the acceptance criteria.

3.1.3 EVALUATION OF TEST RESULTS

Table 3.1-2 gives the minimum and maximum allowable flow rates for three different pump combinations, along with the measured flow rates for each listed condition. It can be seen that the measured flow rates are well within the acceptance criteria, and that the flow imbalance with four reactor coolant pumps was also well within the acceptance criteria of 2 percent.

* This coefficient was changed after the test program to reflect the final flow determination in Section 4.9.

Figure 3.1-1 shows the minimum acceptable reactor coolant flow rate versus time for a four pump coastdown. Also included are the measured reactor coolant flows versus time for the coastdowns of four, two and one reactor coolant pumps from an initial four pump operating condition. It can be seen that during the four pump coastdown the flow remained above the acceptance curve which was normalized to the steady state initial flow rate of 109.9% design flow.

Delay time analysis during the four, two and one reactor coolant pump trips from an initial four pump operating condition is shown in Figures 3.1-2, 3.1-3 and 3.1-4 with the results tabulated in Table 3.1-3 for snubber positions 3 and 4. The data taken at snubbered position 4 indicate that the resulting time delay was well below the acceptance criteria.

3.1.4 CONCLUSIONS

The measured reactor coolant flow rate is approximately 109.9% of the design value. This flow provides adequate margin to both the maximum and minimum allowable flow rates. This flow was preliminary. A final flow measurement was performed as part of the NSSS Heat Balance Test.

The measured reactor coolant flow rate versus time for a loss of four reactor coolant pumps was above the minimum allowable flow coastdown curve.

Snubber position 4 combined adequate filtering with a delay time response well within the acceptance criteria.

Table 3.1-1

Summary Of Testing Done During The Performance Of Reactor Coolant Pump Flow And Flow Coastdown Test

Test Number	Pumps Running				Pumps Tripped				Data Reported	General Comment
	A1	A2	B1	B2	A1	A2	B1	B2		
A.	Reactor Coolant Pump Steady State Flow									
1	X	X	X	X					Tab. 3.1-2	Normal Four Pump Flow
2	X	X		X					Tab. 3.1-2	Minimum Three Pump Flow
3		X		X					Tab. 3.1-2	Minimum Two Pump Flow
B.	Reactor Coolant Pump Flow Coastdowns.									
4	X	X	X	X	X	X	X	X	Fig. 3.1-1	Loss of Four Pumps
5	X	X	X	X	X		X		Fig. 3.1-1	Loss of Highest Flow Pump in Each Loop During Four Pump Operation
6	X	X	X	X			X		Fig. 3.1-1	Loss of Highest Flow Pump During Four Pump Operation
C.	Delay Time Analysis During Flow Coastdowns.									
7	X	X	X	X	X	X	X	X	Tab. 3.1-3 Fig. 3.1-2	Response of Snubber Position 3 and 4 to the Loss of Four Pumps
8	X	X	X	X	X		X		Tab. 3.1-3 Fig. 3.1-3	Response of Snubber Position 3 and 4 to the Loss of Two Pumps
9	X	X	X	X			X		Tab. 3.1-3 Fig. 3.1-4	Response of Snubber Position 3 and 4 to the Loss of One Pump

Table 3.1-2

Comparison Of Measured Reactor Coolant Flow Rates For Various Pump Combinations To The Acceptance Criteria At Reference Conditions Of 532°F And 2155 Psig

Pump Combination	Minimum Acceptable Flow Rate (10^6 lbm/hr)	Maximum Acceptable Flow Rate (10^6 lbm/hr)	Measured Flow Rate (10^6 lbm/hr)	Absolute Flow Imbalance (%)
Four Pumps	142.1	153.3	148.7	0.47
Three Pumps	105.8	153.3	111.7	NA
One Pump Each Loop	69.6	153.3	73.4	1.72

Note: Design core flow rate is equal to 135.3 X 10^6 lbm/hr at 532°F and 2155 Psig.

Note: The measured flow rates stated above are preliminary. A final flow measurement was performed as part of the NSSS Heat Balance Test --- see Section 4.9.

Table 3.1-3

Comparison Of Measured Time Delays Between Snubbered And Unsnubbered Reactor Coolant Flow Rates For Various Pump Combinations From Four Pump Initial Conditions Of 532°F And 2155 Psig

Pump Trip Combination	Snubber Position	Time Reactor Trip Should Occur (Seconds)	Time Delay At Trip (Seconds)	Steady State Noise Level (%)
Four Pumps	3	1.03	0.91	0.67
	4		0.63	1.01
One Pump Each Loop	3	1.30	1.08	0.56
	4		0.66	0.80
One Pump	3	2.59	1.98	0.71
	4		0.99	1.01

Note: The " Time Reactor Trip Should Occur " is defined as that time after the pump trip when the unsnubbered reactor coolant flow rate has been reduced to a flux to flow ratio of 1.044.

Note: The " Steady State Noise Level " is defined as the absolute percentage variation in the reactor coolant flow rate at two standard deviations of the mean value.

Note: The acceptance criteria on time delay for a two and four pump trip, and for a one pump trip is less than 1.00 and 1.25 seconds respectively.

Measured Reactor Coolant Flow Rate Following The Trip Of One, Two, And Four Reactor Coolant Pumps From Four Pump Initial Conditions Of 532°F And 2155 Psig

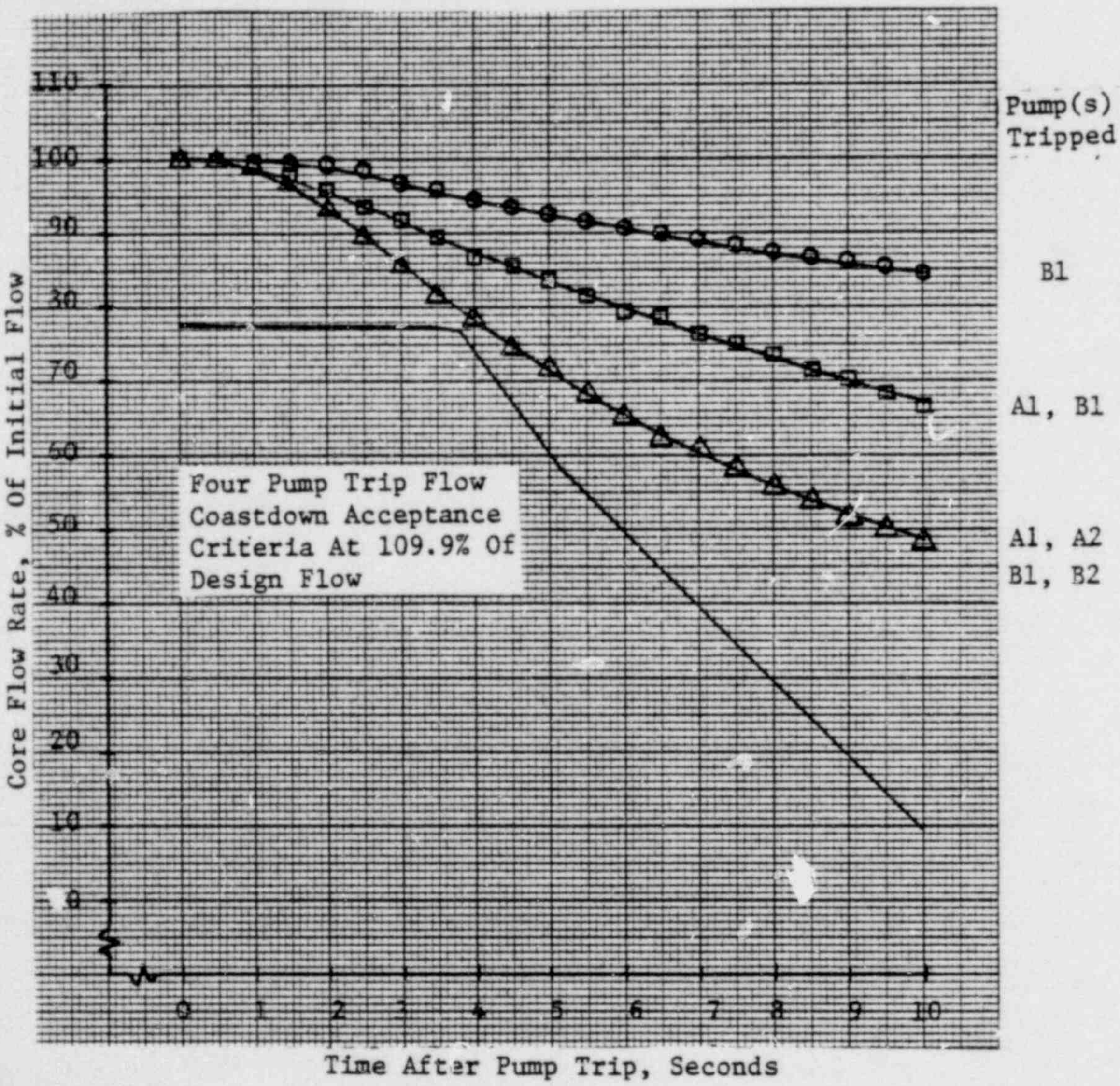

Note: The Measure Flow Coastdown Data Is Taken From Snubber Position (4).

Figure 3.1-1

Measured Time Delay Between Snubbered And Unsnubbered Reactor Coolant Flow Rates Following The Loss Of Four Reactor Coolant Pumps From Four Pump Initial Conditions Of 532°F And 2155 Psig

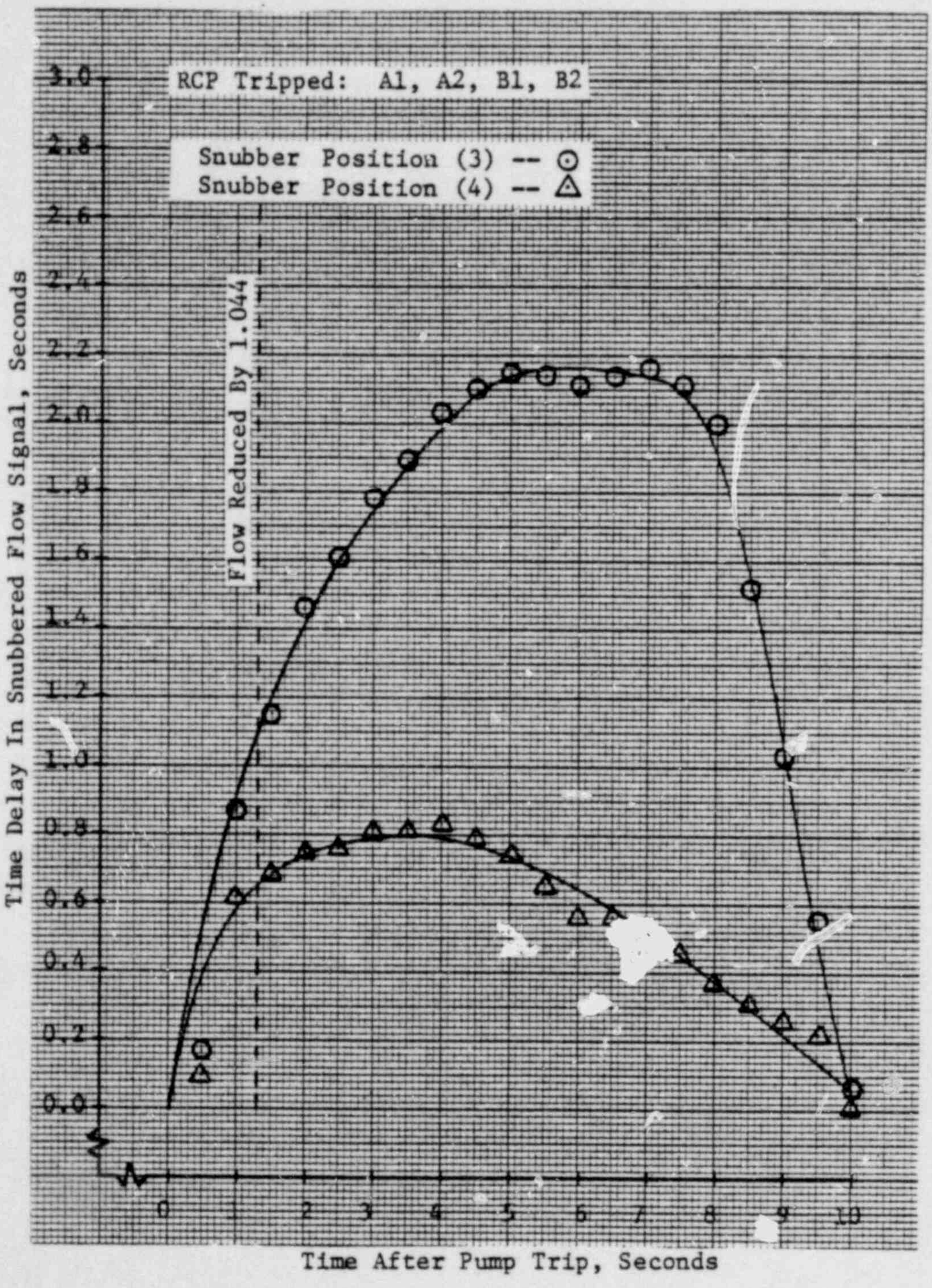

Figure 3.1-2

Measured Time Delay Between Snubbered And Unsnubbered Reactor Coolant Flow Rates Following The Loss Of Two Reactor Coolant Pumps From Four Pump Initial Conditions Of 532°F and 2155 Psig

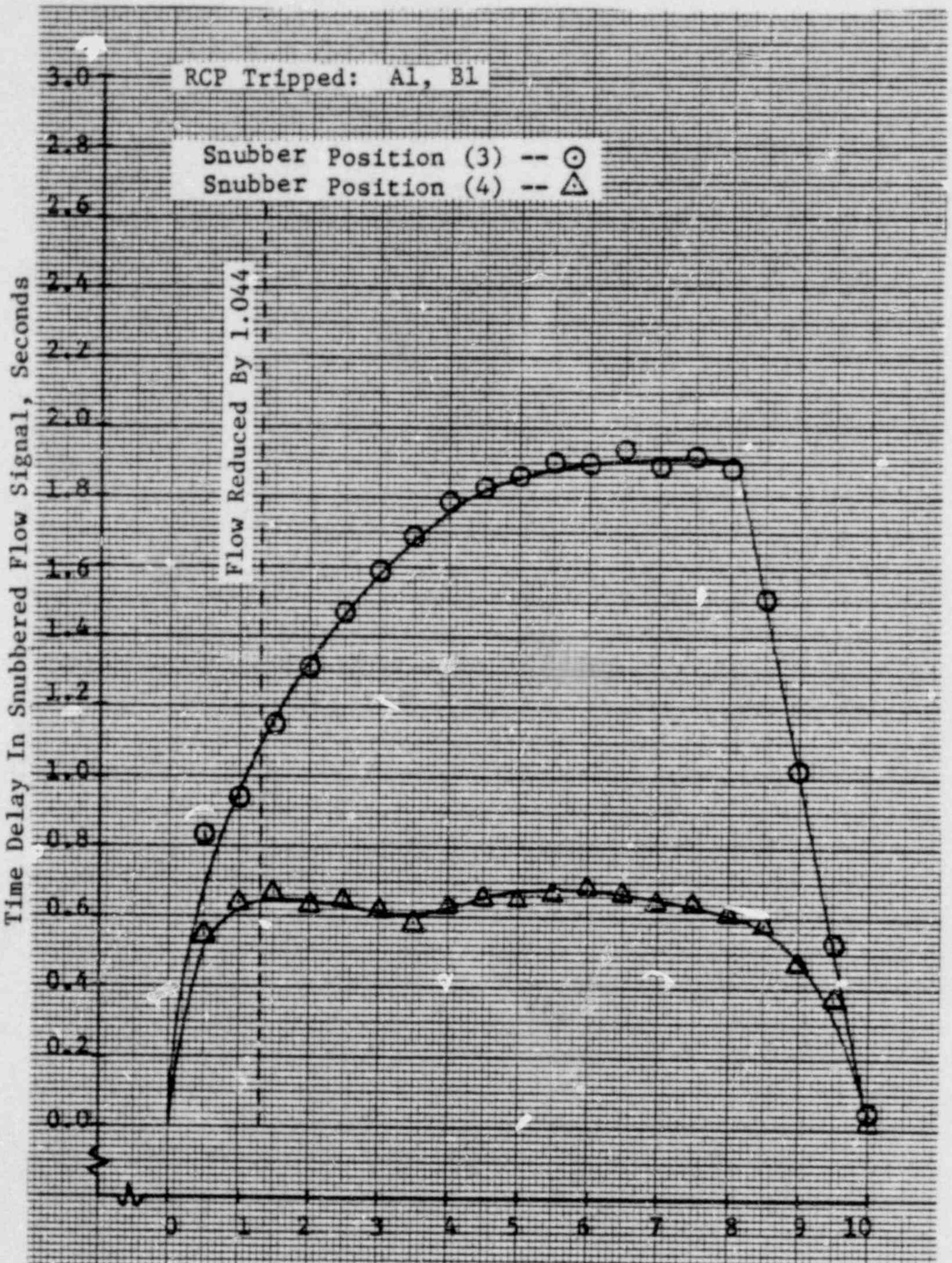

Figure 3.1-3

Measured Time Delay Between Snubbered And Unsnubbered Reactor Coolant Flow Rates Following The Loss Of One Reactor Coolant Pump From Four Pump Initial Conditions Of 532°F And 2155 Psig

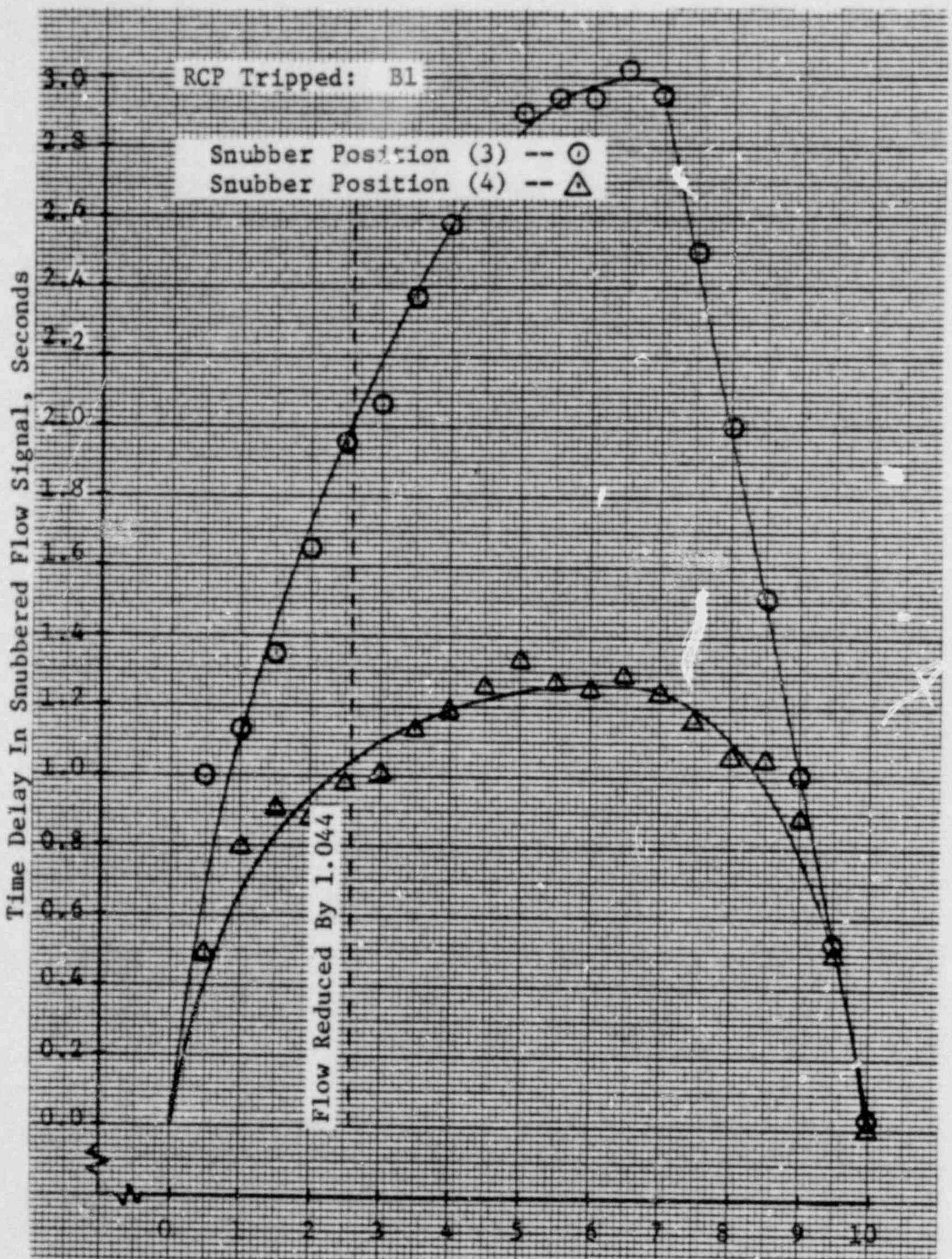

Figure 3.1-4

3.2 CONTROL ROD DRIVE DROP TIME TEST

3.2.1 PURPOSE

The purpose of the Control Rod Drive Drop Time Test was to verify the functional trip capability of the Control Rod Drive System. This was done by fulfilling the following test objectives:

(a) To verify, for each control rod assembly, that the total elapsed drop time from the initiation of the trip signal until the control rod assembly was three-fourths inserted, was less than a predetermined limit at different unit conditions.

(b) To verify the repeatability of the drop time measurement by dropping the fastest and slowest control rod assemblies an additional ten times each.

(c) To verify that the partial length rods (APSR's) cannot be tripped.

Two acceptance criteria are specified for the Control Rod Drive Drop Time Test as listed below:

(1) The individual safety and regulating control rod assembly drop times at zero and full flow, and $\geq$ 525°F is less than 1.400 and 1.660 seconds, respectively.

(2) The partial length control rods (APSR's) do not trip on a trip command.

3.2.2 TEST METHOD

The Control Rod Drive Drop Time Test was performed using strip chart recorders to time the rod drops. Each control rod group was pulled to 100% withdrawn and then dropped into the core using the manual trip pushbutton. A zero time signal was furnished to the test recorders for each control rod assembly from a contact on the manual trip switch. A second signal to indicate three-fourths insertion was furnished to the recorders by a reed switch located on the position indicator tube of each control rod drive. The test was conducted at various combinations of temperature and flow at the following defined test conditions:

Test Condition	Flow	Temperature	Mode
1	No Flow	$\leq$ 280°F	Cold Shutdown
2	One Pump Each Loop	$\leq$ 280°F	Cold Shutdown
3	No Flow	$\geq$ 525°F	Hot Standby
4	Four Pumps	$\geq$ 525°F	Hot Standby

After the drop time measurements on all the groups were completed, the rods with the fastest and slowest trip insertion times at test condition 4 were tripped ten additional times to demonstrate repeatability of the measurement. Measurements were also performed on the Group 8 control rods to verify that they did not drop into the core when power to the control rod drive trip breaker undervoltage coils was interrupted.

3.2.3 EVALUATION OF TEST RESULTS

The results of the rod drop times for the four test conditions stated above are presented in Tables 3.2-1 and 3.2-2. As can be seen, the fastest dropped control rods were H-12, F-14, B-06, M-03 and E-13, and the slowest dropped control rods were C-11, M-09 and H-10 during the performance.

Analysis of the drop times showed that the slowest dropped control rods under zero and full flow conditions yielded drop times of 1.092 and 1.275 seconds respectively, which were well within the acceptance criteria of 1.400 seconds for zero flow and 1.660 seconds for full flow.

Rod H-10 (the slowest) and E-13 (the fastest) at test condition 4 were dropped an additional ten times and produced rod drop times of 1.243 + 0.007/-0.009 and 1.262 + 0.008/-0.013 seconds, respectively.

3.2.4 CONCLUSIONS

The rod drop times were well within the acceptance criteria stated in section 3.1.3.4 of the Technical Specifications, of 1.660 seconds at full flow and greater than 525°F conditions. Also, as would be expected, all drop times under no flow conditions were shorter than under flow conditions.

Table 3.2-1

Control Rod Drive Drop Times For The Fastest And Slowest Control Rod At Each Test Condition

Test Condition	Pumps Running	Mean Drop Time (sec)	Fastest Rod Location	Fastest Rod Time (sec)	Slowest Rod Location	Slowest Rod Time (sec)
1	0	1.099	H-12	1.080	C-11	1.125
2	2	1.167	H-12, F-14, B-06	1.145	C-11	1.195
3	0	1.075	H-12	1.051	M-9	1.092
4	4	1.249	M-3, E-13	1.230	H-10	1.275

Note: The fastest control rod (E-13) and the slowest control rod (H-10) at test condition (4) were dropped an additional ten times. The results are given below:

Fastest control rod time (sec) = 1.243 + 0.007 / -0.009

Slowest control rod time (sec) = 1.262 + 0.008 / -0.013

Note: The mean drop time is the average of all 61 control rod drive drop times. As would be expected, the mean drop time increases with increasing reactor coolant flow.

Table 3.2-2

Summary Of Control Rod Drive Drop Time Measurements Obtained
During The Performance Of Control Rod Drive Drop Time Test

Core Position	Rod Group	Rod Number	Rod Drive Drop Times In Seconds At Test Condition (1)	(2)	(3)	(4)
E9	1	1	1.100	1.180	1.085	1.263
G11	1	2	1.110	1.170	1.078	1.266
K11	1	3	1.098	1.170	1.075	1.249
M9	1	4	1.110	1.180	1.092	1.272
M7	1	5	1.110	1.180	1.080	1.264
K5	1	6	1.120	1.170	1.080	1.256
G5	1	7	1.120	1.150	1.070	1.253
E7	1	8	1.100	1.160	1.078	1.254
F8	2	1	1.095	1.170	1.080	1.265
F10	2	2	1.090	1.175	1.080	1.265
H10	2	3	1.100	1.185	1.080	1.275
L10	2	4	1.110	1.185	1.077	1.257
L8	2	5	1.100	1.180	1.080	1.263
L6	2	6	1.100	1.170	1.081	1.257
H6	2	7	1.090	1.180	1.080	1.270
F6	2	8	1.100	1.180	1.085	1.265
C9	3	1	1.095	1.170	1.082	1.246
G13	3	2	1.100	1.170	1.085	1.245
K13	3	3	1.100	1.170	1.088	1.252
O9	3	4	1.085	1.160	1.078	1.232
O7	3	5	1.100	1.170	1.085	1.246
K3	3	6	1.095	1.180	1.085	1.245
G3	3	7	1.090	1.160	1.077	1.245
C7	3	8	1.095	1.170	1.087	1.246
B8	4	1	1.085	1.170	1.070	1.259
D12	4	2	1.095	1.175	1.072	1.259
H14	4	3	1.100	1.180	1.072	1.262
N12	4	4	1.085	1.165	1.070	1.250
P8	4	5	1.095	1.180	1.082	1.269
N4	4	6	1.090	1.170	1.070	1.250
H2	4	7	1.085	1.170	1.070	1.267
D4	4	8	1.095	1.180	1.071	1.268

Table 3.2-2 (Cont'd)

Summary Of Control Rod Drive Drop Time Measurements Obtained
During The Performance Of Control Rod Drive Drop Time Test

Core Position	Rod Group	Rod Number	Rod Drive Drop Times In Seconds At Test Condition (1)	(2)	(3)	(4)
C11	5	1	1.125	1.195	1.087	1.264
G9	5	2	1.100	1.165	1.063	1.250
E13	5	3	1.105	1.160	1.067	1.230
M13	5	4	1.100	1.165	1.075	1.250
K9	5	5	1.090	1.165	1.068	1.252
O11	5	6	1.100	1.165	1.070	1.243
O5	5	7	1.100	1.160	1.070	1.248
K7	5	8	1.100	1.160	1.057	1.241
M3	5	9	1.085	1.155	1.055	1.230
K3	5	10	1.110	1.170	1.081	1.265
G7	5	11	1.100	1.170	1.073	1.260
C5	5	12	1.100	1.170	1.070	1.258
D8	6	1	1.100	1.150	1.070	1.256
E11	6	2	1.110	1.170	1.078	1.266
H12	6	3	1.080	1.145	1.051	1.232
M11	6	4	1.090	1.160	1.062	1.252
N8	6	5	1.100	1.155	1.070	1.248
M5	6	6	1.090	1.155	1.058	1.254
H4	6	7	1.100	1.170	1.079	1.263
E5	6	8	1.095	1.155	1.069	1.259
H8	7	1	1.100	1.160	1.075	1.255
B10	7	2	1.095	1.150	1.069	1.236
F14	7	3	1.095	1.145	1.069	1.243
L14	7	4	1.100	1.160	1.079	1.244
P10	7	5	1.110	1.155	1.073	1.245
P6	7	6	1.115	1.160	1.085	1.256
L2	7	7	1.110	1.160	1.075	1.252
F2	7	8	1.115	1.155	1.088	1.249
B6	7	9	1.100	1.145	1.062	1.242

3.3 PRESSURIZER TEST

3.3.1 PURPOSE

Pressurizer operational testing was conducted after initial fuel loading and prior to initial criticality. The purpose was to set pressurizer spray and bypass spray flows at prescribed setpoints.

Two acceptance criteria are specified for the pressurizer test as listed below:

(1) The pressurizer spray flow must be set at 190 + 19 / -6 gpm.

(2) The pressurizer bypass spray flow must be set at 1.00 + 2.00 / -0.25 gpm.

3.3.3 TEST METHOD

The technique used to set the pressurizer spray and bypass flows was based upon balancing the heat input to the heat losses from the pressurizer. Initial steady state pressure and temperature conditions were established in the pressurizer without spray or bypass flow. The power input from the pressurizer heaters necessary to maintain steady state conditions was recorded. The additional heat input required to balance spray and bypass flow was then calculated using Equation 3.3-1.

$$F = \frac{K\ V_{fs}\ (Q - Q_o)}{H_{fp} - H_{fs}} \qquad \text{EQ. (3.3-1)}$$

Where:
- F = Spray Or Bypass Spray Flow, gpm
- K = Conversion Constant, 425.36 gpm BTU/Ft^3 kW
- V_{fs} = Specific Volume Of Spray Water, Ft^3/lbm
- Q = Heater Input With Spray Flow, kW
- Q_o = Heater Input Without Spray Flow, kW
- H_{fp} = Enthalpy Of Pressurizer Water, BTU/lbm
- H_{fs} = Enthalpy Of Spray Water, BTU/lbm

Heat input to the pressurizer from the heaters was then increased by the amount calculated. The bypass and spray valve flows were increased to balance the additional heat input and maintain the pressurizer temperature and pressure at their initial values. An initial nominal pressure of 1300 psig was chosen for the spray flow measurement to ensure adequate heater capacity to overcome the 190 gpm spray flow and maintain steady state conditions.

3.3.3 EVALUATION OF TEST RESULTS

The measured results from setting the pressurizer spray and spray valve bypass flows are listed in Table 3.3-1. The bypass and spray flows were set at 1.56 gpm and 190.15 gpm, respectively. The measured pressurizer heat loss was in excess of 169 kW at system conditions of 532^{o}F and 2155 psig.

3.3.4 CONCLUSIONS

The pressurizer spray flow was set within the acceptance criteria limit of 190 + 19 / -6 gpm. The pressurizer spray bypass flow was set within the acceptance criteria limit of 1.00 + 2.00 / -0.25 gpm.

Table 3.3-1

Measured Results For Determination Of Pressurizer Spray And Bypass Spray Flows

RCS COOLANT TEMPERATURE (DEG F)	RCS COOLANT PRESSURE (PSIG)	PRESSURIZER TEMPERATURE (DEG F)	HEATER POWER (KW)	CONVECTIVE LOSSES (KW)	SPRAY FLOW (GPM)	ACCEPTANCE CRITERIA (GPM)	VALVE POSITION (TURNS)
A. Pressurizer Bypass Flow Measurement, RCV-149							
534.0	2145.0	647.0	198.6	169.6	1.56	1.00 +2.00/-0.25	1/8
B. Pressurizer Spray Flow Measurement (With Bypass Flow), RCV-14F							
533.0	1303.0	580.0	1503.1	195.6	190.15	190 +19/-6	1/4

3.4 ZERO POWER PHYSICS TEST

Zero power physics testing on Crystal River Unit 3 commenced with initial criticality on January 14, 1977. Part way through the testing, the FPC grid electrical system was impacted by a severe cold spell. The license was at that time restricted to 5.0% full power. The decision was therefore made to interrupt testing to save the approximately 30 MWe required to run the reactor coolant pumps and other plant equipment. Testing was finally concluded after the aforementioned eight day delay on January 29, 1977. The program which was intended to verify the nuclear design parameters of the core prior to escalation into the power range was performed at 532°F and 2155 Psig.

Each section of the report addresses a specific test which was conducted during the zero power physics testing program. The analyzed results are presented and comparisons made to predicted values and Technical Specification limits. The specific sections include the following:

Initial criticality
Nuclear instrumentation overlap
Sensible heat determination
Reactivity calculations
"ALL RODS OUT" critical boron concentration
Control rod group worths
Soluble poison worths
Ejected control rod worth
Stuck control rod worth
Shutdown margin determination
Temperature coefficient of reactivity
Temperature normalization constant

3.4.1 PURPOSE

The Zero Power Physics Test was performed to verify the nuclear design parameters used in the safety analysis, the Technical Specification limits, and the operational parameters. The purpose of the test was to direct testing at the 532°F and 2155 Psig plateau and included the following:

(a) To direct the initial approach to criticality

(b) To measure selected reactor physics parameters at zero power following initial fuel loading and before escalation into the power range.

(c) To verify that source and intermediate range nuclear instrumentation have sufficient overlap.

(d) To determine the reactor coolant system temperature normalization constant.

Four acceptance criteria are specified for the Zero Power Physics Test as listed below:

(1) Measured values when compared to the predicted values shall agree within the tolerance bands given in Table 3.4-1.

(2) Shutdown margin with the measured worst case stuck rod fully withdrawn shall be more negative than -1.00% $\Delta k/k$.

(3) Measured worst case ejected rod shall not be in excess of +1.00% $\Delta k/k$.

(4) Moderator coefficient shall be less positive than $+0.90 \times 10^{-4} \Delta k/k/^{\circ}F$.

3.4.2 TEST METHOD

Initial criticality was achieved by control rod group withdrawal and boron dilution of the reactor coolant system after the system had been heated up to hot conditions using the reactor coolant pumps. During the initial approach to criticality, plots of inverse multiplication versus boron concentration, rod group position, demineralized water added, and time were maintained by using the source range nuclear instrumentation channels NI-1 and NI-2. After each rod group withdrawal and at every 30 minutes during deboration, the plots were updated and criticality was predicted. After reaching criticality, the nuclear power was increased and the source and intermediate range nuclear instrumentation overlap was verified to be in excess of one decade. During the same increase in power, the point of sensible heat was determined and the current range under which Zero Power Physics Test would be conducted was established. Upon completion of this test, steady state conditions were obtained and the reactor coolant and hot leg temperatures were normalized to indicate a core ΔT of zero.

Measurement of the following physics parameters at 532°F and 2155 Psig was then begun:

(a) "All rods out" boron concentration

(b) Temperature coefficient of reacitivity at three boron concentrations.

(c) Differential and integral rod worth of Groups 8, 7, 6, 5, 4 and part of Group 3 by boron swap.

(d) Total rod worth of part of Group 3 and Groups 2 and 1 by rod drop techniques.

(e) Differential boron worth over large boron changes.

(f) Stuck rod worth by static rod swap techniques.

(g) Determination of the minimum shutdown margin.

(h) Ejected rod worth by static rod swap techniques.

Measurements of reactivity during this test were accomplished by the Babcock & Wilcox Reactimeter which utilizes periodic neutron flux sampling from an intermediate range nuclear instrumentation channel to calculate reactivity. In the case of the Reactimeter, the neutron flux is sampled every 0.2 seconds and the reactivity result is updated after each sample. The Reactimeter can also sample as often as once every 0.2 seconds, the analog or digital signals representing reactor and unit parameters other than neutron flux. This data logging capability was used extensively throughout the test program.

3.4.3 EVALUATION OF TEST RESULTS

3.4.3.1 INITIAL CRITICALITY

Initial criticality was achieved on January 14, 1977 at 0845 hours at reactor coolant conditions of 532°F, 2155 Psig, and 1394 ppmB. Control rod groups 1 through 4 had previously been withdrawn as part of the heatup procedure with reactor coolant boron concentration at 1777 ppmB. The approach to critical began by withdrawing control rod groups 8, 5, and 6 to 100% and group 7 to 75% withdrawn. The reactor coolant system was then deborated until the measured boron concentration fell 50 ppmB below the original predicted value of 1521 ppmB. After an evaluation was made, deboration continued until initial criticality was achieved.

Throughout the approach to criticality, inverse multiplication curves versus time, reactor coolant system boron concentration, and quantity of demineralized water added were maintained for the source range detectors by two independent persons. At the end of each control rod group withdrawal and every 30 minutes during the deboration cycle, the count rate was taken from each source range detector by way of the scaler-counters. The ratio of the initial average count rate to the count rate at the end of each reactivity addition was plotted.

The approach used to obtain initial criticality is outlined below in three basic steps.

(1) Control rod group withdrawal:

Groups 1 - 4 already at 100% withdrawn		
Group	8	100% withdrawn
Group	5	100% withdrawn
Group	6	100% withdrawn
Group	7	75% withdrawn

(2) Deboration from 1777 ppmB at a letdown and makeup flow of 70 gpm until the plot of boron concentration versus time indicated a reactor coolant system boron concentration of 1471 ppmB. At that time demineralized water addition was suspended; the reactor coolant system and makeup tank were allowed to come to equilibrium (i.e. approximately 1440 ppmB); and and evaluation was made:

(a) A lab standard was used to insure that the measured boron concentrations were valid.

(b) Rod position indication was checked to verify that all control rods were fully withdrawn except Group 7.

(c) The 1/M plots were checked for consistency and reasonability. Criticality projections indicated that an additional 30-50 ppm boron reduction was required to reach criticality.

(d) Possible error in the predicted critical boron concentration was speculated. This value was later found to be in error and officially revised to 1434 ppmB.

(e) Agreement between Babcock and Wilcox and Florida Power Corporation to continue deboration was obtained after each reviewed the above results.

(3) Deboration from the above condition to criticality at a makeup and letdown rate of 40 gpm. Control Rod Group 7 inserted to maintain criticality as required. Throughout both deboration steps a plot of reactor coolant system boron concentration versus time was maintained as shown in Figure 3.4-1.

The above procedure was followed, with initial criticality occurring at a reactor coolant system boron concentration of 1394 ppmB. The plots of inverse multiplication versus time, reactor coolant boron concentration, reactivity, removed, demineralized water added are shown in Figures 3.4-2, 3.4-3 and 3.4-4 a & b, respectively, and utilize the data from each of the source range channels. From these plots, the excellent response of the source range detector to subcritical multiplication can be seen.

In summary, initial criticality was obtained in an orderly manner. Analysis of the measured critical boron concentration of 1394 ppmB and the revised predicted value of 1434 ppmB indicated favorable agreement with the difference ascribed to a slightly larger measured differential boron worth at 532°F and 2155 Psig than predicted.

3.4.3.2 NUCLEAR INSTRUMENTATION OVERLAP

Technical Specifications state that prior to operation in the intermediate nuclear instrumentation range, at least a one decade overlap between the source range and intermediate range must be observed. This means that before the source range count rate equals 10^5cps the intermediate range must be on scale. If the one decade is not observed, the approach to the intermediate range cannot be continued until the situation has been corrected.

To satisfy the above overlap requirements after initial criticality was reached, core power was slowly increased until the intermediate range channels came on scale. Detector signal response was thus recorded for both the intermediate and source range channel. This was repeated for another decade to assist in determining the number of decades of overlap.

The results of the Nuclear Instrumentation overlap at 532°F and 2155 Psig have been tabulated in Table 3.4-2 and plotted in Figure 3.4-5. Examination of Table 3.4-2 shows that the overlap between the source and intermediate range is constant at an average value of 2.21 decades which is well above the minimum of one decade overlap stated in Technical Specifications. Examination of Figure 3.4-5 shows that the linearity, overlap, and absolute output of both the intermediate and source range detectors are within specifications and performing satisfactorily.

3.4.3.3 SENSIBLE HEAT DETERMINATION

Determination of the intermediate range current level at which the production of sensible nuclear heat occurs is important to the Zero Power Physics Test program in that it establishes the upper power level limit. Thus by restricting reactor power operation to a level reduced by a factor of three below the sensible heat level, the effects of temperature feedback are eliminated in the measurement of physics parameters.

The test method was to increase the intermediate range current level in one third decade increments until the detection of sensible heat. Since turbine bypass valves and pressurizer levels were maintained constant, heat production in the core was observed by change in the core outlet temperature and makeup tank level. To ensure that the changes observed were caused by the core power production, the heatup rate was plotted versus intermediate range current level. The point at which there was a definite heatup rate was 6.75×10^{-8} amps. Therefore, during the test 6.75×10^{-8} amps on channel NI-3 was defined as the "sensible heat" point. From this the upper zero power physics test current limit was established at 2.25×10^{-8} amps.

After setting the upper zero power physics test current limit, temperature feedback measurements were performed to verify that the above limit was adequate. This was done by adding a +20 pcm over a current range of 1.5×10^{-8} to 3.0×10^{-8} amps and verifying that it remained constant. The results indicated that no temperature feedback effects were present over the current range indicated.

An additional part of the measurement was to ensure that all power range channels were indicating between 1.0 to 2.0 percent full power at the point of sensible heat. This was done to ensure that the overpower trip protection was adequate. At the point of sensible heat, the indication on NI-5, NI-6, NI-7 and NI-8 were 1.3, 1.2, 1.2 and 0.8 percent full power. Thus, all power range channels except NI-8 were within their recommended tolerances. Since all channels were set near their maximum sensitivity no change in the calibration of this channel was performed.

During evaluation of test results, additional evaluation was performed. Figure 3.4-6 shows these results. There was a very small heatup rate at relatively low powers. Using this curve it is possible to establish a relationship between current and power. Thus, 5.4×10^{-8} amps is about 1 MWt and the 2.25×10^{-8} amps used as the upper limit is 0.4 MWt.

3.4.3.4 REACTIVITY CALCULATIONS

Reactimeter is the name given to the Babcock and Wilcox reactivity meter which solves the one-dimensional, inverse kinetics equation with six delayed neutron groups for core net reactivity based upon periodic samples of neutron flux. In addition to reactivity and neutron flux, the Reactimeter can also record 23 other analog and digital signals from the plant.

After initial criticality and prior to the first physics measurement, an on-line functional check of the reactimeter was performed to verify its readiness for use in the test program. After steady state conditions with a constant neutron flux were established, a small amount of negative reactivity was inserted in the core by inserting control rod group 7. Stop watches were used to measure the doubling time of the neutron flux and the reactivity inserted was determined from period-reactivity curves. The measurement was repeated for several values of reactivity inserted by rod group 7, from $\pm$ 0.025 to $\pm$ 0.075% $\Delta k/k$. The reactivities determined from doubling time measurements were then compared with the reactivities calculated by the reactimeter.

The results of the reactimeter verification measurements are summarized in Table 3.4-4. In each case except for the -0.075%$\Delta k/k$ reactivity insertion , the reactivity calculated by the reactimeter was within the acceptance criteria limit of $\pm$ 5% of the reactivity determined from doubling times. Since the reactimeter checkout did not meet the acceptance criteria at -0.075% $\Delta k/k$, reactivity additions were limited to $\pm$ 0.050% $\Delta k/k$ for all measurements except rod drops during the remainder of the test program.

3.4.3.5 "ALL RODS OUT" CRITICAL BORON CONCENTRATION

The "all rods out" critical boron concentration was measured at one isothermal temperature test plateau of 532°F. The measurements actually were made with rod group 7 partially inserted, but the measured boron concentration was adjusted to the all rods out condition using the results of rod worth measurement to determine the reactivity worth, in terms of ppm boron, of the inserted control rods.

The results are tabulated in Table 3.4-3. These results show that the measured boron concentration was within the revised acceptance criteria of 1445 +/- 100 ppmB.

3.4.3.6 CONTROL ROD GROUP WORTHS

The layout of the core according to the standard alpha-numeric mesh showing the initial location of the control rod groups and the location of the 52 incore detector strings is given in Figure 3.4-7. The number of rods in each group and the reactivity control function of each group is listed below.

Rod Group No.	No. of Rods	Control Function
1	8	Safety
2	8	Safety
3	8	Safety
4	8	Safety
5	12	Power Doppler
6	8	Power Doppler
7	9	Transient
8	8	Axial Power Shaping
	69	

Predicted beginning of life control rod group reactivity worths for the normal withdrawal sequence were supplied at two unit conditions of 532°F and 2155 Psig and 579°F and 2155 Psig, and at two APSR positions of 35 and 100 percent withdrawn. These predictions were made using the PDQ-7 code with either a two or three dimensional model of the core. Measurements of the beginning of life control rod group reactivity worth for the normal withdrawal sequence were determined during zero power physics testing at unit condition of 532°F and 2155 Psig, with APSR's at 35 percent withdrawn, using the boron swap and rod drop method. The boron swap method was used to determine the integral and differential worth for groups 8, 7, 6, 5, 4 and part of group 3. This method consisted of setting up a deboration rate and compensating for the change in reactivity by small step changes in rod group positions. The calculation of reactivity on a continuous basis is made by the Reactimeter. The output of reactivity in terms of percent milli k (PCM) is recorded on a strip chart and also on a magnetic tape by the Reactimeter.

The rod-drop method was used to determine the worth of the control rod groups not measured by boron swap. For this measurement, the reactor was adjusted to a critical state with all of the control rod groups to be measured out of the core and at a power level near the Zero Power Physics Test upper current limit. The control rod groups were then simultaneously dropped into the core and the neutron flux and resulting reactivity recorded by the Reactimeter every 0.2 seconds. An uncorrected value for the reactivity introduced by the rod drop was obtained by averaging reading between 20 and 52 seconds after the drop. The corrected reactivity worth was then obtained by multiplying by a correction factor (1.28) to account for the change in the spatial flux shape during the rod drop. The correction factor was determined by plotting measured rod drop reactivity worth versus inserted group worth as measured by the boron swap method. The results of this analysis are shown in Figure 3.4-14.

The results of both the predicted rod group worths and the measured group worths are tabulated in Table 3.4-5 for a moderator temperature and pressure of 532°F 2155 Psig respectively. The total worth of groups 1, 2 and 43% of group 3 was measured by the rod drop method. The sum of groups 1 and 2 worths was then determined by subtracting the group 3 partial worth based on extrapolation of the boron-swap data. Finally, the individual worths of these groups were established by assuming that the percentage deviation between the measured and predicted value was identical on both groups (i.e. groups 1 and 2). The results are presented in Table 3.4-6. Comparison between measured and predicted rod worth shows groups 5-8 agreed within -3.1 percent and groups 1-4 agreed within -28.3 percent. The general acceptance for rod worths calls for analysis and resolution of measurements more than 20% different from predictions. Groups 1-4 did not meet this acceptance criteria. However, when the low worth of those groups is combined with the low stuck rod worth (3.4.3.9) an acceptable shutdown margin exists. Also presented in Table 3.4-6 are the expected control rod group worths at 579°F and 2155 Psig with the APSR's at 35% wd. These values were obtained by applying the percent deviation between the measured and predicted worths at 532°F to the predicted worths at 579°F.

The results of the measured and normalized differential rod worth shapes for control rod groups (3-4) and (5-7) at 532°F and 2155 Psig are plotted for group (8) at 35% wd in Figures 3.4-8 and 2.4-9, respectively. As can be seen the transient, power doppler and safety groups all had similar shapes. The normalized differential rod worth shape for control rod group (8) was also measured and is shown in Figure 3.4-10. Normalized integral rod worth shapes were then developed by integrating the above differential shapes and are presented in Figures 3.4-11 through 3.4-13.

3.4.3.7 SOLUBLE POISON WORTHS

Soluble poison in the form of dissolved boric acid is added to the moderator to provide additional reactivity control beyond that available from the control rods. The primary function of the soluble poison control system is to control the excess reactivity of the fuel throughout each core life cycle.

The reactivity worth of the boric acid in terms of ppm boron was predicted by using both the one-dimensional LIFET Code and the multi-dimensional PDQ-7 Code as developed or modified by Babcock & Wilcox. The predictions were at three moderator temperature and pressure conditions of 300°F and 800 Psig, 532°F and 2155 Psig, and 579°F and 2155 Psig.

Measurement of the soluble poison differential worth has been completed at 532°F and 2155 Psig. The measured value was determined by summing the incremental reactivity values measured during the rod worth measurements over a known boron concentration range from 1403 to 916 ppmB.

The result of the differential soluble poison worth measurement is tabulated in Table 3.4-7 and plotted in Figure 3.4-15 against the predicted value. This measured value along with various reactivity balance calculations performed during the test program were then used to establish the integral boron reactivity worth curve shown in Figure 3.4-16.

In summary, the measured differential boron worth at zero power was within 5.3 percent of the predicted worth which is within the acceptance criteria of $\pm$ 10 percent.

3.4.3.8 EJECTED CONTROL ROD WORTH

Pseudo ejected control rod reactivity worth was measured at hot, zero power conditions of 532°F, and 2155 Psig for control rod 7-8. The purpose of this measurement was to verify the safety analysis calculations relating to the assumed accidental ejection of the most reactive control rod which is fully inserted in the core during normal power operation. The acceptance criterion for the ejected control rod test is that the reactivity worth of the most reactive control rod does not exceed 1.0%Δk/k at hot zero power conditions. Since the ejected control rod worth increases as more rods are inserted into the core, the measurement was performed at the minimum allowable rod position of 45% wd on group 5 as specified by Technical Specifications.

The ejected worth of control rod 7-8 was measured by the rod swap method. The test method was to initially position Group 5 to between 45 to 55 percent withdrawn with the ejected control rod 100% withdrawn. Then the ejected rod and control rod groups 5 and 6 were swapped until the ejected rod was 0% withdrawn. The change in Groups 5 and 6 positions was then converted to reactivity by using a previously generated rod worth to curve to determine the measured ejected rod worth.

Since the measured rod position did not precisely equal group 5 at 45% withdrawn, the measured ejected rod worth was adjusted to the Technical Specifications position by adding 0.02%Δk/k as determined using the equation below:

Where: $\rho(ER) = F \times \rho(R) + \rho(M)$ EQ. (3.4-1)

$\rho(ER)$ = The measured ejected rod worth at the maximum allowable inserted group worth.

F = Empirically derived constant of 0.45 which relates ejected rod worth and total inserted group worth.

$\rho(R)$ = The initial worth of Group 5 minus the worth of Group 5 at 45% wd.

$\rho(M)$ = The measured worth of the ejected rod which corresponds to the worth changes in Groups 5 and 6.

To ensure that the above ejected rod worth was conservative, it was multiplied by an uncertainty factor of 1.05. The results of the above analysis is given in Table 3.4-8.

The predicted and measured ejected control rod reactivity worth at the Technical Specifications rod position of 45% wd on group 5 (i.e. inserted group worth of -2.95%Δk/k) are tabulated in Figure 3.4-17 which also gives the core location of the ejected control rod relative to the out-of-core intermediate range detectors. The measured and worst case ejected control rod worth were determined to be 0.44 and 0.46%Δk/k, respectively.

3.4.3.9 STUCK CONTROL ROD WORTH

The control rod calculated to have the highest withdrawn worth with all other groups fully inserted is rod 4-3 in core location H-14, or those symmetric to it. On Crystal River Unit 3, a stuck rod worth of +4.00%Δk/k was predicted with the APSR's at 35% withdrawn.

The stuck control rod worth was measured during the Zero Power Physics Test program using the rod swap method. In this method the stuck rod was swapped out of the core with control rods and boron until a critical state was achieved with the stuck rod fully withdrawn, the APSR's at 35% wd and the remainder of the control rod groups fully inserted. The stuck rod was then driven into the core and the reactor retaken critical using the normal withdrawal sequence holding reactor coolant system boron constant. The amount of reactivity removed by the control rods to regain criticality is equal to the stuck rod worth. The worth of the control rod groups withdrawn from the core was then determined by the rod drop method.

The result of the stuck rod worth measurement is presented in Table 3.4-9. The measured worth of the stuck rod was determined to be 2.34%Δk/k, which establishes a worst case stuck rod worth of 2.57%Δk/k (i.e., measured value increased 10.0 percent as required by procedure for conservatism). Comparison of the predicted and measured stuck control rod reactivity worths are tabulated in Figure 3.4-18 which also gives the core location of the stuck control rod relative to the out-of-core intermediate range detectors. The large difference between the predicted and measured worth is attributed to the difficulty in PDQ-7 to predict individual rod worths in heavily rodded cores.

The measured stuck rod worth is below the acceptance criteria of ± 30 percent of the predicted value. However, this is in the conservative direction.

3.4.3.10 SHUTDOWN MARGIN DETERMINATION

Shutdown margin is defined as the instantaneous amount of reactivity by which the reactor is or would be subcritical from its present condition assuming:

(1) The worst case stuck rod is fully withdrawn

(2) No change in APSR position

(3) All control rod groups (safety and regulating) are fully inserted

Technical Specification section 3.1.1.1 states that the shutdown margin shall not be less than -1.00%Δk/k during all modes of Unit Operation after fuel is loaded in the core. The predicted minimum shutdown margin during unit criticality at beginning of life conditions is projected to occur at 532°F and 2155 Psig with a control rod position of group 5 at 45% withdrawn.

Upon determination of the necessary core physics parameters, as measured at 532°F and 2155 Psig during the Zero Power Physics Test, a calculation to determine the minimum shutdown margin was performed at the condition specified above as shown in Table 3.4-10. The results using the method called out in the test procedure indicate that a conservative minimum shutdown margin of -2.93%Δk/k was present which adequately satisfies the acceptance criteria of -1.00%Δk/k.

A review of the test results by Babcock and Wilcox revealed that the procedure applied an uncertainty to the stuck rod worth in two different steps of the procedure. Elimination of this double uncertainty yields a minimum shutdown margin of -3.39%Δk/k.

3.4.3.11 TEMPERATURE COEFFICIENTS OF REACTIVITY

The temperature coefficient of reactivity is defined as the fractional change in the excess reactivity of the core per unit change in core temperature. The temperature coefficient is normally divided into two components as shown in Equation (3.4-2).

$$\alpha T = \alpha M + \alpha D \qquad \text{EQ. (3.4-2)}$$

Where: αT = Temperatue Coefficient of Reactivity

αM = Moderator Coefficient of Reactivity

αD = Doppler Coefficient of Reactivity

The technique used to measure the 532°F and 2155 Psig isothermal temperature coefficient at zero power was to first establish steady state conditions by maintaining reactor flux, reactor coolant pressure, turbine header pressure and core average temperature constant, with the reactor critical at approximately 1×10^{-8} amps if a negative feedback effect was expected from a temperature decrease or at approximately 1×10^{-9} amps if a positive feedback effect was expected. Equilibrium boron concentration was established in the reactor coolant system, make-up tank and pressurizer to eliminate reactivity effects due to boron changes during the subsequent temperature swings. The reactimeter and the brush recorders were connected to monitor selected core parameters with the reactivity value calculated by the reactimeter and the core average temperature displayed on a two channel recorder.

Once steady state conditions were established, a negative heatup rate was started by opening the turbine bypass valves. As the reactivity changed about ± 40 PCM, control rods were moved in step changes to keep the reactivity values on scale and also to keep core power in the range necessary to produce an adequate intermediate range signal. After the core average temperature decreased by about 5°F coolant temperature and reactivity were stabilized. This process was then reversed except that the core average temperature was increased by about 10°F. After stabilizing coolant temperature and reactivity, the core average temperature was then returned to its original value. The measurement of the temperature coefficient from the data obtained was then performed by dividing the change in reactivity by the corresponding changes in core temperature over a specific time period.

Isothermal temperature coefficient measurements were conducted at three different reactor coolant boron concentrations during the Zero Power Physics test program. The results of the measurements are summarized in Table 3.4-11 along with the predicted values which are included for comparison. In all cases the measured results compared favorably with the predicted values. All measured temperature coefficients of reactivity were within the acceptance criteria of $\pm$ 0.40 X 10^{-4} $\Delta k/k/^{o}F$ of the predicted value.

The moderator coefficient cannot be directly measured in an operating reactor because a change in moderator temperature causes a similar change in the fuel temperature. However, since the moderator coefficient has safety implications, it is an important reactivity coefficient. As specified in Technical Specifictions the moderator temperature coefficient shall not be positive at power levels above 95 percent full power and shall be less than +0.9 X $10^{-4}\Delta k/k/^{o}F$ at all other power levels. To obtain the moderator coefficient from the measured temperature coefficient, a Doppler correction of 0.6 X $10^{-4}\Delta k/k/^{o}F$ must be added. Determination of the moderator coefficient has been completed and shows that this coefficient is well within the limits stated above.

In conclusion, all temperature coefficients of reactivity that were measured at the 532°F and 2155 Psig plateau were within the acceptance criteria of $\pm$ 0.40 X $10^{-4}\Delta k/k/^{o}F$ of the predicted value. In addition, calculation of the moderator coefficient indicates that it is well within the requirements of the Technical Specification 3.1.1.3.

3.4.3.12 TEMPERATURE NORMALIZATION CONSTANTS

Isothermal temperature normalization constants on the reactor coolant system cold and hot leg were determined as part of the Zero Power Physics test program. The intent of this measurement is to normalize the ΔT across the core to zero and to verify that these temperature indications are reasonable. The importance for normalization lies in the fact that the ΔT across the core is directly related to core thermal power. Thus, if normalization is performed, this quantity can be used during power operation for power level determination.

Measurements of the normalization constants for the cold and hot leg RTD temperature indication on the primary system were performed at 532°F and 2155 Psig, and are reported in Table 3.4-12. In all cases only minor corrections were necessary with the maximum deviation from the average of all RTD readings of -2.2°F.

3.4.4 CONCLUSION

Zero Power Physics Test commenced with initial criticality on January 14, 1977 and continued 5 days until a severe electrical shortage due to cold weather caused it to be interrupted. Testing resumed on January 27, 1977 and was successfully completed on January 29, 1977. The program which was intended to verify the nuclear design parameters of the core prior to escalation into the power range was performed at 532°F and 2155 Psig. The Zero Power Physics Test was conducted with good agreement between measured and predicted results on all physics parameters except the reactivity worths of groups (1-4) and the stuck rod. A summary of each of the measurements performed during the Zero Power Physics Test is given in Table 3.4-13.

Table 3.4-1

Acceptance Criteria Deviation Limits Between Measured And Predicted Values

	Core Physics Parameters	Allowable Deviation Between Predicted And Measured Values
A.	Control Rod Worths	
	Group Worths (1 - 8)	$\pm$ 20%
	Total Worth (1 - 8)	$\pm$ 15%
	Ejected Rod Worth	$\pm$ 30%
	Stuck Rod Worth	$\pm$ 30%
B.	Temperature Coefficients	$\pm 0.4 \times 10^{-4}\ \Delta k/k/{}^{o}F$
C.	Differential Boron Worth	$\pm$ 10%
D.	All Rods Out Boron Concentration	$\pm$ 100 ppmB

Table 3.4-2

Summary Of Nuclear Instrumentation Overlap Measurements During Zero Power Physics Test

Data Set	Source Range Indication		Intermediate Range Indication		Average SR Indication (CPS)	Average IR Indication (AMPS)	Overlap (Decades)
	NI-1 (CPS)	NI-2 (CPS)	NI-3 (AMPS)	NI-4 (AMPS)			
01	8.0×10^{3}	8.0×10^{3}	1.1×10^{-11}	1.3×10^{-11}	8.0×10^{3}	1.2×10^{-11}	2.18
02	8.0×10^{4}	8.0×10^{4}	1.2×10^{-10}	1.5×10^{-10}	8.0×10^{4}	1.4×10^{-10}	2.23
						Average =	2.21

Note(1): Overlap is obtained between the Source and Intermediate Range by using the average indications in the equation below.

$$\text{Overlap} = (6 - \text{Log SR}) + (\text{Log IR} + 11)$$

Table 3.4-3

All Rods Out Critical Boron Concentration (PPM Boron)

Moderator Temperature	Predicted Results	Measured Results
532^{o}F	1445	1403 (1)

Note (1): This number is based on the as measured boron concentration with a 2 ppmB correction to account for the fact the rods were not quite at 100% withdrawn.

Table 3.4-4

Comparison Of Reactimeter And Doubling Time (DT) Reactivity Measurements

Case No.	DT (Sec)	DT Converted Reactivity (% Δk/k)	Reactimeter Reactivity (% Δk/k)	Absolute Error (%)
1	228.0	-0.029	-0.028	3.6
2	219.4	+0.024	+0.025	4.0
3	147.7	-0.047	-0.046	2.2
4	96.3	+0.049	+0.047	4.3
5	102.7	-0.078	-0.073	6.9
6	50.3	+0.082	+0.079	3.8

NOTE: The Absolute Error Between DT Converted Reactivity And Reactimeter Reactivity Is Defined By The Equation Below:

$$E\ (\%) = 100\ (\rho R - \rho DT)\ /\ (\rho R)$$

NOTE: Since The Reactimeter Checkout Failed To Meet The Acceptance Criteria At -0.078 % Δk/k, Reactivity Additions And Insertion Were Limited To $\pm$ 0.050 % Δk/k for all measurements except rod drops during the remainder of the test program.

Table 3.4-5

Comparison Of Predicted And Measured Control Rod Group Reactivity Worth

A. Moderator Temperature at 532°F, APSR's at 35% Withdrawn

Rod Group	Number Of Rods	Predicted Worth (%Δk/k)	Measured Worth (%Δk/k)	Percent Deviation (%) (1)
1	8	-1.05	-0.80	-31.8
2	8	-3.20	-2.43	-31.8
3	8	-0.75	-0.59	-27.1
4	8	-1.75	-1.43	-22.4
5	12	-1.16	-1.14	-1.8
6	8	-1.27	-1.21	-5.0
7	9	-1.17	-1.11	-5.4
8	8	-0.36	-0.36	-0.0
Total	69	-10.71	-9.07	-18.3

B. Moderator Temperature at 579°F, APSR's at 35% Withdrawn

Rod Group	Number of Rods	Predicted Worth (%Δk/k)	Estimated Worth (%Δk/k) (2)	Percent Deviation (%) (1)
1	8	-1.38	-1.05	-31.8
2	8	-3.69	-2.80	-31.8
3	8	-0.77	-0.61	-27.1
4	8	-1.55	-1.27	-22.4
5	12	-1.47	-1.44	-1.8
6	8	-1.43	-1.36	-5.0
7	9	-1.13	-1.07	-5.4
8	8	-0.42	-0.42	0.0
Total	69	-11.84	-10.02	-18.3

NOTE (1): Percent deviation is determined assuming that the measured values are correct.

NOTE (2): Estimated worth is determined by applying the percent deviations between predicated to measured results at 532°F to the predicted results at 579°F.

Table 3.4-6

Determination Of The Remaining Worth Of The Safety Groups Not Measured By Boron Swap Using The Rod Drop Method

Rod Group Number	Position Interval (%wd)	Predicted Worth (%Δk/k)	Measured Rod Drop Worth (%Δk/k)	Corrected To Boron Swap Worth (%Δk/k)	Absolute Error (%)
1	100 to 0	-1.05		-0.80	
2	100 to 0	-3.20		-2.43	
3	43 to 0	-0.56		-0.42	
TOTAL		-4.81	-2.85	-3.65	-31.8

Note: The Boron Swap Worth Is Equal To 1.28 Times The Rod Drop Worth. This constant (1.28) Was Established From Figure 3.4-14 And Relates The Rod Drop Worth To Boron Swap Worth.

Table 3.4-7

Differential Boron Reactivity Worth Measurements During Zero Power Physics Test

Rod Position, % wd								Measured Boron Conc. (ppm)	Average Boron Conc. (ppm)	Delta Boron Conc. (ppm)	Boron Worth (%Δk/k)	Differential Worth %Δk/k/ppmB	
1	2	3	4	5	6	7	8					Measured	Predicted
100	100	100	100	100	100	100	100	1403	1160	487	5.48	0.0113	0.0108
100	100	35	0	0	0	0	35	916					

Note: The linear least squares best fitted differential boron worth using all steady state data points yielded a values of 0.01142%Δk/k/ppmB.

Table 3.4-8

Determination Of The Ejected Rod Worth At Zero Power, BOL, And 532°F Conditions

Rod Position, %wd								Inserted Reactivity (%Δk/k)	RCS Boron Concentration (ppmB)	Ejected Rod Position (%Δk/k)	Change In Reactivity (%Δk/k)	Ejected Rod Worth, %Δk/k	
1	2	3	4	5	6	7	8					Measured	Worst Case
100	100	100	100	51	0	0	35	2.89	1181	100	0.42	0.44	0.46
100	100	100	100	100	16	0	35	2.47		0			

Note: The measured ejected rod worth has been normalized to the Technical Specifications minimum allowable rod index of 45% wd by the addition of 0.02%Δk/k.

Note: The worst case ejected rod worth is obtained by application of an uncertainty factor of 1.05.

Table 3.4-9

Determination Of The Stuck Rod Worth At Zero Power, BOL, And 532°F Conditions

Rod Position, %wd								Withdrawn Reactivity (%Δk/k)	RCS Boron Concentration (ppmB)	Stuck Rod Position (%wd)	Change In Reactivity (%Δk/k)	Stuck Rod Worth, (%Δk/k)	
1	2	3	4	5	6	7	8					Measured	Worst Case
15	0	0	0	0	0	0	0	0.10	819	100	2.34	2.34	2.57
0	34	0	0	0	0	0	0	2.44		0			

Note: The measured stuck rod worth was obtained by dropping group 1 and part of group 2 from the above conditions and by adjusting this value for the amount of reactivity withdrawn at the start of the measurement.

$$(SR) = (1.28) \times (1.91) - 0.10 = 2.34\%\Delta k/k$$

Note: The worst case stuck rod worth is obtained by application of an uncertainty factor of 1.10

Table 3.4-10

Determination Of Minimum Shutdown Margin

The Reactor must have a minimum reactivity shutdown margin of -1% Δk/k at all times with the highest reactivity worth control rod stuck in its most reactive position of 100% withdrawn.

1.0 Measured Rod Worth available, if trip occurred at the maximum allowable inserted group worth (i.e. Group (5) at 45% withdrawn).

Group 1	(at 100% wd)	=	-0.80%Δk/k
Group 2	(at 100% wd)	=	-2.43%Δk/k
Group 3	(at 100% wd)	=	-0.59%Δk/k
Group 4	(at 100% wd)	=	-1.43%Δk/k
Group 5	(at 4[illegible]% wd)	=	-0.86%Δk/k
	TOTAL	=	-6.11%Δk/k

The above value should be reduced by ten percent (10%) for measurement uncertainties -5.50%Δk/k

2.0 The worst case stuck rod worth

The above value is obtained by increasing the measured stuck rod worth by ten percent (10%) for measurement uncertainties +2.57%Δk/k

3.0 The minimum shutdown margin (SUM of above terms) -2.93%Δk/k

NOTE: The shutdown margin should be more negative than -1.0%Δk/k

Table 3.4-11

Summary Of Measured, Calculated, And Predicted Coefficients Of Reactivity At Zero Power

Rod Position, %wd								Average Temperature (Deg F)	RCS Boron Concentration (ppmB)	Reactivity Coefficients, 1.0E-04 $\Delta k/k/^{o}F$			
										Temperature Coefficient		Moderator Coefficient	
1	2	3	4	5	6	7	8			Measured	Predicted	Calculated	Predicted
100	100	100	100	100	100	86	100	532	1400	+0.36	+0.21	+0.52	+0.37
100	100	100	100	07	0	0	35	532	1070	-0.61	-0.69	-0.45	-0.53
100	100	35	0	0	0	0	35	532	916	-0.64	-0.48	-0.48	-0.32

Note: The Predicted Temperature And Moderator Coefficient Were Adjusted For The Difference Between Predicted And Actual All-Rods-Out Critical Boron Concentration (-0.17×10^{-4} $\Delta k/k/^{o}F$).

Note: The calculated moderator coefficient has been determined from the measured temperature coefficient of -0.16×10^{-4} $\Delta k/k/^{o}F$.

Table 3.4-12

Reactor Coolant System Cold And Hot Leg RTD Temperature Normalization Constants

Unit Parameter	Temperature Transmitter	Computer Point ID	Normalization Constant CN (Deg. F)	Percent Error (%)
RCS LP (A) Hot Leg Temperature	RC4A-TT4	R212	+1.6	+0.30
RCS LP (A) Hot Leg Temperature	RC4A-TT1	R212	+0.8	+0.15
RCS LP (B) Hot Leg Temperature	RC4B-TT4	R213	-2.1	-0.40
RCS LP (B) Hot Leg Temperature	RC4B-TT1	R213	-2.2	-0.41
RCS LP (A1) Cold Leg Temperature	RC5A-TT1	R214	+0.6	+0.11
RCS LP (A2) Cold Leg Temperature	RC5A-TT3	R215	+0.5	+0.09
RCS LP (B1) Cold Leg Temperature	RC5B-TT1	R216	+0.5	+0.09
RCS LP (B2) Cold Leg Temperature	RC5B-TT3	R217	+0.5	+0.09

Table 3.4-13

Comparison Of Measured And Predicted Results Obtained During Zero Power Physics Test

	Physic Parameter	Units	Measured	Predicted	Acceptance Requirements	Comparison
1.	All Rods Out Critical Boron	ppmB	1403	1445	Measured value must be within 100 ppmb of predicted value	OK (42 ppm)
2.	Sensible Heat	amps	2.25×10^{-8}		None	
3.	NI Overlap	decades	2.21		Greater than 1.0 decade	OK (> 1.0)
4.	Control Rod Group Worth	% Δ k/k			Percent deviation of group worth should be less than 20%.	
	Group 8		-0.36	-0.36		OK (0.0%)
	Group 7		-1.11	-1.17		OK (-5.4%)
	Group 6		-1.21	-1.27		OK (-5.0%)
	Group 5		-1.14	-1.16		OK (-1.8%)
	Group 4		-1.43	-1.75		NOT OK (-22.4%)
	Group 3		-0.59	-0.75		NOT OK (-27.1%)
	Group 2		-2.43	-3.20		NOT OK (-31.8%)
	Group 1		-0.80	-1.05		NOT OK (-31.8%)
	TOTAL		-9.07	-10.71	Percent deviation of total worth should be less than 15%	NOT OK (-18.1%)
5.	Shutdown Margin	% Δk/k	-2.93		Measured value must be less than -1% Δ k/k	OK (-1.0)
6.	Stuck Rod Worth (4-3)	% Δk/k	-2.34	-4.00	Percent deviation of stuck rod worth should be within 30% of the predicted value.	NOT OK (-70.9%)
7.	Ejected Rod Worth (7-8)	% Δk/k	+0.44	+0.47	Percent deviation of ejected rod worth must be within 30% of the predicted value. Also value must be more negative than +1.0%Δk/k.	OK (-6.8%) OK (<+1.0)
8.	Temperature Coefficient	10^{-4} Δk/k°F				
	At 1400 ppmB		+0.36	+0.21	Measured value must be within 0.4 X 10^{-4} Δk/k/°F of the predicted value.	OK (.15)
	At 1070 ppmB		-0.61	-0.69		OK (.08)
	At 916 ppmB		-0.64	-0.48		OK (.16)

Table 3.4-13 (Cont'd)

Comparison Of Measured And Predicted Results Obtained During Zero Power Physics Test

	Physic Parameter	Units	Measured	Predicted	Acceptance Requirements	Comparison
9.	Moderator Coefficient	$10^{-4}\ \Delta k/k/^{o}F$			Maximum positive moderator coefficient must be less than $0.9 \times 10^{-4}\ \Delta k/k/^{o}F$	
	At 1400 ppmB		+0.52	+0.37		OK (<.90)
	At 1070 ppmB		-0.45	-0.53		OK (<.90)
	At 916 ppmB		-0.48	-0.32		OK (<.90)
10.	Differential Boron Worth	$\% \Delta k/k/$ ppmB				
	At 1160 ppmB		-0.0113	-0.0107	Percent deviation must be less than 10%	OK (-5.6)

NOTE: Percent Deviation is defined by the following formula:

$$\% \text{ Deviation} = \frac{\text{Measured Value} - \text{Predicted Value}}{\text{Measured Value}} \times 100$$

RCS Boron Concentration Versus Time For Approach To Initial Criticality

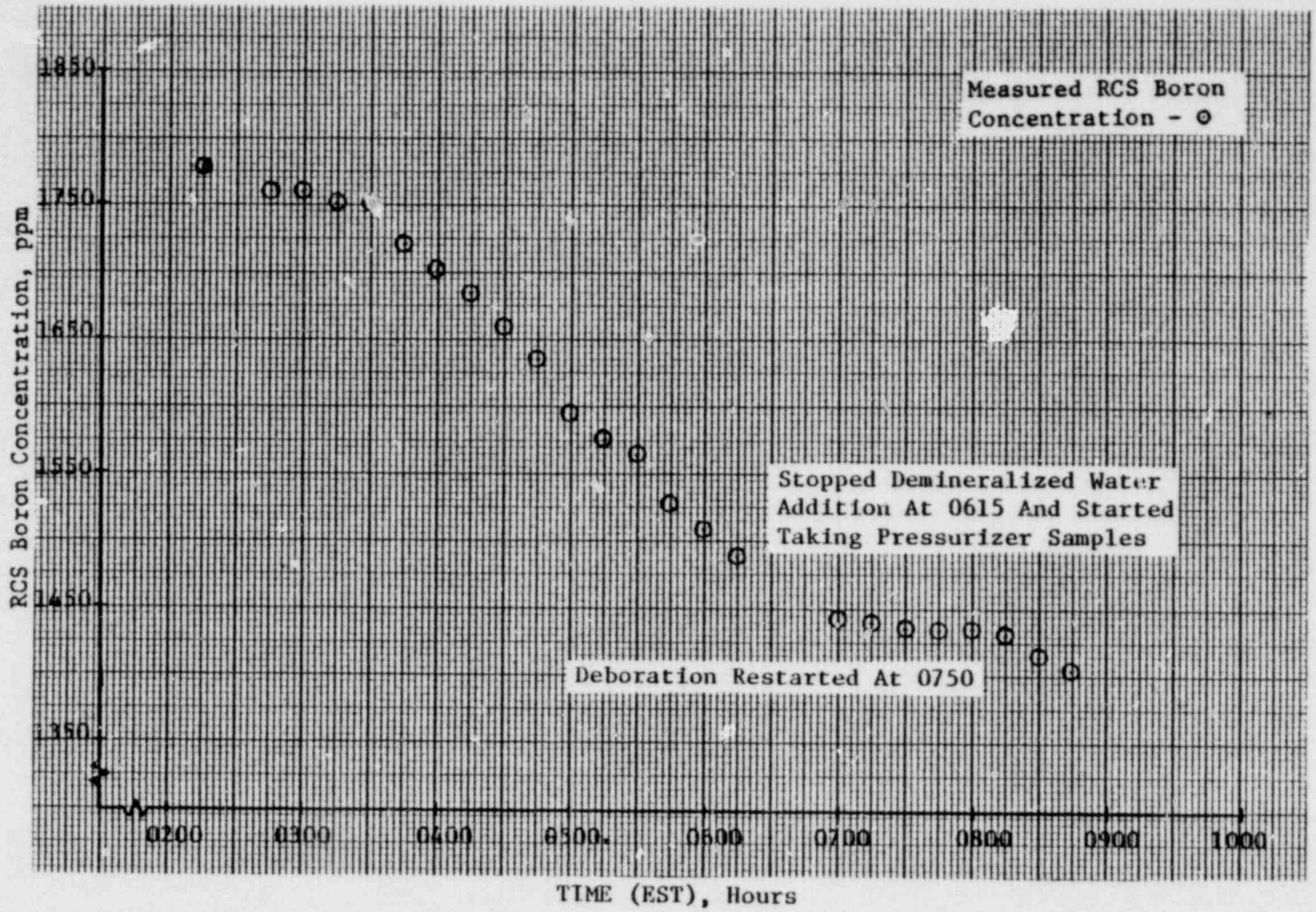

Figure 3.4-1

Inverse Multiplication For Detectors NI-1 And NI-2 Versus
Time For Approach To Initial Criticality

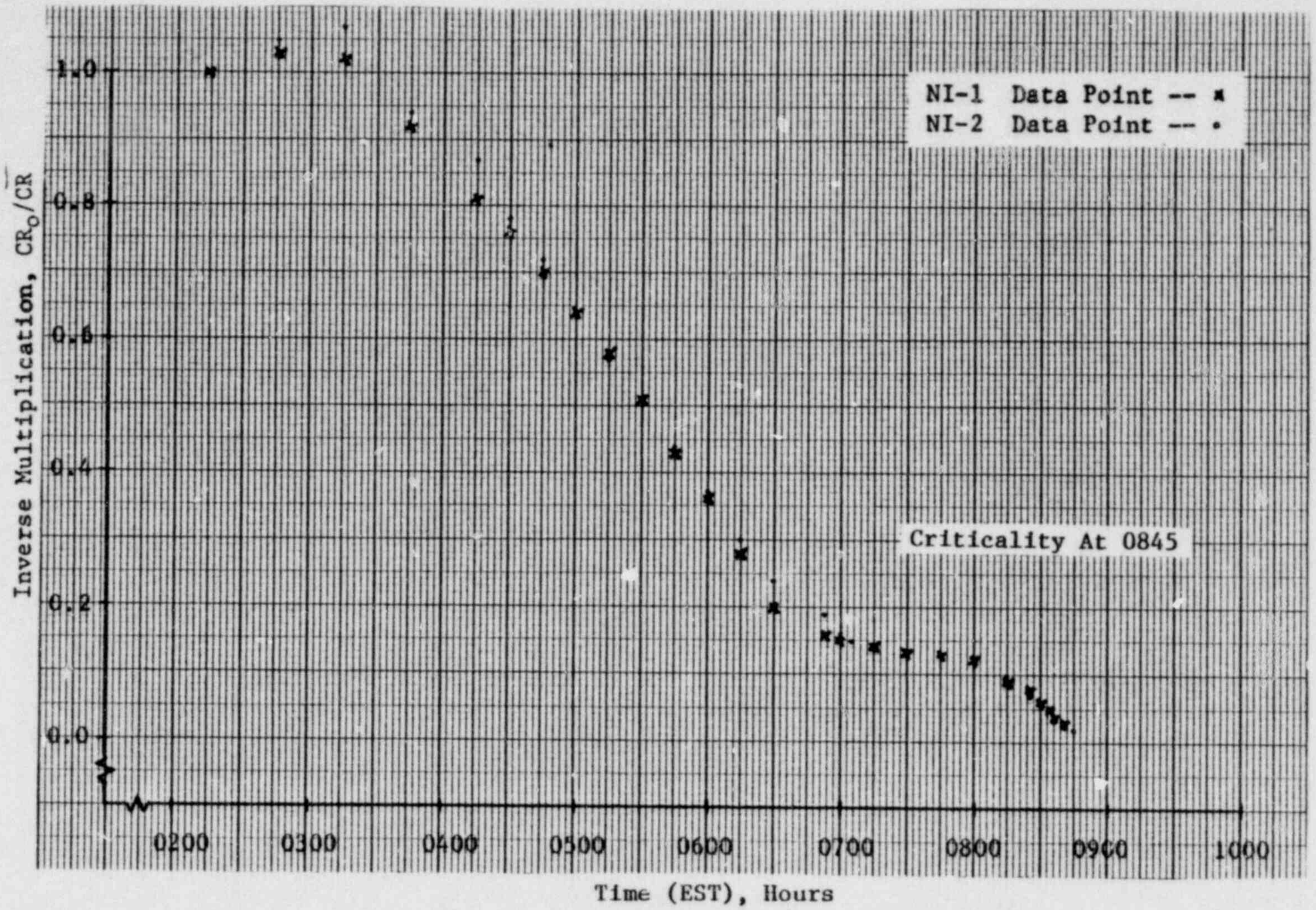

Figure 3.4-2

Inverse Multiplication For Detectors NI-1 And NI-2 Versus
RCS Boron Concentration For Approach To Initial Criticality

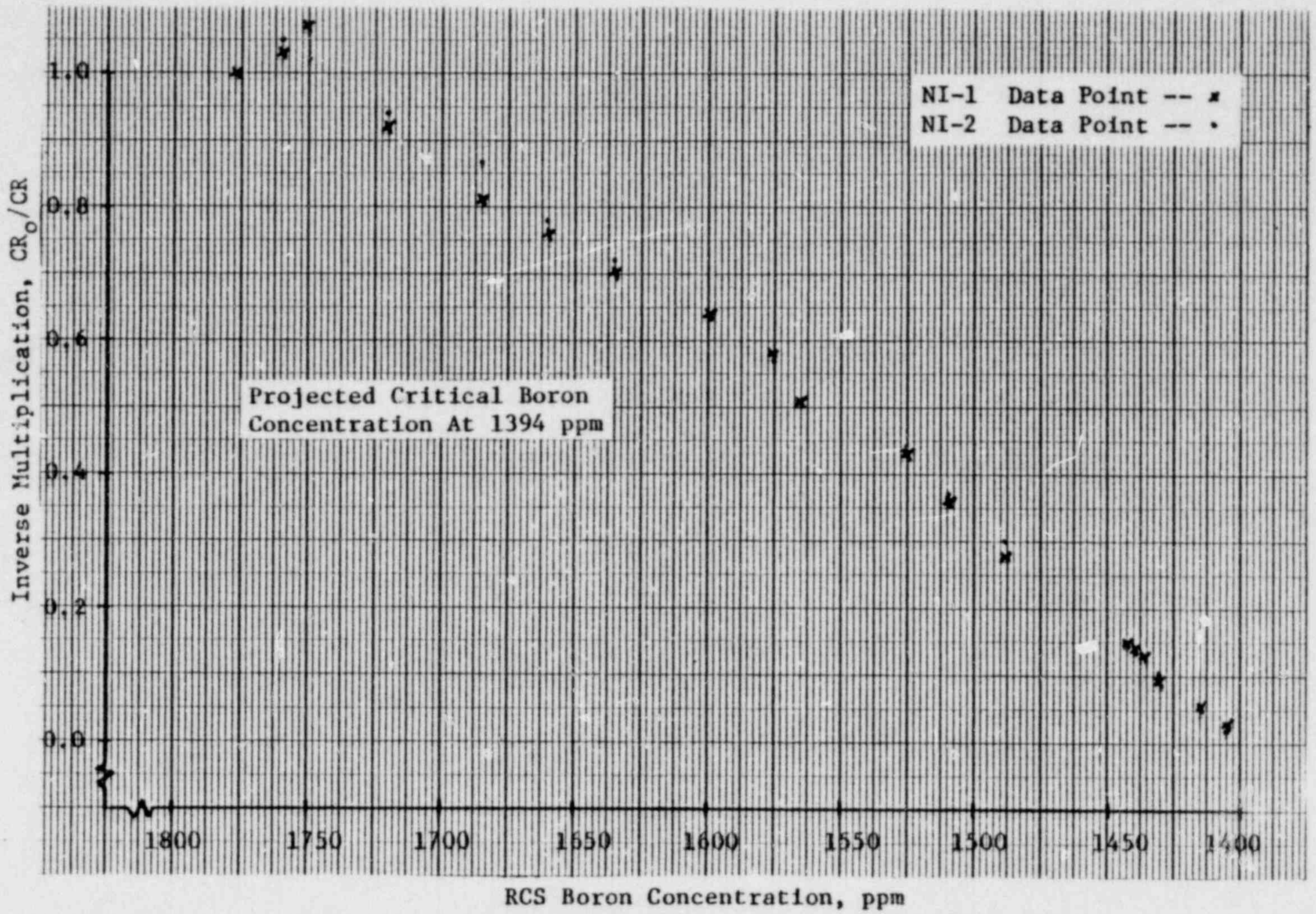

Figure 3.4-3

Inverse Multiplication For Detectors NI-1 And NI-2 Versus
Reactivity Removed For Approach To Initial Criticality

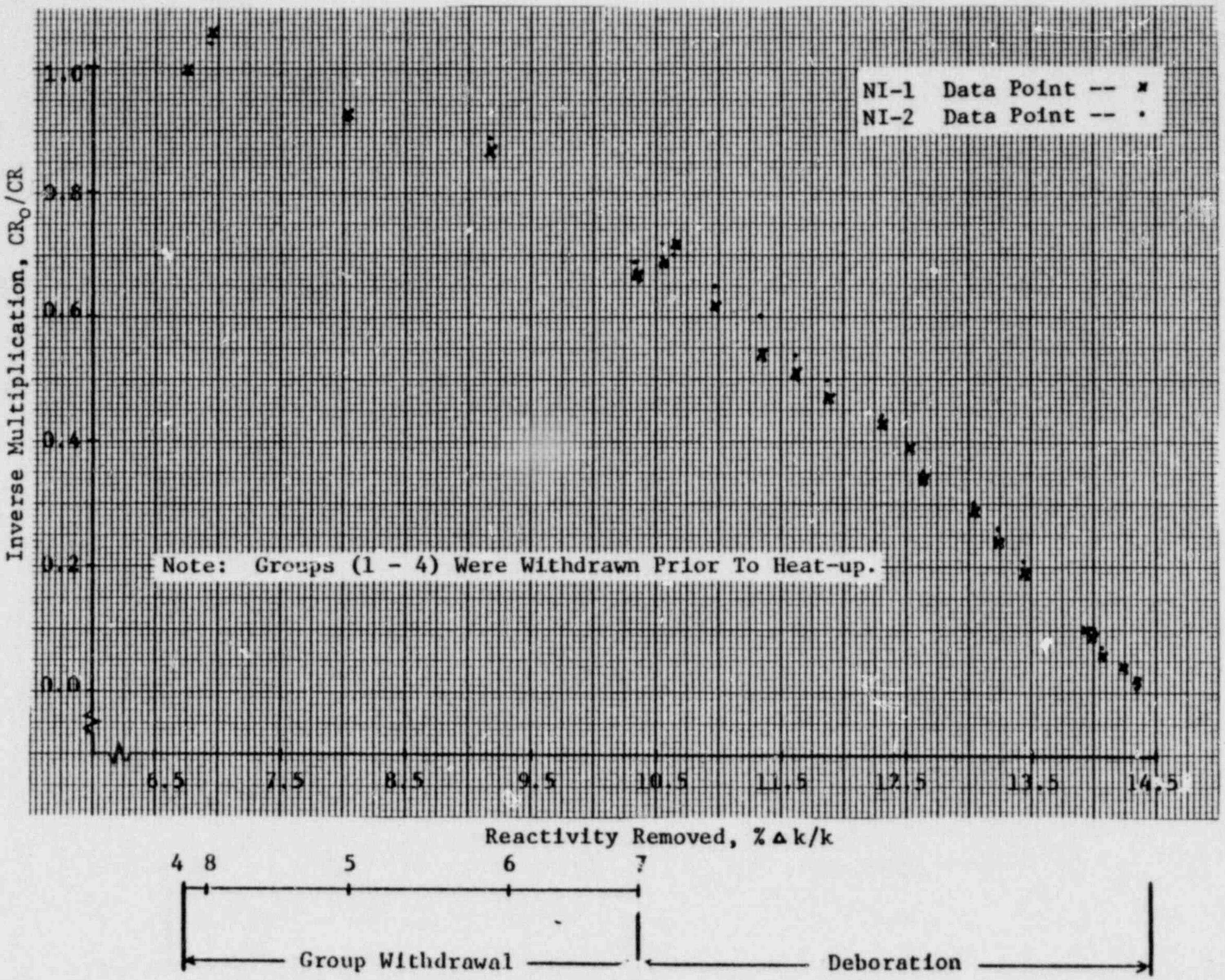

Figure 3.4-4a

Inverse Multiplication For Detectors NI-1 And NI-2 Versus
Demineralized Water Added For Approach To Initial Criticality

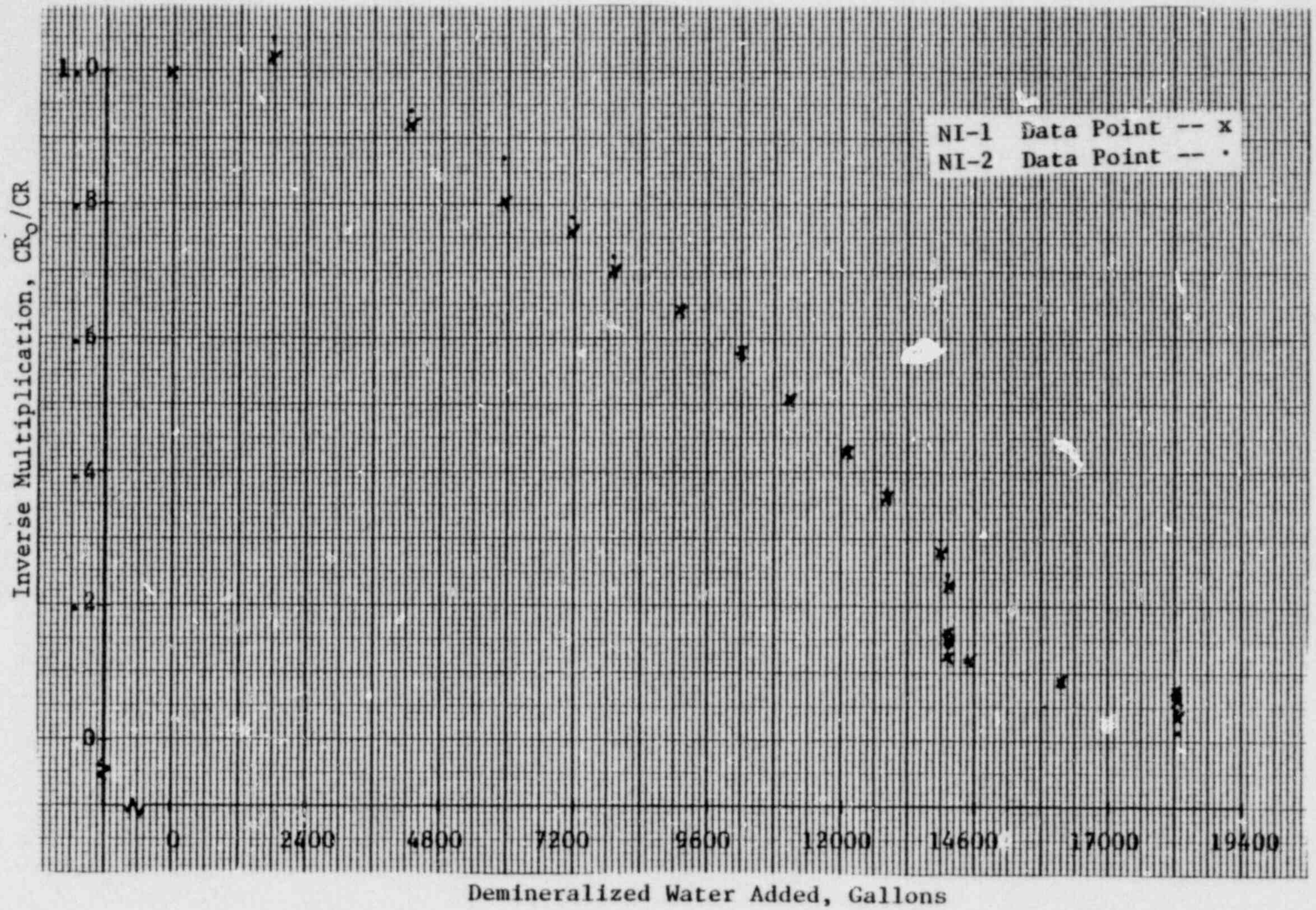

Figure 3.4-4b

Core Power Versus Detector Response

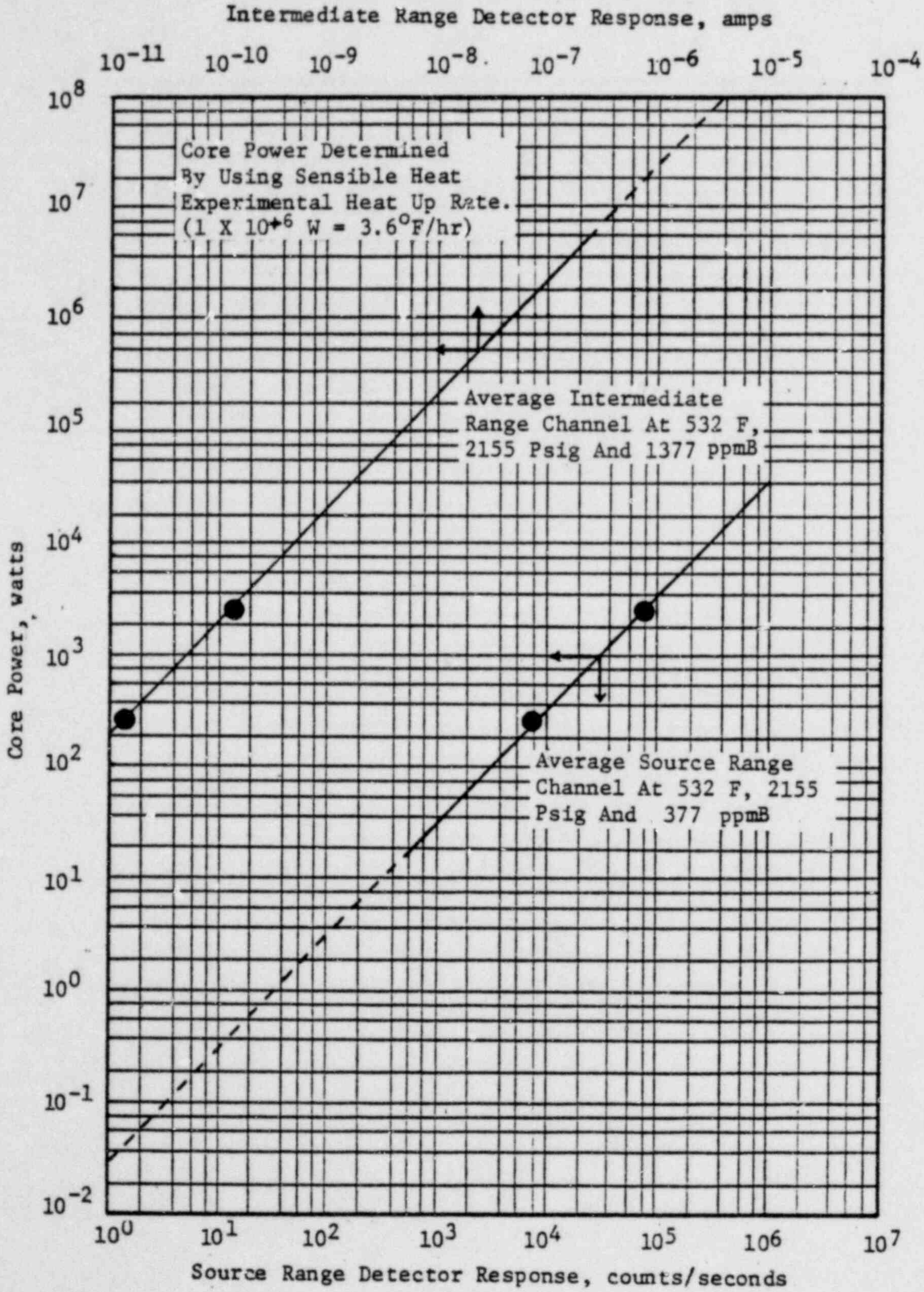

Figure 3.4-5

Reactor Coolant System Heatup Rate Versus Intermediate Range Current Level For The Determination Of The Point Of Sensible Heat.

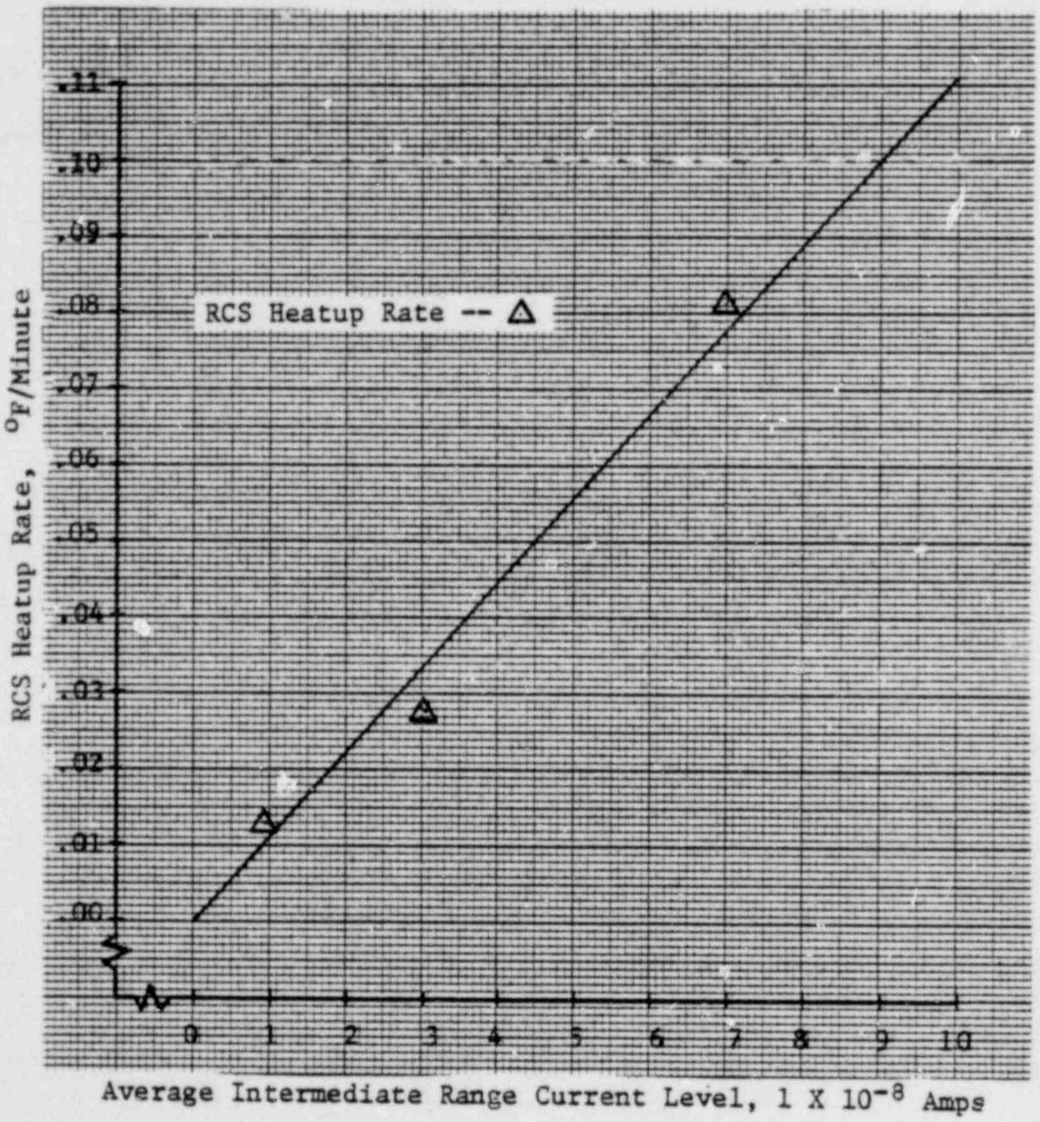

Figure 3.4-6

Cycle 1 Core Locations Of Control Rods, Incore Monitor Assemblies, And Out-Of-Core Detectors.

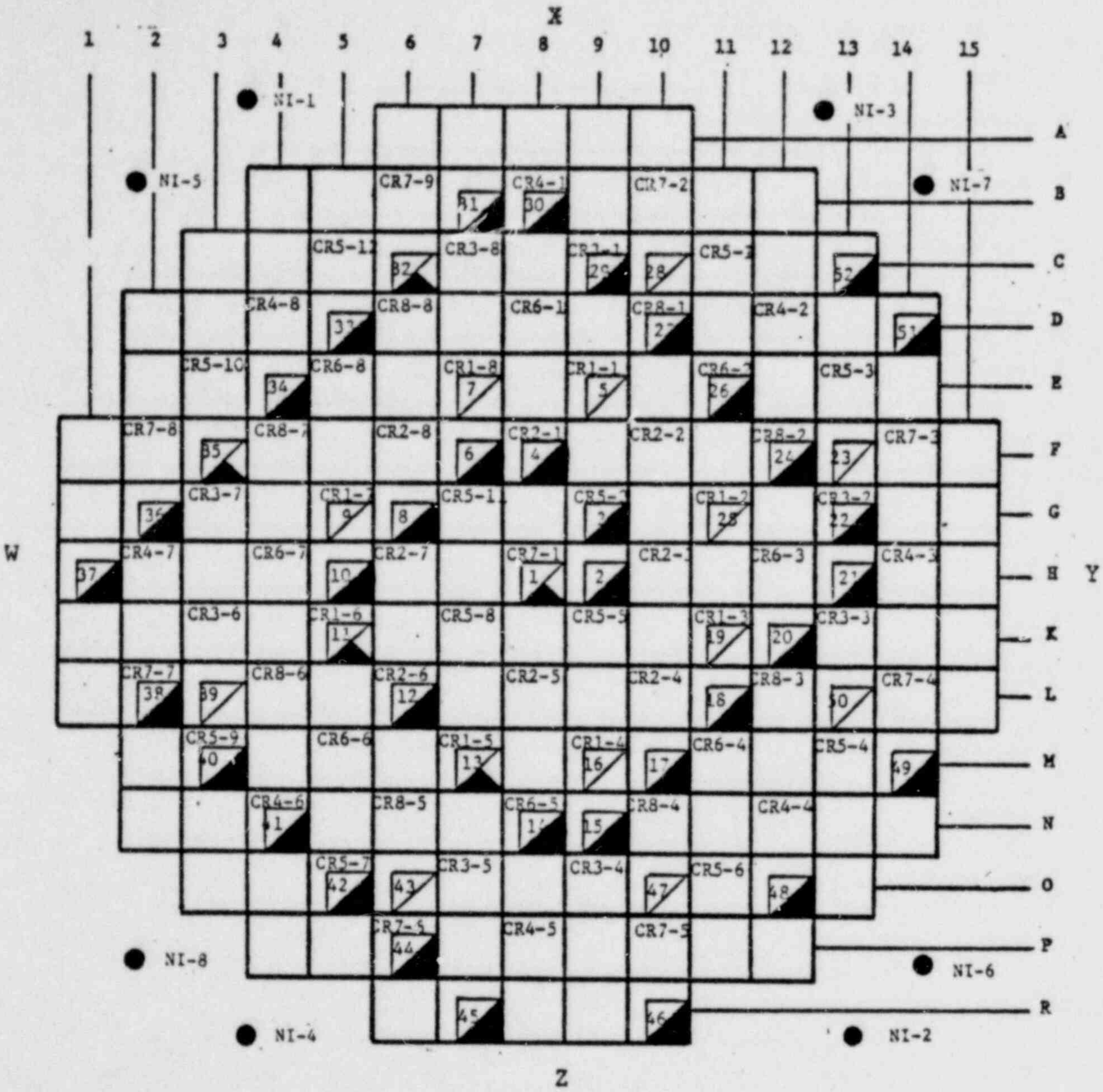

Z – Total Core Monitor

Z – Total Core And Symmetry Monitor

Z – Symmetry Monitor

Z – Incore Monitor Number

CRX-Y – Control Rod Number Y Of Control Rod Group X

Figure 3.4-7

Normalized Differential Shapes Of Control Rod Groups 3-4 Versus Withdrawal Position, For Beginning Of Life, Zero Power Conditions

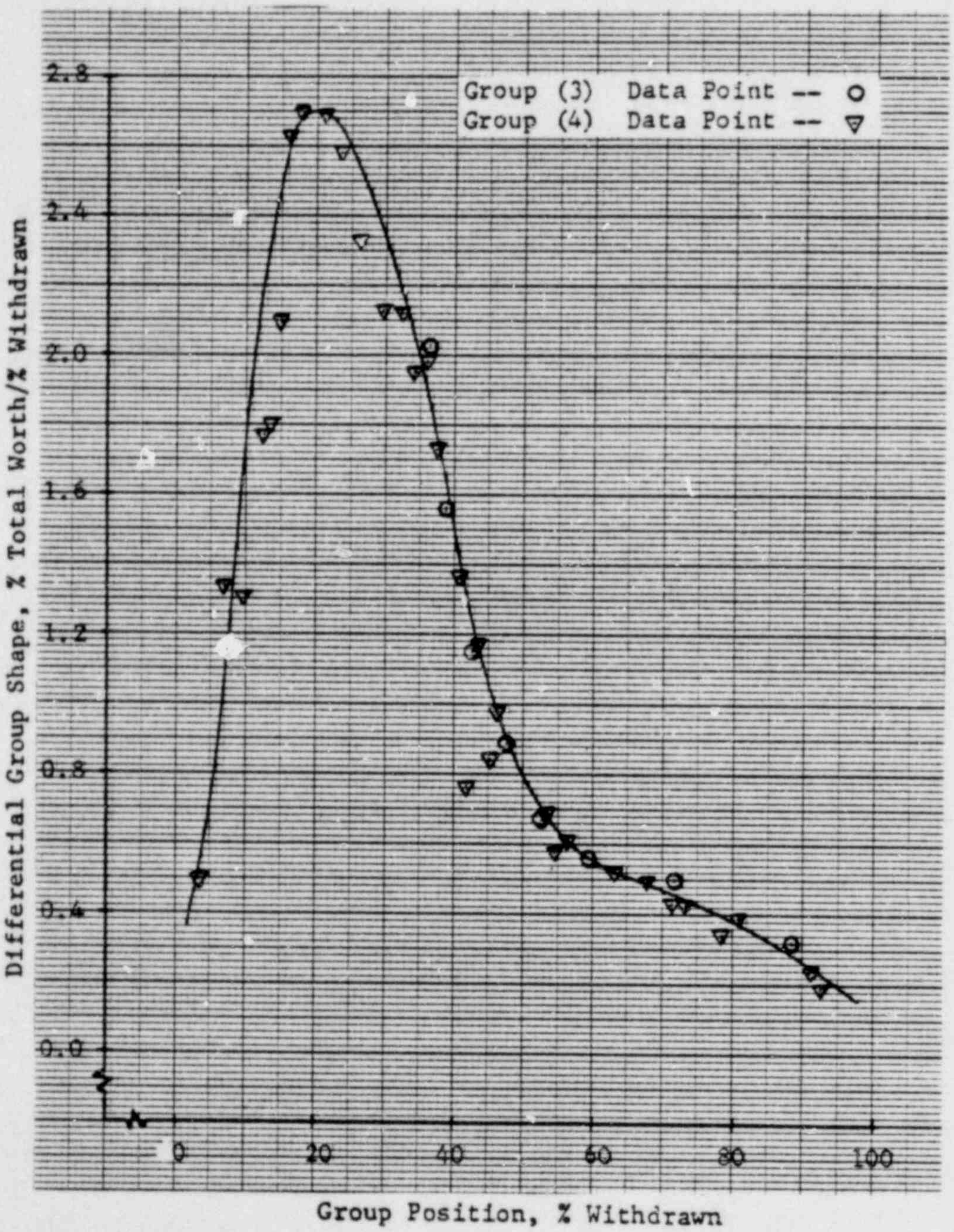

Figure 3.4-8

Normalized Differential Shapes Of Control Rod Groups 5-7 Versus
Withdrawal Position, For Beginning Of Life, Zero Power Conditions

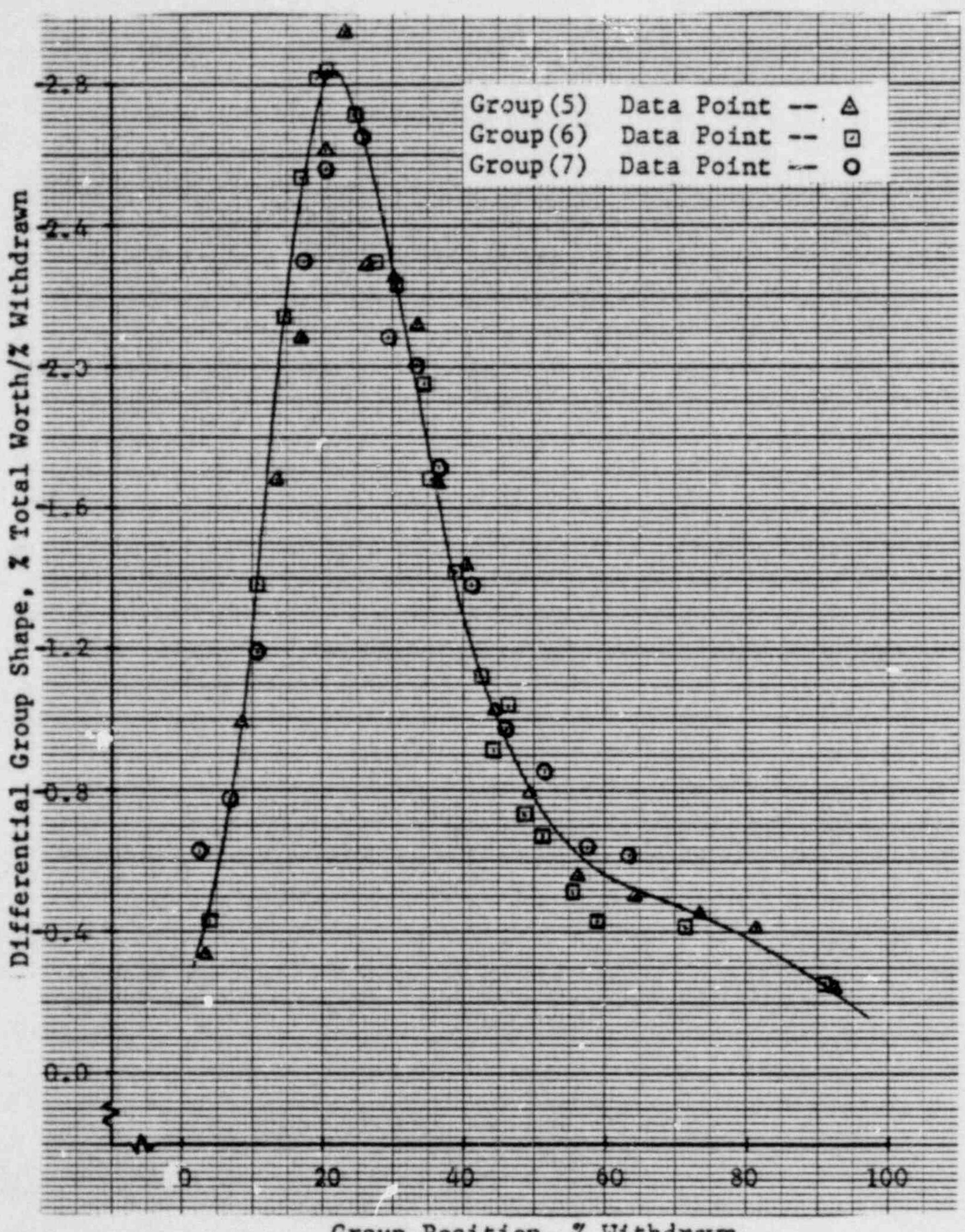

Figure 3.4-9

Normalized Differential Shape Of Control Rod Group 8 Versus
Withdrawal Position, For Beginning Of Life, Zero Power Conditions

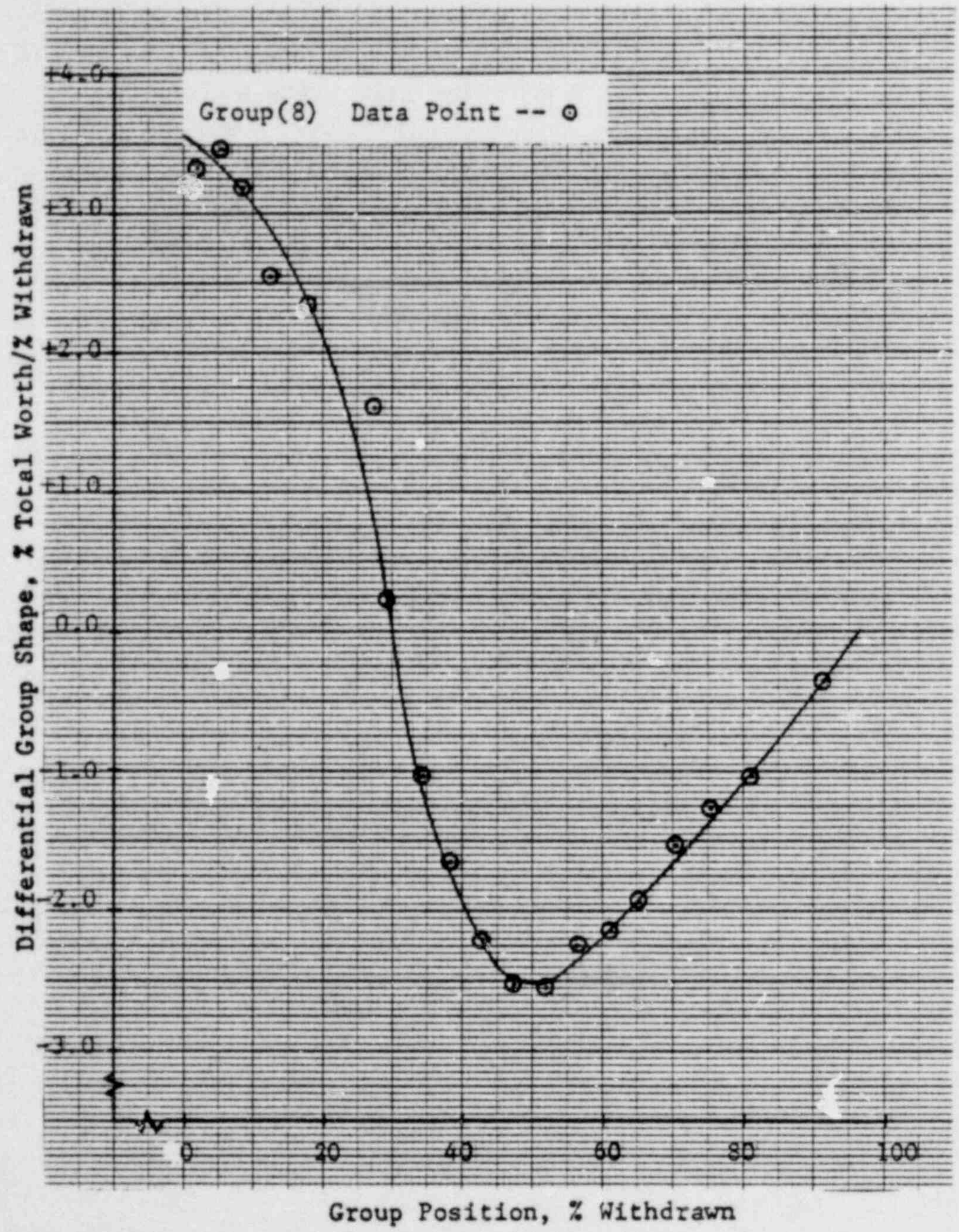

Figure 3.4-10

Normalized Integral Shapes Of Control Rod Groups 3-4 Versus Withdrawal Position, For Beginning Of Life, Zero Power Conditions

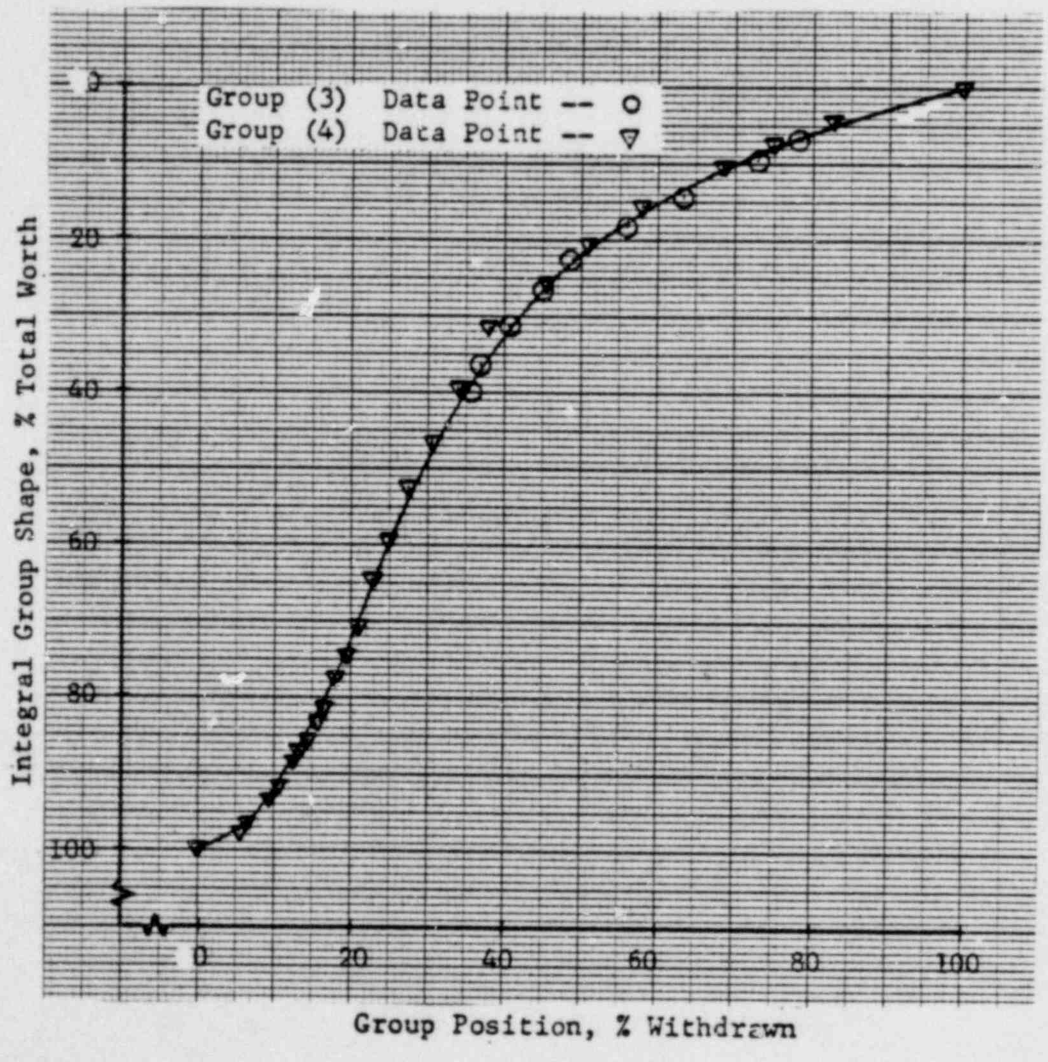

Figure 3.4-11

Normalized Integral Shapes Of Control Rod Groups 5-7 Versus Withdrawal Position, For Beginning Of Life, Zero Power Conditions

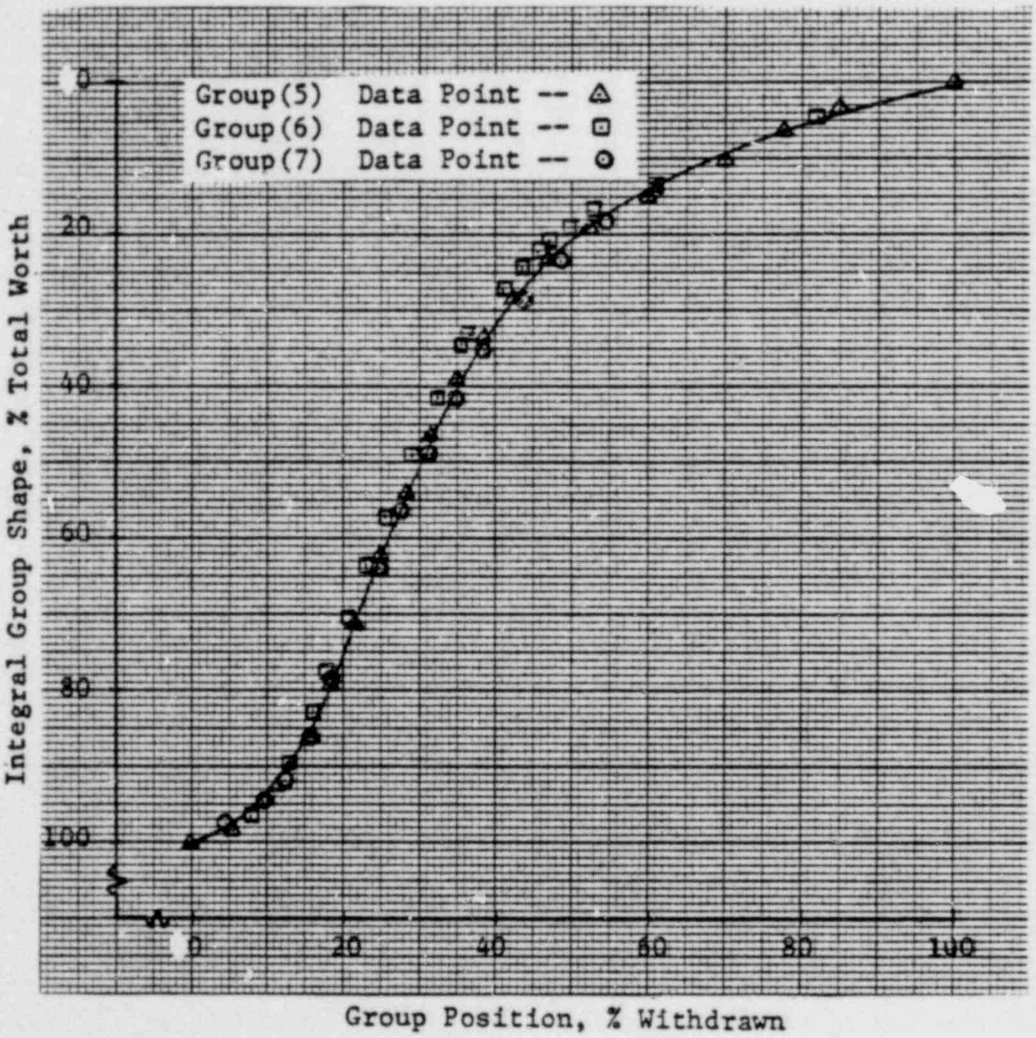

Figure 3.4-12

Normalized Integral Shape Of Control Rod Group 8 Versus Withdrawal Position, For Beginning Of Life, Zero Power Conditions

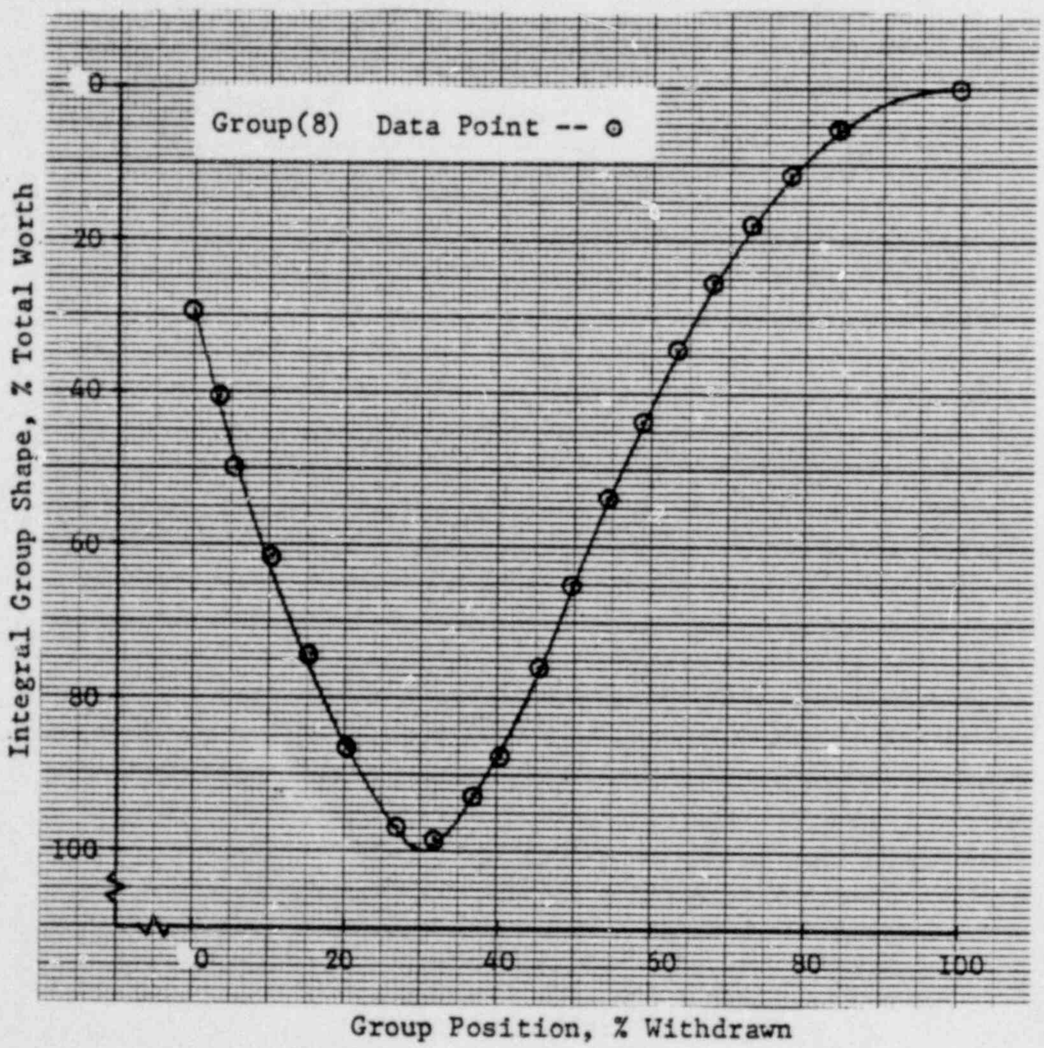

Figure 3.4-13

Measured Reactivity Worth Versus Inserted Group Worth For The Determination Of The Rod Drop To Boron Swap Correction Factor

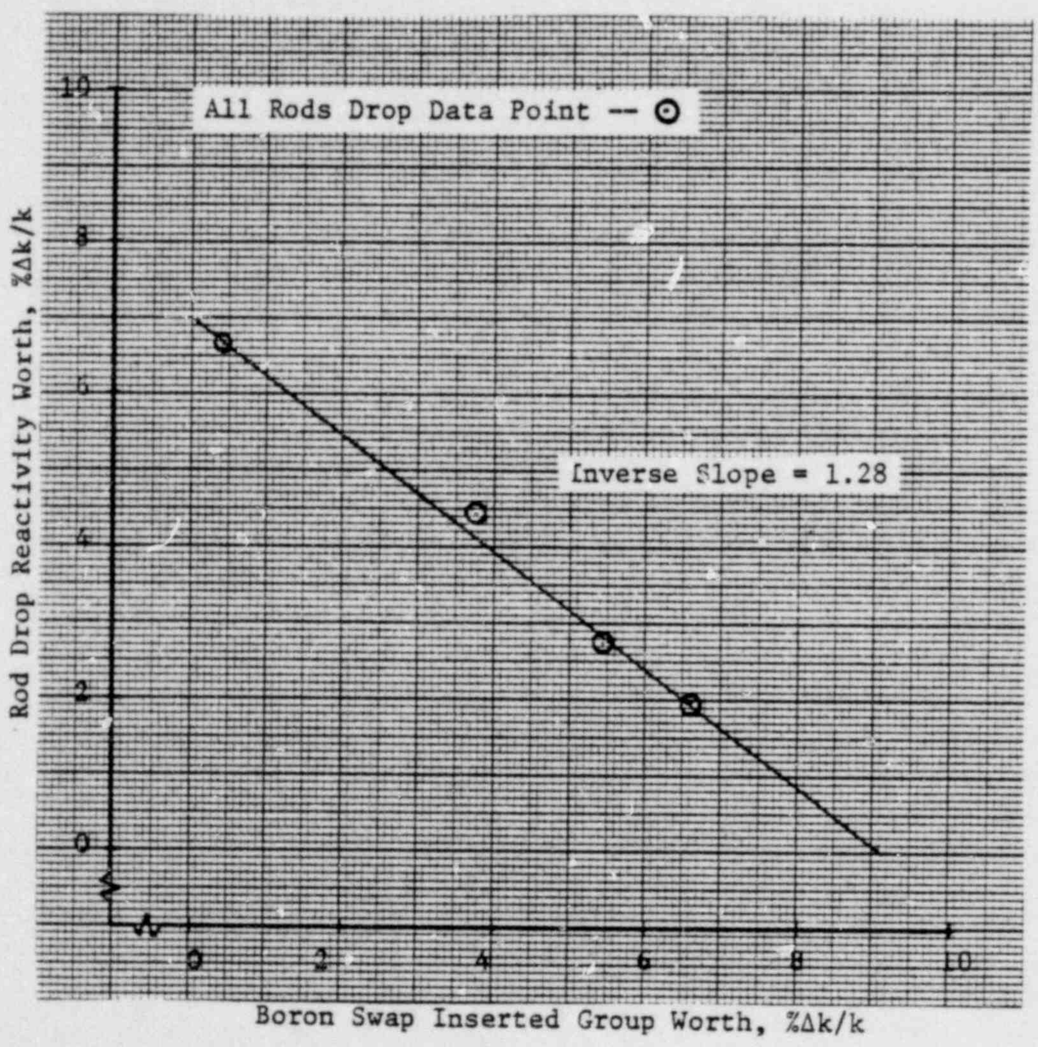

Figure 3.4-14

Comparison Of Measured And Predicted Differential Reactivity Worth of Soluble Boron Versus Boron Concentration For Beginning Of Life Conditions

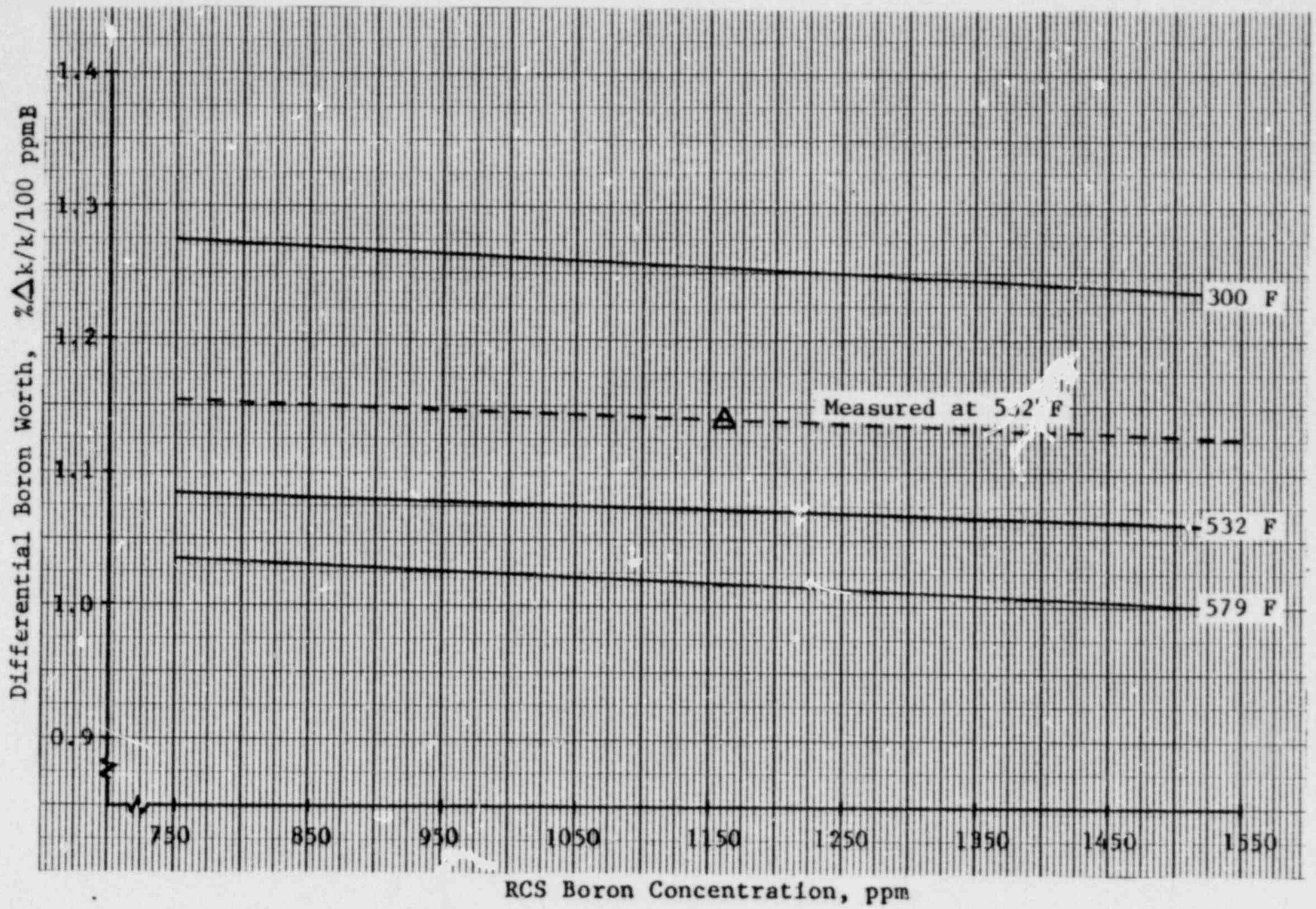

Figure 3.4-15

Comparison Of Measured And Predicted Integral Reactivity Worth Of Soluble Boron Versus Boron Concentration For Beginning Of Life Conditions

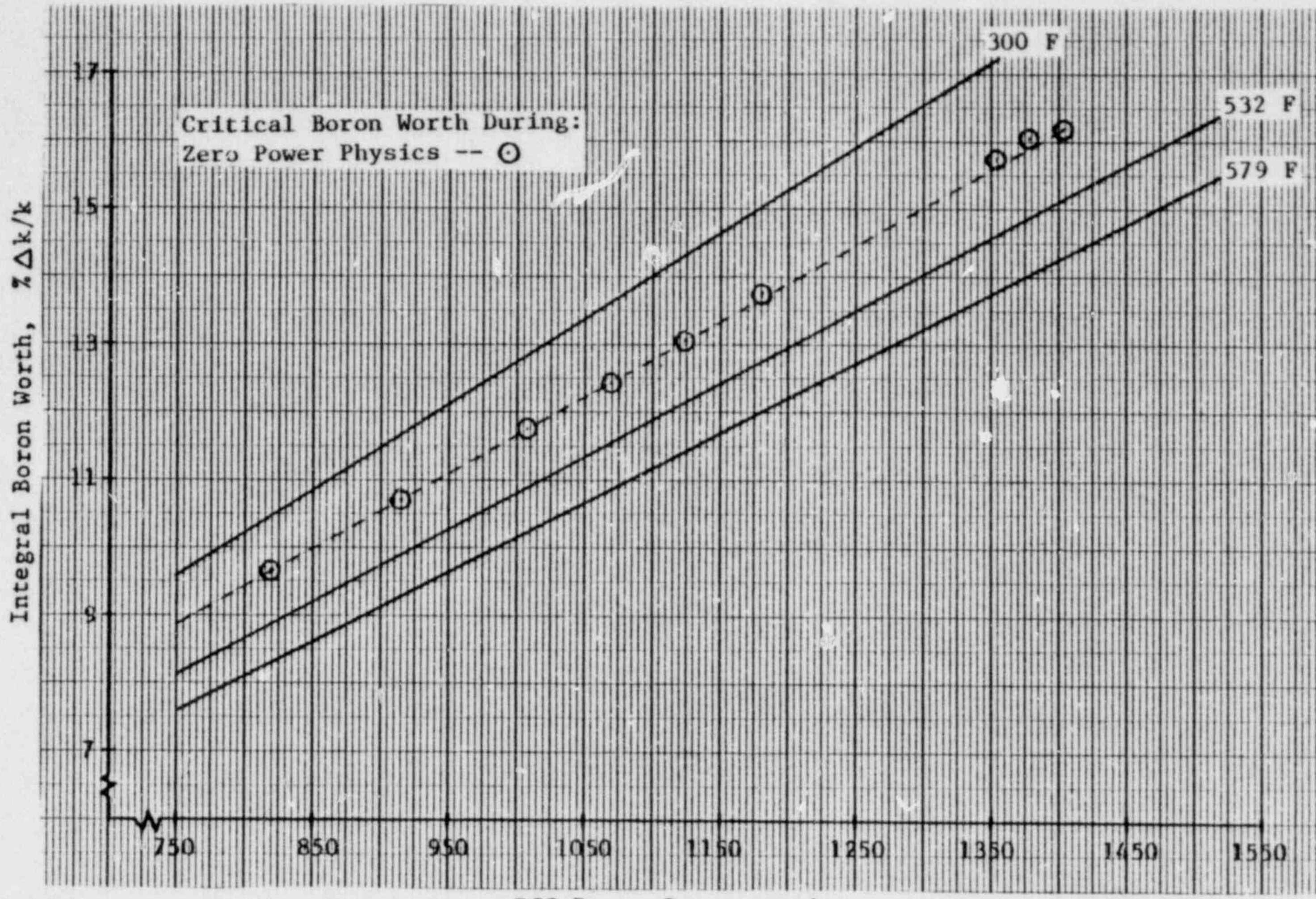

Figure 3.4-16

Ejected Control Rod Reactivity Worth At Zero Power, Beginning Of Life, And 532 Degree F Conditions.

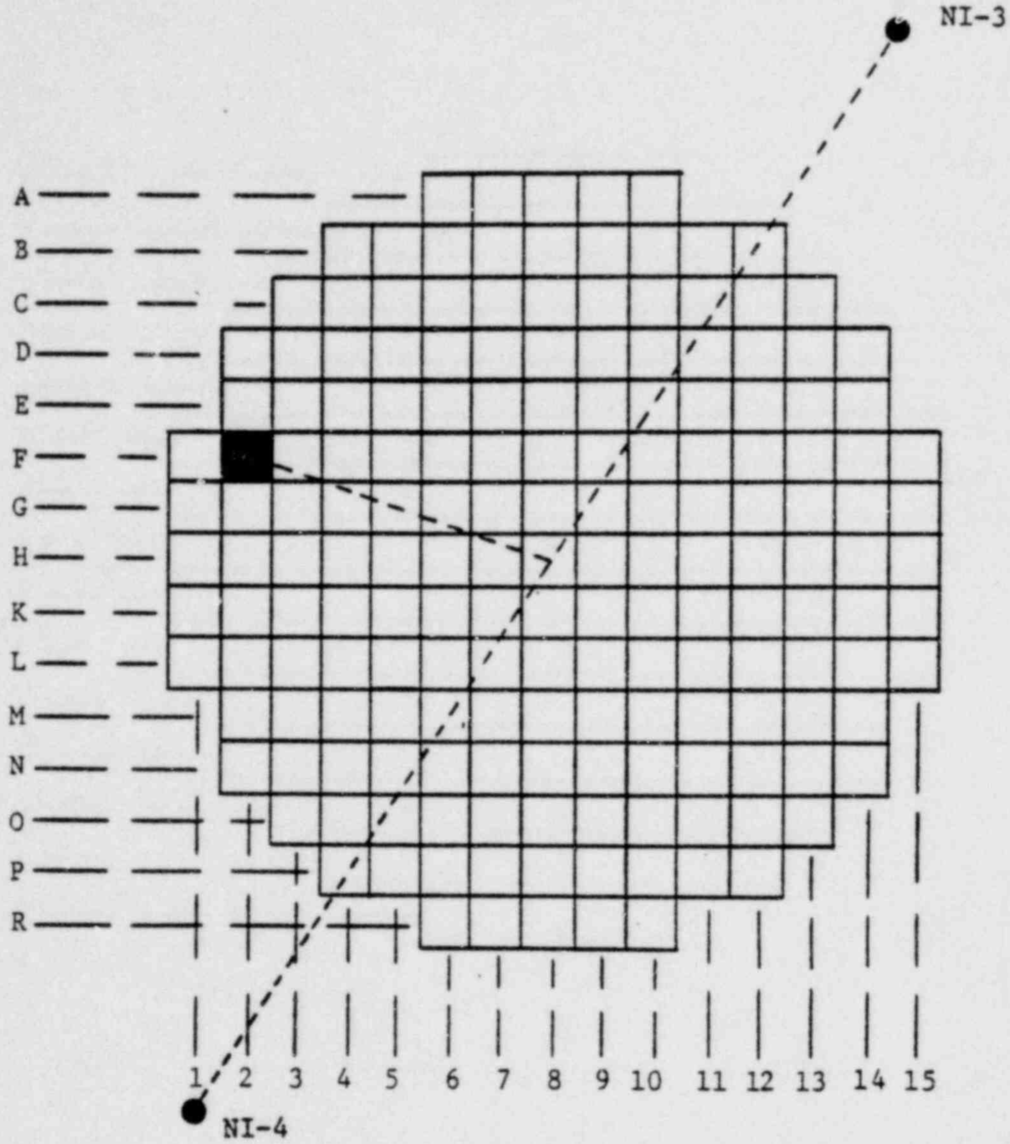

CONTROL ROD	CORE POSITION	CONTROL ROD WORTH, % Δk/k PREDICTED	MEASURED
7-8	F-02	0.47	0.44

Figure 3.4-17

Stuck Control Rod Reactivity Worth At Zero Power, Beginning Of Life, And 532 Degree F Conditions

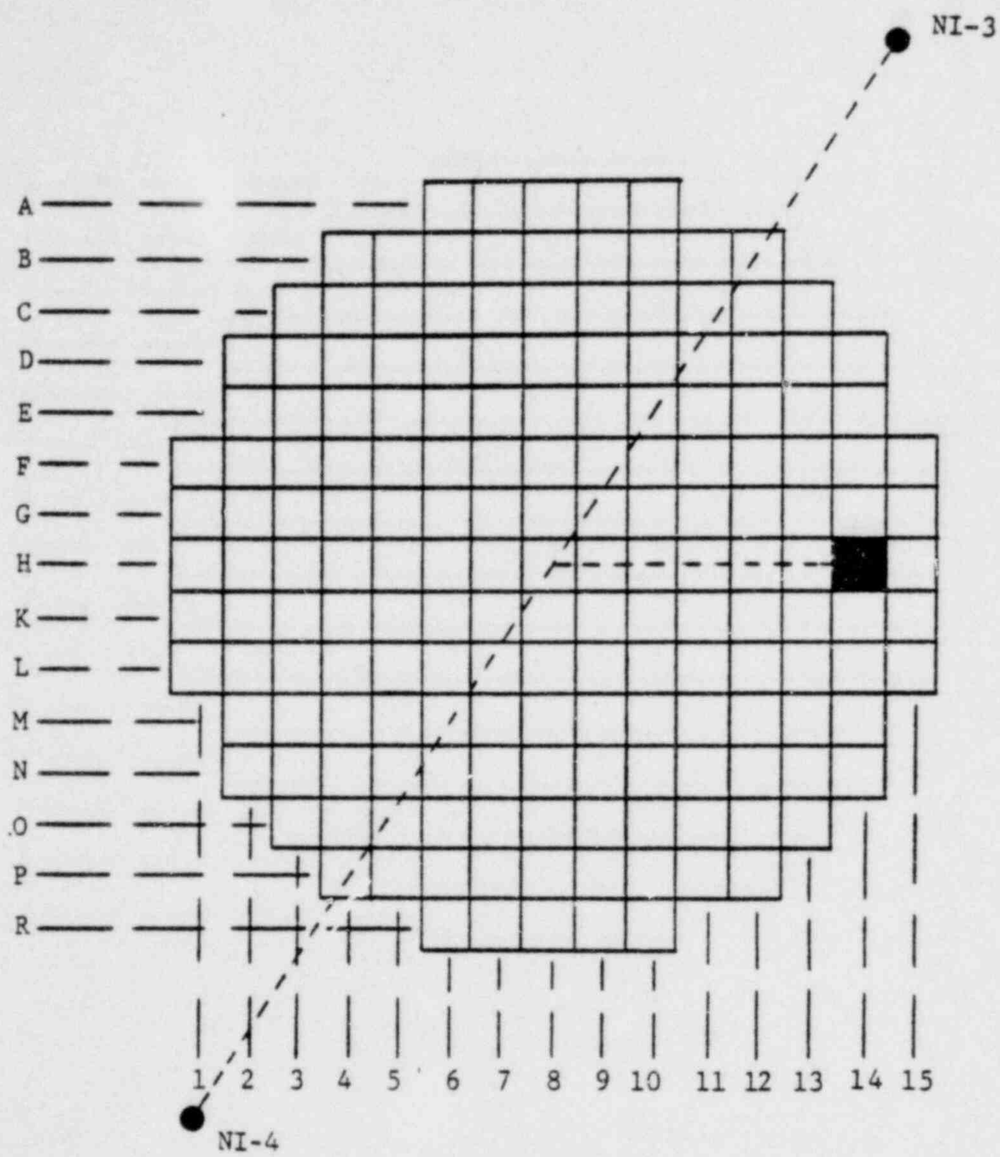

CONTROL ROD	CORE POSITION	CONTROL ROD WORTH, % $\Delta k/k$ PREDICTED	MEASURED
4-3	H-14	4.00	2.34

Figure 3.4-18

4.0 POWER ESCALATION TESTS

Following the completion of Zero Power Physics Testing, initial power escalation commenced on January 29, 1977 with the first nuclear electrical power produced at 1800 on January 30, 1977 (a small amount of power was produced for six minutes on July 17, 1976, during turbine testing as part of Hot Functional Testing). The power escalation test program was conducted at four major test plateaus of 15, 40, 75, and 100% full power with minor testing performed at intermediate power levels as required by the controlling procedure for power escalation. All testing was completed by 2400 hours on April 26, 1977. The average daily power level history during the power escalation test program is shown in Figure 4.0-1. The major power levels were achieved as follows:

Power Level (Percent of Full Power - % FP)	Date Achieved
15	February 1, 1977
40	February 27, 1977
75	March 14, 1977
100	April 1, 1977

Test results review was performed concurrently with testing. This allowed immediate review and approval by the Test Working Group (TWG), Plant Review Committee (PRC), and Testing/Operations management. Escalation to a new power level always followed promptly behind completion of the approval process.

The test program was written to comply with the Technical Specifications and structured in accordance with NRC Regulatory Guide 1.68, November, 1973. The tests reported in this section cover all required power escalation testing. A brief summary of tests reported, along with the appropriate section number of this report and the power level at which they were performed, is given in Table 4.0-1. These tests and the reports written on each, represent all unit and physics parameters necessary for experimental verification to assure that continued operation of Crystal River Unit 3 is within the limits as imposed by Technical Specifications.

A summary of performance indicators during the test period are tabulated in Table 4.0-2. As can be seen, a net time for the test program was 87.6 days. This time includes 23 days for the one major delay encountered.

Average Daily Power Level Versus Time During The Power Escalation Test Program

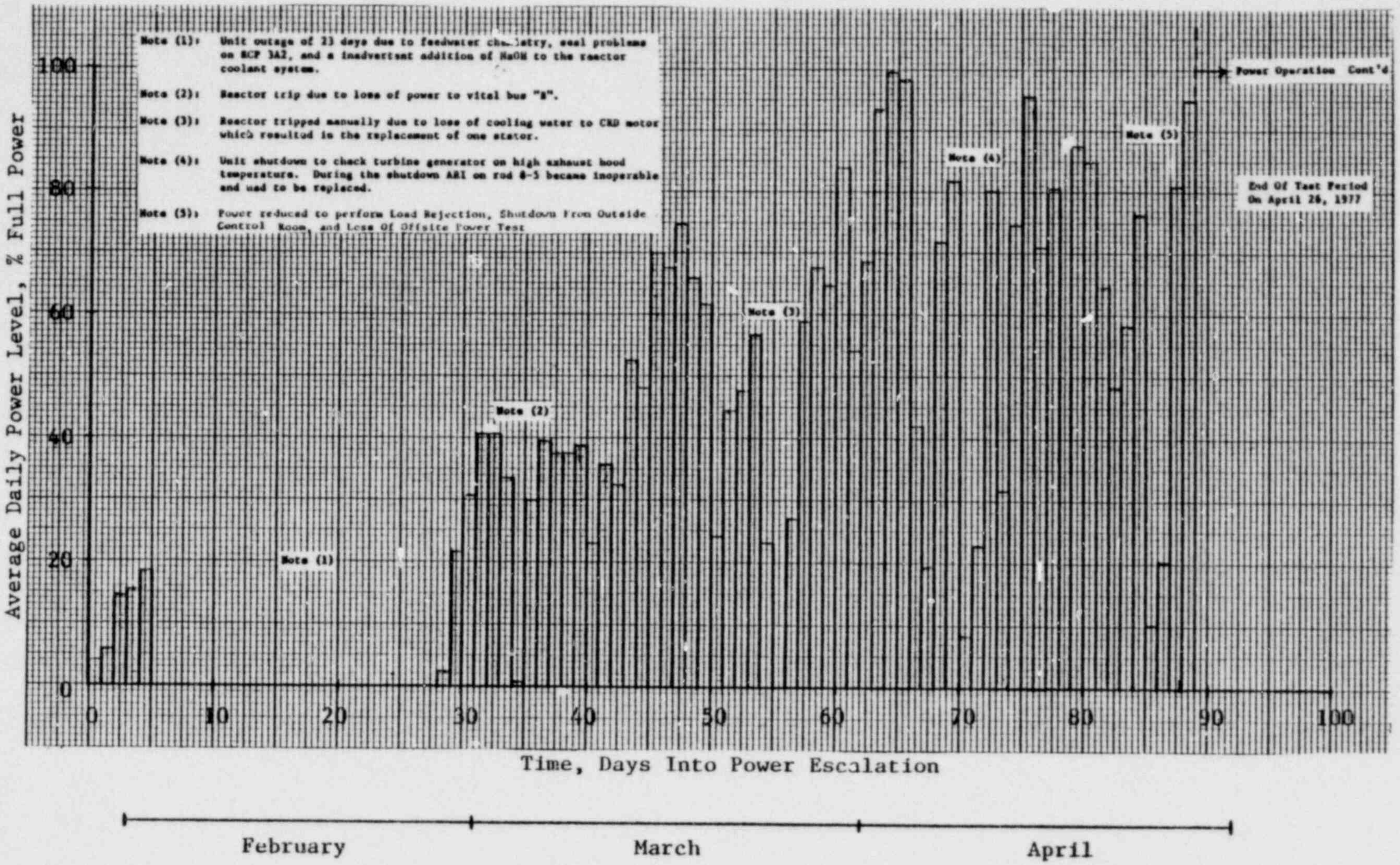

Figure 4.0-1

Table 4.0-1

Summary Of Power Escalation Tests Reported In Section 4.0

Report Section	Title of Section		Test Power Levels							
			0-5	15	25	40	65	75	92	100
4.1	Nuclear Instrumentation Calibration at Power Test		X	X		X		X	X	X
4.2	Biological Shield Survey Test		X			X				X
4.3	Reactivity Coefficients At Power Test					X		X		X
4.4	Core Power Distribution Test			X		X		X		X
4.5	Unit Loss Of Electrical Load Test									X
4.6	Turbine/Reactor Trip Test	Turbine Plus Reactor				X				
		Turbine Only						X		X
4.7	Incore Detector Test					X		X		
4.8	Power Imbalance Detector Correlation Test					X		X		
4.9	Nuclear Steam Supply System Heat Balance Test			X		X		X	X	X
4.10	Unit Load Steady State Test		X	X	X	X	X	X	X	X
4.11	Unit Load Transient Test					X		X		X
4.12	Shutdown From Outside The Control Room									X*
4.13	Pseudo Rod Ejection Test					X				
4.14	Dropped Control Rod Test					X		X		
4.15	Loss Of Offsite Power Test									X*

* Note: Done from 15% full power as part of the 100% full power plateau.

Table 4.0-2

Summary Of Power Escalation Performance Indicators

Test Plateau (%FP)	Testing Duration (Days)	Major Delays (Days)	Net Time (Days)	Unit Capacity Factor* Measured	Unit Capacity Factor* Estimated
15	3.3	0	3.3	0.66	0.65
40	14.3	23.0	37.3	0.75	0.85
75	19.3	0	19.3	0.74	0.78
100	27.7	0	27.7	0.62	0.75
Total	64.6	23.0	87.6	0.69	0.76

* Based on total MWh that could have been produced at a given test plateau.

4.1 NUCLEAR INSTRUMENTATION CALIBRATION AT POWER TEST

The power range instrumentation has four linear channels, (NI-5, NI-6, NI-7, NI-8) originating in four detector assemblies, each of which contains two uncompensated ion chambers. These ion chambers are positioned to represent the top and bottom halves of the core. The individual currents from the chambers are fed into individual linear amplifiers. The sum of the top and bottom neutron signals is the total reactor power. The difference between the top and bottom neutron signal multiplied by a gain factor is the power imbalance of the core. The outputs are directly proportional to reactor power and cover the range of 0 to 125% full power for the total power and -62.5 to +62.5% full power for the power imbalance. Each channel supplies power level information to the reactor protection system (RPS) and to the integrated control system (ICS). The gain of each linear amplifier is adjustable, providing a means for calibrating the outputs against a thermal heat balance and an incore axial imbalance measurement. The location of the out-of-core detectors relative to the reactor core is shown in Figure 4.1-1.

4.1.1 PURPOSE

The purpose of the Nuclear Instrumentation Calibration At Power Test was to calibrate the power range nuclear instrumentation to within 2.0% full power of the thermal power as determined by a heat balance and to within 3.5% incore axial offset as determined by the incore monitoring system. Additional purposes during the power escalation program were as follows:

(a) To adjust the high power level trip setpoint when required by the power escalation test procedure.

(b) To confirm that the nuclear instrumentation calibration procedure can adequately adjust the power range channels to a heat balance and an incore offset.

(c) To verify that at least one decade overlap exists between the intermediate and power range nuclear instrumentation.

Four acceptance criteria are specified for the Nuclear Instrumentation Calibration At Power Test as listed below:

(1) The power range nuclear instrumentation indicates the power level within 2.0% full power of the heat balance and within 3.5% incore axial offset. The incore axial offset criteria does not apply below 30% full power.

(2) The high power level trip bistable is set to trip at the desired value within a tolerance of +0.00 to -0.31% full power.

(3) The power range nuclear instrumentation can be calibrated adequately using the nuclear instrumentation calibration procedure.

(4) The overlap between the intermediate and power range is in excess of one decade overlap.

4.1.2 TEST METHOD

As required during power escalation, the top and bottom linear amplifier gains were adjusted to make the power range nuclear instrumentation channels indicate the measured heat balance power. The most conservative indication of reactor thermal power was obtained using weighted average heat balance on the unit computer. The gains were adjusted keeping their ratios the same if the offset was within tolerance of plus or minus 3.5 percent as determined by the incore monitoring system. If the offset needed to be adjusted, the gains were adjusted to correct the offset and heat balance mismatch at the same time.

During each adjustment, data was also taken to verify overlap between the intermediate and power range channels. The required overlap was a minimum of one decade between these two nuclear instrumentation ranges.

After all required testing was completed and approved at a major test plateau, the power escalation procedure then directed the high flux trip bistable setpoint to be re-adjusted. The major settings during power escalation are given below:

Test Plateau (%FP)	Bistable Setpoint (%FP)
15	35
40	50
75	85
100	104.7

The verification of the trip setpoint was then performed by placing each channel in the test mode and slowly increasing a test power signal until each bistable tripped. The difference between the actual power at which the bistable tripped and the setpoint trip power was the trip error recorded during each adjustment.

4.1.3 EVALUATION OF TEST RESULTS

An analysis of test results indicates that changes in reactor coolant system boron, cold leg temperature, control rod configuration, and xenon buildup or burnout affected the power indication as observed by the nuclear instrumentation. This was as expected since the power range nuclear instrumentation measured reactor neutron leakage which is directly related to the above changes in system conditions. As system conditions were changed, this resulted in a nuclear power range increase or decrease which often fell outside the calibration tolerances, thus requiring them to be calibrated. Early in the power escalation test program, some difficulties were experienced until procedural errors were resolved and instrumentation personnel experience increased. Also near the completion of the 40% full power plateau, the procedural method was modified from an on-line to off-line technique to assist in removing time dependent drift. However, each time that it was necessary to calibrate the power range nuclear instrumentation, the acceptance criteria of calibration to the heat balance power of ± 2.0%FP was met without any difficulty. Also each time it was necessary to calibrate the power range nuclear instrumentation, the ± 3.5% axial offset criteria as determined by the incore monitoring system was also met. Table 4.1-1 is a summary of the data taken during calibration at different power levels during power escalation testing.

The performance of the power imbalance detector correlation test has indicated that an acceptable relationship between incore and out-of-core imbalance on offset is obtained when a gain factor of 3.90 is employed. A detailed report on this gain factor adjustment is included in section 4.8 of this report.

The high flux level trip bistable was adjusted to 35, 50, 85, and 104.7% FP prior to escalation of power to 15, 40, 75, and 100% FP, respectively. Acceptance criteria of adjusting the setpoint to the above values within ± 0.00 to -0.31% FP was met each time without difficulty. The maximum trip error recorded was -0.08% FP when setting the high flux trip at 100% FP.

The actual overlap measured during the startup program exceeded the one decade overlap requirement. The overlap between the intermediate and power range channels covers the total span of the power range. Figure 4.1-2 shows the overlap of all three nuclear instrumentation channels.

4.1.4 CONCLUSIONS

The power range channels were calibrated to within 2.0% full power and to within 3.5% axial offset several times during the startup program. Total power was determined by a thermal heat balance, and axial incore offset was determined using the incore monitoring system as input to the calibration. The calibrations were required due to changes in xenon worth, reactor coolant system boron concentration and rod configuration during the power escalation test program. The calibration method has therefore, been thoroughly tested and has proven satisfactory.

The high flux level trip bistable was adjusted prior to each power level escalation to its respective trip setpoint. Verification of trip setpoint in all cases indicated that the maximum error in the setting is well within the acceptance criteria.

Table 4.1-1

Summary Of Nuclear Instrumentation Calibrations Performed At Power During The Power Escalation Test Program

Core Power (%FP)	Incore Offset (%)	Maximum NI Quad Tilt (%)	Power Before And After Calib. %FP				Offset Before And After Calib. %			
			NI-5	NI-6	NI-7	NI-8	NI-5	NI-6	NI-7	NI-8
15.38	+ 5.07	NA	15.95	15.28	14.91	15.19	+ 6.37	+ 7.02	+ 8.84	+ 6.18
15.08	- 0.86	NA	14.91	14.78	14.44	14.69	- 2.21	- 2.03	+ 0.13	- 1.84
26.72	+10.97	-1.03	24.07	22.35	22.22	23.10	+31.10	+15.20	+17.70	+10.60
25.65	- 0.97	-1.03	26.69	26.66	26.88	27.04	- 3.56	- 3.34	- 2.27	- 2.74
40.43	- 1.41	-0.93	40.60	40.40	40.90	40.90	- 6.33	- 5.45	- 5.31	- 4.99
38.94	- 4.52	-0.93	39.60	39.60	39.73	39.7	- 6.06	- 6.14	- 4.21	- 5.16
76.60	+ 0.67	-2.22	74.33	74.02	73.77	75.33	+ 0.07	+ 0.11	+ 0.37	- 1.92
76.50	- 1.30	-2.07	76.67	76.52	76.42	76.71	- 2.14	- 0.43	+ 0.14	- 0.03
91.02	- 4.46	-2.18	89.18	88.90	88.93	89.08	- 8.12	- 6.21	- 5.58	- 5.95
90.78	- 9.48	-2.37	92.02	91.71	91.24	92.55	- 7.09	-10.54	- 6.52	- 7.44
99.62	- 4.70	-2.28	97.62	98.56	96.81	98.40	- 1.84	- 1.84	- 1.37	- 2.28
100.47	- 7.73	-2.28	101.90	101.52	101.52	101.71	-10.54	-10.54	-10.40	-10.39

Nuclear Instrumentation Detector Location

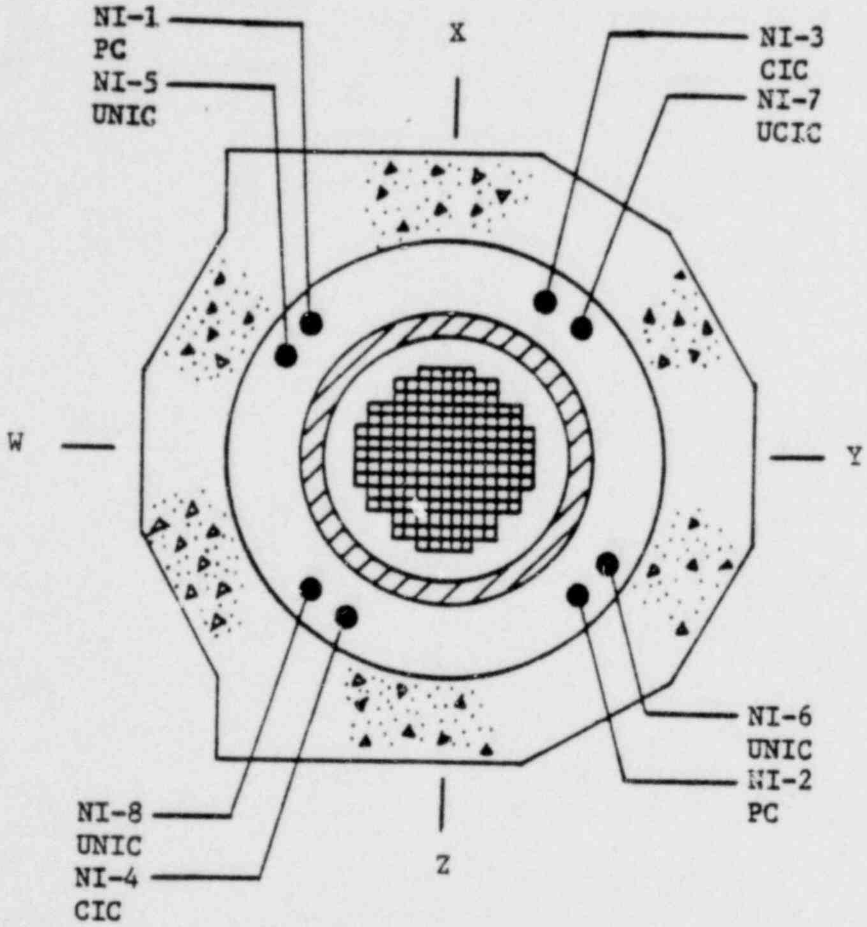

PC - Proportional Counter -------------- Source Range Detector

CIC - Compensated Ion Chamber ---------- Intermediate Range Detector

UNIC - Uncompensated Ion Chamber --------- Power Range Detector

Figure 4.1-1

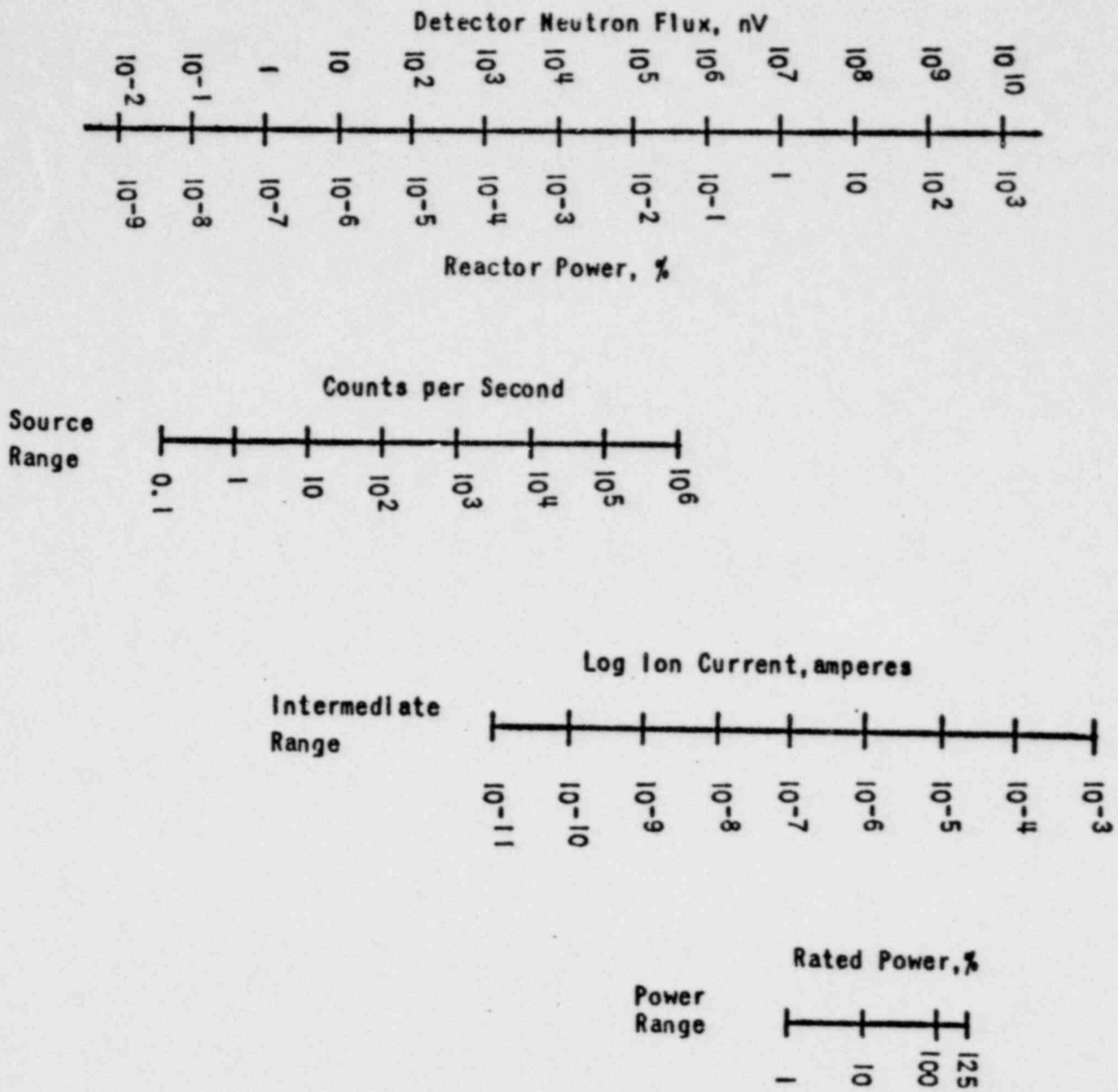

Figure 4.1-2

Nuclear Instrumentation Flux Ranges

4.2 BIOLOGICAL SHIELD SURVEY TEST

The biological shield on Crystal River Unit 3 is designed to attenuate radiation levels throughout the unit, from direct and scattered radiation, to the dose rate levels which comply with the radiation exposure limits specified in the Final Safety Analysis Report (FSAR). These limits are listed below for each type of zone classification:

Zone Classification	Dose Rate (mRem/hr)	Typical Location
Unlimited Occupancy	$\leq$ 0.5	Office, Control Room and Turbine Building
Normal Continuous Occupancy	$\leq$ 2.5	Auxiliary Building: Accessible Areas
Controlled, Limited Access	$\leq$15.0	Valve Galleries
Controlled, Limited Access	$\leq$ 25	Reactor Building: Accessible Areas
Restricted Access	>100	Restricted Access: Inside Secondary Shield

To ascertain that the above design criteria in regard to radiation fields have been met, testing of the installed biological shield was required during the power escalation test program.

This report presents the results of the biological shield survey test performed on Crystal River Unit 3 at 0, 40, and 100 percent full power. The test program was based on ANSI N18.9-1972 Program for Testing Biological Shielding in Nuclear Reactor Plants.

4.2.1 PURPOSE

The general purpose of the biological shield survey test was to measure dose rates in all accessible locations of the unit adjacent to the biological shield. The specific purposes were:

(a) To measure and record radiation levels of the normally accessible areas of the nuclear unit.

(b) To identify those locations where radiation levels do not meet design criteria.

(c) To obtain base-line radiation levels at various power levels for comparison with future measurements of activity buildup with operation.

(d) To identify and label radiation and high radiation areas.

Three acceptance criteria are specified for the Biological Shield Survey Test and are listed below:

(1) Radiation levels of the normally accessible areas of the nuclear unit have been measured with those locations not meeting the design criteria noted.

(2) Base-line radiation levels at various power levels have been established for future reference and comparison.

(3) Radiation and high radiation areas have been identified and posted.

4.2.2 TEST METHOD

The biological shield is defined as the effective shielding between the measurement location and the reactor vessel. Its principle shielding components are the primary shield wall, the secondary shield wall, the reactor building and the auxiliary building.

During the initial escalation in power from 0 to 100% FP, biological shield measurements at power levels of 0, 40, and 100% FP were performed to verify its ability to attenuate gamma and neutron radiation.

The test was performed by dividing all accessible areas into three different groups, each requiring a survey. The particular group surveys were:

(1) Reactor Building Interior Survey

(2) Reactor Building Periphery Survey

(3) Selected Unit Locations Survey

The reactor building interior survey was performed by a walk through survey of the normally accessible areas of the reactor building interior. At least one dose rate measurement was recorded for each stairway flight and each intermediate landing. If during the walk through, locally high radiation levels were encountered a complete scan of this area was performed. These areas were surveyed by traversing the survey instrument approximately waist-high and recording the highest reading observed.

The reactor building periphery survey was intended to scan normally accessible areas adjacent to the reactor building. Prior to performing this survey, accessible portions of the reactor building periphery were divided into a grid network. Each grid was then assigned a unique designation number of the form LLL-T-SSS, where:

LLL - Denoted the major floor, ground, or roof elevation in feet

T - Denoted the grid type: "A" indicated a grid from floor elevation to 4 feet above and "B" indicated a grid from 4 feet above floor elevation to 8 feet above

SSS - Denoted the section sequence number

During the measurement the entire extent of each grid section was scanned by holding the detector approximately 2 inches from the surface, with the highest reading encountered recorded.

The selected unit location survey consisted of 60 locations throughout the unit. These areas were confined to the following locations:

(1) Auxiliary Building

(2) Access Corridor To Reactor Building

(3) Intermediate Building

(4) Control Complex

(5) Turbine Building

(6) Reactor Building

At each location only gamma radiation measurements were required provided the reactor building periphery survey indicated no detectable neutron radiation. During the survey instrumentation was held approximately waist-high when taking readings.

Prior to performance of the above shield surveys at each power level, calibration of the survey instruments were performed. This calibration was also repeated at the completion of the surveys at each power levels. The surveys were obtained utilizing portable ionization and Geiger-Muller Detectors for gamma and BF_3 detectors for neutron.

4.2.3 EVALUATION OF TEST RESULTS

The reactor building interior survey was confined to floor elevations of 95 and 119 feet, since admittance within the secondary shield was prohibited when reactor power was greater than 1.0E-07 amps on the intermediate range detectors ($\sim$1% FP). On these two reactor building levels, points which represented whole body exposure were established alphabetically from A to Z as shown in Figures 4.2-1 and 4.2-2. Additional areas were also monitored whenever significant localized radiation was observed. During the survey, all locations except E, N, O and P met the design requirement of less than or equal to 25 mRem/hr as shown in Table 4.2-1. Of these only "E" was of a sufficient level to be considered a high radiation zone (i.e. >100 mRem/hr). The problem observed at "E" was that the shield penetration for the cavity cooling fans was providing a path for neutron and gamma streaming. Additional sources of high radiation levels were also caused by numerous localized penetrations which were providing paths for neutron and gamma streaming. In some cases, these localized areas did exceed 100 mRem/hr.

The reactor building periphery survey was conducted at elevations of 95, 119, 143, 162, and 195 feet and incorporated the survey of 582 grids. Each grid location at which radiation levels were observed during the shield test are listed in Table 4.2-2, with the levels measured at each plateau listed. As can be seen, only gamma type radiation was observed. The radiation levels in general have been lower than expected, with only a few areas having levels higher that the design value of less than or equal to 2.5 mRem/hr. The high values are attributable to piping within the auxiliary building.

The selected unit location survey was designed to monitor the radiation levels at specific points throughout the unit. The intent was to verify that normally accessible areas were within their respective design values. Table 4.2-3 presents the radiation levels monitored at these locations for the three test plateaus. In all cases, the dose rates measured were within their designed values.

4.2.4 CONCLUSIONS

Upon completion of the Biological Shield Survey Test, the following conclusions were reached:

(1) Radiation and high radiation areas have been identified and posted.

(2) Radiation levels at various points around the nuclear unit have been established for future reference and comparison.

(3) Areas in which radiation levels exceed their design values are undergoing further design evaluation. In the meantime they have been appropriately identified and marked.

Measured Dose Rates On Crystal River Unit 3
During The Reactor Building Interior Survey

POINT INDEX (X)	DESIGN DOSE RATE (mRem/hr)	0% FP PLATEAU DOSE RATE, mRem/hr			40% FP PLATEAU DOSE RATE, mRem/hr			100% FP PLATEAU DOSE RATE, mRem/hr		
		NEUTRON	GAMMA	TOTAL	NEUTRON	GAMMA	TOTAL	NEUTRON	GAMMA	TOTAL
A	$\leq$ 25.0	ND	ND	ND	ND	0.5	0.5	< 0.5	< 0.5	< 1.0
B	$\leq$ 25.0	ND	ND	ND	ND	1.5	1.5	0.5	< 0.5	< 1.0
C	$\leq$ 25.0	ND	ND	ND	ND	1.5	1.5	3.0	2.5	5.5
D	$\leq$ 25.0	ND	ND	ND	5.0	30.0	35.0	5.0	1.5	6.5
E	$\leq$ 25.0	ND	ND	ND	25.0	5.0	30.0	125.0	20.0	145.0
F	$\leq$ 25.0	ND	ND	ND	ND	1.5	1.5	2.0	3.0	5.0
G	$\leq$ 25.0	ND	ND	ND	ND	2.0	2.0	1.0	4.0	5.0
H	$\leq$ 25.0	ND	ND	ND	ND	3.5	3.5	0.5	6.0	6.5
I	$\leq$ 25.0	ND	ND	ND	ND	0.5	0.5	< 0.5	< 0.5	< 1.0
J	$\leq$ 25.0	ND	ND	ND	ND	0.5	0.5	< 0.5	< 0.5	< 1.0
K	$\leq$ 25.0	ND	ND	ND	0.5	0.5	1.0	< 0.5	0.5	< 1.0
L	$\leq$ 25.0	ND	ND	ND	ND	0.5	0.5	< 0.5	< 0.5	< 1.0
M	$\leq$ 25.0	ND	ND	ND	1.0	0.5	1.5	1.5	0.5	2.0
N	$\leq$ 25.0	ND	ND	ND	ND	15.0	15.0	< 0.5	55.5	<56.0
O	$\leq$ 25.0	ND	ND	ND	ND	30.0	30.0	< 0.5	55.5	<56.0
P	$\leq$ 25.0	ND	ND	ND	ND	45.0	45.0	< 0.5	80.0	<80.5
Q	$\leq$ 25.0	ND	ND	ND	ND	0.5	0.5	< 0.5	0.5	< 1.0
R	$\leq$ 25.0	ND	ND	ND	ND	0.5	9.5	< 0.5	10.0	<10.5
S	$\leq$ 25.0	ND	ND	ND	ND	5.0	5.0	< 0.5	15.0	<15.5
T	$\leq$ 25.0	ND	ND	ND	ND	2.0	2.0	< 0.5	0.5	< 1.0
U	$\leq$ 25.0	ND	ND	ND	1.5	0.5	2.0	2.5	2.0	4.5
V	$\leq$ 25.0	ND	ND	ND	ND	0.5	0.5	< 0.5	3.0	< 3.5
W	$\leq$ 25.0	ND	ND	ND	ND	20.0	20.0	< 0.5	18.0	<18.5
X	$\leq$ 25.0	ND	ND	ND	ND	0.5	0.5	< 0.5	0.5	< 1.0
Y	$\leq$ 25.0	ND	ND	ND	ND	0.5	0.5	< 0.5	0.5	< 1.0
Z	$\leq$ 25.0	ND	ND	ND	ND	0.5	0.5	< 0.5	0.5	< 1.0

Note: The definition of (ND) is none detected

Table 4.2-1

Table 4.2-2

Measured Dose Rates On Crystal River Unit 3 During
The Reactor Building Periphery Survey

POINT INDEX (LLL-T-SSS)	DESIGN DOSE RATE (mRem/hr)	0% FP PLATEAU DOSE RATE, mRem/hr			40% FP PLATEAU DOSE RATE, mRem/hr			100% FP PLATEAU DOSE RATE, mRem/hr		
		NEUTRON	GAMMA	TOTAL	NEUTRON	GAMMA	TOTAL	NEUTRON	GAMMA	TOTAL
095-A-001	≤ 2.5	ND	ND	ND	ND	ND	ND	ND	0.20	0.20
095-B-001	≤ 2.5	ND	ND	ND	ND	0.50	0.50	ND	0.20	0.20
095-A-002	≤ 2.5	ND	ND	ND	ND	ND	ND	ND	0.20	0.20
095-B-002	≤ 2.5	ND	ND	ND	ND	ND	ND	ND	0.60	0.60
095-A-003	≤ 2.5	ND	ND	ND	ND	ND	ND	ND	0.60	0.60
095-B-003	≤ 2.5	ND	ND	ND	ND	ND	ND	ND	0.60	0.60
095-A-004	≤ 2.5	ND	ND	ND	ND	ND	ND	ND	0.80	0.80
095-B-004	≤ 2.5	ND	ND	ND	ND	ND	ND	ND	0.80	0.80
095-A-005	≤ 2.5	ND	ND	ND	ND	0.50	0.50	ND	2.00	2.00
095-B-005	≤ 2.5	ND	ND	ND	ND	0.50	0.50	ND	2.00	2.00
095-A-006	≤ 2.5	ND	ND	ND	ND	ND	ND	ND	2.50	2.50
095-B-006	≤ 2.5	ND	ND	ND	ND	0.50	0.50	ND	3.50	3.50
095-A-007	≤ 2.5	ND	ND	ND	ND	ND	ND	ND	2.50	2.50
095-B-007	≤ 2.5	ND	ND	ND	ND	2.00	2.00	ND	3.50	3.50
095-A-008	≤ 2.5	ND	ND	ND	ND	ND	ND	ND	2.50	2.50
095-B-008	≤ 2.5	ND	ND	ND	ND	1.50	1.50	ND	4.00	4.00
095-A-009	≤ 2.5	ND	ND	ND	ND	ND	ND	ND	2.50	2.50
095-B-009	≤ 2.5	ND	ND	ND	ND	0.50	0.50	ND	5.00	5.00
095-A-010	≤ 2.5	ND	ND	ND	ND	ND	ND	ND	2.50	2.50
095-B-010	≤ 2.5	ND	ND	ND	ND	ND	ND	ND	3.50	3.50
095-A-011	≤ 2.5	ND	ND	ND	ND	ND	ND	ND	2.00	2.00
095-B-011	≤ 2.5	ND	ND	ND	ND	ND	ND	ND	2.50	2.50
095-A-012	≤ 2.5	ND	ND	ND	ND	ND	ND	ND	2.00	2.00
095-B-012	≤ 2.5	ND	ND	ND	ND	ND	ND	ND	2.50	2.50
095-A-013	≤ 2.5	ND	ND	ND	ND	ND	ND	ND	1.50	1.50
095-B-013	≤ 2.5	ND	ND	ND	ND	ND	ND	ND	1.50	1.50
095-A-014	≤ 2.5	ND	ND	ND	ND	ND	ND	ND	1.50	1.50
095-B-014	≤ 2.5	ND	ND	ND	ND	ND	ND	ND	1.50	1.50
095-A-015	≤ 2.5	ND	ND	ND	ND	ND	ND	ND	1.00	1.00
095-B-015	≤ 2.5	ND	ND	ND	ND	ND	ND	ND	1.00	1.00
095-A-016	≤ 2.5	ND	ND	ND	ND	ND	ND	ND	1.00	1.00

Note: Only grid sections with measurable radiation reported
Note: The definition of (ND) is none detec

Table 4.2-2 (Cont'd)

Measured Dose Rates On Crystal River Unit 3 During
The Reactor Building Periphery Survey

POINT INDEX (LLL-T-SSS)	DESIGN DOSE RATE (mRem/hr)	0% FP PLATEAU DOSE RATE, mRem/hr			40% FP PLATEAU DOSE RATE, mRem/hr			100% FP PLATEAU DOSE RATE, mRem/hr		
		NEUTRON	GAMMA	TOTAL	NEUTRON	GAMMA	TOTAL	NEUTRON	GAMMA	TOTAL
095-B-016	≤ 2.5	ND	ND	ND	ND	ND	ND	ND	1.00	1.00
095-A-017	≤ 2.5	ND	ND	ND	ND	ND	ND	ND	1.00	1.00
095-B-017	≤ 2.5	ND	ND	ND	ND	ND	ND	ND	1.00	1.00
095-A-018	≤ 2.5	ND	ND	ND	ND	ND	ND	ND	1.00	1.00
095-B-018	≤ 2.5	ND	ND	ND	ND	ND	ND	ND	1.00	1.00
095-A-019	≤ 2.5	ND	ND	ND	ND	ND	ND	ND	0.18	0.18
095-B-019	≤ 2.5	ND	ND	ND	ND	ND	ND	ND	0.18	0.18
095-A-020	≤ 2.5	ND	ND	ND	ND	ND	ND	ND	0.18	0.18
095-B-020	≤ 2.5	ND	ND	ND	ND	ND	ND	ND	0.18	0.18
095-A-021	≤ 2.5	ND	ND	ND	ND	ND	ND	ND	0.16	0.16
095-B-021	≤ 2.5	ND	ND	ND	ND	ND	ND	ND	0.18	0.18
095-A-022	≤ 2.5	ND	ND	ND	ND	ND	ND	ND	0.16	0.16
095-B-022	≤ 2.5	ND	ND	ND	ND	ND	ND	ND	0.16	0.16
095-A-023	≤ 2.5	ND	ND	ND	ND	ND	ND	ND	0.14	0.14
095-B-023	≤ 2.5	ND	ND	ND	ND	ND	ND	ND	0.14	0.14
095-A-024	≤ 2.5	ND	ND	ND	ND	ND	ND	ND	0.08	0.08
095-B-024	≤ 2.5	ND	ND	ND	ND	ND	ND	ND	0.08	0.08
095-A-025	≤ 2.5	ND	ND	ND	ND	ND	ND	ND	0.06	0.06
095-B-025	≤ 2.5	ND	ND	ND	ND	ND	ND	ND	0.06	0.06
095-A-026	≤ 2.5	ND	ND	ND	ND	ND	ND	ND	0.04	0.04
095-B-026	≤ 2.5	ND	ND	ND	ND	ND	ND	ND	0.04	0.04
095-A-027	≤ 2.5	ND	ND	ND	ND	ND	ND	ND	0.04	0.04
095-B-027	≤ 2.5	ND	ND	ND	ND	ND	ND	ND	0.04	0.04
095-A-028	≤ 2.5	ND	ND	ND	ND	ND	ND	ND	0.02	0.02
095-B-028	≤ 2.5	ND	ND	ND	ND	ND	ND	ND	0.02	0.02
095-A-093	≤ 2.5	ND	ND	ND	ND	ND	ND	ND	0.10	0.10
095-B-093	≤ 2.5	ND	ND	ND	ND	ND	ND	ND	0.04	0.04
095-A-094	≤ 2.5	ND	ND	ND	ND	ND	ND	[illegible]	1.00	1.00
095-B-094	≤ 2.5	ND	ND	ND	ND	ND	ND	ND	0.50	0.50
095-A-095	≤ 2.5	ND	ND	ND	ND	ND	ND	ND	0.02	0.02
095-B-095	≤ 2.5	ND	ND	ND	ND	ND	ND	ND	0.14	0.14

Note: Only grid sections with measurable radiation reported
Note: The definition of (ND) is none detected

Table 4.2-2 (Cont'd)

Measured Dose Rates On Crystal River Unit 3 During
The Reactor Building Periphery Survey

POINT INDEX (LLL-T-SSS)	DESIGN DOSE RATE (mRem/hr)	0% FP PLATEAU DOSE RATE, mRem/hr			40% FP PLATEAU DOSE RATE, mRem/hr			100% FP PLATEAU DOSE RATE, (mRem/hr)		
		NEUTRON	GAMMA	TOTAL	NEUTRON	GAMMA	TOTAL	NEUTRON	GAMMA	TOTAL
095-A-096	$\leq$ 2.5	ND	ND	ND	ND	ND	ND	ND	0.02	0.02
095-B-096	$\leq$ 2.5	ND	ND	ND	ND	ND	ND	ND	0.02	0.02
119-A-004	$\leq$ 2.5	ND	ND	ND	ND	1.50	1.50	ND	4.50	4.50
119-B-004	$\leq$ 2.5	ND	ND	ND	ND	2.00	2.00	ND	4.00	4.00
119-A-005	$\leq$ 2.5	ND	ND	ND	ND	1.00	1.00	ND	2.00	2.00
119-B-005	$\leq$ 2.5	ND	ND	ND	ND	1.00	1.00	ND	3.00	3.00
119-A-006	$\leq$ 2.5	ND	ND	ND	ND	1.00	1.00	ND	1.50	1.50
119-B-006	$\leq$ 2.5	ND	ND	ND	ND	1.00	1.00	ND	2.00	2.00
119-A-007	$\leq$ 2.5	ND	ND	ND	ND	1.50	1.50	ND	2.00	2.00
119-B-007	$\leq$ 2.5	ND	ND	ND	ND	2.00	2.00	ND	2.00	2.00
119-A-008	$\leq$ 2.5	ND	ND	ND	ND	1.50	1.50	ND	1.50	1.50
119-B-008	$\leq$ 2.5	ND	ND	ND	ND	1.00	1.00	ND	1.50	1.50
119-A-009	$\leq$ .25	ND	ND	ND	ND	1.50	1.50	ND	0.50	0.50
119-B-009	$\leq$ 2.5	ND	ND	ND	ND	1.00	1.00	ND	1.00	1.00
119-A-010	$\leq$ 2.5	ND	ND	ND	ND	1.00	1.00	ND	1.00	1.00
119-B-010	$\leq$ 2.5	ND	ND	ND	ND	1.00	1.00	ND	1.00	1.00
119-A-011	$\leq$ 2.5	ND	ND	ND	ND	1.50	1.50	ND	1.00	1.00
199-B-011	$\leq$ 2.5	ND	ND	ND	ND	1.50	1.50	ND	1.00	1.00
119-A 012	$\leq$ 2.5	ND	ND	ND	ND	1.50	1.50	ND	1.00	1.00
119-B-012	$\leq$ 2.5	ND	ND	ND	ND	1.50	1.50	ND	1.00	1.00
119-A-013	$\leq$ 2.5	ND	ND	ND	ND	1.00	1.00	ND	1.00	1.00
119-B-013	$\leq$ 2.5	ND	ND	ND	ND	1.50	1.50	ND	1.50	1.50
119-A-014	$\leq$ 2.5	ND	ND	ND	ND	1.50	1.50	ND	1.00	1.00
119-B-014	$\leq$ 2.5	ND	ND	ND	ND	1.50	1.50	ND	1.00	1.00
119-A-015	$\leq$ 2.5	ND	ND	ND	ND	1.50	1.50	ND	1.00	1.00
119-B-015	$\leq$ 2.5	ND	ND	ND	ND	1.00	1.00	ND	1.00	1.00
119-A-016	$\leq$ 2.5	ND	ND	ND	ND	1.00	1.00	ND	1.00	1.00
119-B-016	$\leq$ 2.5	ND	ND	ND	ND	1.00	1.00	ND	1.00	1.00
119-A-017	$\leq$ 2.5	ND	ND	ND	ND	0.50	0.50	ND	1.00	1.00
119-B-017	$\leq$ 2.5	ND	ND	ND	ND	0.50	0.50	ND	1.00	1.00
119-A-018	$\leq$ 2.5	ND	ND	ND	ND	1.00	1.00	ND	1.00	1.00

Note: Only grid sections with measurable radiation reported
Note: The definition of (ND) is none det[illegible]d

Table 4.2-2 (Cont'd)

Measured Dose Rates On Crystal River Unit 3 During The Reactor Building Periphery Survey

POINT INDEX (LLL-T-SSS)	DESIGN DOSE RATE (mRem/hr)	0% FP PLATEAU DOSE RATE, mRem/hr			40% FP PLATEAU DOSE RATE, mRem/hr			100% FP PLATEAU DOSE RATE, mRem/hr		
		NEUTRON	GAMMA	TOTAL	NEUTRON	GAMMA	TOTAL	NEUTRON	GAMMA	TOTAL
119-B-018	≤ 2.5	ND	ND	ND	ND	1.00	1.00	ND	0.02	0.02
162-A-004	≤ 2.5	ND	ND	ND	ND	ND	ND	ND	0.02	0.02
162-B-004	≤ 2.5	ND	ND	ND	ND	ND	ND	ND	0.04	0.04
162-A-005	≤ 2.5	ND	ND	ND	ND	ND	ND	ND	0.04	0.04
162-B-005	≤ 2.5	ND	ND	ND	ND	ND	ND	ND	0.06	0.06
162-A-006	≤ 2.5	ND	ND	ND	ND	ND	ND	ND	0.06	0.06
162-B-006	≤ 2.5	ND	ND	ND	ND	ND	ND	ND	0.06	0.06
162-A-007	≤ 2.5	ND	ND	ND	ND	ND	ND	ND	0.06	0.06
162-B-007	≤ 2.5	ND	ND	ND	ND	ND	ND	ND	0.06	0.06
162-A-008	≤ 2.5	ND	ND	ND	ND	ND	ND	ND	0.06	0.06
162-B-008	≤ 2.5	ND	ND	ND	ND	ND	ND	ND	0.06	0.06
162-A-009	≤ 2.5	ND	ND	ND	ND	ND	ND	ND	0.04	0.04
162-B-009	≤ 2.5	ND	ND	ND	ND	ND	ND	ND	0.04	0.04
162-A-010	≤ 2.5	ND	ND	ND	ND	ND	ND	ND	0.02	0.02
162-B-010	≤ 2.5	ND	ND	ND	ND	ND	ND	ND	0.02	0.02

Note: Only grid sections with measurable radiation reported
Note: The definition of (ND) is none detected

Table 4.2-3

Measured Dose Rates On Crystal River Unit 3 During
The Selected Unit Locations Survey

POINT INDEX (XX)	DESIGN DOSE RATE (mRem/hr)	0% FP PLATEAU			40% FP PLATEAU			100% FP PLATEAU		
		DOSE RATE, mRem/hr			DOSE RATE, mRem/hr			DOSE RATE, mRem/hr		
		NEUTRON	GAMMA	TOTAL	NEUTRON	GAMMA	TOTAL	NEUTRON	GAMMA	TOTAL
A. Auxiliary Building										
01	≤ 2.5	ND	ND	ND	ND	ND	ND	NR	< 0.5	< 0.5
02	≤ 2.5	ND	ND	ND	ND	ND	ND	NR	< 0.5	< 0.5
03	≤ 2.5	ND	ND	ND	ND	ND	ND	NR	< 0.5	< 0.5
04	≤ 2.5	ND	ND	ND	ND	ND	ND	NR	< 0.5	< 0.5
05	≤ 2.5	ND	ND	ND	ND	ND	ND	NR	< 0.5	< 0.5
06	≤ 2.5	ND	ND	ND	ND	ND	ND	NR	< 0.5	< 0.5
07	≤ 2.5	ND	ND	ND	ND	ND	ND	NR	< 0.5	< 0.5
08	≤ 2.5	ND	ND	ND	ND	ND	ND	NR	< 0.5	< 0.5
09	≤ 2.5	ND	ND	ND	ND	ND	ND	NR	< 0.5	< 0.5
10	≤ 2.5	ND	ND	ND	ND	ND	ND	NR	< 0.5	< 0.5
11	≤ 2.5	ND	ND	ND	ND	ND	ND	NR	< 0.5	< 0.5
12	≤ 2.5	ND	ND	ND	ND	ND	ND	NR	< 0.5	< 0.5
13	≤ 2.5	ND	ND	ND	ND	< 0.5	< 0.5	NR	< 0.5	< 0.5
14	≤ 2.5	ND	ND	ND	ND	ND	ND	NR	< 0.5	< 0.5
15	≤ 2.5	ND	ND	ND	ND	ND	ND	NR	< 0.5	< 0.5
16	≤ 2.5	ND	ND	ND	ND	1.5	1.5	NR	< 0.5	< 0.5
17	≤ 2.5	ND	ND	ND	ND	ND	ND	NR	< 0.5	< 0.5
18	≤ 2.5	ND	ND	ND	ND	ND	ND	NR	< 0.5	< 0.5
19	≤ 2.5	ND	ND	ND	ND	ND	ND	NR	< 0.5	< 0.5
20	≤ 2.5	ND	ND	ND	ND	ND	ND	NR	< 0.5	< 0.5
21	≤ 2.5	ND	ND	ND	ND	1.5	1.5	NR	1.5	1.5
22	≤ 2.5	ND	ND	ND	ND	ND	ND	NR	< 0.5	< 0.5
23	≤ 2.5	ND	ND	ND	ND	ND	ND	NR	< 0.5	< 0.5
24	≤ 2.5	ND	ND	ND	ND	ND	ND	NR	< 0.5	< 0.5
25	≤ 2.5	ND	ND	ND	ND	ND	ND	NR	< 0.5	< 0.5
26	≤ 2.5	ND	ND	ND	ND	ND	ND	NR	< 0.5	< 0.5
B. Access Corridor To Reactor Building										
27	≤ 2.5	ND	ND	ND	ND	ND	ND	NR	< 0.5	< 0.5

Note: The definition of (ND) is none detected
Note: The definition of (NR) is not requ[illegible]

Table 4.2-3 (Cont'd)

Measured Dose Rates On Crystal River Unit 3 During
The Selected Unit Locations Survey

POINT INDEX (XX)	DESIGN DOSE RATE (mRem/hr)	0% FP PLATEAU DOSE RATE, mRem/hr			40% FP PLATEAU DOSE RATE, mRem/hr			100% FP PLATEAU DOSE RATE, mRem/hr		
		NEUTRON	GAMMA	TOTAL	NEUTRON	GAMMA	TOTAL	NEUTRON	GAMMA	TOTAL
28	≤ 2.5	ND	ND	ND	ND	ND	ND	NR	< 0.5	< 0.5
29	≤ 2.5	ND	ND	ND	ND	ND	ND	NR	< 0.5	< 0.5
30	≤ 2.5	ND	ND	ND	ND	ND	ND	NR	< 0.5	< 0.5
31	≤ 2.5	ND	ND	ND	ND	ND	ND	NR	< 0.5	< 0.5
32	≤ 2.5	ND	ND	ND	ND	ND	ND	NR	< 0.5	< 0.5
C. Intermediate Building										
33	≤ 2.5	ND	ND	ND	ND	ND	ND	NR	< 0.5	< 0.5
34	≤ 2.5	ND	ND	ND	ND	ND	ND	NR	< 0.5	< 0.5
35	≤ 2.5	ND	ND	ND	ND	ND	ND	NR	< 0.5	< 0.5
36	≤ 2.5	ND	ND	ND	ND	ND	ND	NR	< 0.5	< 0.5
37	≤ 2.5	ND	ND	ND	ND	ND	ND	NR	< 0.5	< 0.5
38	≤ 2.5	ND	ND	ND	ND	ND	ND	NR	< 0.5	< 0.5
39	≤ 2.5	ND	ND	ND	ND	ND	ND	NR	< 0.5	< 0.5
D. Control Complex										
40	≤ 0.5	ND	ND	ND	ND	ND	ND	NR	< 0.5	< 0.5
41	≤ 0.5	ND	ND	ND	ND	ND	ND	NR	< 0.5	< 0.5
42	≤ 0.5	ND	ND	ND	ND	ND	ND	NR	< 0.5	< 0.5
43	≤ 0.5	ND	ND	ND	ND	ND	ND	NR	< 0.5	< 0.5
44	≤ 0.5	ND	ND	ND	ND	ND	ND	NR	< 0.5	< 0.5
45	≤ 0.5	ND	ND	ND	ND	ND	ND	NR	< 0.5	< 0.5
46	≤ 0.5	ND	ND	ND	ND	ND	ND	NR	< 0.5	< 0.5
47	≤ 0.5	ND	ND	ND	ND	ND	ND	NR	< 0.5	< 0.5
48	≤ 0.5	ND	ND	ND	ND	ND	ND	NR	< 0.5	< 0.5
49	≤ 0.5	ND	ND	ND	ND	ND	ND	NR	< 0.5	< 0.5
E. Turbine Building										
50	≤ 0.5	ND	ND	ND	ND	ND	ND	NR	< 0.5	< 0.5
51	≤ 0.5	ND	ND	ND	ND	ND	ND	NR	< 0.5	< 0.5

Note: The definition of (ND) is none detected
Note: The definition of (NR) is not required

Measured Dose Rates On Crystal River Unit 3 During
The Selected Unit Locations Survey

POINT INDEX (XX)	DESIGN DOSE RATE (mRem/hr)	0% FP PLATEAU DOSE RATE, mRem/hr			40% FP PLATEAU DOSE RATE, mRem/hr			100% FP PLATEAU DOSE RATE, mRem/hr		
		NEUTRON	GAMMA	TOTAL	NEUTRON	GAMMA	TOTAL	NEUTRON	GAMMA	TOTAL
52	≤ 2.5	ND	ND	ND	ND	ND	ND	NR	< 0.5	< 0.5
53	≤ 2.5	ND	ND	ND	ND	ND	ND	NR	< 0.5	< 0.5
54	≤ 2.5	ND	ND	ND	ND	ND	ND	NR	< 0.5	< 0.5
55	≤ 2.5	ND	ND	ND	ND	ND	ND	NR	< 0.5	< 0.5
56	≤ 2.5	ND	ND	ND	ND	ND	ND	NR	< 0.5	< 0.5
57	≤ 2.5	ND	ND	ND	ND	ND	ND	NR	< 0.5	< 0.5
58	≤ 2.5	ND	ND	ND	ND	ND	ND	NR	< 0.5	< 0.5
59	≤ 2.5	ND	ND	ND	ND	ND	ND	NR	< 0.5	< 0.5
F. Reactor Building										
60	≤ 25.0	ND	ND	ND	ND	ND	ND	NR	< 0.5	< 0.5

Note: The definition of (ND) is none detected
Note: The definition of (NR) is not requi

Table 4.2-3 (Cont'd)

Location Of Whole Body Exposure Points Inside The Reactor Building At Elevation Of 95 Feet

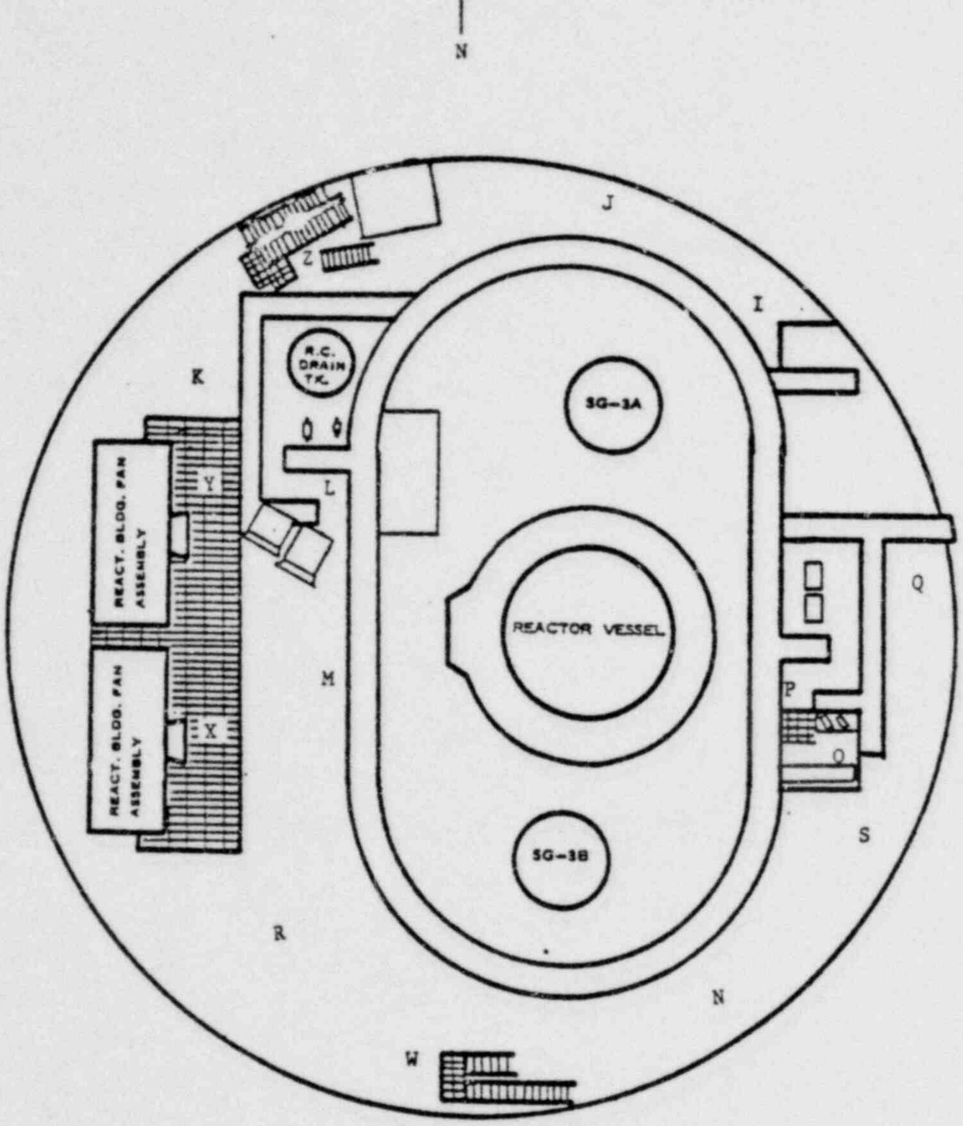

Figure 4.2-1

Location Of Whole Body Exposure Points Inside The Reactor Building At Elevation Of 119 Feet

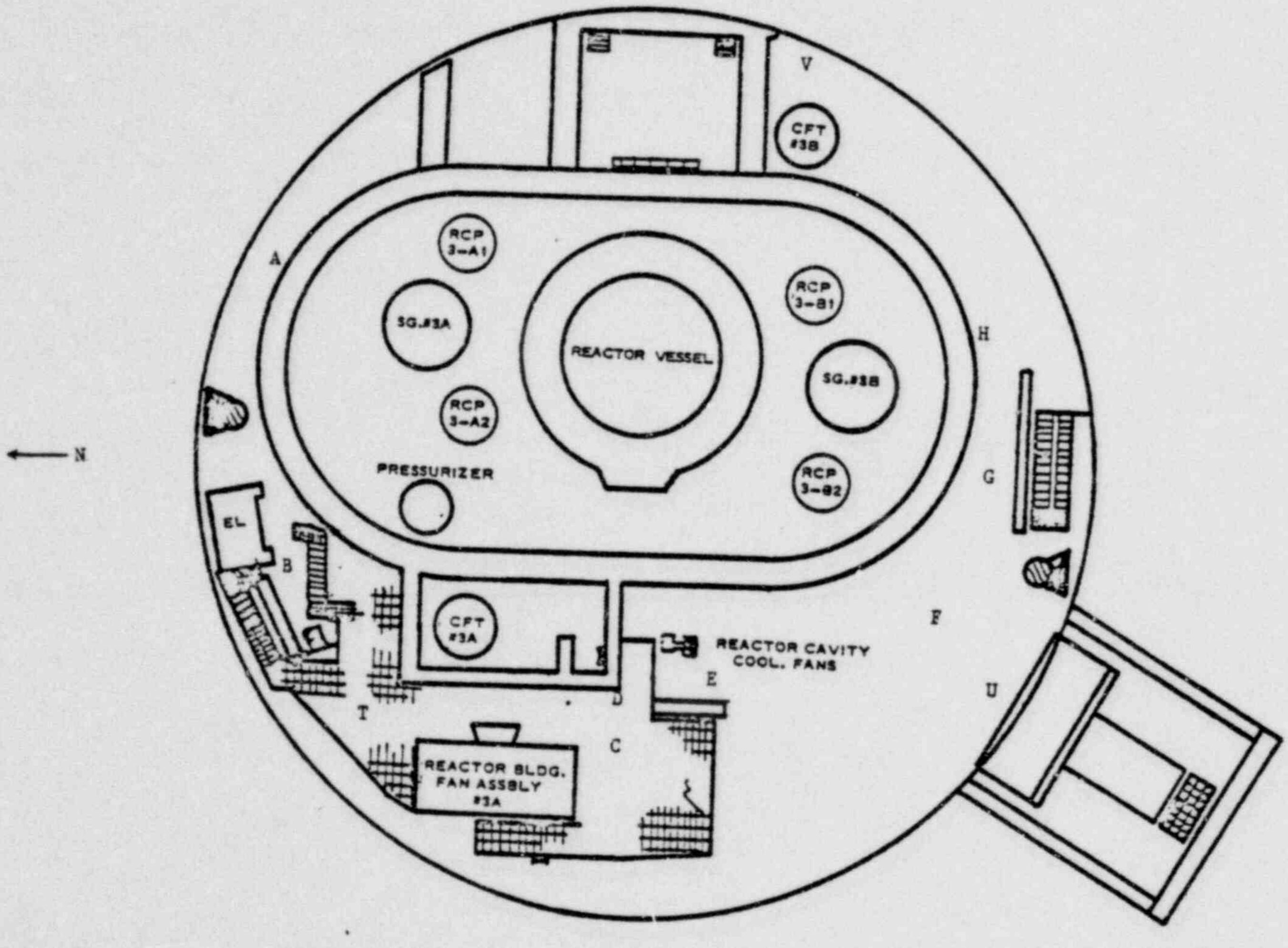

Figure 4.2-2

4.3 REACTIVITY COEFFICIENTS AT POWER TEST

4.3.1 PURPOSE

The purpose of this test was to measure reactivity coefficients during power operation at 40, 75, and 100 percent full power, and to verify that they were conservative with respect to the FSAR. The following coefficients were either measured or calculated from the data obtained.

(a) Temperature coefficient of reactivity, defined as the fractional change in the reactivity of the core per unit change in fuel and moderator temperature.

(b) Moderator coefficient of reactivity, defined as the fractional change in the reactivity of the core per unit change in moderator temperature.

(c) Power Doppler coefficient of reactivity, defined as the fractional change in the reactivity of the core per unit change in power.

(d) Doppler coefficient of reactivity, defined as the fractional change in the reactivity of the core per unit change in fuel temperature.

Three acceptance criteria are specified for the Reactivity Coefficients at Power Test and are listed below:

(1) The moderator coefficient of reactivity measured at 40 and 75% full power shall be less than $+0.90 \times 10^{-4} \Delta k/k/^{\circ}F$.

(2) The moderator coefficient of reactivity measured at 100% full power shall be less than $0.00 \times 10^{-4} \Delta k/k/^{\circ}F$.

(3) The power Doppler coefficient of reactivity shall be more negative than $-0.55 \times 10^{-4} \Delta k/k/\%FP$.

4.3.2 TEST METHOD

Reactivity coefficient measurements were made during the power escalation test program at core power levels of 40, 75, and 100% full power. No measurements were made at 15% full power because of the change in control mode from changing T_{AVE} to constant T_{AVE} which occurs around 15% full power. This change makes reactivity coefficient measurements impractical at 15% full power.

Differential rod worth measurements were executed at each steady state plateau during the reactivity coefficient measurement in order to generate rod worth data for the specific test conditions. For temperature coefficients, average reactor coolant temperature was increased or decreased about 5°F and data recorded. For power Doppler coefficients, power was decreased about 5 percent full power and data recorded. From the measured temperature and power Doppler coefficients, the moderator and Doppler coefficients were calculated.

4.3.2.1 TEMPERATURE AND MODERATOR COEFFICIENTS

The temperature coefficient of reactivity is defined as the fractional change in the reactivity of the core per unit change in fuel and moderator temperature. The temperature coefficient is normally divided into two components as shown in equation 4.3-1.

$\alpha_T = \alpha_M + \alpha_D$ EQ. (4.3-1)

Where: α_T = Temperature Coefficient of Reactivity

α_M = Moderator Coefficient of Reactivity

α_D = Doppler Coefficient of Reactivity

The moderator coefficient cannot be directly measured in an operating reactor because a change in the moderator temperature also causes a similar change in the fuel temperature. Therefore, the moderator coefficient must be calculated using equation 4.3-1 after the temperature and Doppler coefficients have been determined. Technical Specifications, section 3.1.1.3, requires that the moderator coefficient be less than $+0.90 \times 10^{-4} \Delta k/k/^{\circ}F$ at power levels below 95% full power and non-positive at or above 95% full power.

Temperature and moderator coefficients were theoretically predicted at various power levels as shown in Figures 4.3-1 and 4.3-2 using the distributed moderator and fuel temperatures instead of the isothermal values which were used for zero power physics predictions. For these predictions, the normal mode of operation with critical boron and rod conditions was assumed which set the average core moderator temperature equal to 579°F.

The measurement method used at power is to change the reactor coolant temperature setpoint at the reactor control station with the integrated control system in automatic effecting an approximate 5°F change in the reactor coolant temperature. The reactivity change caused by the temperature change of the core was measured by recording the change in the position of the controlling control rod group and converting this change to reactivity using differential rod worth values measured during the test. Prior to running the test, steady state equilibrium xenon conditions including a stable boron concentration and no significant control rod motion during the last 30 minutes prior to taking data were required as prerequisite system conditions.

4.3.2.2 POWER DOPPLER AND DOPPLER COEFFICIENTS

The Doppler coefficient relates the change in core reactivity to a corresponding change in fuel temperature. The Doppler effect is a negative reactivity contribution arising from the Doppler broadening of the U-238 neutron capture cross sections in the resonance or high energy region. An increase in fuel temperature increases the effective absorption of neutrons within the fuel which decreases the core excess reactivity. The Doppler coefficient of reactivity is not measured directly in an operating reactor because the fuel temperature cannot be readily measured. However, the Doppler coefficient must be determined in order to calculate the moderator temperature coefficient. Thus an indirect approach is taken: The power Doppler coefficient of reactivity is measured and the Doppler coefficient is calculated using the calculated fuel temperature change associated with a power level change according to Figure 4.3-3. Mathematically, the Doppler coefficient is related to the power Doppler coefficient as follows:

$\alpha_D = (\Delta P/\Delta T_f)\ \alpha_{PD}$ EQ. (4.3-2)

Where: α_D = Doppler Coefficient of Reactivity

α_{PD} = Power Doppler Coefficient of Reactivity

$\Delta P/\Delta T_f$ = Change in Power per Unit Change in Fuel Temperature

The power Doppler coefficient relates the change in core reactivity to a corresponding change in power. Theoretical predictions of the power Doppler coefficient were made using a three-dimensional PDQ code with thermal feedback. The predicted power Doppler coefficients using this code are presented in Figure 4.3-4.

The measurement method used was to change the reactor power level 5 percent full power. This change in power level was initiated by manually decreasing the reactor power at the reactor master control station. After obtaining approximately ten minutes of steady state data at the reduced power level, reactor power was returned to the initial power.

The calculation of the power Doppler coefficient uses the measured change in the controlling rod group position converted to an equivalent reactivity value and the measured change in reactor power determined by using the normalized core ΔT which is the primary side heat balance.

4.3.2.3 DIFFERENTIAL ROD WORTH AT POWER

The method by which the differential rod worth was determined at power is the fast insertion/withdrawal method. In this measurement, the controlling rod group is inserted for approximately six seconds, followed immediately by a withdrawal for approximately six seconds. Since the total elapsed time is on the order of the primary loop recirculation time, the moderator temperature effects are eliminated and the reactivity versus time is essentially a combination of the effects due to the control rod motion and the fuel power variation. A typical plot of the response of the reactivity, rod position, and fuel power is shown in Figure 4.3-6.

Determination of the differential rod worth was then found by using the measured reactivity and rod positions, compensating the data by a predicted fuel power correction factor. Mathematically, this is expressed as:

$$d\rho/dh = (CF)\ (2\rho 2 - \rho 1 - \rho 3)\ /\ (2H2 - H1 - H3) \quad \text{EQ. (4.3-3)}$$

Where:
- H1 = CRA (s) position (%) prior to motion
- H2 = CRA (s) position (%) after the insertion but prior to withdrawal
- H3 = CRA (s) position (%) after the withdrawal is terminated
- $\rho 1$ = Reactivity prior to CRA motion ($\Delta k/k$)
- $\rho 2$ = Reactivity after the insertion but prior to the withdrawal ($\Delta k/k$)
- $\rho 3$ = Reactivity after the withdrawal is terminated ($\Delta k/k$)
- CF = Fuel Power Correction Factor (none)

The fuel power correction factor accounts for the time delay involved in fuel temperature change during the measurement and is given by the equation below:

$$CF = 1 + (CC)\ (P1)$$

Where:
- CF = Fuel Power Correction Factor (none)
- CC = Correlation constant (BOL = $0.0053\%FP^{-1}$)
- P1 = Fuel power prior to motion (%FP)

By application of the above two equations, the differential rod worth during the reactivity coefficient at power test was determined.

4.3.3 EVALUATION OF TEST RESULTS

The results of the measured temperature and calculated moderator coefficients at power are tabulated in Table 4.3-1 and plotted in Figures 4.3-1 and 4.3-2 which also shows the predicted temperature and moderator coefficient results. A tabulation of the measured data used to determine the temperature coefficient at the 40, 75, and 100% full power plateaus is also furnished for each measurement in Tables 4.3-2 through 4.3-4.

Examination of the calculated moderator coefficients as plotted in Figure 4.3-2 indicates that the limit of a non-positive value will not be exceeded at 95 percent full power unless the soluble poison concentration is in the range of 1120 ppmB. Measured results show that the soluble poison concentration for equilibrium-xenon all-rods-out condition is about 1020 ppmB. This confirmed that during power operation at or above 95 percent full power the moderator coefficient will be negative even if all control rods are withdrawn from the core.

The results of the measured and predicted power Doppler coefficient of reactivity are tabulated in Table 4.3-1 and plotted in Figure 4.3-4. A tabulation of the measured data used to determine the power Doppler coefficient at the 40, 75, and 100% full power plateau is also furnished for each measurement in Tables 4.3-5 through 4.3-7.

The acceptance criterion for the measured power Doppler coefficient is that the coefficient must be more negative than $-0.55 \times 10^{-4} \Delta k/k/\%FP$. Figure 4.3-4 shows that all measured coefficients are below this value and that the acceptance criterion is adequately met. In addition, all calculated Doppler coefficients were also within their respective acceptance criteria.

Examination of the measured power Doppler coefficient indicates a slightly more negative value than predicted which results in a reactivity deficit versus power more negative than originally predicted. A comparison of the measured and predicted power Doppler reactivity deficit versus power level is shown in Figure 4.3-5. The total measured reactivity deficit between 0 and 100 percent full power is estimated at -1.10 percent $\Delta k/k$ in core excess reactivity available for Cycle 1 lifetime.

The results of the differential rod worth measurement performed as part of the Reactivity Coefficient At Power Test are shown in Tables 4.3-8 through 4.3-10. It should be noted that the maximum value measured was $0.0202\%\Delta k/k/\%wd$ which is well within the maximum allowable design value of less than $0.0303\%\Delta k/k/\%wd$ at hot full power.

To ensure that these differential rod worths were correct, verification of the correlation constant used in the fuel power correction factor was also performed at 40, 75, and 100% full power. In all cases, favorable agreement was obtained.

4.3.4 CONCLUSIONS

The measured results at 40, 75, and 100% full power indicates that the moderator coefficient of reactivity will be negative during power operation above 95% full power. Comparison between predicted and measured temperature coefficients of reactivity showed favorable agreement.

Analyzed data for the power Doppler coefficient versus power level indicates that the least negative coefficient is $-1.02 \times 10^{-4} \Delta k/k/\%FP$ which is sufficiently below the acceptance criterion of $-0.55 \times 10^{-4} \Delta k/k/\%FP$. The total power Doppler deficit from this measured data is projected at $-1.10\% \Delta k/k$.

Table 4.3-1

Summary Of Measured, Calculated, And Predicted Coefficients Of Reactivity At Power

Average Power (%FP)	Incore Offset (%)	Rod Position, % wd				Boron Conc. (ppm)	Core Burnup (EFPD)	Coefficient of Reactivity, 10^{-4} $\Delta k/k$			
		1-5	6	7	8			Measured	Predicted	Calculated	Predicted
A. Temperature And Moderator Coefficient								Temperature		Moderator	
40.0	-2.0	100	96	21	18	1034	1.9	-0.34	-0.24	-0.14	-0.06
70.8	+0.6	100	88	10	17	956	7.7	-0.52	-0.40	-0.34	-0.25
93.6	-2.1	100	94	15	8	916	18.3	-0.46	-0.49	-0.28	-0.36
B. Power Doppler And Doppler Coefficient								Power Doppler		Doppler	
36.9	-2.0	100	94	19	18	1034	1.9	-1.12	-0.99	-0.20	-0.18
71.8	+0.6	100	88	13	17	956	7.7	-1.05	-0.97	-0.18	-0.17
91.1	-2.1	100	93	12	8	916	18.3	-1.02	-0.96	-0.18	-0.17

Table 4.3-2

Temperature Coefficient Measurement Calculation At 40% Full Power

REACTIVITY CONTROLLING PARAMETERS	TEMPERATURE COEFFICIENT ANALYSIS (Up)	(Down)	UNITS
T_1 (initial avg. reactor coolant temp.)	578.58	583.57	°F
T_2 (final avg. reactor coolant temp.)	583.57	576.81	°F
$\Delta T = (T_1 - T_2)$	-4.89	+6.76	°F
H_1 (initial controlling CRA Group Position)	96.48/20.90	96.49/20.90	%wd
H_2 (final controlling CRA Group Position)	96.49/20.90	96.50/20.90	%wd
ΔH (change in rod position during measurement)	0.01/0.00	0.01/0.00	%wd
$\Delta k/k/\Delta H$ (differential rod worth values)	0.0168	0.0168	$\%\Delta k/k/\Delta H$
P_1 (initial power level)	40.76	39.16	%FP
P_2 (final power level)	39.16	41.01	%FP
ΔP (change in power due to temperature change)	-1.60	+1.85	%FP
α_{PD} (Power doppler coefficient)	-0.0112	-0.0112	$\%\Delta k/k/\Delta P$
Boron Concentration	1034	1034	ppmB
$\rho_{xe\ 1}$ (initial xenon reactivity worth)	-2.0234	-2.0245	$\%\Delta k/k$
$\rho_{xe\ 2}$ (final xenon reactivity worth)	-2.0245	-2.0256	$\%\Delta k/k$
* $(\Delta k/k/\Delta H)(\Delta H)$	0.0000	0.0000	$\%\Delta k/k$
* $(\alpha_{PD})(\Delta P)$	+0.0179	-0.0208	$\%\Delta k/k$
* $\Delta\rho_{xe}$ (avg. reactivity change due to Xe)	-0.0006	-0.0011	$\%\Delta k/k$
* $\Delta\rho$ excess reactivity inserted due to temperature change	±0.0001	±0.0020	$\%\Delta k/k$
RHO = total of * items above	+0.0174	-0.0217	$\%\Delta k/k$
α_T (temperature coefficient) = RHO/ΔT	-0.0036	-0.0032	$\%\Delta k/k/\Delta T$

Table 4.3-3

Temperature Coefficient Measurement Calculation At 75% Full Power

REACTIVITY CONTROLLING PARAMETERS	TEMPERATURE COEFFICIENT ANALYSIS (Up)	(Down)	UNITS
T_1 (initial avg. reactor coolant temp.)	578.79	583.55	°F
T_2 (final avg. reactor coolant temp.)	583.55	577.96	°F
$\Delta T = (T_1 - T_2)$	-4.76	+5.59	°F
H_1 (initial controlling CRA Group Position)	88.49/10.51	87.82/9.73	%wd
H_2 (final controlling CRA Group Position)	87.82/9.73	87.48/9.40	%wd
ΔH (change in rod position during measurement)	-0.67/-0.78	-0.34/-0.33	%wd
$\Delta k/k/\Delta H$ (differential rod worth values)	0.0112	0.0112	$\%\Delta k/k/\Delta H$
P_1 (initial power level)	72.84	69.44	%FP
P_2 (final power level)	69.44	71.61	%FP
ΔP (change in power due to temperature change)	-3.40	+2.17	%FP
α_{PD} (Power doppler coefficient)	-0.0105	-0.0105	$\%\Delta k/k/\Delta P$
Boron Concentration	956	956	ppmB
$\rho_{xe\ 1}$ (initial xenon reactivity worth)	-2.5642	-2.5652	$\%\Delta k/k$
$\rho_{xe\ 2}$ (final xenon reactivity worth)	-2.5652	-2.5671	$\%\Delta k/k$
* $(\Delta k/k/\Delta H)\ (\Delta H)$	-0.0082	-0.0038	$\%\Delta k/k$
* $(\alpha_{PD})\ (\Delta P)$	+0.0357	-0.0227	$\%\Delta k/k$
* $\Delta\rho_{xe}$ (avg. reactivity change due to Xe)	-0.0010	-0.0019	$\%\Delta k/k$
* $\Delta\rho$ excess reactivity inserted due to temperature change	-0.0008	+0.0004	$\%\Delta k/k$
RHO = total of * items above	+0.0251	-0.0280	$\%\Delta k/k$
α_T (temperature coefficient) = RHO/ΔT	-0.0054	-0.0050	$\%\Delta k/k/\Delta T$

Table 4.3-4

Temperature Coefficient Measurement Calculation At 100% Full Power

REACTIVITY CONTROLLING PARAMETERS	TEMPERATURE COEFFICIENT ANALYSIS (Up)	(Down)	UNITS
T_1 (initial avg. reactor coolant temp.)	578.69	584.12	°F
T_2 (final avg. reactor coolant temp.)	584.18	579.02	°F
$\Delta T = (T_1 - T_2)$	+5.49	-5.10	°F
H_1 (initial controlling CRA Group Position)	93.24/14.30	94.77/15.53	%wd
H_2 (final controlling CRA Group Position)	95.30/16.29	93.26/13.66	%wd
ΔH (change in rod position during measurement)	+2.06/+1.99	1.51/1.87	%wd
$\Delta k/k/\Delta H$ (differential rod worth values)	0.0146	0.0141	$\%\Delta k/k/\Delta H$
P_1 (initial power level)	94.19	92.70	%FP
P_2 (final power level)	94.72	92.86	%FP
ΔP (change in power due to temperature change)	+0.53	+0.16	%FP
α_{PD} (Power doppler coefficient)	-0.0102	-0.0102	$\%\Delta k/k/\Delta P$
Boron Concentration	916	916	ppmB
$\rho_{xe\ 1}$ (initial xenon reactivity worth)	-2.7201	-2.7198	$\%\Delta k/k$
$\rho_{xe\ 2}$ (final xenon reactivity worth)	-2.7201	-2.7198	$\%\Delta k/k$
* $(\Delta k/k/\Delta H)\ (\Delta H)$	+0.0296	-0.0238	$\%\Delta k/k$
* $(\alpha_{PD})\ (\Delta P)$	-0.0054	-0.0016	$\%\Delta k/k$
* $\Delta\rho_{xe}$ (avg. reactivity change due to Xe)	0.0000	0.0000	$\%\Delta k/k$
* $\Delta\rho$ excess reactivity inserted due to temperature change	+0.0001	+0.0013	$\%\Delta k/k$
RHO = total of * items above	+0.0243	-0.0241	$\%\Delta k/k$
α_T (temperature coefficient) = RHO/ΔT	-0.0044	-0.0047	$\%\Delta k/k/\Delta T$

Table 4.3-5

Power Doppler Coefficient Measurement Calculation At 40% Full Power

REACTIVITY CONTROLLING PARAMETERS	POWER DOPPLER COEFFICIENT ANALYSIS (Down)	(Up)	UNITS
P_1 (initial power level)	39.98	33.77	%FP
P_2 (final power level)	33.77	40.21	%FP
$\Delta P = (P_1 - P_2)$	6.21	-6.44	%FP
H_1 (initial controlling CRA Group Position)	95.69/20.23	92.43/16.73	%wd
H_2 (final controlling CRA Group Position)	92.43/16.73	96.88/21.58	%wd
ΔH (change in rod position during measurement)	-3.26/-3.50	4.45/4.85	%wd
$\Delta k/k/\Delta H$ (differential rod worth values)	0.0181	0.0166	$\%\Delta k/k/\Delta H$
T_1 (initial avg. reactor coolant temperature)	578.30	578.14	^oF
T_2 (final avg. reactor coolant temperature)	578.14	578.35	^oF
ΔT (change in temperature due to power change)	-0.16	+0.21	^oF
α_T (temperature coefficient)	-0.0034	-0.0034	$\%\Delta k/k/\Delta T$
Boron Concentration	1034	1034	ppmB
$\rho_{xe\ 1}$ (initial xenon reactivity worth)	-2.0355	-2.0438	$\%\Delta k/k$
$\rho_{xe\ 2}$ (final xenon reactivity worth)	-2.0438	-2.0475	$\%\Delta k/k$
* $(\Delta k/k/\Delta H)$ (ΔH)	-0.0613	+0.0772	$\%\Delta k/k$
* (α_T) (ΔT)	+0.0005	-0.0006	$\%\Delta k/k$
* $\Delta \rho_{xe}$ (avg. reactivity change due to Xe)	-0.0083	-0.0037	$\%\Delta k/k$
* $\Delta \rho$ excess reactivity inserted due to power change	-0.0003	-0.0009	$\%\Delta k/k$
RHO = total of * items above	-0.0694	+0.0720	$\%\Delta k/k$
α_{PD} (Power doppler coefficient = RHO/ΔP)	-0.0112	-0.0112	$\%\Delta k/k/\Delta P$

Table 4.3-6

Power Doppler Coefficient Measurement Calculation At 75% Full Power

REACTIVITY CONTROLLING PARAMETERS	POWER DOPPLER COEFFICIENT ANALYSIS (Down)	(Up)	UNITS
P_1 (initial power level)	74.13	69.55	%FP
P_2 (final power level)	69.78	74.09	%FP
$\Delta P = (P_1 - P_2)$	4.35	-4.54	%FP
H_1 (initial controlling CRA Group Position)	88.19/14.04	86.66/12.32	%wd
H_2 (final controlling CRA Group Position)	85.70/11.25	89.09/14.96	%wd
ΔH (change in rod position during measurement)	-2.49/-2.79	2.43/2.64	%wd
$\Delta k/k/\Delta H$ (differential rod worth values)	0.0187	0.0185	$\%\Delta k/k/\Delta H$
T_1 (initial avg. reactor coolant temperature)	578.01	578.66	°F
T_2 (final avg. reactor coolant temperature)	578.40	578.73	°F
ΔT (change in temperature due to power change)	+0.39	+0.07	°F
α_T (temperature coefficient)	-0.0052	-0.0052	$\%\Delta k/k/\Delta T$
Boron Concentration	956	956	ppmB
$\rho_{xe\ 1}$ (initial xenon reactivity worth)	-2.5667	-2.[illegible]	$\%\Delta k/k$
$\rho_{xe\ 2}$ (final xenon reactivity worth)	-2.5667	-2.5749	$\%\Delta k/k$
* $(\Delta k/k/\Delta H)$ (ΔH)	-0.0494	+0.0469	$\%\Delta k/k$
* (α_T) (ΔT)	-0.0020	-0.0003	$\%\Delta k/k$
* $\Delta\rho_{xe}$ (avg. reactivity change due to Xe)	0.0000	-0.0004	$\%\Delta k/k$
* $\Delta\rho$ excess reactivity inserted due to power change	+0.0008	0.0000	$\%\Delta k/k$
RHO = total of * items above	-0.0466	+0.0461	$\%\Delta k/k$
α_{PD} (Power doppler coefficient = RHO/ΔP)	-0.0107	-0.0102	$\%\Delta k/k/\Delta P$

Table 4.3-7

Power Doppler Coefficient Measurement Calculation At 100% Full Power

REACTIVITY CONTROLLING PARAMETERS	POWER DOPPLER COEFFICIENT ANALYSIS (Down)	POWER DOPPLER COEFFICIENT ANALYSIS (Up)	UNITS
P_1 (initial power level)	93.66	88.34	%FP
P_2 (final power level)	88.34	94.11	%FP
$\Delta P=(P_1 - P_2)$	5.32	5.77	%FP
H_1 (initial controlling CRA Group Position)	93.93/14.10	90.56/10.37	%wd
H_2 (final controlling CRA Group Position)	90.56/10.37	95.36/15.10	%wd
ΔH (change in rod position during measurement)	-3.37/-3.73	+4.80/+4.73	%wd
$\Delta k/k/\Delta H$ (differential rod worth values)	0.0136	0.0134	$\%\Delta k/k/\Delta H$
T_1 (initial avg. reactor coolant temperature)	578.77	578.88	^oF
T_2 (final avg. reactor coolant temperature)	578.88	578.69	^oF
ΔT (change in temperature due to power change)	+0.10	-0.19	^oF
α_T (temperature coefficient)	-0.0046	-0.0046	$\%\Delta k/k/\Delta T$
Boron Concentration	916	916	ppmB
$\rho_{xe\ 1}$ (initial xenon reactivity worth)	-2.7341	-2.7386	$\%\Delta k/k$
$\rho_{xe\ 2}$ (final xenon reactivity worth)	-2.7386	-2.7434	$\%\Delta k/k$
* $(\Delta k/k/\Delta H)$ (ΔH)	-0.0483	+0.0639	$\%\Delta k/k$
* (α_T) (ΔT)	-0.0005	+0.0009	$\%\Delta k/k$
* $\Delta\rho_{xe}$ (avg. reactivity change due to Xe)	-0.0045	-0.0048	$\%\Delta k/k$
* $\Delta\rho$ excess reactivity inserted due to power change	-0.0005	-0.0002	$\%\Delta k/k$
RHO = total of * items above	-0.0538	+0.0598	$\%\Delta k/k$
α_{PD} (Power doppler coefficient = RHO/ΔP)	-0.0101	-0.104	$\%\Delta k/k/\Delta P$

Table 4.3-8

Summary Of Measured Differential Rod Worths At 40% Full Power

Initial Power P1 (% FP)	Correction Factor CF (NONE)	Control Rod Group Position H1 (%WD)	H2 (% WD)	H3 (%WD)	DH (%WD)	Reactivity $\rho 1$ (PCM)	$\rho 2$ (PCM)	$\rho 3$ (PCM)	$D\rho$ (PCM)	Average Position HA (%WD)	Differential Worth CF $D\rho$/ DH (PCM/%WD)
A. Temperature And Moderator Coefficient											
40.76	1.220	20.2	18.3	20.1	-3.7	0.0	-25.0	+10.0	-60.0	19.2	19.8
40.76	1.220	20.1	18.2	19.8	-3.5	0.0	-24.0	+ 9.0	-57.0	19.4	19.9
B. Power Doppler And Doppler Coefficient											
39.98	1.212	20.8	19.0	20.7	-3.5	-3.5	-22.0	+ 8.4	-51.1	19.9	17.7
39.98	1.212	20.1	18.3	20.0	-3.5	-1.4	-19.2	+ 7.1	-44.1	19.2	15.3
33.77	1.186	16.5	14.7	16.1	-3.2	-1.0	-23.4	+ 6.1	-52.1	15.5	19.3
33.77	1.186	17.0	15.3	16.7	-3.1	+1.0	-22.5	+ 6.8	-52.8	16.1	20.2
40.21	1.213	21.1	19.5	20.9	-3.0	-2.0	-20.8	+ 9.0	-48.6	20.3	19.6
40.21	1.213	20.1	18.2	20.0	-3.7	-1.8	-23.0	+ 8.1	-52.3	19.1	17.1

Note: CF = (1 + 0.0053 xP1)
DH = (2H2 - H1 - H3)
$D\rho$ = ($2\rho 2 - \rho 1 - \rho 3$)
HA = (2H2 + H1 + H3) / 4

Table 4.3-9

Summary Of Measured Differential Rod Worths At 75% Full Power

Initial Power	Correction Factor	Control Rod Group Position				Reactivity				Average Position	Differential Worth
P1	CF	H1	H2	H3	DH	$\rho 1$	$\rho 2$	$\rho 3$	$D\rho$	HA	$CF\ D\rho / DH$
(% FP)	(NONE)	(%WD)	(% WD)	(%WD)	(%WD)	(PCM)	(PCM)	(PCM)	(PCM)	(%WD)	(PCM/%WD)
A. Temperature And Moderator Coefficient											
72.84	1.386	10.6	8.9	10.6	-3.4	0.0	- 9.1	+ 6.3	-24.5	9.8	10.0
72.84	1.386	10.2	8.4	10.1	-3.5	0.0	-10.5	+ 4.9	-25.9	9.3	10.3
69.44	1.368	9.2	7.2	9.1	-3.9	0.0	-14.1	+ 6.4	-34.6	8.1	12.2
69.44	1.368	9.1	7.2	9.0	-3.7	0.0	-12.7	+ 7.6	-33.0	8.1	12.2
B. Power Doppler And Doppler Coefficient											
74.13	1.393	13.6	11.8	13.6	-3.6	0.0	-18.0	+11.3	-47.3	12.7	18.3
74.13	1.393	13.5	11.8	13.5	-3.4	0.0	-17.0	+10.0	-44.0	12.7	18.0
69.55	1.369	11.7	9.9	11.8	-3.7	0.0	-19.3	+11.0	-49.6	10.8	18.3
69.55	1.369	11.7	10.0	11.7	-3.4	0.0	-19.3	+11.2	-49.8	10.9	20.0
74.09	1.393	9.1	7.4	9.2	-3.5	0.0	-16.3	+10.9	-43.5	8.3	17.3
74.09	1.393	9.2	7.4	9.2	-3.6	0.0	-18.7	+ 9.7	-47.1	8.3	18.2

Note: CF = (1 + 0.0053 xP1)
DH = (2H2 - H1 - H3)
$D\rho$ = ($2\rho 2$ - $\rho 1$ - $\rho 3$)
HA = (2H2 + H1 + H3) / 4.

Table 4.3-10

Summary Of Measured Differential Rod Worths At 100% Full Power

Initial Power	Correction Factor	Control Rod Group Position				Reactivity				Average Position	Differential Worth
P1	CF	H1	H2	H3	DH	$\rho 1$	$\rho 2$	$\rho 3$	$D\rho$	HA	CF $D\rho$/ D H
(% FP)	(NONE)	(%WD)	(% WD)	(%WD)	(%WD)	(PCM)	(PCM)	(PCM)	(PCM)	(%WD)	(PCM/%WD)
A. Temperature And Moderator Coefficient											
94.19	1.499	14.20	12.50	14.20	-3.20	0.00	-12.50	+8.30	-33.30	13.35	15.60
94.19	1.499	14.30	12.50	14.30	-3.60	0.20	-13.00	+9.00	-35.20	13.40	14.66
94.72	1.502	16.00	14.10	15.90	-3.70	0.00	-12.75	+9.00	-34.50	15.03	14.01
94.72	1.502	15.60	13.60	15.30	-3.70	0.00	-13.00	+9.00	-35.00	14.53	14.21
92.86	1.492	13.50	11.60	13.25	-3.55	0.20	-13.00	+8.20	-34.40	12.49	14.46
92.86	1.492	13.30	11.50	13.30	-3.60	0.20	-12.00	+9.00	-33.20	12.40	13.76
B. Power Doppler And Doppler Coefficient											
93.66	1.496	14.10	12.30	14.10	-3.60	0.30	-12.00	9.00	-33.30	13.20	13.84
93.66	1.496	14.10	12.20	14.10	-3.80	0.00	-12.30	8.90	-33.50	13.15	13.19
88.34	1.468	10.80	9.00	10.70	-3.50	0.50	-12.00	8.00	-32.50	9.88	13.63
88.34	1.468	10.70	9.00	10.70	-3.40	0.20	-11.50	8.60	-31.80	9.85	13.73
94.11	1.499	14.50	12.50	14.30	-3.80	0.00	-12.00	7.90	-31.90	13.45	12.58
94.11	1.499	14.30	12.50	14.30	-3.60	0.30	-11.80	9.20	-33.10	13.40	13.78

Note: CF = (1 + 0.0053 xP1)
DH = (2H2 - H1 - H3)
Dρ = (2ρ2 - ρ1 - ρ3)
HA = (2H2 + H1 + H3) / 4

Temperature Coefficient Of Reactivity Versus Boron Concentration For Critical Boron And Rod Conditions At 579°F, 2155 PSIG, And 0 EFPD

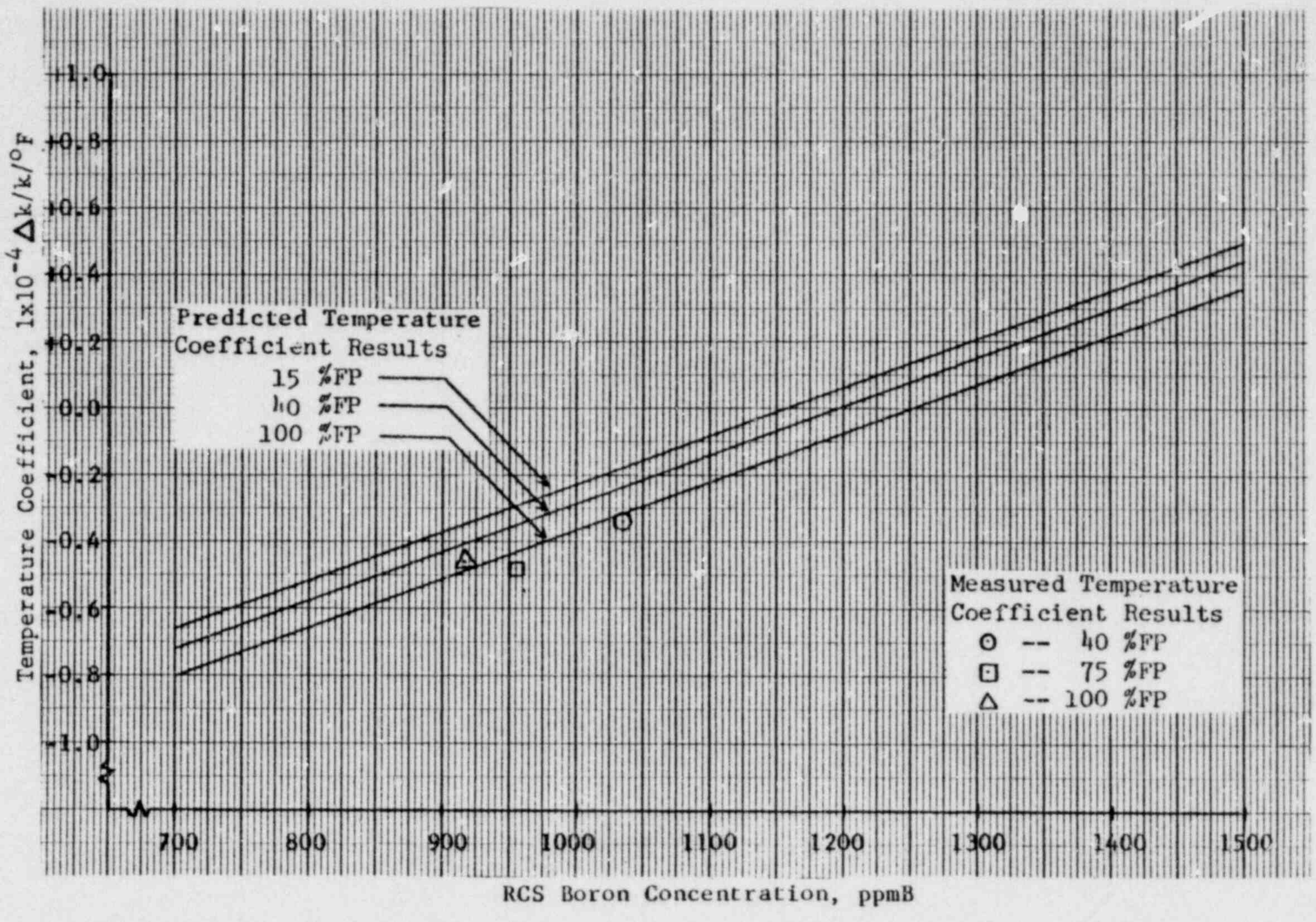

Figure 4.3-1

Moderator Coefficient Of Reactivity Versus Boron Concentration For Critical Boron And Rod Conditions At 579°F, 2155 PSIG, And 0 EFPD

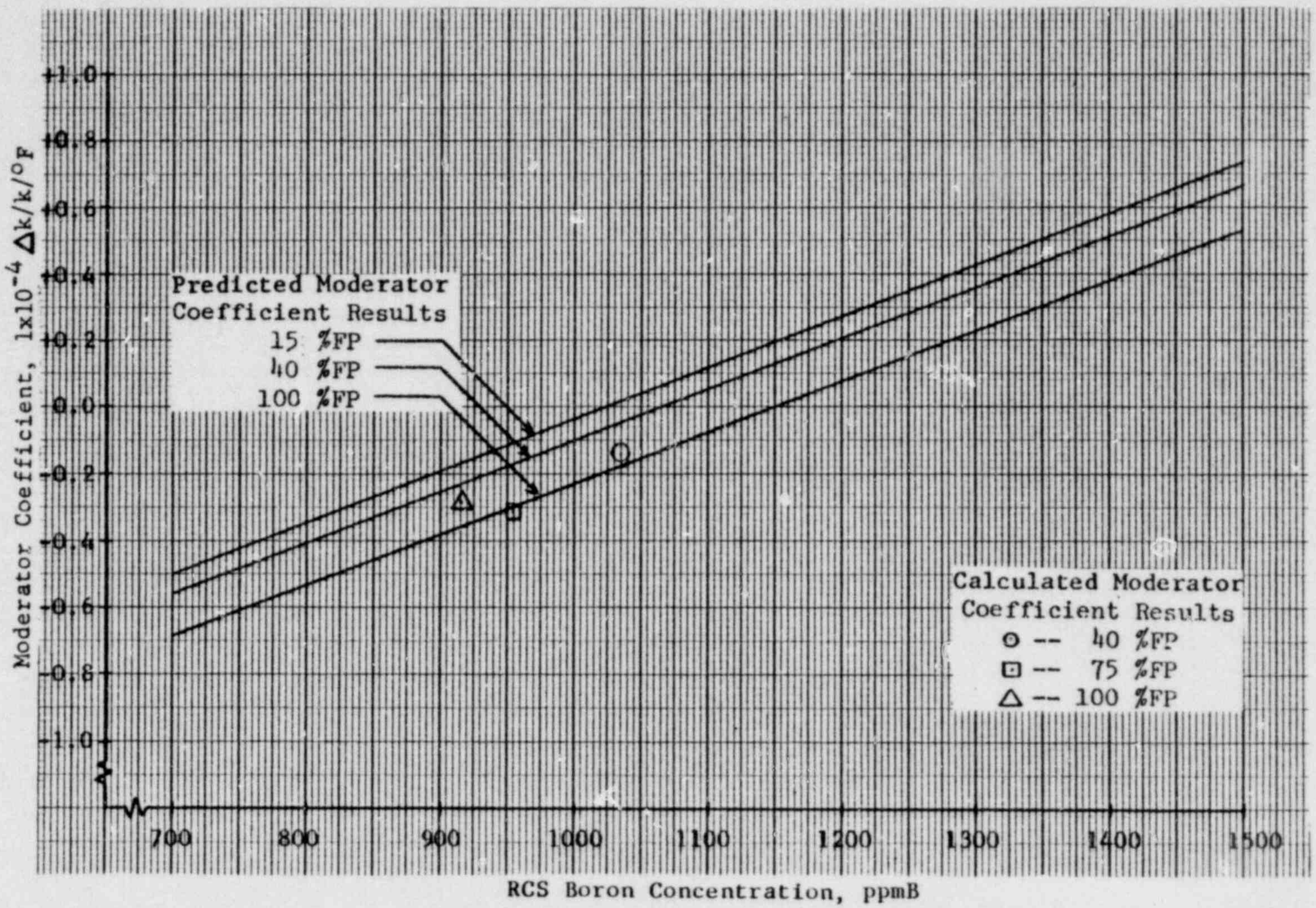

Figure 4.3-2

Average Fuel Temperature Versus Power Level At 0 EFPD

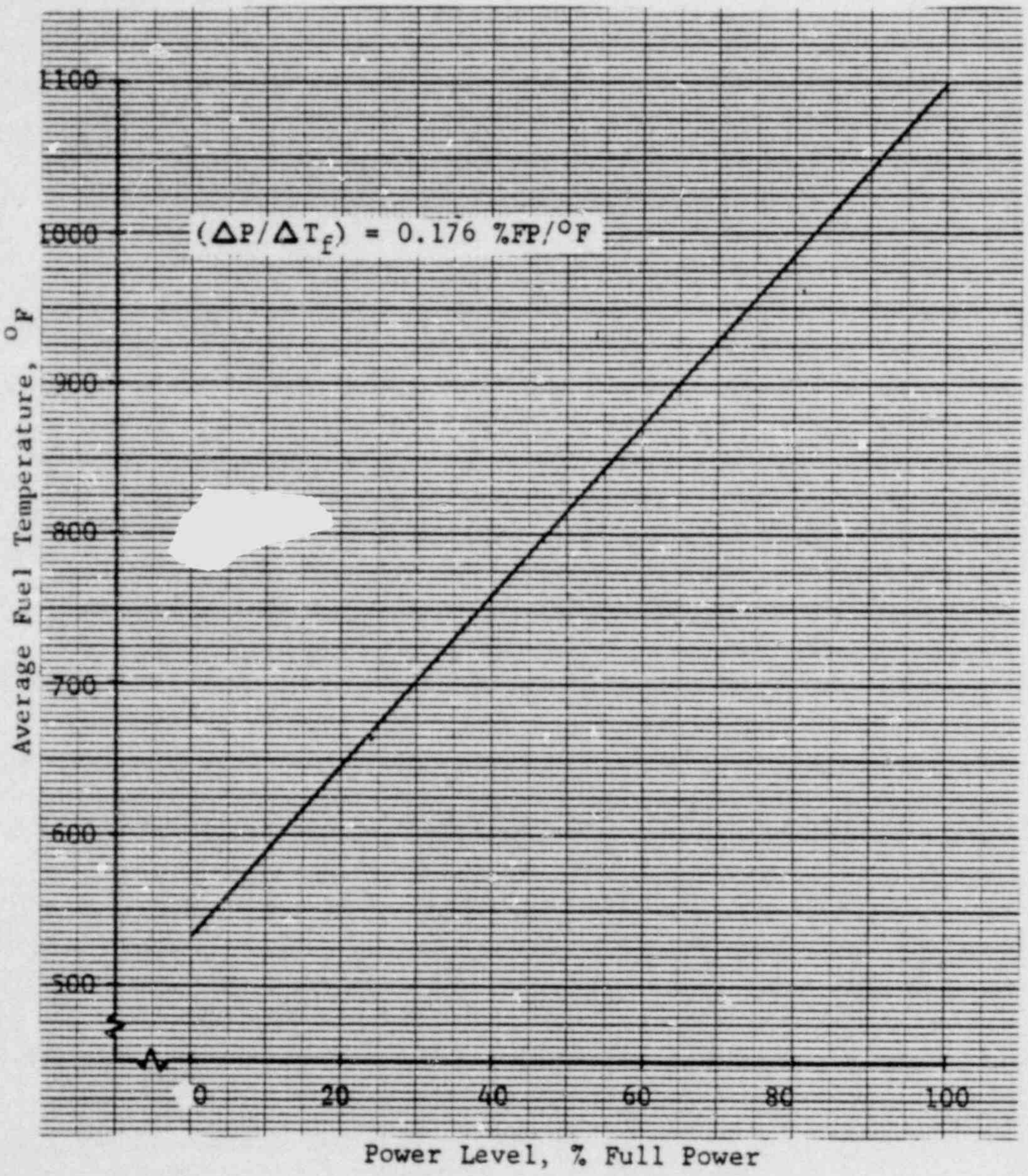

Figure 4.3-3

Power Doppler Coefficient Of Reactivity Versus Power Level

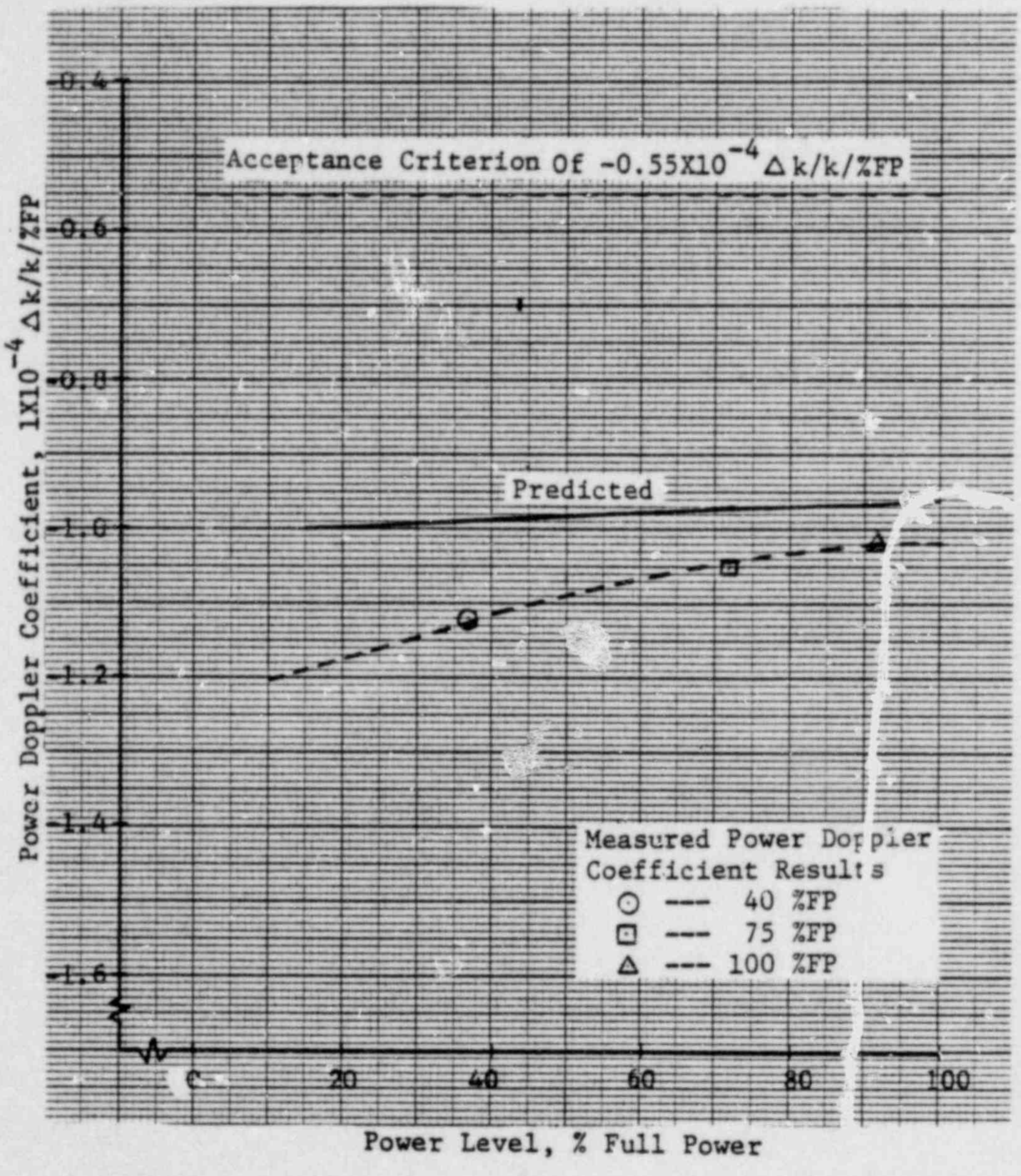

Figure 4.3-4

Power Doppler Reactivity Deficit Versus Power Level

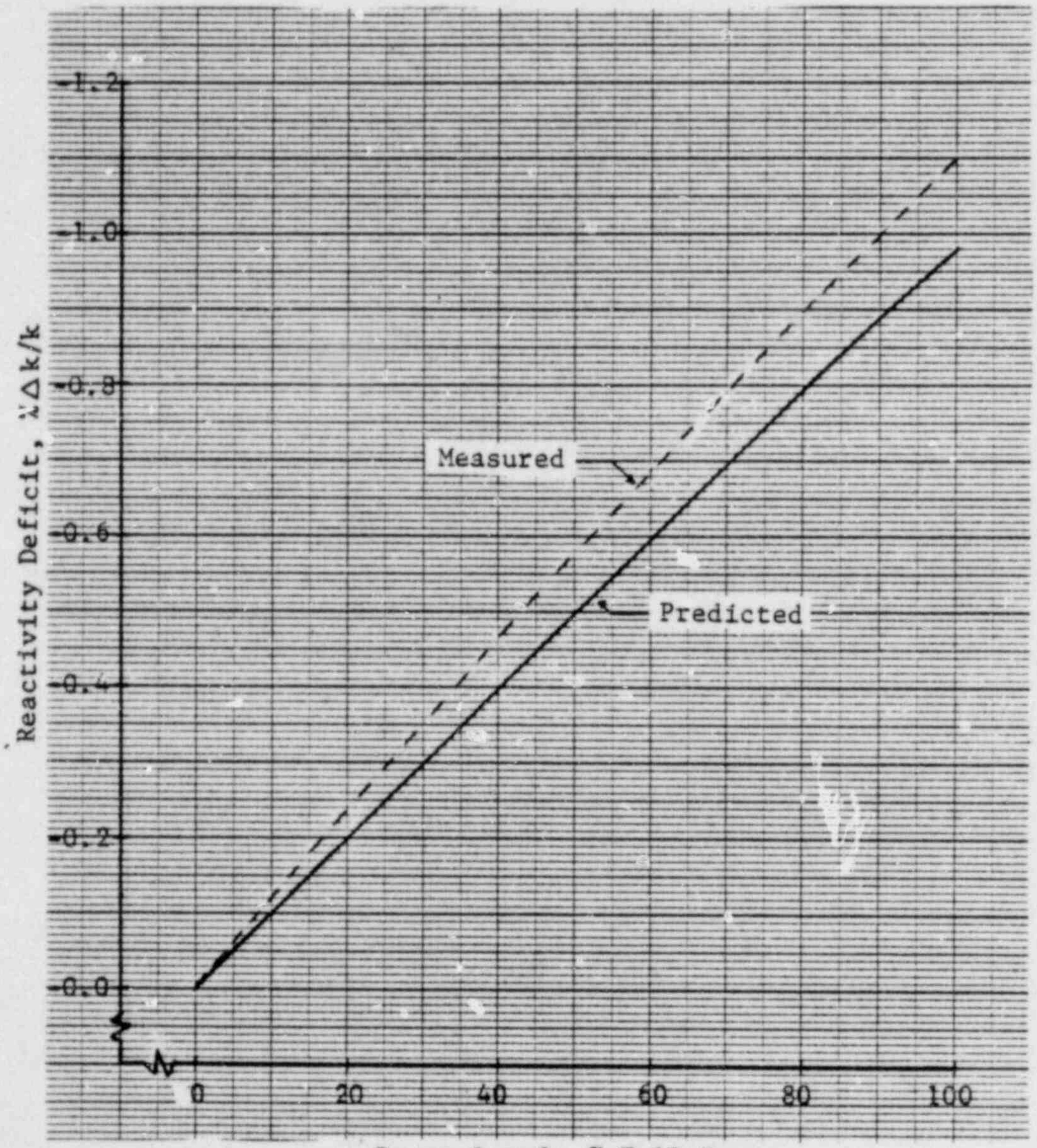

Figure 4.3-5

Reactivity, Group Position, And Fuel Power During A Typical Differential Rod Worth Measurement At Power

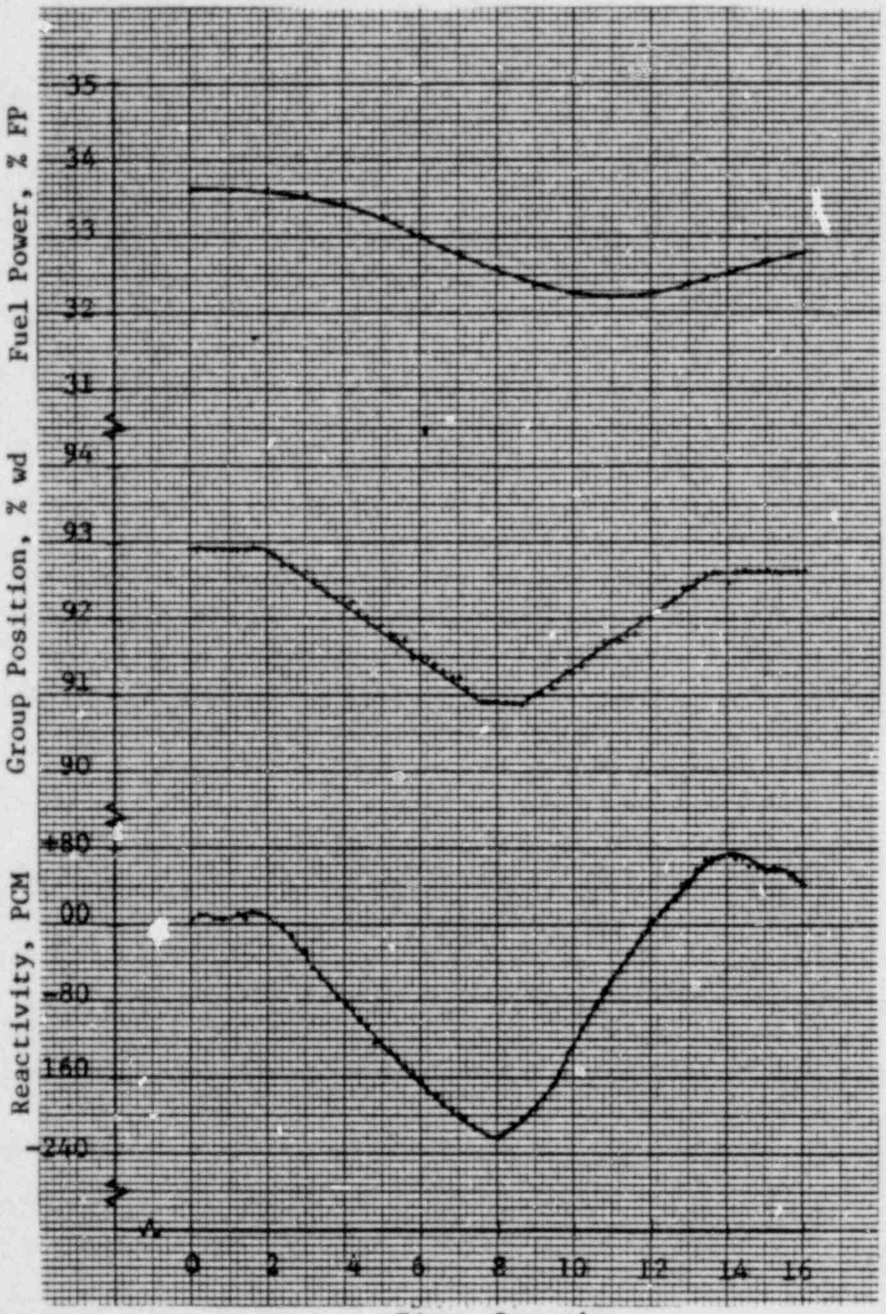

Time, Seconds

Figure 4.3-6

4.4 CORE POWER DISTRIBUTION TEST

Core power distributions were taken as required during the power escalation test program as a part of the following individual tests.

Core Power Distribution Test
Power Imbalance Detector Correlation Test
Incore Detector Test
Pseudo Ejected Control Rod Test
Dropped Control Rod Test

Continuous monitoring of the core power density at 364 core locations is accomplished by the incore monitoring system. This system is comprised of 52 detector strings each having 7 individual neutron detectors equally spaced at seven axial elevations in the center of 52 fuel assemblies. This system is capable of producing detailed core power distributions for either eighth core or quarter core symmetry conditions. A detailed description of the incore monitoring system and the calibration test results are presented in Section 4.7. The output of the incore detectors is connected to the unit computer and is corrected for background, fuel depletion and the as-built dimensions to provide accurate outputs of relative neutron flux. The computer output of the corrected signals is used to develop core power distributions which provide power peaking information necessary to determine core performance in terms of DNBR and LHR.

Because the incore monitoring system does not immediately respond to prompt changes in core conditions, the above limits are maintained on the bases of core power and core power imbalance as measured by the out-of-core nuclear instrumentation. Implementation of the core power and core power imbalance safety limits, in terms of the reactor protection setpoints, is shown in Figure 4.4-1.

The results of the core power distributions taken during the test program as part of the power escalation sequence are discussed by dividing this section into three subsections as follows:

(1) Normal Operating Core Power Distributions

(2) Worst Case Minimum DNBR And Maximum LHR Calculations

(3) Quadrant Power Tilt And Axial Power Imbalance

Numerous core power distributions were taken during power escalation testing. Generally, the detailed analyses presented herein are those required by the Core Power Distribution Test, TP 7 1 800 11. Additional analyses of the core power distributions taken as a part of other tests are presented in their appropriate sections.

4.4.1 PURPOSE

The purposes of the steady state core power distribution measurements are as follows:

(a) To measure core power distribution and thermal-hydraulic data at the major test plateaus as required by the power escalation test program.

(b) To compare the measured and predicted core power distributions at 40, 75, and 100% full power.

(c) To verify acceptable core thermal-hydraulic parameters at 40, 75, and 100% full power.

Four acceptance criteria are specified for the Core Power Distribution Test and are listed below.

(1) The core power distribution and thermal-hydraulic parameters have been measured, evaluated, and deemed reasonable.

(2) The highest measured radial and total peaking factors are not more than 5.0 and 7.5 percent greater than predicted, respectively.

(3) The measured worst case minimum DNBR is greater than 1.30 and the measured worst case maximum LHR is less than 18.00 kW/ft.

(4) The extrapolated worst case minimum DNBR is greater than 1.30 and the extrapolated worst case maximum LHR is less than 19.70 kW/ft, or the extrapolated imbalance falls outside the power imbalance trip envelope as shown in Figure 4.4-1.

4.4.2 TEST METHOD

When required by the test program, computer printouts of the core power distribution and thermal hydraulics conditions were obtained after establishing steady state conditions at the required power level and rod configurations as determined by the Controlling Procedure for Power Escalation, TP 7 1 800 00. In order to compare measured results to predicted results, some cases required two-dimensional or three-dimensional equilibrium xenon. When three-dimensional equilibrium xenon was required, the APSR's were maintained at a constant position and the axial incore imbalance was maintained within +/-2% FP of zero for approximately eight hours prior to taking data.

4.4.3 EVALUATION OF THE TEST RESULTS

4.4.3.1 NORMAL OPERATING CORE POWER DISTRIBUTIONS

Normal operating, equilibrium xenon core power distributions were measured and predicted for various operating control rod patterns at each of the major power escalation test plateaus. Measured results of four core power distributions covering various control rod patterns and core power levels are tabulated in detail in Tables 4.4-2 through 4.4-5. These tables give complete 1/8 core power distribution maps using the corrected signal outputs from 203 incore detectors located in 29 different fuel assemblies which describe the entire core, assuming eighth core symmetry. A summary of each measured core power distribution presented in the above tables is given in Table 4.4-1 which tabulates the core power level, control rod positions, core burnup, boron concentration, axial imbalance, maximum quadrant tilt, maximum LHR, minimum DNBR and power peaking data for each measurement. The measurements covered the following control rod patterns and core power levels:

Case Number	Power Level % FP	Control Rod Position, %wd Gp (1-5)	Gp (6)	Gp (7)	GP (8)	Xenon Equil. Status
1	15	100	94	19	20	Yes/2-D
2	40	100	95	18	18	Yes/3-D
3	75	100	97	18	08	Yes/3-D
4	100	100	86	10	08	Yes/3-D

The results of these measured core power distributions taken at operating control rod configurations indicate a maximum radial peaking factor between 1.36 and 1.42, and a maximum total peaking factor between 1.62 and 1.92 for the four cases studied. Examination of the maximum radial peaking factor indicates that this value is a monotonically decreasing function of power level at a given control rod configuration. This is basically ascribed to thermal feedback effects between 15 and 100 percent full power. Figure 4.4-2 shows the degree of power flattening on the radial power profile as observed along the X-Z plane at row 08 for various power levels. As can be seen, a relatively flat radial power distribution at 100 percent full power was observed. Examination of the maximum total peaking factor indicates that it also is a function of power level and strongly dependent on the incore offset and core lifetime at a given control rod configuration. As quoted above, the range of total peaking factors observed during normal operation was well below the design maximum total peaking factor of 2.67.

Core power distribution predictions at steady state conditions were predicted using the three-dimensional PDQ-7 code with thermal feedback. The results of the steady state PDQ predictions are given in the Physics Test Manual for different unit conditions in terms of the maximum radial and total peaking factors. The four cases reported in this section have been compared (measured versus predicted) in Table 4.4-6 to demonstrate the degree of agreement. In all instances, measured maximum radial and total peaking factors were within the acceptance criteria of not being more than 5.0 and 7.5 percent greater than those predicted by PDQ-7. A comparison of the measured and predicted core power distribution using (1/8) core analysis, was also performed on an assembly type basis (lump burnable poison, fuel enrichment, rod and unrodded, or a combination of the aforementioned). These results are presented in Figures 4.4-3 and 4.4-4. As can be seen, PDQ-7 is adequately predicting the radial and total peaking factors independent of the location and assembly type.

In summary, the comparison between the measured and predicted radial and total power distributions as expressed in peaking factors indicated favorable agreement, well within the acceptance criteria. Examination of the measured core power distribution relative to that predicted by PDQ-7 indicates that Crystal River Unit 3 has a better power distribution (i.e. flatter radial power profile and lower maximum peaking factors) than had initially been predicted.

4.4.3.2 WORST CASE MINIMUM DNBR AND MAXIMUM LHR CALCULATIONS

To maintain the integrity of the fuel cladding and to prevent fission product release, it is necessary to prevent overheating of the cladding under normal peaking conditions. The two primary core thermal limits which are indicative of fuel thermal performance are fuel melting and departure from nucleate boiling. These limits are independent; each must be evaluated to ensure core safety for a given power peaking situation. Fuel melting is basically a function of the local power generated in the fuel which is a combination of radial and axial peaking. The parameter used to define this limit is the maximum linear heat rate given in terms of kW/ft.

The upper boundary of the nucleate boiling region is termed "departure from nucleate boiling" (DNB). At this point, there is a sharp reduction of the heat transfer coefficient, which would result in high cladding temperature and the possibility of cladding failure. The local DNB ratio, (DNBR), defined as the ratio of the heat flux that would cause DNB at a particular core location to the actual heat flux at that location, is indicative of the margin to DNB.

Although DNB is not an observable parameter during reactor operation, the observable parameters of neutron power, reactor coolant flow, temperature and pressure can be related to DNB through the use of the W-3 correlation. The W-3 correlation has been developed to predict DNB and the location of DNB for uniform and non-uniform axial heat flux distributions. The minimum value of the DNBR, during steady-state operation, normal operational transients, and anticipated transients is limited to 1.30. A DNBR of 1.30 corresponds to 94.5% probability at a 99% confidence level that DNB will not occur; this is considered a conservative margin to DNB for all operational conditions.

Technical Specifications Limits related to DNBR and LHR limits of 1.30 and 19.70 kW/ft respectively, are given in terms of core axial imbalance, power level, reactor coolant flow, temperature and pressure. Figure 4.4-1 gives the protective limits in terms of core power level and axial imbalance for four reactor coolant pump operation.

This section presents the results of the worst case minimum DNBR and maximum LHR calculations based on measured core power distributions taken during the power escalation test program through the 100 percent full power test plateau. The analyses presented are based on the output of the unit computer where measured data is printed out in a reduced form and/or analyzed by the various computer packages. Both worst case minimum DNBR and maximum LHR calculations were performed by the unit computer and printed as part of the standard core power distribution analysis.

WORST CASE MINIMUM DNBR DETERMINATION

The worst case minimum DNBR values were calculated by the unit computer for each core power distribution taken as part of the power escalation test program. The results of various worst case minimum DNBR values calculated at each test plateau under normal rod configurations are plotted in Figure 4.4-5. These results indicate that all measured values were above the design worst case minimum DNBR versus power level and well above the minimum acceptable value of 1.30.

Four normal operating equilibrium xenon core power distributions as required by The Core Power Distribution Test were obtained during the power escalation sequence. Each distribution was subjected to the following analysis:

(a) From each core power distribution, the worst case measured minimum DNBR was selected.

(b) The measured worst case minimum DNBR's were then extrapolated to the overpower trip setpoint and corrected for axial peak location and magnitude.

(c) Verification of acceptable core conditions at the present and next power level of escalation were then performed relative to 1.30.

(d) The measured worst case minimum DNBR's were then extrapolated to the LOCA and design overpower power level and corrected for axial peak location and magnitude.

(e) Margin analysis was then performed on the extrapolated worst case minimum DNBR value relative to the minimum value of 1.30.

The results of these analyses are presented in Table 4.4-7. All measured and worst case minimum DNBR prior to and after extrapolation were above 1.30. In addition, all cases studied resulted in substantial DNBR margins. A minimum worst case minimum DNBR margin of 96.2 and 53.8 percent were observed from the LOCA and design overpower limits, respectively.

WORST CASE MAXIMUM LHR DETERMINATION

Worst case maximum LHR values were calculated by the unit computer for each standard core power distribution taken as part of the power escalation test program. These calculated results were then multiplied by an additional factor of (1.02), to bring the position of the worst case calculation to nine feet above the bottom of the core. Comparison of each case relative to the LOCA limit of 18.00 kW/ft was then performed. In all cases, the above limit was met during the power escalation test program.

Four normal operating equilibrium xenon core power distributions as required by the core power distribution test were obtained during the power escalation sequence. Each distribution was subjected to the following analysis:

(a) From each core power distribution, the measured worst case maximum LHR was selected.

(b) The measured worst case maximum LHR values were multiplied by an additional factor of (1.02) and then extrapolated to the overpower trip setpoint.

(c) Verification of acceptable core conditions at the present and next power level of escalation was then performed relative to the acceptance criteria values of 18.00 and 19.70 kW/ft, respectively.

(d) The measured worst case maximum LHR values were multiplied by an additional factor of (1.02) and then extrapolated to the LOCA and design overpower levels.

(e) Margin analysis was then performed on the extrapolated worst case maximum LHR values relative to the LOCA and design overpower limits of 18.00 and 19.70 kW/ft, respectively.

The results of these analyses are presented in Table 4.4-7. All worst case values prior to and after the extrapolation to the overpower trip setpoint were within their respective acceptance criteria of 18.00 and 19.70 kW/ft, respectively. In addition, all cases studied resulted in adequate LHR margins. A minimum worst case maximum LHR margin of 22.0 and 21.7 percent were observed from the LOCA and design overpower limits, respectively.

4.4.3.3 QUADRANT POWER TILT AND AXIAL POWER IMBALANCE

QUADRANT POWER TILT

Quadrant power tilt limits have been established in the Technical Specifications. These limits, when used in conjunction with the control rod position limits, assure that the design peak heat rate criterion is not exceeded during normal power operation.

Quadrant power tilt is defined by the following equation and is expressed in percent.

$$\text{Quadrant Power Tilt} = \left[\frac{\text{Power in Any Core Quadrant}}{\text{Average Power of All Quadrants}} - 1\right] \times 100 \qquad \text{EQ. (4.4-1)}$$

During the startup testing program, maximum quadrant power tilt was determined using the corrected signals from the 16 symmetric incore monitoring assemblies. Table 4.4-1 shows the maximum quadrant power tilt for each standard core power distribution taken as required by the Core Power Distribution Test. These maximum quadrant power tilts are representative of the values observed during the startup test program.

During the performance of the Power Imbalance Detector Correlation Test, the quadrant power tilt as indicated by the corrected signals from the 16 symmetric incore monitoring assemblies was shown to be relatively independent of the degree of incore axial offset. This trend was as expected since quadrant power tilt theoretically is not dependent on the magnitude of the incore axial offset. The results of this study for the 40 and 75% full power plateaus are shown in Figure 4.4-6.

AXIAL POWER IMBALANCE

Results from the Standard Core Power Distributions taken at 40 and 75% FP during the performance of the Power Imbalance Detector Correlation Test, show that the imbalance trip envelope (Figure 4.4-1) of the reactor protective system is sufficient to protect the unit from exceeding the DNBR and the LHR limits under all core imbalance conditions when a gain factor of 3.90 is set into the delta flux amplifier. In addition, analyses indicate that the largest thermal margins (measured by DNBR and LHR) exist when a negative 5.0 to 10.0 incore axial offset is present.

During the startup test program, the calculation of axial core imbalance was performed by the unit computer using signals from the 364 incore detectors. A minimum and maximum core imbalance value over the test period of -29.80 and +5.91% FP was observed during the performance of Power Imbalance Detector Correlation Test. It should be noted the core preferred to have a negative imbalance and achieving positive imbalances of any magnitude was difficult.

The core imbalances measured in conjunction with the core power distributions of this section are shown in Table 4.4-1. These results confirm that under normal operating rod configurations no difficulty in maintaining an approximate zero percent full power imbalance was observed.

4.4.4 CONCLUSIONS

Four normal operating equilibrium xenon core power distributions taken at 15, 40, 75, and 100 percent full power under various core rod positions and incore axial imbalance were examined. The maximum radial and total peaking factors were not more than 5.0 and 7.5 percent greater than those predicted by PDQ-7.

Comparison between measured and predicted radial and total core power distributions as expressed in peaking factors on a 1/8 core power distribution showed favorable agreement on all core locations.

The worst case minimum DNBR and maximum LHR measured as part of this test were subject to various types of analyses. On the bases of this study, the following were determined:

(a) All measured worst case minimum DNBR and maximum LHR were within their respective acceptance criteria of 1.30 and 18.00 kW/ft.

(b) Acceptable core conditions at the trip setpoint of the next power level of escalation were verified prior to escalating reactor power.

(c) Margin analysis on the minimum DNBR and maximum LHR values at the LOCA and design overpower limits resulted in substantial margins.

The results of the quadrant power tilt and axial power imbalance calculations for a variety of different core power distributions taken during the power escalation test program yield the following conclusions:

(a) All maximum quadrant power tilts determined during normal power operation were well within the Technical Specifications Limit of 4%.

(b) The reactor protective system will provide sufficient protection against exceeding DNBR and LHR limits when the delta flux amplifier has a gain factor of 3.90.

Table 4.4-1

Summary Of Measured Core Power Distribution Results At Equilibrium Xenon Conditions For Various Control Rod Patterns And Core Power Levels Of 15, 40, 75, And 100 Percent Full Power

Date	Time	Power Level (%FP)	Rod Position, %wd				Core Burnup (EFPD)	Boron Conc. (ppmB)	Axial Imb. (%FP)	Maximum Tilt (%)	Thermal		Maximum	
			1-5	6	7	8					DNBR	LHR	P(R)	P(RXA)
02/01/77	0620	16.20	100	94	19	20	0.28	1155	+1.47	+0.53	21.64	2.23	1.42	1.92
03/01/77	0206	40.21	100	95	17	18	1.56	1031	-0.82	+0.94	10.13	4.44	1.40	1.62
03/15/77	2230	73.94	100	97	18	08	7.62	960	+0.61	+0.74	4.66	8.93	1.36	1.79
04/03/77	1240	99.65	100	86	10	08	18.27	908	-0.91	+1.60	3.03	12.70	1.37	1.83

Measured Core Power Distribution Results At 15 % Full Power

Control Rod Group Positions

Gps 1-5 100 % wd GP 7 19 % wd
Gp 6 94 % wd GP 8 20 % wd
Core Power Level 16.2 % FP
Boron Concentration 1155 ppmB
Core Burnup 0.28 EFPD
Axial Imbalance +1.47 % FP
Xenon Conditions
Equilibrium Conc. YES Yes or No
Reactivity Worth -1.08 % Δk/k
Max Quadrant Tilt +0.53 %

1/8 Core Fuel Assy. Location	Incore Detector Number	Weighting Factor	Pmax/ $\bar{P}$core Local	P/$\bar{P}$ Fuel Assembly
H-08	1	1	1.13	0.92
G-08	2	4	1.60	1.27
F-08	4	4	1.71	1.27
E-08	10	4	1.92	1.38
D-08	14	4	1.70	1.23
C-08	21	4	1.76	1.31
B-08	30	4	1.85	1.42
A-08	37	4	1.19	0.92
G-09	3	4	1.64	1.24
F-10	12	4	1.76	1.27
E-11	26	4	1.54	1.07
D-12	41	4	1.32	0.93
C-13	52	4	0.73	0.52
F-09	6	8	1.87	1.37
E-09	5	8	1.70	1.23
D-09	15	8	1.81	1.29
C-09	29	8	1.48	1.09
B-09	31	8	1.36	1.05
A-09	45	8	1.01	0.78
E-10	17	8	1.85	1.30
D-10	27	8	1.52	1.30
C-10	28	8	1.34	0.98
B-10	44	8	0.82	0.66
A-10	46	8	0.55	0.46
D-11	33	8	1.59	1.11
C-11	42	8	1.21	0.87
B-11	49	8	0.82	0.64
C-12	48	8	1.13	0.82
B-12	51	8	0.61	0.46

Table 4.4-2

Measured Core Power Distribution Results At 40 % Full Power

Control Rod Group Positions

Gps 1-5 100 % wd GP 7 17 % wd
Gp 6 95 % wd GP 8 18 % wd
Core Power Level 40.2 % FP
Boron Concentration 1031 ppmB
Core Burnup 1.56 EFPD
Axial Imbalance -0.82 % FP
Xenon Conditions
Equilibrium Conc. YES Yes or No
Reactivity Worth -1.97 % $\Delta k/k$
Max Quadrant Tilt +0.94%

1/8 Core Fuel Assy. Location	Incore Detector Number	Weighting Factor	$P_{max}/\bar{P}_{core}$ Local	$P/\bar{P}$ Fuel Assembly
H-08	1	1	1.36	0.96
G-08	2	4	1.46	1.26
F-08	4	4	1.50	1.27
E-08	10	4	1.61	1.33
D-08	14	4	1.53	1.23
C-08	21	4	1.56	1.31
B-08	30	4	1.62	1.40
A-08	37	4	1.10	0.94
G-09	3	4	1.46	1.19
F-10	12	4	1.56	1.26
E-11	26	4	1.37	1.07
D-12	41	4	1.22	0.96
C-13	52	4	0.69	0.59
F-09	6	8	1.62	1.35
E-09	5	8	1.50	1.22
D-09	15	8	1.59	1.26
C-09	29	8	1.34	1.10
B-09	31	8	1.21	1.06
A-09	45	8	0.92	0.79
E-10	17	8	1.62	1.26
D-10	27	8	1.36	0.98
C-10	28	8	1.22	0.98
B-10	44	8	1.01	0.67
A-10	46	8	0.60	0.49
D-11	33	8	1.39	1.10
C-11	42	8	1.12	0.89
B-11	49	8	0.78	0.66
C-12	48	8	1.04	0.84
B-12	51	8	0.59	0.49

Table 4.4-3

Measured Core Power Distribution Results At 75 % Full Power

Control Rod Group Positions

Gps 1-5 100 % wd GP 7 18 % wd
Gp 6 97 % wd GP 8 08 % wd
Core Power Level 73.9% FP
Boron Concentration 960 ppmB
Core Burnup 7.62 EFPD
Axial Imbalance +0.61% FP
Xenon Conditions
Equilibrium Conc. YES Yes or No
Reactivity Worth -2.57% Δk/k
Max Quadrant Tilt +0.74%

1/8 Core Fuel Assy. Location	Incore Detector Number	Weighting Factor	Pmax/ $\bar{P}$core Local	P/$\bar{P}$ Fuel Assembly
H-08	1	1	1.21	0.93
G-08	2	4	1.58	1.25
F-08	4	4	1.67	1.26
E-08	10	4	1.77	1.31
D-08	14	4	1.79	1.26
C-08	21	4	1.73	1.33
B-08	30	4	1.73	1.36
A-08	37	4	1.20	0.92
G-09	3	4	1.54	1.22
F-10	12	4	1.66	1.28
E-11	26	4	1.59	1.15
D-12	41	4	1.35	1.01
C-13	52	4	0.76	0.58
F-09	6	8	1.73	1.33
E-09	5	8	1.65	1.25
D-09	15	8	1.70	1.25
C-09	29	8	1.42	1.11
B-09	31	8	1.29	1.03
A-09	45	8	0.94	0.75
E-10	17	8	1.76	1.31
D-10	27	8	1.45	0.98
C-10	28	8	1.36	1.03
B-10	44	8	0.82	0.62
A-10	46	8	0.60	0.47
D-11	33	8	1.50	1.09
C-11	42	8	1.22	0.89
B-11	49	8	0.85	0.65
C-12	48	8	1.11	0.82
B-12	51	8	0.63	0.48

Table 4.4-4

Measured Core Power Distribution Results At 100 % Full Power

Control Rod Group Positions

Gps 1-5 100 % wd GP 7 10 % wd
Gp 6 86 % wd GP 8 8 % wd
Core Power Level 99.80 % FP
Boron Concentration 908 ppmB
Core Burnup 18.27 EFPD
Axial Imbalance -0.91 % FP
Xenon Conditions
Equilibrium Conc. YES Yes or No
Reactivity Worth -2.75 % $\Delta k/k$
Max Quadrant Tilt +1.60 %

1/8 Core Fuel Assy. Location	Incore Detector Number	Weighting Factor	Pmax/ $\bar{P}$core Local	$P/\bar{P}$ Fuel Assembly
H-08	1	1	0.92	1.27
G-08	2	4	1.28	1.64
F-08	4	4	1.26	1.69
E-08	10	4	1.34	1.83
D-08	14	4	1.29	1.82
C-08	21	4	1.34	1.76
B-08	30	4	1.33	1.69
A-08	37	4	0.88	1.17
G-09	3	4	1.20	1.52
F-10	12	4	1.30	1.69
E-11	26	4	1.17	1.65
D-12	41	4	1.01	1.37
C-13	52	4	0.58	0.76
F-09	6	8	1.31	1.74
E-09	5	8	1.27	1.68
D-09	15	8	1.37	1.81
C-09	29	8	1.11	1.48
B-09	31	8	1.02	1.25
A-09	45	8	0.71	0.92
E-10	17	8	1.33	1.79
D-10	27	8	0.98	1.50
C-10	28	8	0.96	1.28
B-10	44	8	0.63	0.73
A-10	46	8	0.46	0.60
D-11	33	8	1.07	1.49
C-11	42	8	0.90	1.17
B-11	49	8	0.64	0.86
C-12	48	8	0.81	1.10
B-12	51	8	0.47	0.63

Table 4.4-5

Table 4.4-6

Comparison Of Measured And Predicted Maximum Radial And Total Peaking Factors

Case Number (dim)	Power Level (%FP)	Maximum Predicted Peaking Factors Radial (dim)	Maximum Predicted Peaking Factors Total (dim)	Maximum Measured Peaking Factors Radial (dim)	Maximum Measured Peaking Factors Total (dim)	Percentage Error Radial (%)	Percentage Error Total (%)
1	15	1.49	2.03	1.42	1.92	-4.93	-5.73
2	40	1.41	1.74	1.40	1.62	-0.71	-7.41
3	75	1.41	1.74	1.36	1.79	-3.68	+2.79
4	100	1.46	1.85	1.37	1.83	-6.50	-1.09

NOTE: Percentage Error = $\left[\frac{\text{Measured - Predicted}}{\text{Measured}}\right] \times 100$

NOTE: The acceptance criteria requires that the radial and total peaking factors are not more than 5.0 and 7.5 percent greater than predicted, respectively.

Table 4.4-7

Minimum DNBR And Maximum LHR Analysis For Core Power Distribution Test

Data Analysis (None)	Power Level (%FP)	Incore Offset (%)	Axial Peak Magnitude (None)	Axial Peak Location (Segment)	Extrapolated Imbalance (% FP)	Worst Case Maximum LHR (kW/ ft)	Worst Case Minimum DNBR (None)
Measured Point	16.20	+ 9.07	1.35	5	+ 1.47	2.23	21.64
Overpower Trip Setpoint	50.00				+ 4.54	6.68	5.98
LOCA Limit	102.00				+ 9.25	14.04	2.55
Design Overpower Limit	112.00				+10.16	15.42	2.00
Measured Point	40.21	- 2.04	1.17	5	- 0.82	4.44	10.13
Overpower Trip Setpoint	85.00				- 1.73	9.39	4.45
LOCA Limit	102.00				- 2.09	11.26	3.75
Design Overpower Limit	112.00				- 2.28	12.37	3.35
Measured Point	73.94	+ 0.82	1.42	5	+ 0.61	8.39	4.66
Overpower Trip Setpoint	104.70				+ 0.86	11.88	2.70
LOCA Limit	102.00				+ 0.84	11.57	2.89
Design Overpower Limit	112.00				+ 0.92	12.71	2.39
Measured Point	99.65	- 0.91	1.37	5	- 0.91	12.70	3.03
Overpower Trip Setpoint	104.70				- 0.95	13.34	2.72
LOCA Limit	102.00				- 0.93	13.00	2.82
Design Overpower Limit	112.00				- 1.02	14.27	2.42

Reactor Protective System Maximum Allowable Envelope
For Four Pump Operation

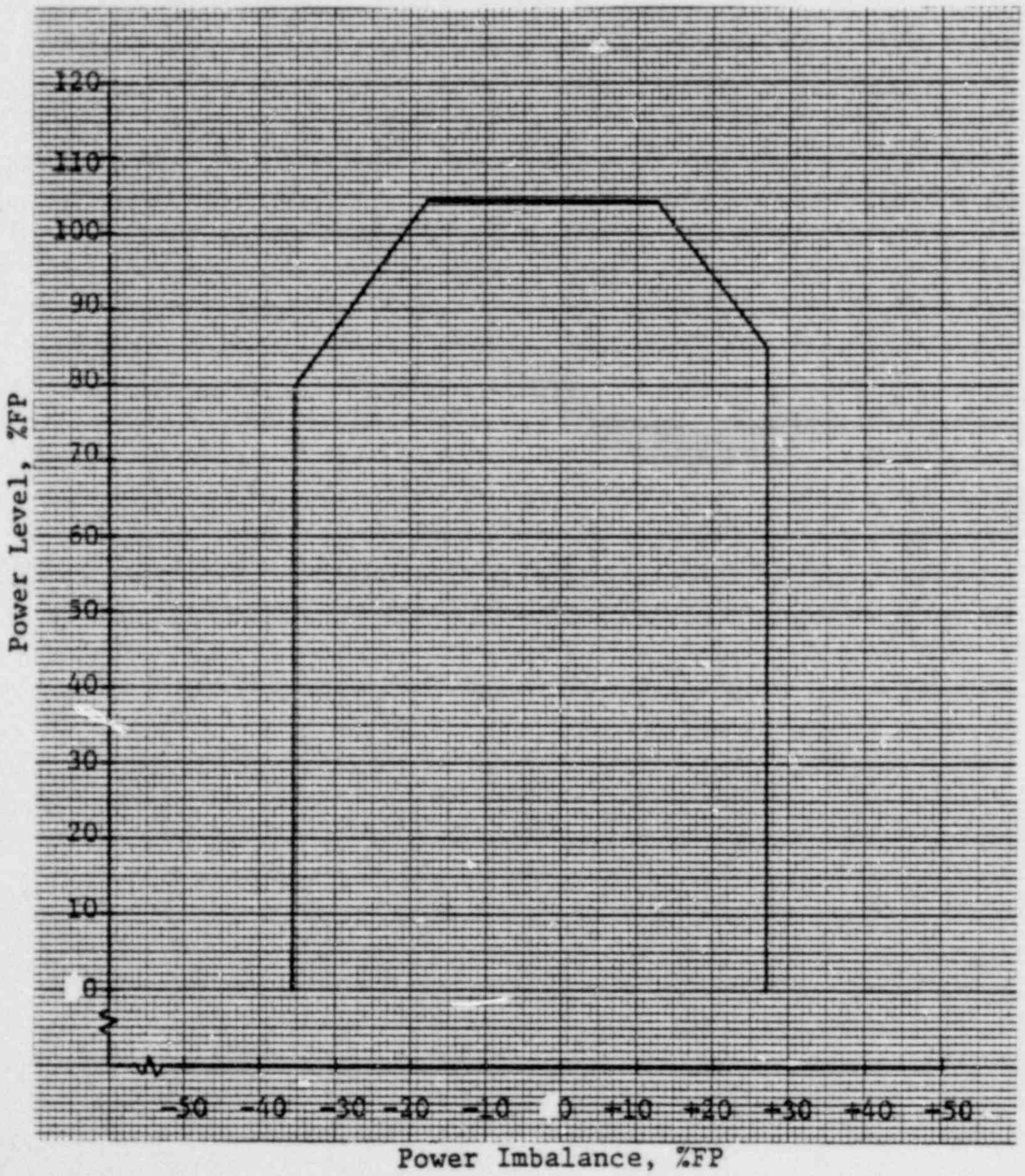

Figure 4.4-1

Comparison Of Measured Radial Core Power Distributions Obtained During The Performance Of Standard Core Power Distributions Test As Taken Along The X-Z Plane At Row 08

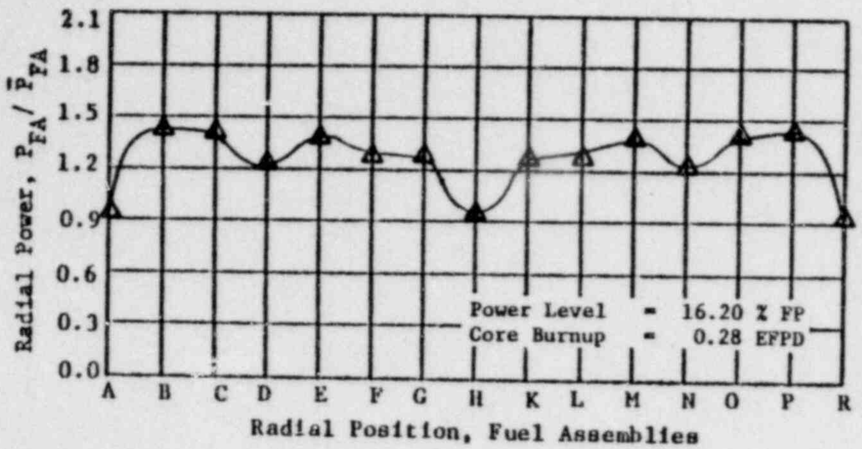

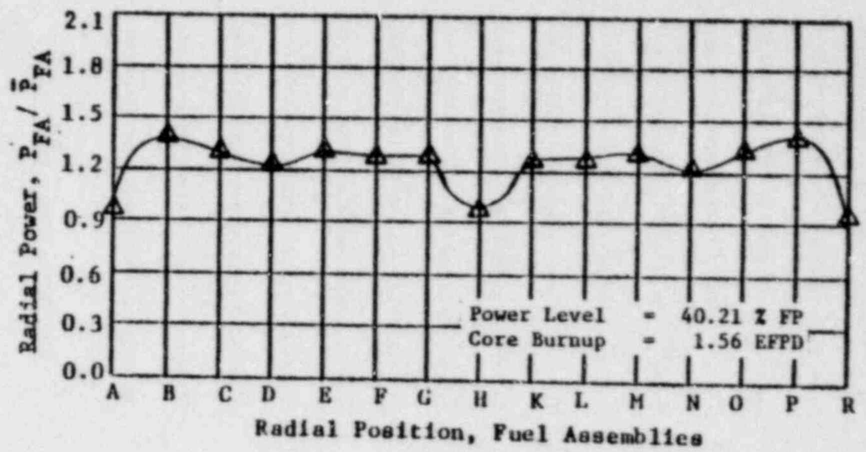

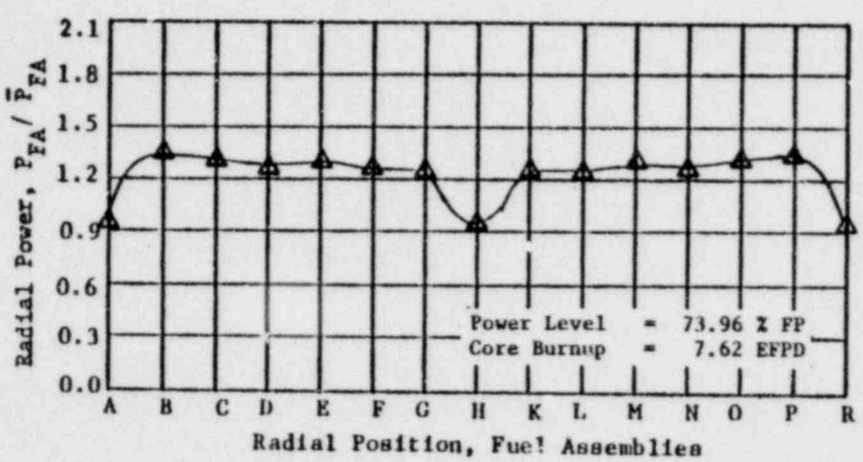

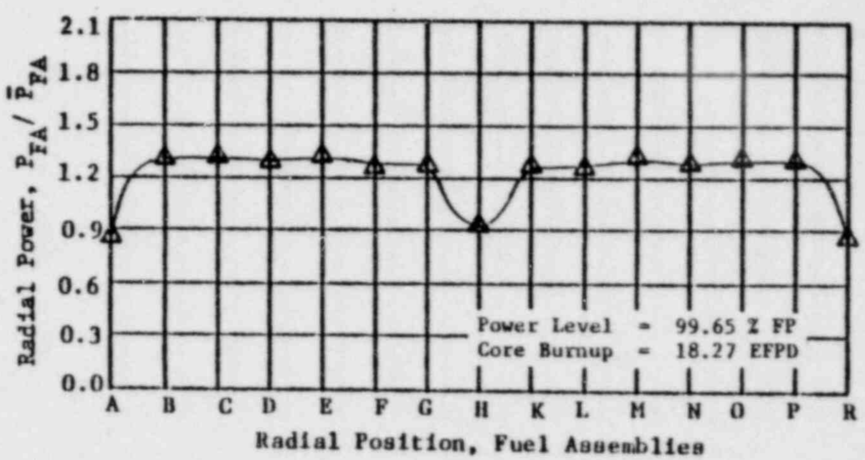

Figure 4.4-2

Comparison Of Predicted And Measured Radial Core Power Distribution Results At Steady State, 3-D Equilibrium Xenon, 40 %FP Conditions

Predicted Conditions

Control Rod Group Positions					
Gps 1-5	100.0 % wd		Core Power Level	40.0	%FP
Gp 6	95.8 % wd		Boron Concentration	NA	ppmB
Gp 7	20.8 % wd		Core Burnup	4.0	EFPD
Gp 8	29.2 % wd		Axial Imbalance	+0.24	%FP
			Max Quadrant Tilt	0.00	%

Measured Conditions

Control Rod Group Positions					
Gps 1-5	100 % wd		Core Power Level	40.2	%FP
Gp 6	95 % wd		Boron Concentration	1031	ppmB
Gp 7	17 % wd		Core Burnup	1.56	EFPD
Gp 8	18 % wd		Axial Imbalance	-0.82	%FP
			Max Quadrant Tilt	+0.94	%

	H	G	F	E	D	C	B	A
8	7 1.01 0.96	1.25 1.26	1.22 1.27	1.41 1.33	6 1.16 1.23	1.28 1.31	1.33 1.40	0.91 0.94
9		5 1.16 1.19	1.41 1.35	1.20 1.22	1.28 1.26	1.01 1.10	0.97 1.06	0.76 0.79
10			1.21 1.26	1.33 1.26	8 0.97 0.98	0.97 0.98	7 0.71 0.67	0.49 0.49
11				6 1.09 1.07	1.14 1.10	5 0.83 0.89	0.72 0.66	
12					0.90 0.96	0.89 0.84	0.55 0.49	
13						0.63 0.59		
14								
15								

℄

X	Control Rod Group (5-8)
X.XX	Predicted Results
X.XX	Measured Results

Figure 4.4-3

Comparison Of Predicted And Measured Total Peaking Core Power Distribution Results At Steady State, 3-D Equilibrium Xenon, 40 %FP Conditions

Predicted Conditions

Control Rod Group Positions			Core Power Level	40.0	%FP
Gps 1-5	100.0	% wd	Boron Concentration	NA	ppmB
Gp 6	95.8	% wd	Core Burnup	4.0	EFPD
Gp 7	20.8	% wd	Axial Imbalance	+0.24	%FP
Gp 8	29.2	% wd	Max Quadrant Tilt	0.00	%

Measured Conditions

Control Rod Group Positions			Core Power Level	40.2	%FP
Gps 1-5	100	% wd	Boron Concentration	1031	ppmB
Gp 6	95	% wd	Core Burnup	1.56	EFPD
Gp 7	17	% wd	Axial Imbalance	-0.82	%FP
Gp 8	18	% wd	Max Quadrant Tilt	+0.94	%

	H	G	F	E	D	C	B	A
8	1.35 [7] 1.36	1.43 1.46	1.47 1.50	1.74 1.61	1.45 [6] 1.53	1.54 1.56	1.55 1.62	1.08 1.10
9		1.38 [5] 1.46	1.71 1.62	1.50 1.50	1.62 1.59	1.22 1.34	1.14 1.21	0.91 0.92
10			1.51 1.56	1.71 1.62	1.34 [8] 1.36	1.18 1.22	1.04 [7] 1.01	0.61 0.60
11				1.41 [6] 1.37	1.47 1.39	1.01 1.12	0.86 0.78	
12					1.13 1.22	1.08 1.04	0.66 0.59	
13						0.77 0.69		
14								
15								

Note: The results represent the maximum total peaking in each assembly

Legend	
X	Control Rod Group (5-8)
X.XX	Predicted Results
X.XX	Measured Results

Figure 4.4-4

Hot Channel Minimum DNBR Versus Core Power Level

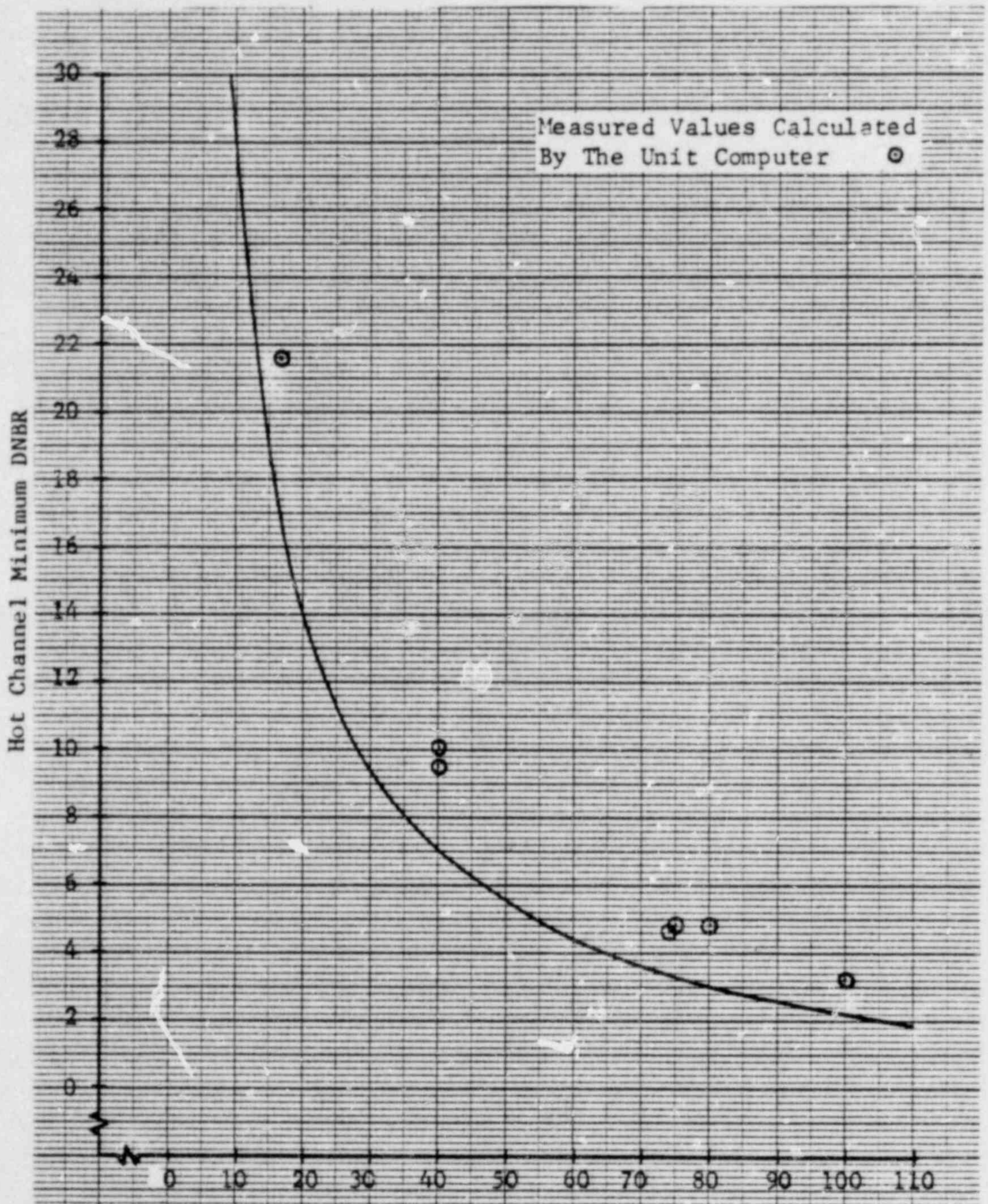

Figure 4.4-5

Maximum Quadrant Power Tilt Versus Full Incore Offset During
The Performance Of Power Imbalance Detector Correlation Test

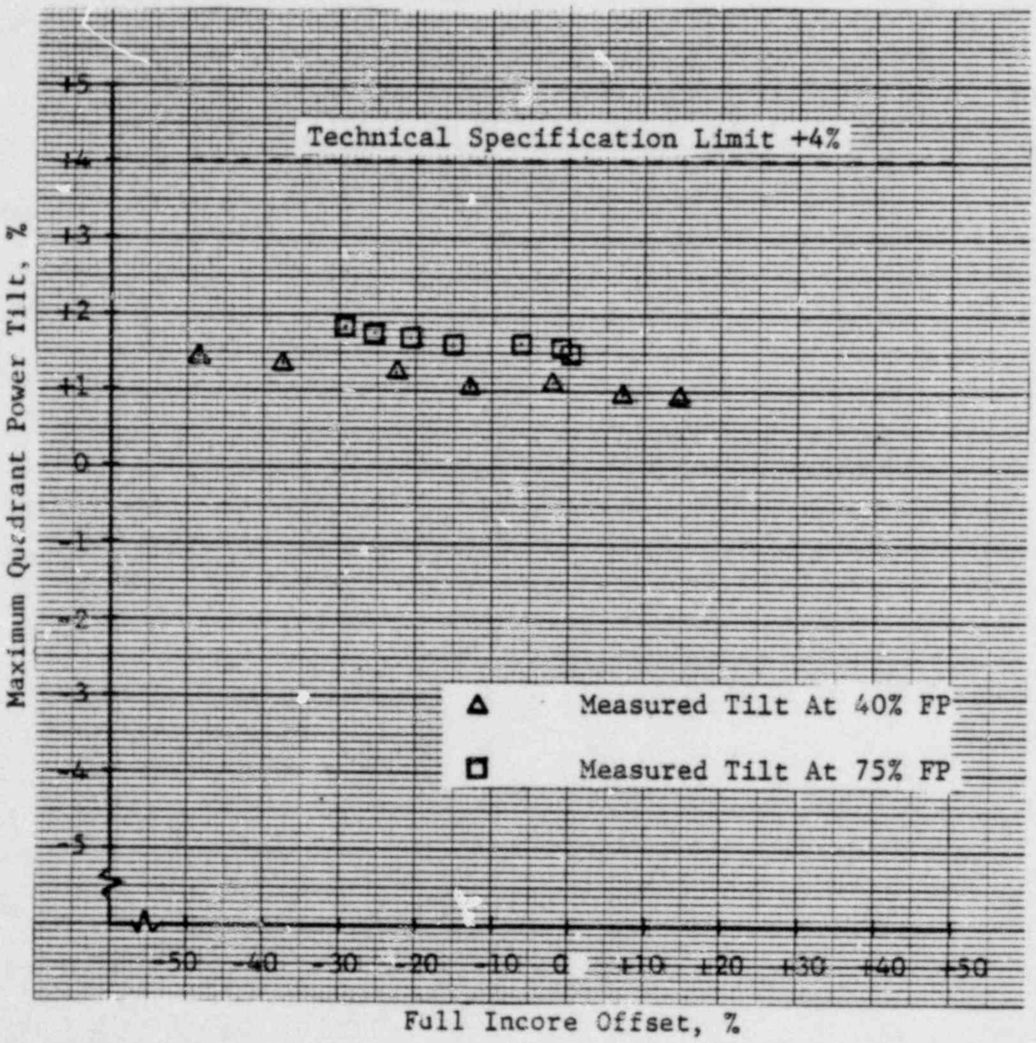

Figure 4.4-6

4.5 UNIT LOSS OF ELECTRICAL LOAD TEST

4.5.1 PURPOSE

The purpose of this test was to ensure that the primary/secondary systems can safely undergo a net load loss at 100% full power. This was accomplished by verifying the automatic response of the reactor and auxiliary systems during a generator separation from the transmission system.

Six acceptance criteria are specified for the Unit Loss Of Electrical Load Test, and are listed below:

(1) Unit 3 auxiliary transformer supplies power to the 6900 volt reactor auxiliary busses 3A and 3B, the 4160 volt unit busses 3A and 3B, and associated motor control centers.

(2) Automatic power reduction to 15% full power at a nominal rate of 20% full power per minute and less than a maximum rate of 50 %FP/min.

(3) The unit frequency will peak at less than the overspeed trip point and decay back to a set frequency in 40 to 50 seconds.

(4) The loss of electrical load does not result in fuel damage (leakage). No increase in RC coolant letdown activity as measured by RM-L1.

(5) Reactor coolant pressure/temperature relationship must remain within the protective system envelope of Figure 4.5-1

(6) Minimum total feedwater flow does not decrease below 5.0 percent of the normal value (10.2 MPPH).

4.5.2 TEST METHOD

This test involved separating unit 3 generator from the line and measuring the system response during the ensuing transient. The turbine-generator output should drop to house load and continue to supply unit power. However, the generator separation might also cause the reactor/turbine to trip. In any case, the primary intent was to verify that the unit can withstand a loss of electrical load.

This test was conducted from 100 percent full power as scheduled by the power escalation test procedure.

4.5.3 EVALUATION OF TEST RESULTS

On April 22, 1977 at approximately 2000, Unit Loss Of Electrical Load Test was performed by tripping the generator output breakers. Upon the separation, the integrated control system smoothly ran reactor power back from 100 to 15% full power within 5.0 minutes at an average ramp rate of 16.8% FP/Min. As shown in Figures 4.5-2 and 4.5-3, excellent control of primary and secondary parameters during the transient was observed. In all cases, large margins to RPS trip setpoints were experienced. After reaching 15% full power, the unit continued to supply power in the fully integrated mode of control until hand control of the turbine was taken at 7.8 minutes into the transient.

During the performance of this test, some difficulty was experienced which should be noted. These areas are listed below:

(1) During the reactor runback, the low load feedwater block valve stuck at approximately 50% shut. This caused a moderate loop temperature mismatch to occur around five minutes into the transient.

(2) The turbine experienced speed oscillations prior to and after reaching 15% full power. The magnitude of the turbine speed variations was approximately ± 40 RPM.

Even though the above did not affect the successful runback of the unit, the second problem did cause the acceptance criteria on unit frequency control not to be met, since it did not decay back to a set frequency in 40 to 50 seconds. Further investigation into this difficulty revealed that the frequency oscillation magnitude was small and did not constitute a hazard to the operating equipment on the unit.

The results of the test when compared to the acceptance criteria minimum and maximum parameter tolerances are shown in Table 4.5-1 which also gives the minimum and maximum deviation in primary and secondary unit parameters both prior to and after the trip. As can be seen, all measured values fell within their allowable limits. An additional acceptance criteria was that the trend in plant fission product activity from RM-L1 did not increase. Indication on RM-L1 (i.e. RCS letdown) revealed a before and after count rate of 3.4×10^3 cpm. These results confirm that no change in the activity of the coolant system (i.e. no fuel failure) was observed.

4.5.4 CONCLUSIONS

Upon completion of The Unit Loss Of Electrical Load Test at 100% full power, the following conclusions were reached:

(1) The unit successfully sustained a net load loss at 100% full power without any fuel or equipment damage.

(2) Unit response to the load loss indicates that the integrated control system successfully ran reactor power back to 15% full power with large margin to RPS trip setpoints.

(3) Frequency oscillations were experienced after the runback to 15 % full power, thus causing the acceptance criteria on frequency control not to be met. Further investigation resulted in the conclusion that since the oscillation magnitude observed was small it did not represent a hazard to the operating equipment.

Summary Of Minimum And Maximum Deviations In Unit Parameters During
The Performance Of Unit Loss Of Electrical Load Test

Unit Parameters	Units	Test Data Prior To Trip		Test Data After Trip		Acceptance Criteria Limits	
		Minimum	Maximum	Minimum	Maximum	Minimum	Maximum
RCS Average Temperature	°F	578.9	579.1	574.2	586.0		
RCS Coolant Pressure	PSIG	2125.2	2143.7	1978.0	2261.5	1800.0	2355.0
RCS Pressurizer Level	Inches	197.5	199.1	170.0	235.0		
RCS Loop Temperature Mismatch	°F	-0.4	+0.3	-4.0	+4.3		
RCS Makeup Tank Level	Inches	NR	NR	NR	NR		
RCS Loop A Exit Temperature	°F	600.0	600.2	578.9	604.7		619.0
RCS Loop B Exit Temperature	°F	601.0	601.2	578.9	505.5		619.0
MS Generator A Level	Inches	142.3	145.8	30.2	149.9		
MS Generator B Level	Inches	147.1	149.1	24.5	147.6		
MS Generator A Temperature	°F	593.1	594.4	581.2	601.5		
MS Generator B Temperature	°F	593.4	593.6	584.6	600.5		
MS Generator A Pressure	PSIG	911.7	913.0	837.9	1049.2		
MS Generator B Pressure	PSIG	914.9	916.4	835.5	1051.8		
FDW Loop A Temperature	°F	447.8	448.5	410.1	448.2		
FDW Loop B Temperature	°F	446.0	446.4	389.5	446.1		
FDW Total Flow	MPPH	10.1	10.2	0.7	10.2	0.5	
Turbine Header Pressure	PSIG	896.4	901.2	835.2	1058.6		
Turbine Speed	RPM	1796.0	1798.0	1732.0	1928.0		

Note: The definition of (NR) is not recorded

Table 4.5-1

Reactor Coolant Pressure/Temperature Safety Limits

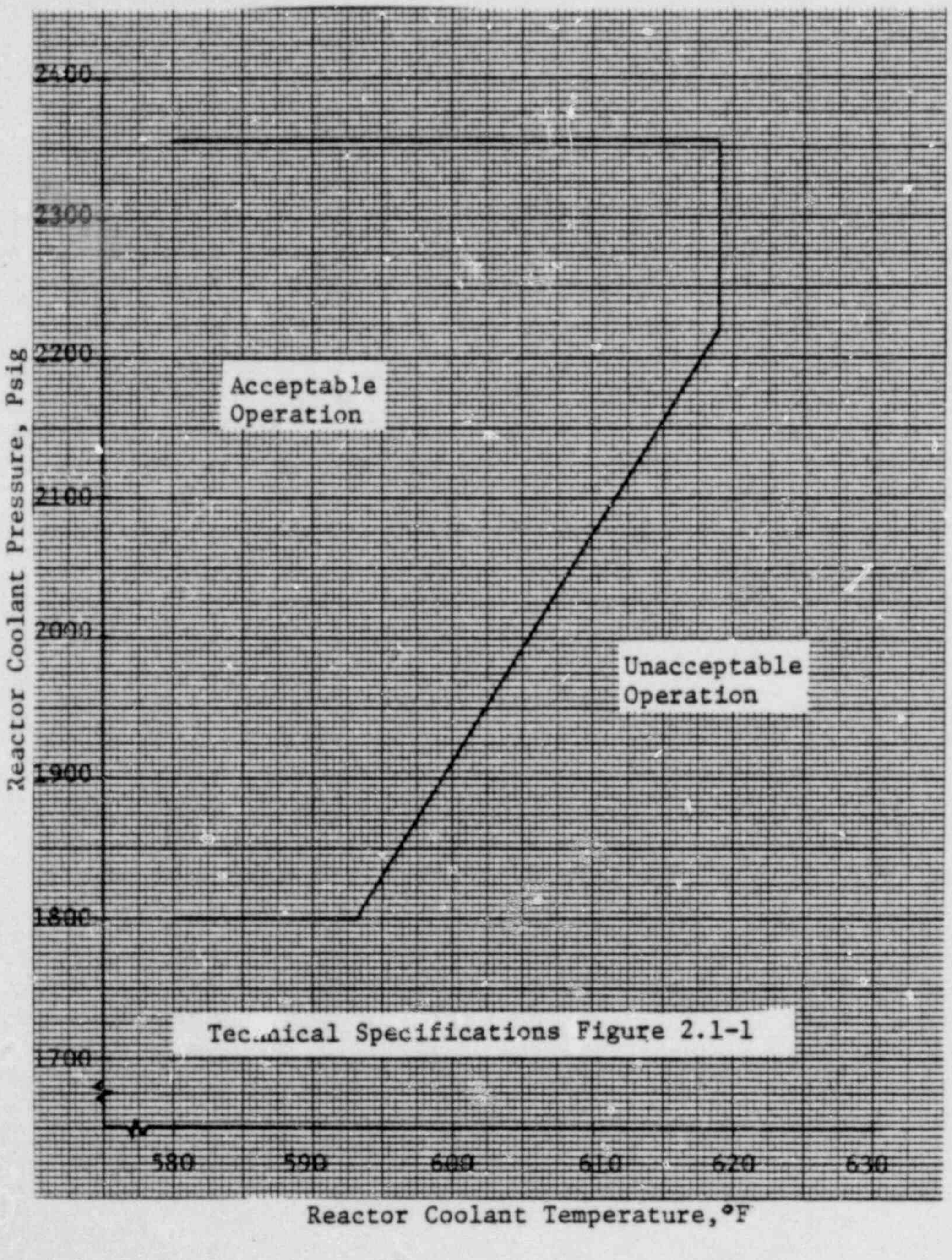

Figure 4.5-1

Primary Side Unit Parameters Versus Time During The Performance Of Unit Loss Of Electrical Load Test

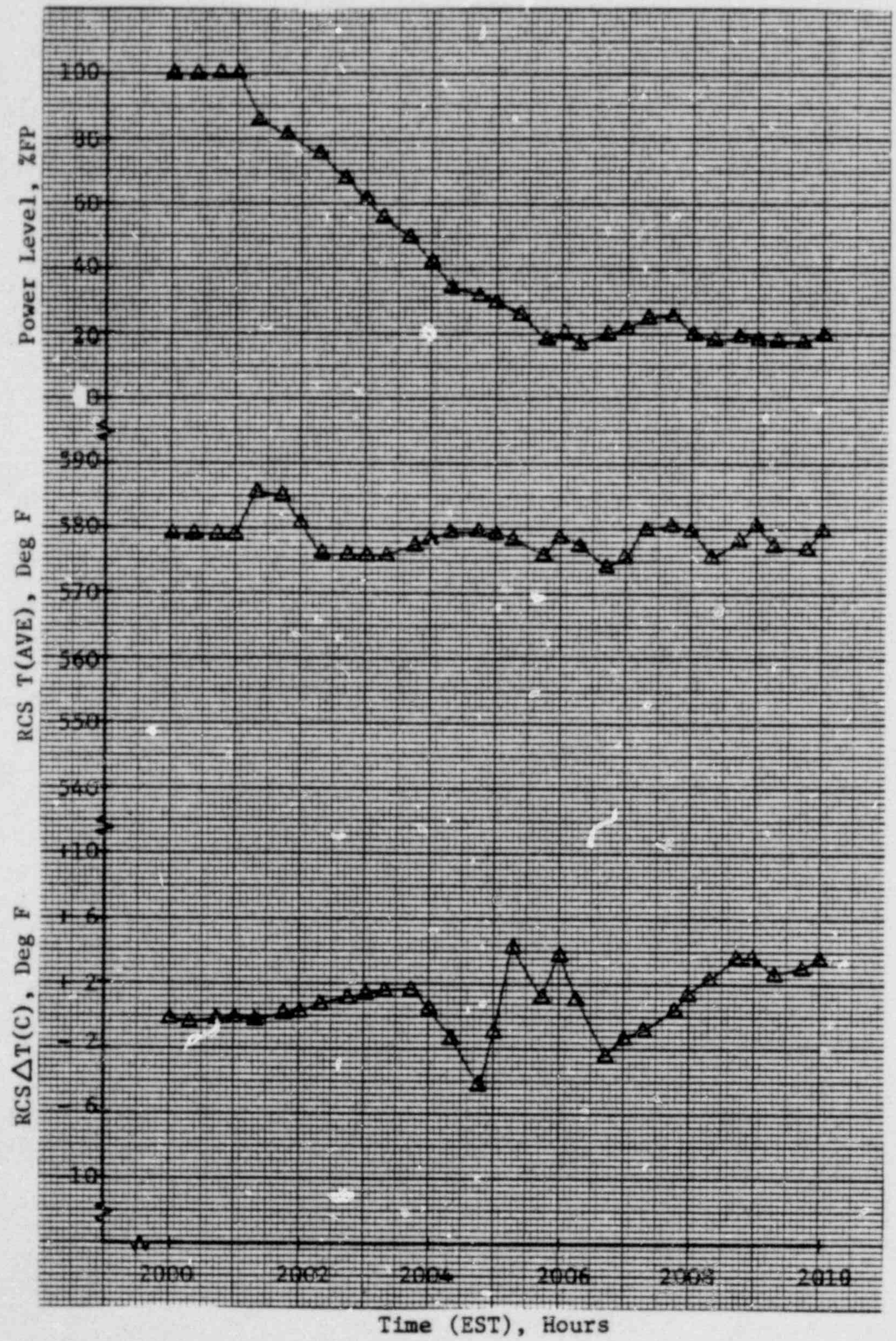

Figure 4.5-2

Primary Side Unit Parameters Versus Time During The Performance Of Unit Loss Of Electrical Load Test

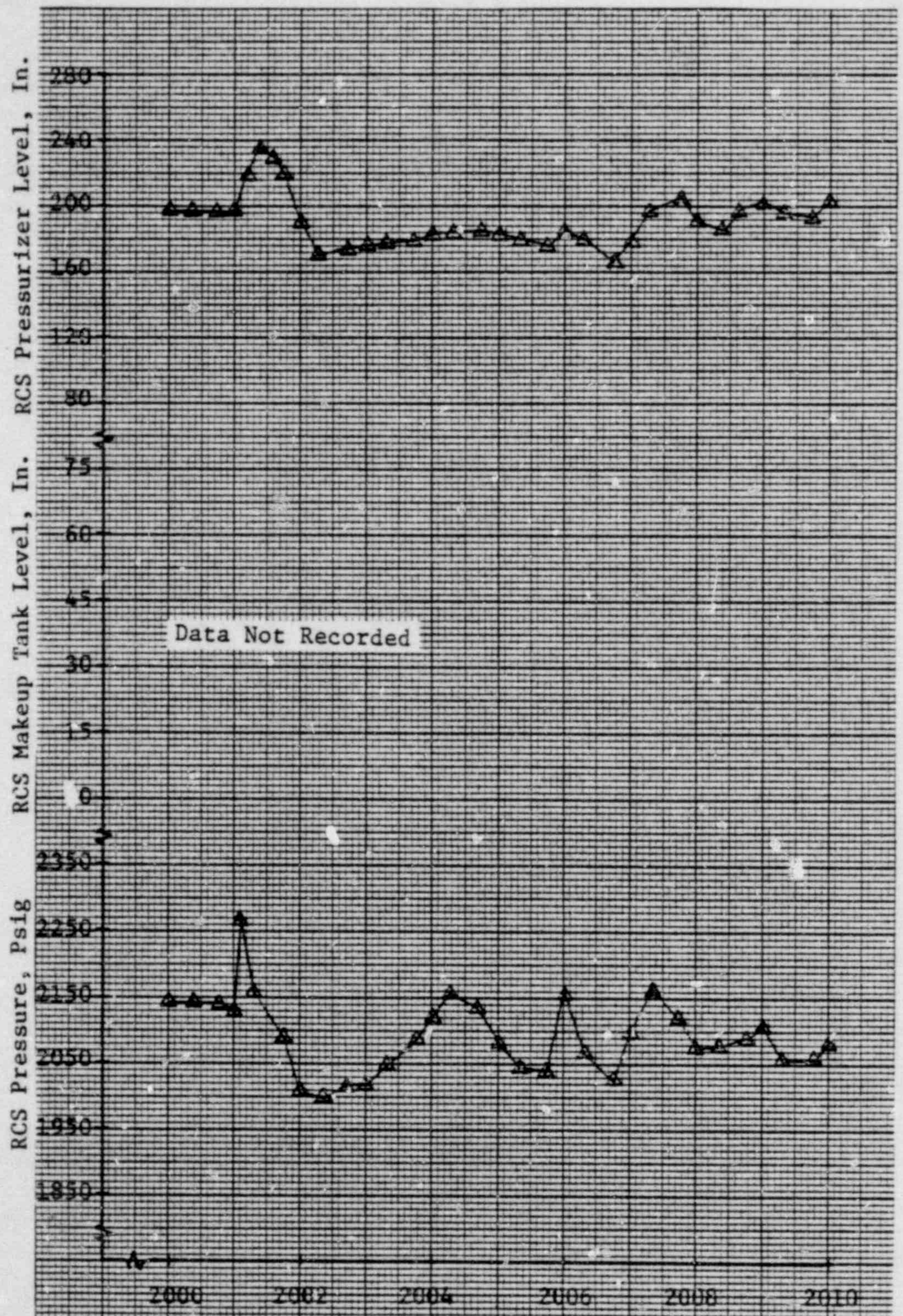

Figure 4.5-2 (Cont'd)

Secondary Side Unit Parameters Versus Time During The Performance
Of Unit Loss Of Electrical Load Test

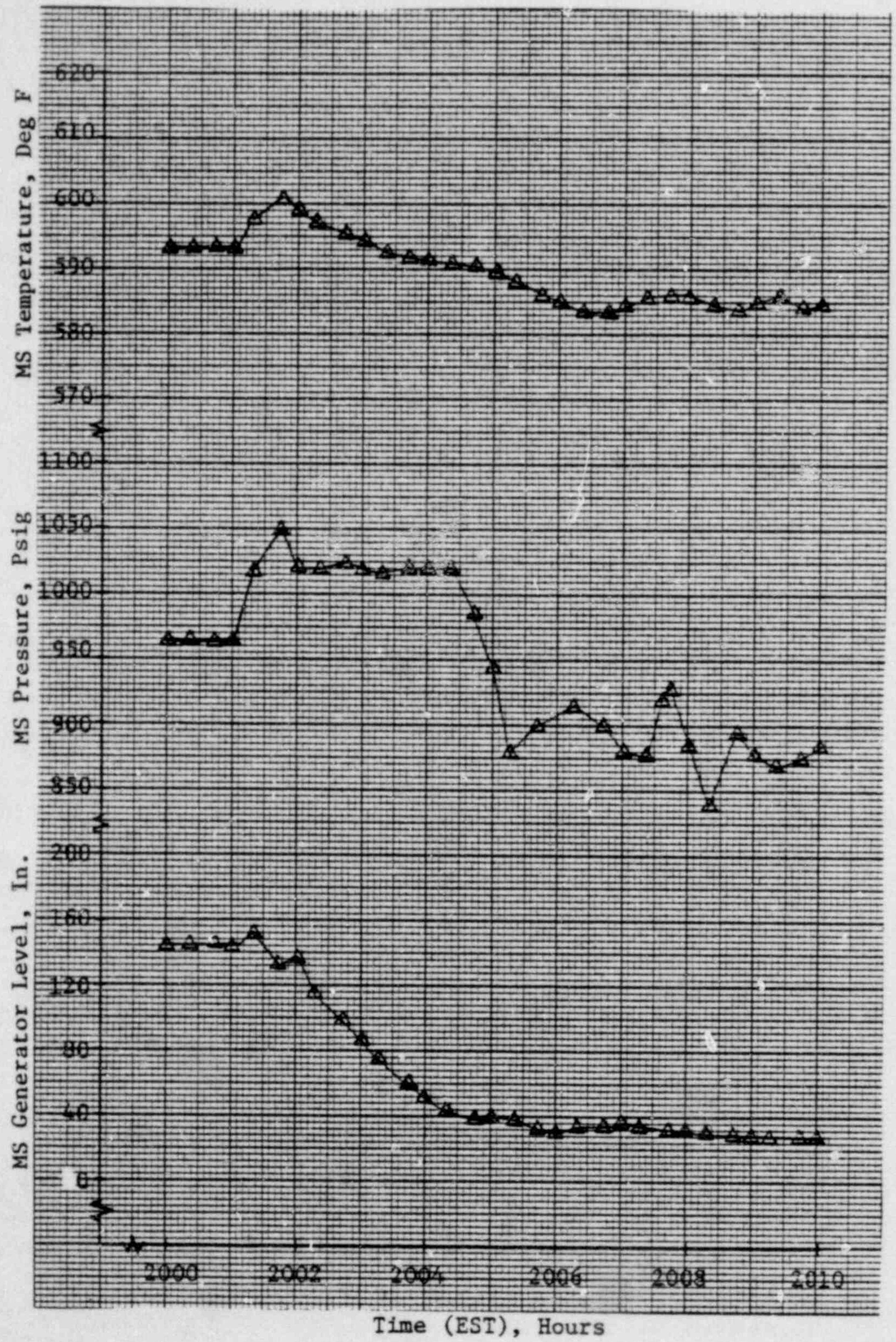

Figure 4.5-3

Secondary Side Unit Parameters Versus Time During The Performance Of Unit Loss Of Electrical Load Test

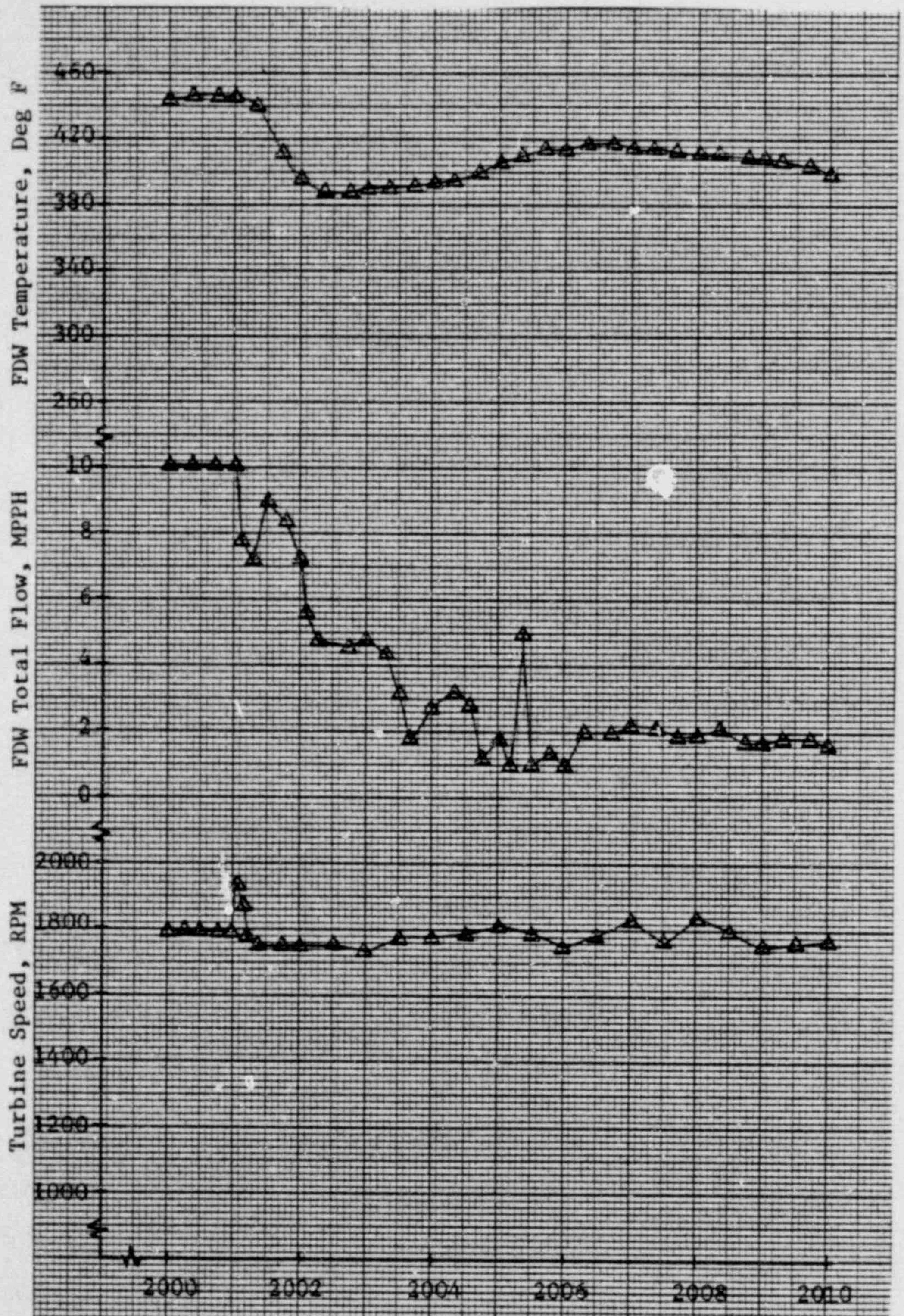

Figure 4.5-3 (Cont'd)

4.6 TURBINE/REACTOR TRIP TEST

The Turbine/Reactor Trip Test consisted of two distinct parts: a reactor trip with subsequent turbine trip at 40 percent full power and turbine trips in which the reactor was not tripped at 75 and 100 percent full power. Its purpose was to measure the plant response during and after a deliberate reactor or turbine trip from power. In order to minimize the number of reactor and/or turbine trips, unit performance data adequate for the analysis of this test was monitored continuously during power operation. An unscheduled trip might have been substituted for a scheduled trip. (This did not happen, however).

The Turbine/Reactor trip test provided data that was used to optimize the performance of the integrated control system and provide baseline data for comparison with future performance data. In addition, it also provided data for use in evaluating the effectiveness of the main steam line snubbers during closure of the main turbine stop valves.

4.6.1 PURPOSE

The general purpose of this test was to measure and evaluate the transient response of the unit during and following a reactor/turbine trip from 40% rated power and a turbine trip from 75 and 100% rated power. Specific purposes were as follows:

(a) Test pressurizer level control, reactor coolant pressure control and reactor coolant temperature control during a reactor or turbine trip.

(b) Test feedwater control and OTSG level control during a reactor or turbine trip.

(c) Test main steam pressure and feedwater temperature control during a reactor or turbine trip.

(d) Test main turbine response during a reactor or turbine trip.

The acceptance criteria for the Turbine/Reactor Trip Test are divided into the individual acceptance criteria for the reactor trip and turbine trip as given in Table 4.6-1.

4.6.2 TEST METHOD

The reactor trip portion of the test was performed at 40% full power by manually tripping the reactor from the control room console. Various unit parameters were monitored using the Reactimeter and six Brush recorders throughout the ensuing transient. Additional performance data was also obtained using the unit computer post trip review program which can printout data thirty minutes prior to and after such an occurrence. Specific data was tabulated as shown in Table 4.6-2 and comparison to the acceptance criteria was performed.

The turbine trip portion of the test was performed at 75 and 100% full power by manually tripping the turbine from the control room console. Unit parameters were monitored during the transient in the same manner as for the reactor trip.

Specific data was then tabulated as shown in Tables 4.6-3 and 4.6-4 and comparison to the acceptance criteria was performed.

During the performance of both parts of the test, the response of primary and secondary parameters were monitored and plotted to verify that the transient performance of the integrated control system to a major pertubation was acceptable. This included evaluating the impact of the spray flow, BTU limits, safety valve settings and various other controlled quantities on the transient response.

4.6.3 EVALUATION OF TEST RESULTS

The evaluation of the test results of the Turbine/Reactor Trip Test has been subdivided into three sections: one for the reactor trip test at 40% full power, one for the turbine trip test at 75% full power, and one for the turbine trip test at 100% full power. In each instance, all the acceptance criteria for this test were met as stated in Table 4.6-1.

4.6.3.1 REACTOR TRIP TEST AT 40% FULL POWER

On March 9, 1977 at approximately 1458, the Turbine/Reactor Trip Test was performed by tripping the reactor. This immediately caused an automatic turbine trip, which transferred house load to the startup transformer. However, during this transfer, the feedwater pump tachometer experienced a momentary loss of power causing a zero speed indication to the feedwater pump controller which tripped the pump. Since feedwater flow was lost, the control room operator put the unit in manual and took control to maintain pressures, temperatures, levels and flows. Thus the ability of the integrated control system to maintain the above quantities was not ascertained. To correct the above problem on future reactor trips, the power supply to each feedwater pump tachometer has been connected to a vital bus.

The response of the primary and secondary unit parameters both during and after the transient is shown in Figures 4.6-1 and 4.6-2. As can be seen, adequate control of the unit was maintained with no unstable conditions developing. Even though sufficient control of the unit was achieved, periodic lifting of safety valve MSV-33 at approximately 1000 Psig (i.e. 50 Psig below its setpoint) was contradicting the ability of the integrated control system turbine bypass valves to control main steam pressure at 1010 Psig. The status of all main safety valves during the test is given in Table 4.6-5. It should be noted that MSV-33 blew for 348 seconds, which had a strong effect on the primary system cooldown rate.

The results of the test were compared to the acceptance criteria minimum and maximum tolerances as shown in Table 4.6-2. Also presented are the minimum and maximum primary and secondary unit parameters both prior to and after the trip. As can be seen, all measured values fell within their allowable limits.

4.6.3.2 TURBINE TRIP TEST AT 75% FULL POWER

On March 30, 1977 at approximately 0814, the Turbine/Reactor Trip Test at 75% full power was performed by manually tripping the turbine. The unit successfully ran reactor power back to 15% full power within 2.8 minutes after the trip with an average ramp rate of approximately 21%FP/Min. As shown in Figures 4.6-3 and 4.6-4, excellent control of primary and secondary parameters during the transient was experienced. After the reactor power had leveled out around 15% full power, periodic oscillation in the primary side unit parameters at a two minute period were present. This, in part, has been attributed to the fact that reactor power is less than that recommended for the fully integrated control mode.

During the turbine trip, some difficulty was experienced when FWV-29 and FWV-30 would not close. The control room operator took manual control and shut the block valves in 216 and 142 seconds, respectively. Since this performance did not meet the acceptance criteria, the torque and limit switches on these valves were adjusted. To ensure that this adjustment was adequate, the turbine was brought back on-line at 15% full power and tripped again. This time FWV-29 and FWV-30 took 28.0 and 27.5 seconds, respectively, to close (i.e. time from a red light to green light indication using a stop watch).

The results of the test were compared to the acceptance criteria minimum and maximum tolerances as shown in Table 4.6-3. Also presented are the minimum and maximum primary and secondary unit parameters both prior to and after the trip. As can be seen, all measured values fell within their allowable limits.

The above test results were also reviewed by the Babcock and Wilcox Control Analysis Section, so that improvements in the ICS transient performance could be incorporated prior to transient testing at 100% full power. As a result of this review, the ICS modifications listed in Table 4.6-6 were incorporated prior to the 100% turbine trip test.

4.6.3.3 TURBINE TRIP TEST AT 100% FULL POWER

On April 18, 1977 at approximately 1100, the Turbine/Reactor Trip Test at 100% full power was performed by manually tripping the turbine. The unit successfully ran reactor power back to 15% full power within 4.0 minutes at an average ramp rate of approximately 21% FP/Min. As shown in Figures 4.6-5 and 4.6-6, excellent control of primary and secondary parameters during the transient was observed. In all parameters, large margins from RPS trip setpoints were experienced. After the reactor power had leveled out around 15% full power periodic oscillations in the primary side unit parameters on a two minute period were present. These oscillations were similar to those experienced during the turbine trip test at 75% full power.

The results of the test were compared to the acceptance criteria minimum and maximum tolerances as shown in Table 4.6-4. Also presented are the minimum and maximum primary and secondary unit parameters both prior to and after the trip. As can be seen, all measured values fell within their allowable limits.

During the test, the closure times on the feedwater block valves FDW-29 and FDW-30 were also recorded using a stop watch. The results indicate that the closure times were less than 30.0 seconds.

4.6.4 CONCLUSIONS

Upon completion of the reactor and turbine trip portions of Turbine/Reactor Trip Test at 40, 75, and 100% full power, the following conclusions were reached:

(a) Analysis of unit parameters during the transient indicates that all acceptance criteria were met.

(b) Unit response to a manual turbine trip indicated that the integrated control system can successfully run reactor power back to 15% full power with large margins to RPS trip setpoints.

(c) The manual reactor trip caused the turbine to trip which ensures that cooldown rates less than $100^{o}F/hr$ can be maintained following reactor trips at power.

(d) After adjustments the feedwater block valves closure times were verified. to be less than 30 seconds.

Table 4.6-1

Summary Of The Turbine/Reactor Trip Test Acceptance Criteria

Criteria Number	Procedural Acceptance Criteria	Acceptance Criteria Met Reactor/Turbine 40 % FP	 Turbine Only 75 % FP	 Turbine Only 100 % FP
1	The reactor trip causes the turbine/generator to trip	Yes	NA	NA
2	The reactor coolant pressure remains above 1800 psig and below 2355 psig	Yes	Yes	Yes
3	The main steam pressure at the OTSG outlet must not exceed 1155 psig	Yes	Yes	Yes
4	The final feedwater temperature remains above 185°F and below 470°F	Yes	Yes	Yes
5	The pressurizer level does not go below 0 inches or above 320 inches	Yes	NA	NA
6	The pressurizer level does not go below 40 inches or above 320 inches	NA	Yes	Yes
7	The turbine speed does not reach or exceed its overspeed trip point of 1998 RPM.	Yes	Yes	Yes
8	The OTSG level remains above 8 inches and below 384 inches	Yes	Yes	Yes
9	The reactor coolant pumps remain in operation	Yes	Yes	Yes
10	Automatic high pressure injection is not initiated by the engineered safeguard system.	Yes	Yes	Yes
11	Main Feedwater block valve FDW-29 and FDW-30 close within 30 seconds of receiving the closure signal	NA	Yes	Yes

Note: The definition of (NA) is not applicable

Table 4.6-2

Summary Of Minimum And Maximum Unit Parameters During The Performance Of Turbine/Reactor Trip Test At 40% Full Power

Unit Parameters	Units	Test Data Prior To Trip		Test Data After Trip		Acceptance Criteria Limits	
		Minimum	Maximum	Minimum	Maximum	Minimum	Maximum
RCS Average Temperature	^{o}F	578.7	579.0	548.5	57[illegible].5		
RCS Coolant Pressure	PSIG	2134.9	2153.6	1921.8	2153.6	1800.0	2355.0
RCS Pressurizer Level	Inches	198.8	201.0	63.1	201.0	0.0	320.0
RCS Loop Temperature Mismatch	^{o}F	-0.2	+0.2	-1.1	+6.4		
RCS Makeup Tank Level	Inches	64.0	64.1	29.9	64.0		
MS Generator A Level	Inches	55.0	57.7	20.2	56.5	8.0	384.0
MS Generator B Level	Inches	53.7	56.0	12.2	55.1	8.0	384.0
MS Generator A Temperature	^{o}F	587.9	588.2	58[illegible].4	599.0		
MS Generator B Temperature	^{o}F	588.5	588.7	588.9	602.4		
MS Generator A Pressure	PSIG	879.9	885.3	884.6	1040.8		1155.0
MS Generator B Pressure	PSIG	881.3	886.6	885.6	1021.2		1155.0
FDW Loop A Temperature	^{o}F	367.8	368.0	226.4	367.9	185.0	470.0
FDW Loop B Temperature	^{o}F	365.9	366.5	358.1	366.4	185.0	470.0
Turbine Header Pressure	PSIG	884.8	890.3	889.1	1047.9		
Turbine Speed	RPM	1795.0	1796.0	948.0	1796.0		1998.0

Table 4.6-3

Summary Of Minimum And Maximum Unit Parameters During The Performance Of Turbine/Reactor Trip Test At 75% Full Power

Unit Parameters	Units	Test Data Prior To Trip		Test Data After Trip		Acceptance Criteria Limits	
		Minimum	Maximum	Minimum	Maximum	Minimum	Maximum
RCS Average Temperature	^oF	579.5	579.5	576.8	591.0		
RCS Coolant Pressure	PSIG	2153.8	2158.9	1923.7	2320.3	1600.0	2[illegible]55.0
RCS Pressurizer Level	Inches	200.3	200.5	164.1	266.1	40.0	320.0
RCS Loop Temperature Mismatch	^oF	0.0	+0.3	-6.8	+3.3		
RCS Makeup Tank Level	Inches	62.3	62.3	48.5	64.8		
MS Generator A Level	Inches	99.8	101.0	25.[illegible]	112.2	8.0	384.0
MS Generator B Level	Inches	101.0	101.9	[illegible]5.8	90.0	8.0	384.0
MS Generator A Temperature	^oF	592.1	592.3	581.5	606.7		
MS Generator B Temperature	^oF	594.2	594.3	589.8	609.7		
MS Generator A Pressure	PSIG	891.9	893.8	859.0	1035.0		1155.0
MS Generator B Pressure	PSIG	894.7	896.7	909.0	1055.0		1155.0
FDW Loop A Temperature	^oF	423.7	423.7	305.3	423.7	185.0	470.0
FDW Loop B Temperature	^oF	422.6	422.6	339.5	422.5	185.0	470.0
Turbine Header Pressure	PSIG	892.0	894.2	860.9	1076.1		
Turbine Speed	RPM	1794	1796	1085	1795		1998.0

Table 4.6-4

Summary Of Minimum And Maximum Unit Parameters During The Performance Of Turbine/Reactor Trip Test At 100% Full Power

Unit Parameters	Units	Test Data Prior To Trip		Test Data After Trip		Acceptance Criteria Limits	
		Minimum	Maximum	Minimum	Maximum	Minimum	Maximum
RCS Average Temperature	^{o}F	578.6	578.7	576.0	586.1		
RCS Coolant Pressure	PSIG	2126.9	2133.9	1975.3	2280.0	1800.0	2355.0
RCS Pressurizer Level	Inches	199.1	199.8	173.2	240.5	40.0	320.0
RCS Loop Temperature Mismatch	^{o}F	-0.6	+0.0	-3.7	+3.3		
RCS Makeup Tank Level	Inches	NR	NR	NR	NR		
MS Generator A Level	Inches	145.7	149.4	26.6	159.3	8.0	384.0
MS Generator B Level	Inches	147.9	150.6	24.8	142.7	8.0	384.0
MS Generator A Temperature	^{o}F	592.5	592.6	583.9	605.8		
MS Generator B Temperature	^{o}F	592.8	592.9	583.0	603.5		
MS Generator A Pressure	PSIG	912.0	913.2	888.4	1049.1		1155.0
MS Generator B Pressure	PSIG	916.4	917.5	899.2	1035.8		1155.0
FDW Loop A Temperature	^{o}F	488.6	449.3	288.8	449.0	185.0	470.0
FDW Loop B Temperature	^{o}F	446.9	447.3	294.7	422.5	185.0	470.0
Turbine Header Pressure	PSIG	897.4	901.1	883.8	1061.9		
Turbine Speed	RPM	1794.0	1795.0	862.0	1794.0		1998.0

Note: The definition of (NR) is not recorded

Table 4.6-5

Main Steam Valves Status During The Performance Of Turbine/Reactor Trip Test At 40, 75 And 100 % Full Power

Main Steam Valve Number (None)	Safety Valve Lift Setting (Psig)	Orifice Size (Inches)	40 % FP Plateau		75 % FP Plateau		100 % FP Plateau	
			Delay Time (Seconds)	Lift Time (Seconds)	Delay Time (Seconds)	Lift Time (Seconds)	Delay Time (Seconds)	Lift Time (Seconds)
Main Steam Line A1								
MSV-34	1050	4.515	NA	NA	10	245	6	180
MSV-38	1070	4.515	NA	NA	11	185	6	180
MSV-43	1090	4.515	NA	NA	11	130	6	180
MSV-40	1100	3.750	NA	NA	NA	NA	NA	NA
Main Steam Line A2								
MSV-33	1050 *	4.515	5	348	10	245	6	240
MSV-37	1070	4.515	NA	NA	11	185	6	240
MSV-42	1090	4.515	NA	NA	11	130	6	240
MSV-46	1100	4.515	NA	NA	NA	NA	NA	NA
Main Steam Line B1								
MSV-35	1050	4.515	5	60	10	245	6	240
MSV-39	1070	4.515	NA	NA	11	185	6	240
MSV-44	1090	4.515	NA	NA	11	130	6	240
MSV-47	1100	4.515	NA	NA	NA	NA	NA	NA
Main Steam Line B2								
MSV-36	1050	4.515	5	60	10	245	6	210
MSV-41	1070	4.515	NA	NA	11	185	6	210
MSV-45	1090	4.515	NA	NA	11	130	6	210
MSV-48	1100	3.750	NA	NA	NA	NA	NA	NA

Note: The definition of (NA) is not applicable

Note(*): Actual setting was approximately 1000 psig

Table 4.6-6

Summary Of ICS Modifications Recommended As A Result Of Turbine Reactor Trip Test At 75% FP. Modifications Incorporated Prior To 100% Trip Test.

Change Number	ICS Modifications	Reason For Modification
1.	Feedwater pump speed kicker circuit was added to loop A and B FDW pumps. This increased feedwater pump speed about 20% in the first four seconds after tripping the turbine or a loss of electrical load.	To prevent a significant reduction of feedwater flow to the steam generators immediately after tripping the turbine or rejecting electrical load.
2.	Added the requirement that both atmospheric dump valves open whenever steam pressure exceedes 1025 psig	To reduce peak steam pressure after a trip. This is important since peak steam and reactor coolant pressure are strongly related to each other.
3.	Added three back-to-back diode "deadband" filter circuits	To eliminate system "hunting" due to noisy error signals.
4.	Changed the characterization of the grid frequency error signal to the unit load demand signal so that the maximum step change to ULD will only be ± 10% not ± 100%	To limit the large frequency error correction to the unit load demand signal.
5.	Changed pressurizer spray valve logic so that the valve receives an immediate "open" signal for five seconds after either a turbine trip or a loss of electrical load.	To assure quick response of the Pressurizer Spray System to high reactor coolant pressure.

Primary Side Unit Parameters Versus Time During The Performance Of Turbine/Reactor Trip Test At 40% FP

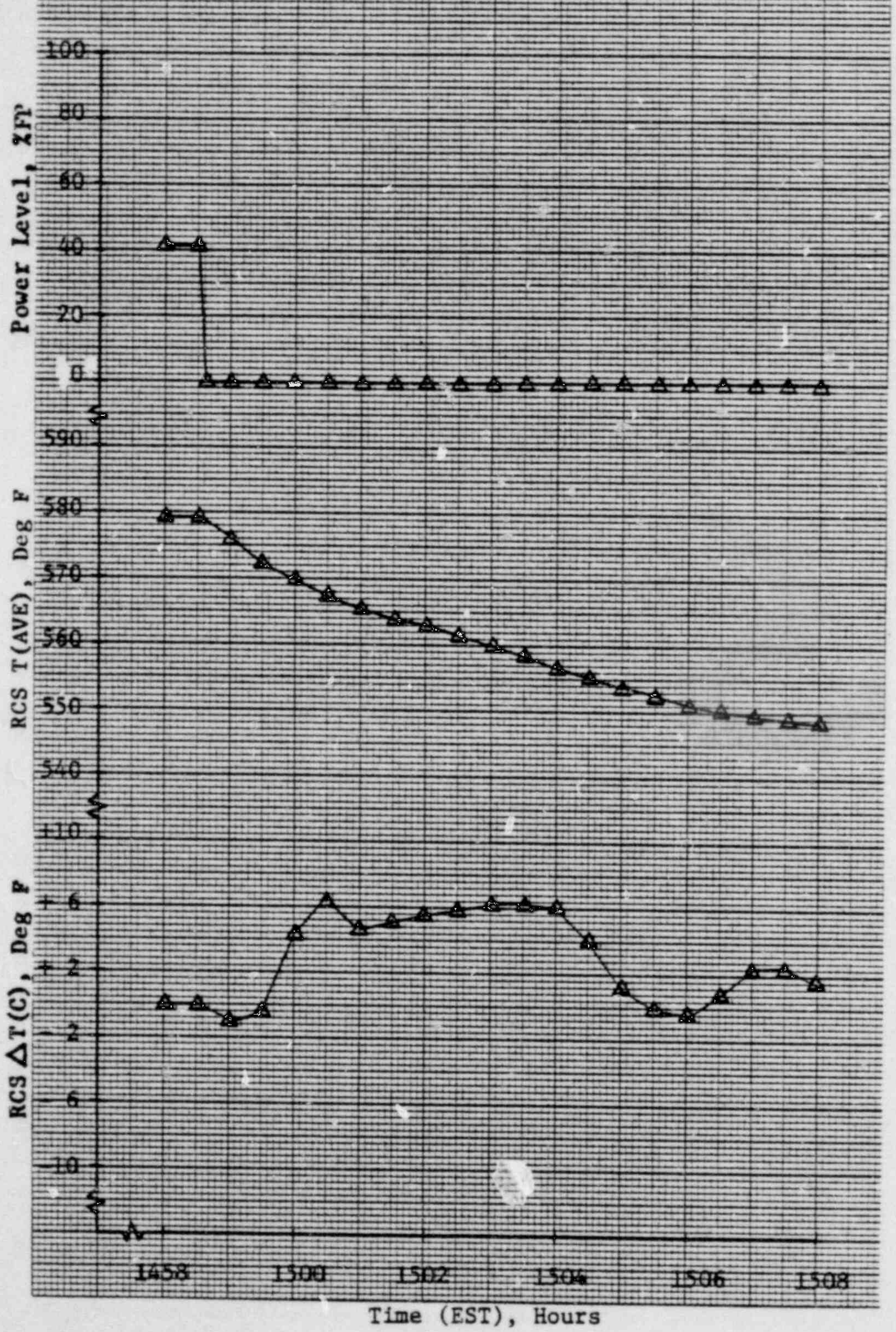

Figure 4.6-1

Primary Side Unit Parameters Versus Time During The Performance
Of Turbine/Reactor Trip Test At 40% FP

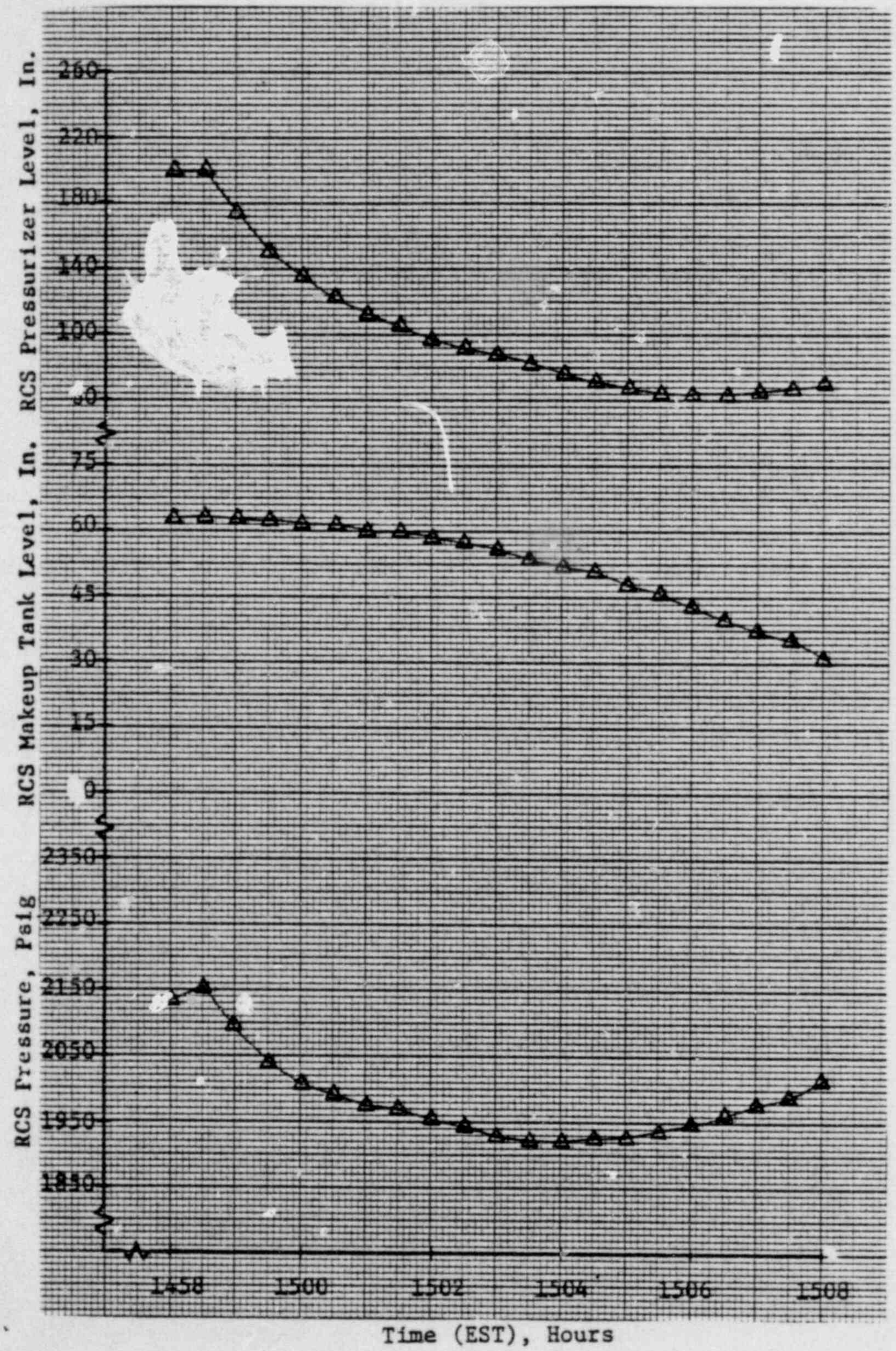

Figure 4.6-1 (Cont'd)

Secondary Side Unit Parameters Versus Time During The Performance Of Turbine/Reactor Trip Test At 40% FP

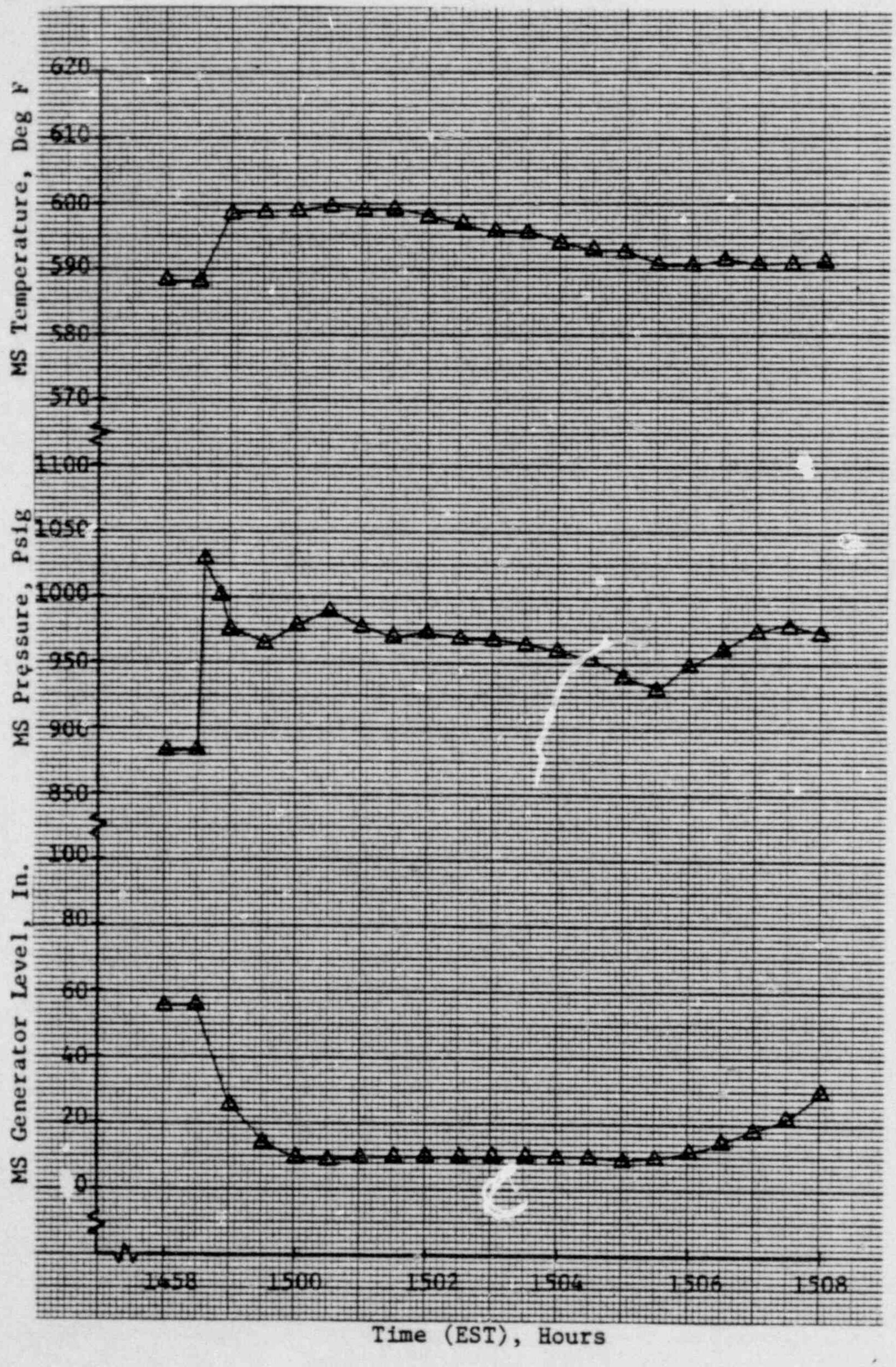

Figure 4.6-2

Secondary Side Unit Parameters Versus Time During The Performance Of Turbine/Reactor Trip Test At 40% FP

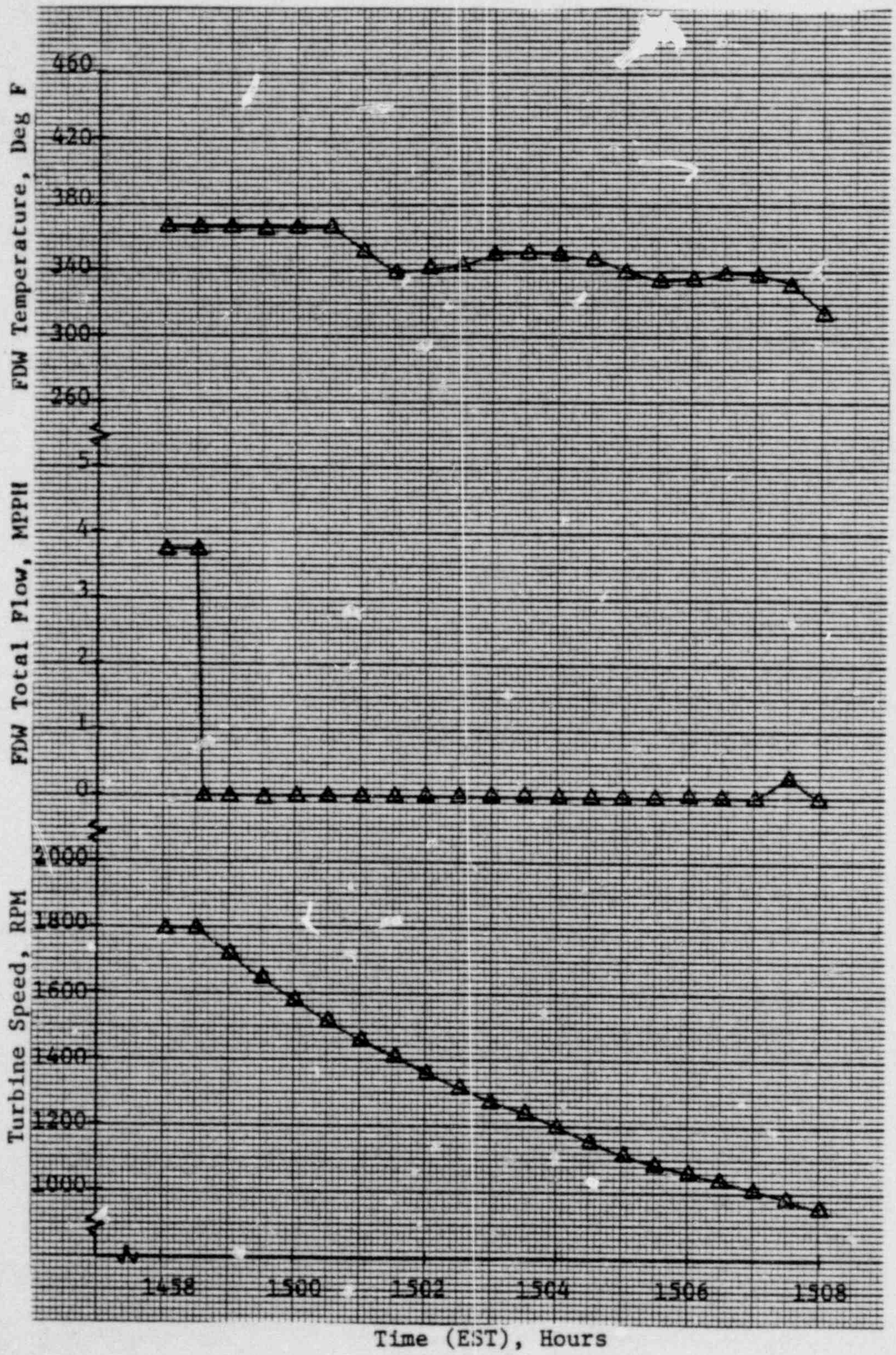

Figure 4.6-2 (Cont'd)

Primary Side Unit Parameters Versus Time During The Performance Of Turbine/Reactor Trip Test At 75% FP

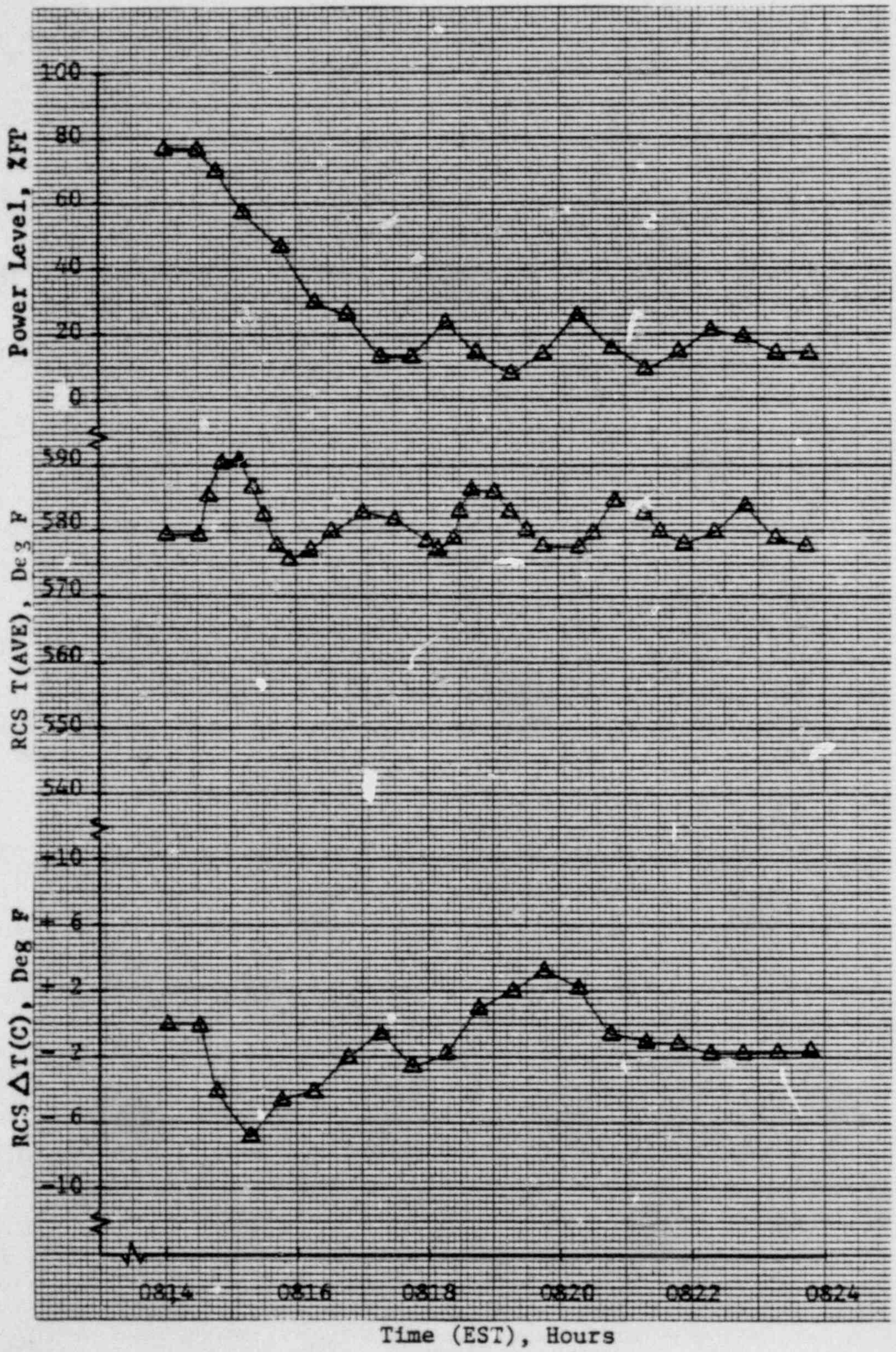

Figure 4.6-3

Primary Side Unit Parameters Versus Time During The Performance Of Turbine/Reactor Trip Test At 75% FP

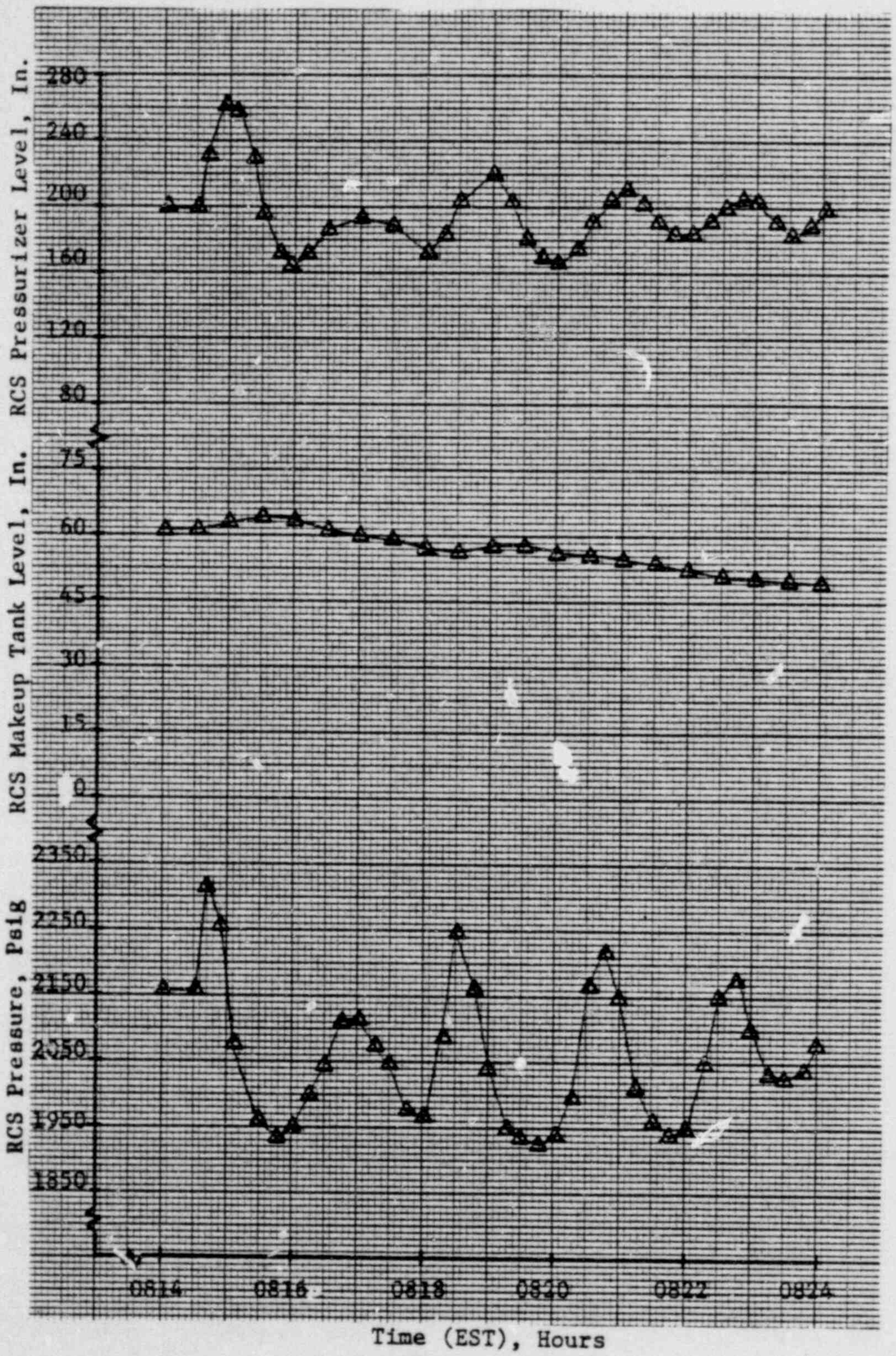

Figure 4.6-3 (Cont'd)

Secondary Side Unit Parameters Versus Time During The Performance Of Turbine/Reactor Trip Test At 75% FP

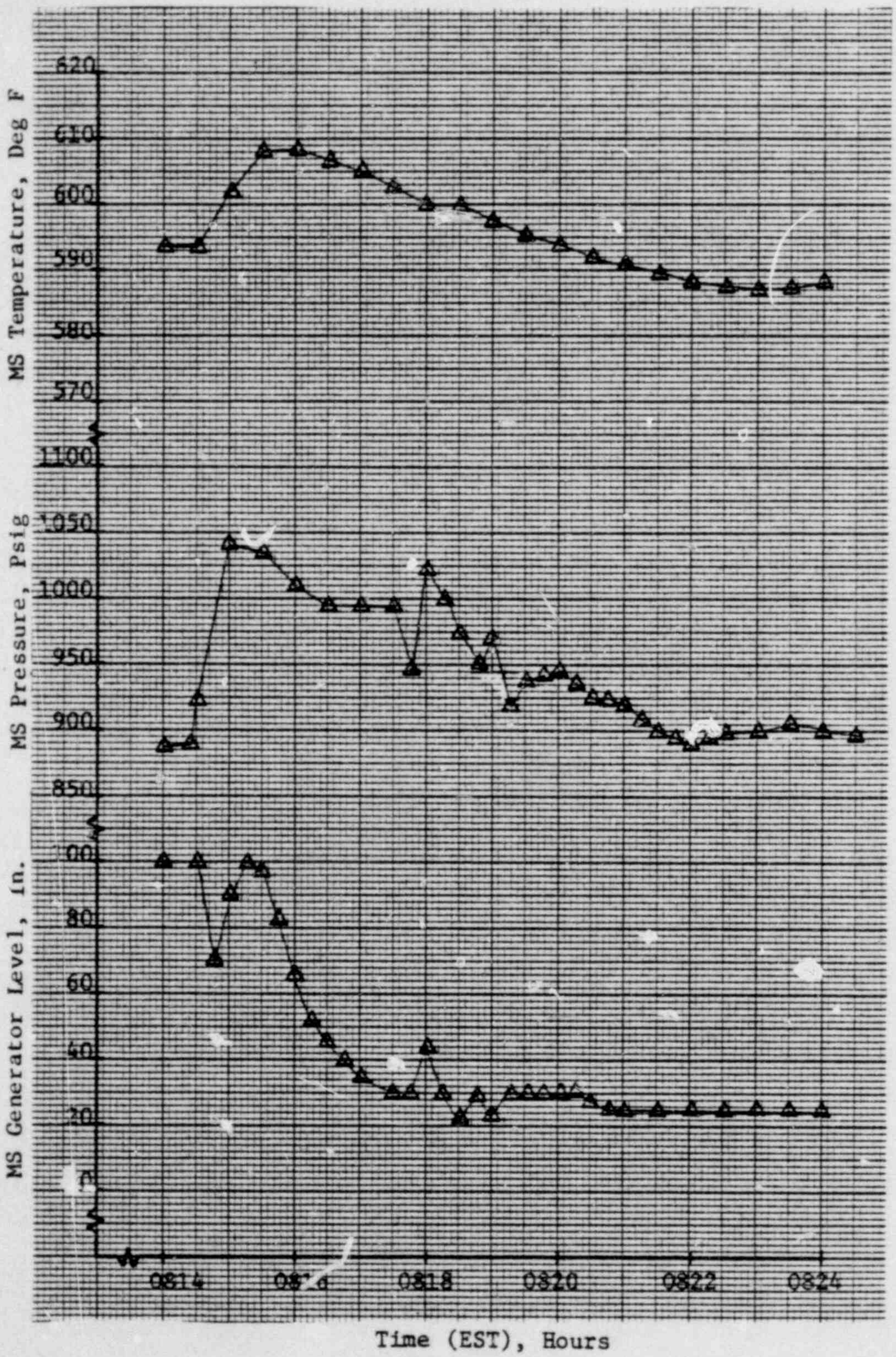

Figure 4.6-4

Secondary Side Unit Parameters Versus Time During The Performance Of Turbine/Reactor Trip Test At 75% FP

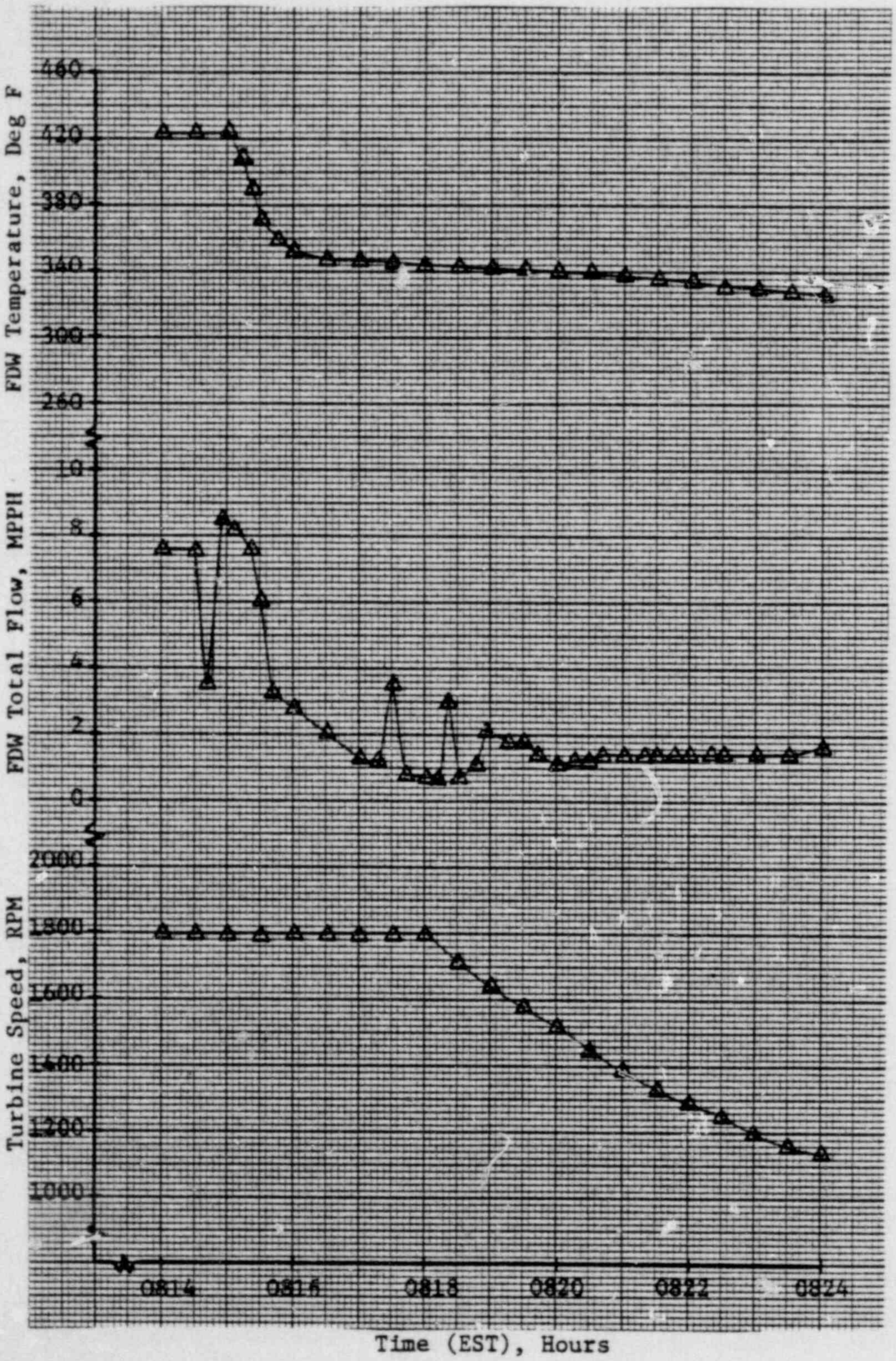

Figure 4.6-4 (Cont'd)

Primary Side Unit Parameters Versus Time During The Performance
Of Turbine/Reactor Trip Test At 100% FP

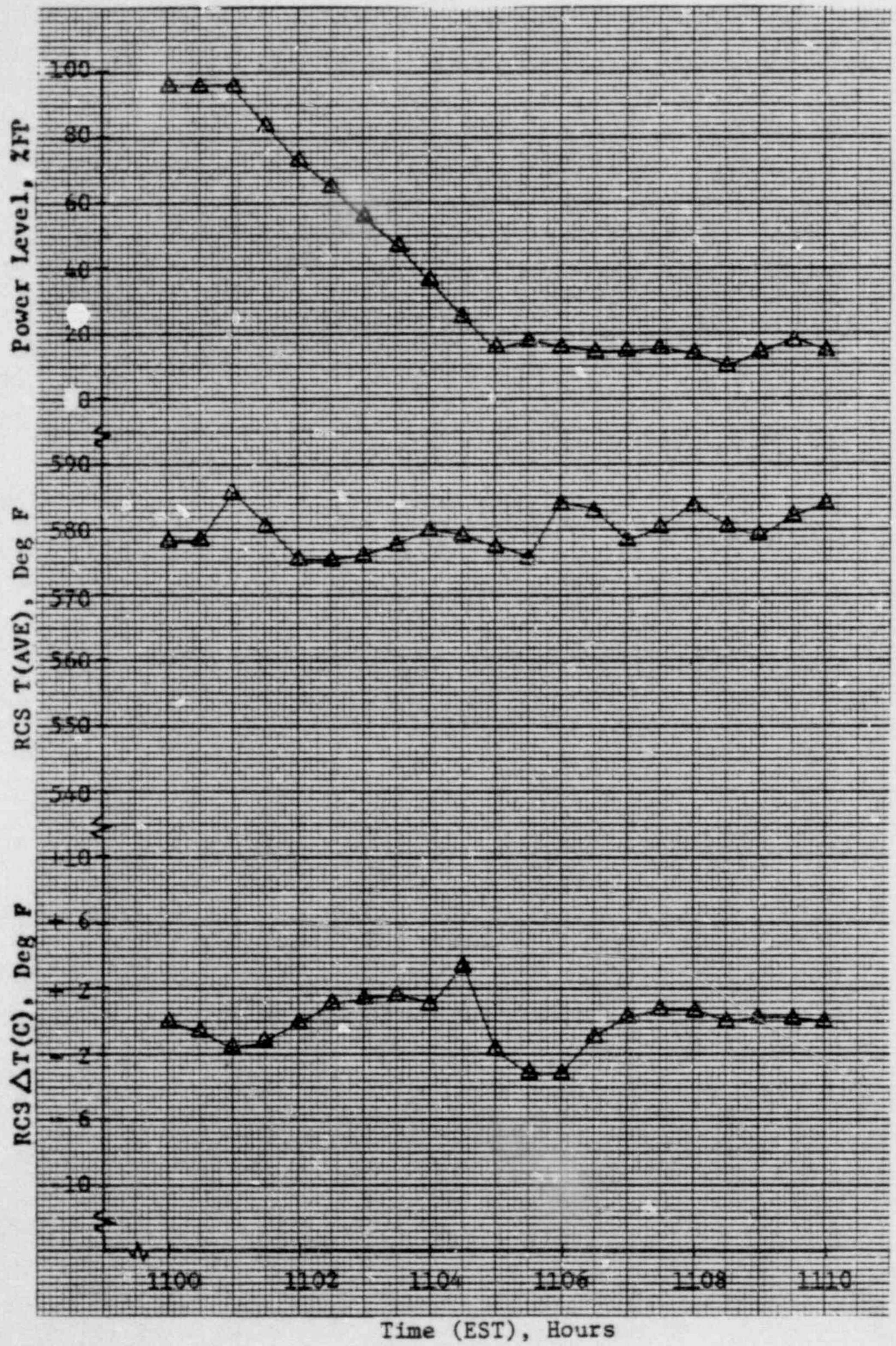

Figure 4.6-5

Primary Side Unit Parameters Versus Time During The Performance Of Turbine/Reactor Trip Test At 100% FP

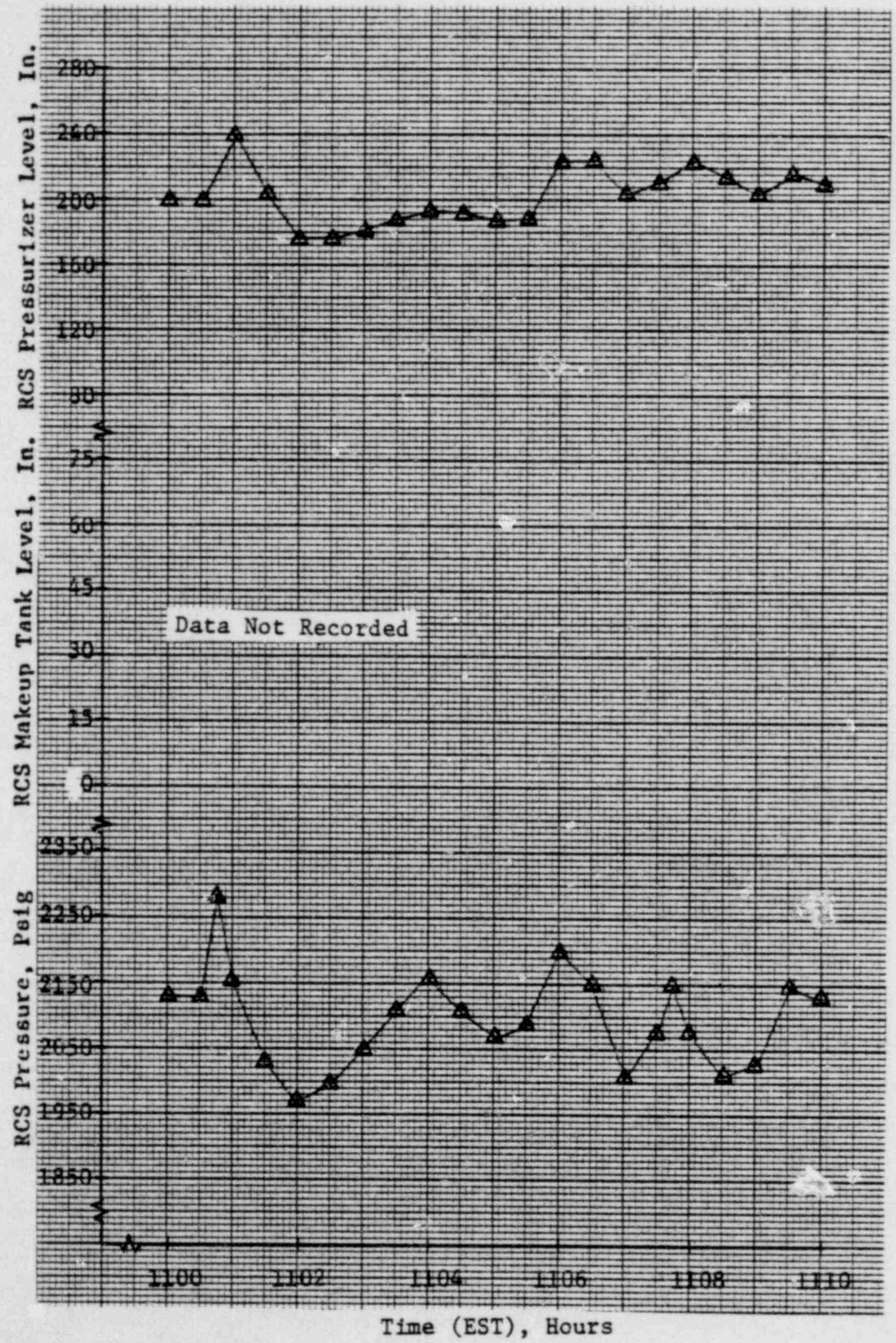

Figure 4.6-5 (Cont'd)

Secondary Side Unit Parameters Versus Time During The Performance Of Turbine/Reactor Trip Test At 100% FP

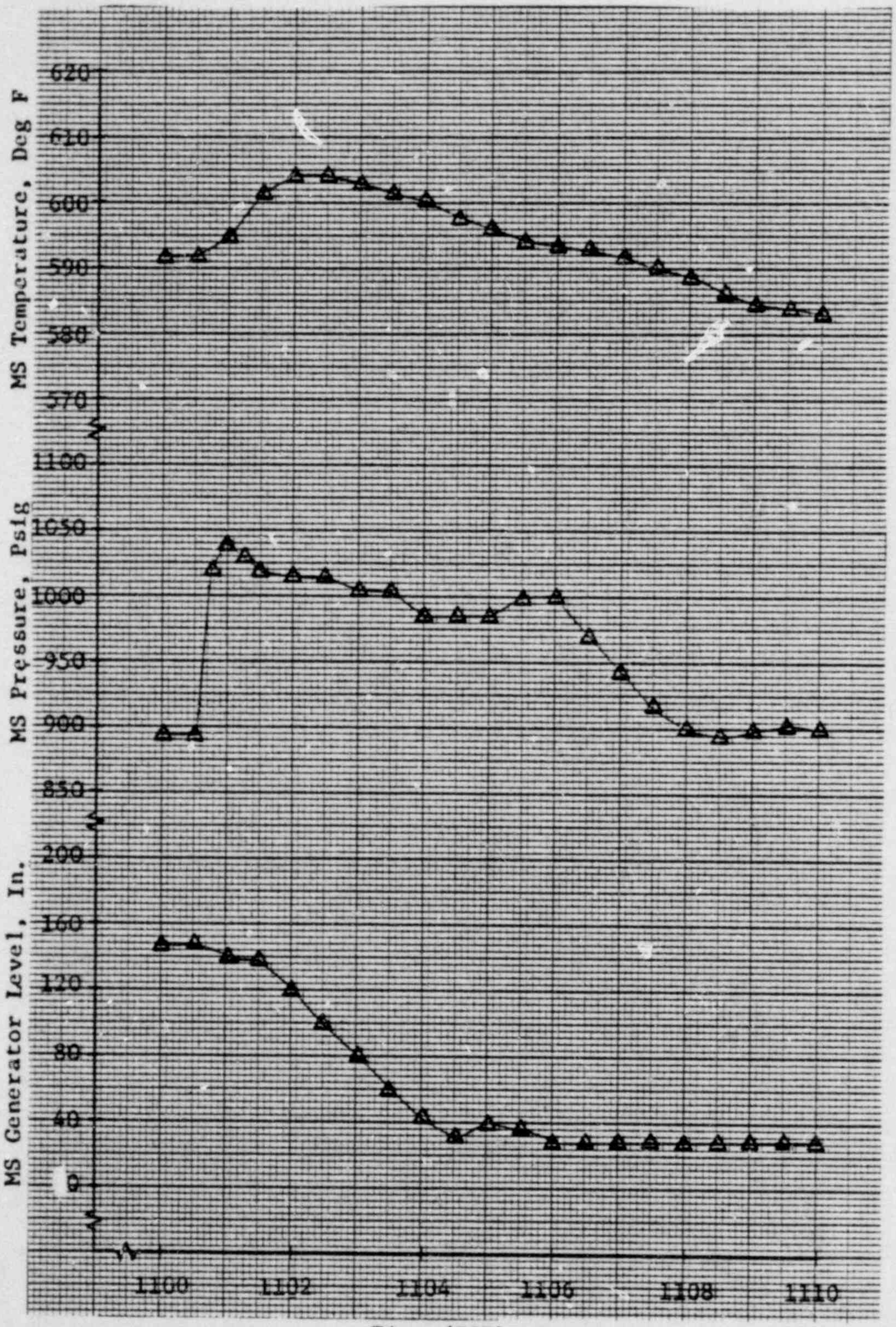

Figure 4.6-6

Secondary Side Unit Parameters Versus Time During The Performance Of Turbine/Reactor Trip Test At 100% FP

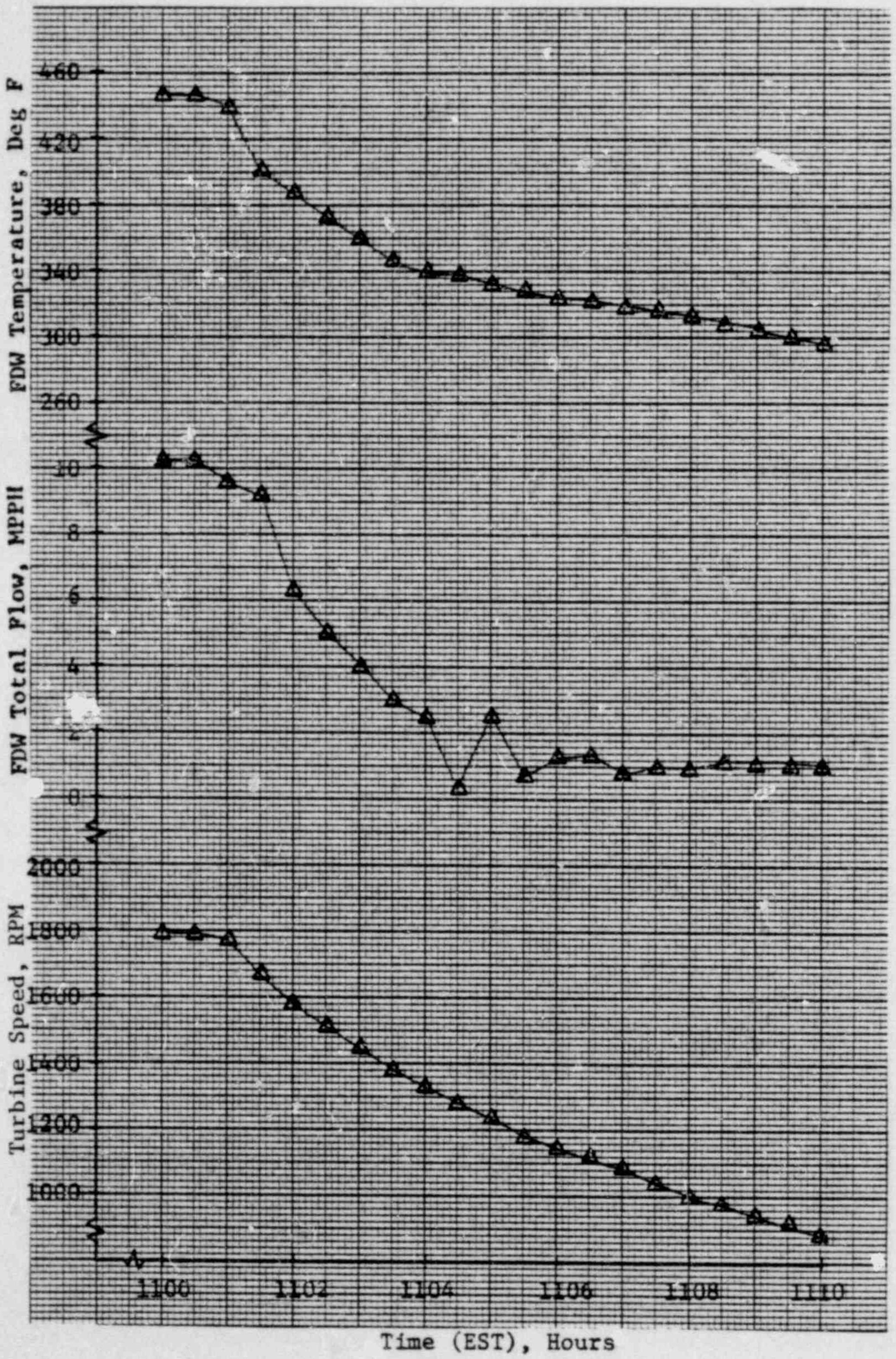

Figure 4.6-6 (Cont'd)

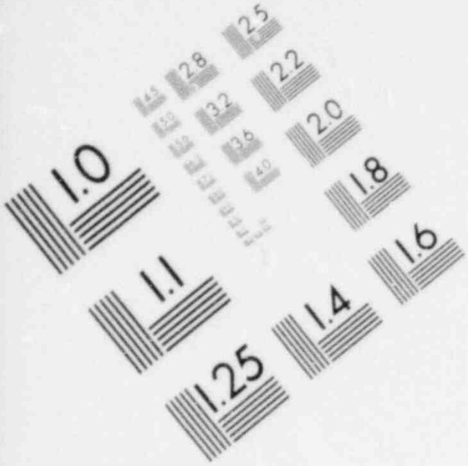

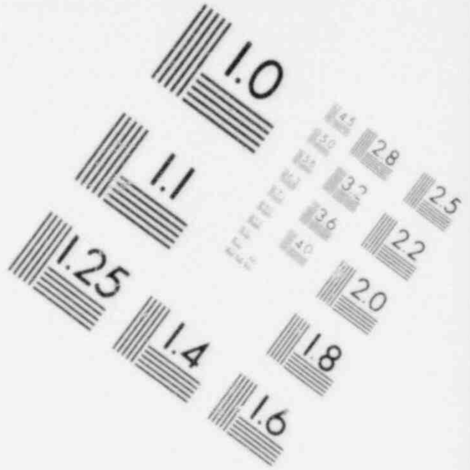

IMAGE EVALUATION
TEST TARGET (MT-3)

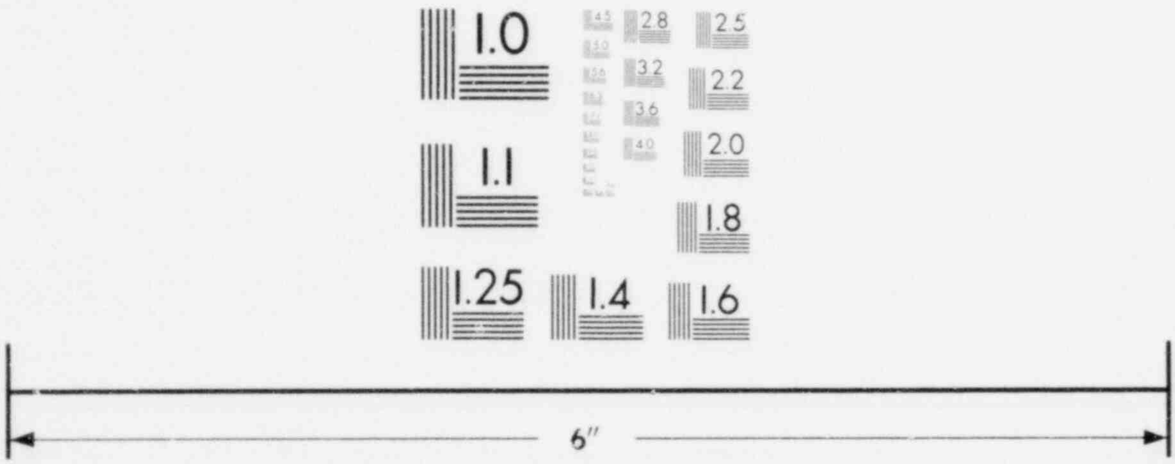

MICROCOPY RESOLUTION TEST CHART

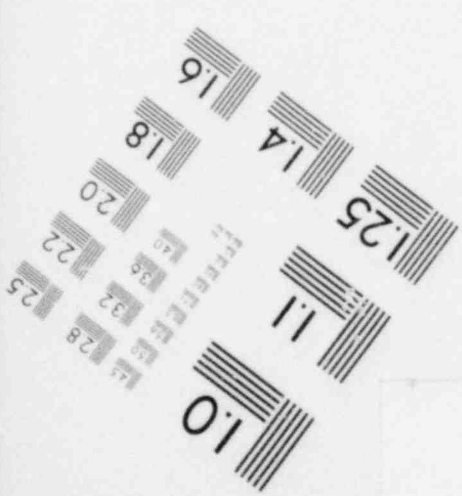

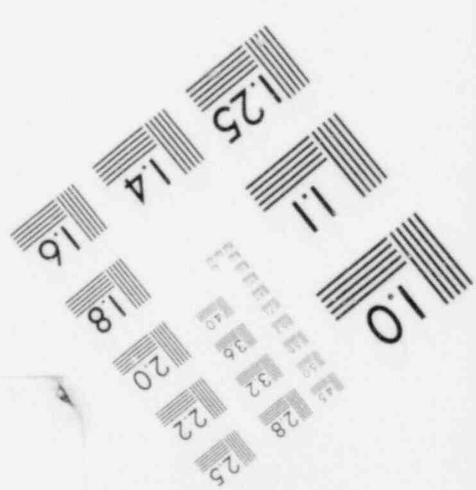

IMAGE EVALUATION
TEST TARGET (MT-3)

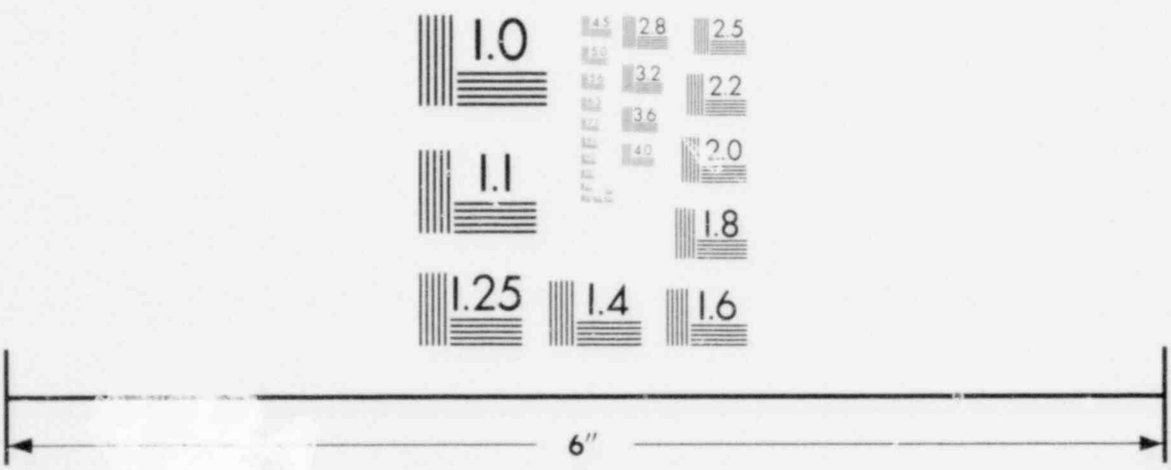

MICROCOPY RESOLUTION TEST CHART

4.7 INCORE DETECTOR TEST

The incore monitoring system consists of 52 detector assemblies each containing 7 neutron detectors equally spaced axially. Of these 52 detector assemblies, all contain rhodium self-powered neutron detectors (SPND) with inconel lead wires. Each also contains one inconel lead wire detector without rhodium for use in background corrections. The power distribution within the core is measured at 364 locations by use of these neutron detectors (7 axial positions in the 52 detector assemblies). The outputs of the SPND's are connected to the unit computer which provides the unit operators with power distribution information. In addition, 48 detector signals are available in the control room on two 24 point recorders for backup in case the unit computer is not operational. The incore monitoring system does not perform direct protective actions or direct control actions. However, the incore instrumentation is used to calibrate the top and bottom out-of-core power range detectors in terms of imbalance (power in top half of core minus power in bottom half of core). Furthermore, the incore instrumentation provides detailed power distribution data that could be used to alert the reactor operators to any adverse power distribution change or trend during operation, and to provide power distribution and fuel burnup data.

The incore monitoring assemblies are placed at preselected radial positions in the core as shown in Figure 4.7-1. Each assembly contains seven equally spaced flux detectors corresponding to seven axial elevations in the core to provide measurement of axial flux shape. As shown in Figure 4.7-1, 17 detector assemblies are positioned to act as symmetry monitors; the remaining 35 assemblies with 5 of the 17 symmetry monitors, monitor other fuel assembly positions assuming core symmetry.

The unit computer utilizes a variety of correction factors which are used to correct the signal of the self-powered neutron detector. The computer provides readouts of the incore detector signals on typewriters and individual digital display.

In order to ascertain that the incore monitoring system and the Bailey 855 unit computer when coupled together were giving an accurate description of the distribution of core power, these systems were qualified during the power escalation test program by comparing certain computer calculated values with similar values calculated by hand. It was not expected that this comparison would give identical values since a number of simplifying assumptions were used in the hand calculation.

The incore monitor system and the Bailey 855 unit computer were qualified for both the 40 and 75% full power test plateau, with a preliminary qualification done at 15% full power. Once the unit computer was qualified, it was then used in lieu of hand calculations for testing at that test plateau. Similarily once it was qualified at 75% full power, it was then used for all testing thereafter.

The results of the incore detector testing done during the test program as part of the power escalation sequence are discussed by dividing this section into five subsections as follows:

(1) Incore Detector Checkout

(2) Incore Detector Signal Corrections

(3) Radial Core Power Distribution Comparison

(4) Worst Case Maximum Linear Heat Rate (LHR) Calculations

(5) Incore Detector Response

4.7.1 PURPOSE

The general purpose of this test is to verify that the incore monitoring system and the Bailey 855 unit computer together provide an accurate description of the core power distribution. This is accomplished by fulfilling the following individual purposes:

(1) To verify that the incore detector outputs are reasonable and to identify any which have failed or have questionable outputs.

(2) To verify that the Bailey 855 unit computer is properly performing the necessary corrections to the incore detector signals.

(3) To verify that the Bailey 855 unit computer is calculating the radial core power distribution and worst case maximum LHR correctly.

Five acceptance criteria are specified for Incore Detector Test and are listed below:

(1) The hand and computer calculated values for the sensitivity, depletion, and background corrected signals shall agree within ± 2 percent.

(2) The hand and computer calculated values for the segment powers shall agree within ± 3 percent.

(3) The hand and computer calculated values for the radial peaking factors shall agree within ± 5 percent.

(4) The hand calculated worst case LHR is less than or equal to the computer worst case LHR.

(5) Any incore detectors which have failed or are questionable have been identified, located, and flagged for further evaluation.

4.7.2 TEST METHOD

The Incore Detector Test was performed at the 40 and 75% full power test plateaus concurrently with the core power distribution test. After three-dimensional equilibrium xenon was established, data was obtained using the performance data output program on the unit computer. This included a listing of the following:

(1) Uncorrected detector signals

(2) Sensitivity, depletion, and background corrected detector signals

(3) Enrichment, rodded/unrodded, and LBP corrected segment power

(4) Radial core power distribution

(5) Thermal hydraulic data

This data was then used in a hand calculation to verify that the computer values for corrected SPND, segment power, radial power distribution and worst case MLHR was being performed satisfactory. To reduce analysis time, hand calculations were performed on a representative sample of four incore monitor assemblies (i.e. 1, 7, 35 and 52) when checking the ability of the unit computer to calculate the various corrections.

4.7.3 EVALUATION OF TEST RESULTS

4.7.3.1 INCORE DETECTOR CHECKOUT

Verification of proper incore detector output was accomplished by comparing the uncorrected detector output and the background detector output of detectors located in similar locations. Since the shape of the curve was the variable being compared, all detector outputs were normalized to the average detector output per assembly. Tables 4.7-1 and 4.7-2 show the results of this comparison at the 40 and 75% full power test plateau, respectively. In all cases, similar flux shapes and normalized background detector outputs for the indicated grouping were obtained, except for IC (17) and IC (32) BG which both had lower values than expected at the 75% full power test plateau. An investigation on these two detectors were performed with the following conclusions reached:

(1) IC (17) level 7 -- This detector was found to be acceptable and thus was not locked out of the computer. The lower than expected inciation was the result of comparing uncorrected level 7 SPND's which inherently have large background corrections.

(2) IC (32) BG -- This background detector was locked out of the computer. The lower than expected indication is believed to be cable related. However, no definite conclusion was reached during the test program.

A comparison was also performed between 52 background detector outputs for consistency. The results of this review indicated that the background detectors were relatively constant at an average ratio of background signal to average assembly rhodium signal of 0.17 and a standard error of 0.03.

4.7.3.2 INCORE DETECTOR SIGNAL CORRECTIONS

The unit computer utilizes a variety of correction factors which are applied to correct the signal from the self-power neutron detectors. During the power escalation test program, hand calculations were performed to verify that the computer was performing these corrections as required. This section covers the results of this investigation.

SENSITIVITY, DEPLETION, AND BACKGROUND CORRECTIONS

To verify proper operation of the unit computer in performing sensitivity, depletion, and background corrections to the rhodium incore detectors, the uncorrected detector outputs and the background detector outputs along with the individual detector sense and charge factors were used to calculate the corrected signals for incore strings 1, 7, 35 and 52. These results were then compared to the corrected SPND values as calculated by the unit computer and a percentage deviation determined. Tab es 4.7-3 and 4.7-4 show the results of these comparisons at 40 and 75% full power, respectively. As can be seen, good agreement between the computer and hand calculated values were obtained with all percentage deviation within the acceptance criteria limit of $\pm$ 2.00 percent. The maximum difference observed was +1.92 percent at the 40% full power test plateau.

ENRICHMENT, RODDED/UNRODDED, AND LBP CORRECTIONS

During the performance of the Incore Detector Test, hand calculations were performed using the computer sensitivity, depletion, and background corrected detector signals and the fuel enrichment, rodded/unrodded, and LBP correction factors given in Table 4.7-5 to generate the segment power for 28 detectors located in incore strings 1, 7, 35, and 52. These particular detectors were chosen because they constituted a representative sample for the corrections being applied. The equation used to perform the above correction is given below:

$$P_i = S_i \times F_A \times F_1 \times F_2 \times F_7 \times F_8 \qquad \text{EQ. (4.7-1)}$$

Where:
- P_i = Segment power at level (i), MWt
- S_i = Corrected detector output at level (i), Amps
- F_A = Fit factor, assumed to be 1.000 at BOL
- F_1 = Megawatt thermal to current conversion factor
- F_2 = Fuel enrichment correction factor
- F_7 = Non rodded/rodded correction factor
- F_8 = Lump burnable poison correction factor

The hand and computer calculated values at 40 and 75% full power were then compared as shown in Tables 4.7-6 and 4.7-7, respectively. As can be seen, good agreement between the computer and hand calculated values were obtained with most values meeting the acceptance criteria limit of $\pm$ 3.00 percent. The maximum difference observed was -3.02 percent at the 75% full power test plateau.

It is important to note the results show a consistent error indicative of the approximate factor used in the hand calculation plus a random error well within the allowable band. Since the segment powers are later normalized to the heat balance, this consistent error is eliminated.

INSULATION LEAKAGE CORRECTIONS

The i lation leakage correction factor is incorporated to account for the det .or current which leaks to the sheath of the detector assembly instead of being transmitted to the computer. To ensure that insulation leakages were small and negligible, direct measurements were performed to determine these factors on various detectors in incore strings 9, 11, 17, 19 and 23. These had low resistances during the pre-operational incore detector checkout. The equation used to calculate the insulation leakage factor for each detector is given below:

$$F_L = 1 + R \times \frac{\Delta I}{\Delta V} \times 10^9 \qquad \text{EQ. (4.7-2)}$$

Where: F_L = Insulation leakage factor

R = Resistance, 20×10^3 Ohms

ΔI = Delta Current $(I_+ - I_-)$, Amps

ΔV = Delta Voltage, 20 Volts

The results of the above investigation revealed a maximum measured value of 1.002 on the selected group of detectors measured. However, these results do imply that the computer insulation leakage factors assumed to be 1.00 at BOL have so far adequately described this correction.

4.7.3.3 RADIAL CORE POWER DISTRIBUTION COMPARISON

To confirm that the unit computer was calculating the radial core power distribution correctly, hand calculation was done using segment powers (i.e. SPNDAA values) from the unit computer. The calculational method was to assume that 1/8 core symmetry existed which allowed the analysis to be performed using 29 characteristic fuel assemblies. From the hand and computer calculated data, the percentage deviation between the two methods was then determined for comparison to the acceptance criteria. Figure 4.7-2 shows the percentage deviation observed during performance of this test at 40 and 75% full power. As can be seen, the maximum deviations at 40 and 75% full power were +0.70 and +0.53%, respectively, which is well within the acceptance criteria limit of ± 5.00%.

4.7.3.4 WORST CASE MAXIMUM LHR CALCULATIONS

As part of the unit computer checkout, hand calculations for determining the worst case maximum LHR were also performed in conjunction with the above 1/8 core analysis. After selection of the fuel assembly which produced the maximum total peaking factor, the worst case maximum LHR was then determined and compared to the value generated by the unit computer. The equation utilized to perform the hand calculation was based on using the maximum LHR times the worst case uncertainty factor as shown below:

$$\text{WC MLHR} = \text{WCF} \times \text{MLHR} \qquad \text{EQ. (4.7-3)}$$

where the definition of the above terms is expressed by the following two equations:

$$\text{MLHR} = \frac{P_R \times A \times \text{Q Rate} \times \text{FNT} \times \text{FOP}}{\text{NA} \times \text{NP} \times \text{AL}} \qquad \text{EQ. (4.7-4)}$$

where:
MLHR = Maximum Linear Heat Rate (kW/ft)
P_{RxA} = Total Peaking Factor
Q Rate = Rated Core Thermal Power (2452×10^3 kW)
FNT = Fraction of power generated in the fuel (0.973)
FOP = Fraction of power level (power in percent/100)
NA = Number of fuel assemblies in the core (177)
NP = Number of fuel pins in each fuel assembly (208)
AL = Active length of each fuel pin (12 ft.)

$$WCF = F_D \times P_{RL} \times P_{AL} \times FQ'' \times PS \times U_P \times U_N \qquad \text{EQ. (4.7-5)}$$

Where: WCF = Worst Case Factor
FD = Fuel Densification Factor (1.021)
P_{RL} = Radial Local Peaking Factor (1.050, 0.00% B_4C)
(1.082, 1.01% B_4C)
(1.098, 1.18% B_4C)
(1.094, 1.34% B_4C)
P_{AL} = Axial Local Peaking Factor (1.026)
FQ" = Hot Channel Factor (1.014)
PS = Power Spike Factor (1.075)
U_P = Power Uncertainty Factor (1.020)
U_N = Nuclear Uncertainty Factor (1.075)

Table 4.7-8 presents the results of these hand calculated worst case maximum LHR for each case along with the unit computer worst case value. As can be seen, good agreement was obtained between the hand and computer calculated values. However, the hand calculated values exceeded the computer calculated values which does not meet the acceptance criterion.

A review of the hand and computer calculational methods has revealed that the unit computer is slightly in error in its method of determining the maximum total peaking factor. This error had been isolated to the two basic difficulties listed below:

(1) The unit computer selects the fuel assembly with the highest radial peaking factor. This fuel assembly however, may not contain the highest total peaking factor required in the calculation.

(2) The unit computer uses a segment averaged total peaking factor instead of the maximum total peaking factor observed. Thus an additional factor of 1.04 (i.e. average segment power to peak) should be incorporated in the computer value.

No change to the unit computer is planned since the small error introduced by using the present output is overshadowed by the 24 percent conservatism presently applied through various factors. However, as a result of this study, Babcock and Wilcox has issued a revised method of obtaining the worst case LHR from the unit computer which corrects the problems noted above.

4.7.3.5 INCORE DETECTOR RESPONSE

The incore detectors have performed according to design during the startup testing. The signal response from the detectors has been measured continuously since power operation began on January 29, 1977. The signal from the detectors is almost exactly proportional to power. Figure 4.7-3 is a plot of measured average incore detector signal in nanoamps versus core power level.

During the startup period a few detectors as measured by the unit computer had low or questionable readings either as a result of a bad detector or cable problems. The problems were worked on and by the end of the test period, there remained only two detectors with low and/or questionable outputs. These detectors are listed below:

(1) IC (32), BG

(2) IC (49), BG

In each case the Bailey 855 is substituting a background signal from another detector to be used in the calculation.

4.7.4 CONCLUSIONS

Upon completion of Incore Detector Testing at 40 and 75% full power, the following was concluded:

(1) The incore monitoring system has performed as expected during the startup period. Verification of flux shapes on symmetric grouping and incore detector response has been excellent.

(2) Computer corrections to the uncorrected detector signals were found to be consistent with hand calculations.

(3) The ability of the computer to determine the radial core power distribution was demonstrated.

(4) Comparison of computer and hand calculated worst case LHR indicates that the computer is slightly in error. No change to the computer is plannned since the error introduced by using the present output is overshadowed by the 24 percent conservatism presently applied.

Table 4.7-1

Comparison Of Incore Monitoring Assemblies Flux Shapes At 40% FP
Using The Indicated Grouping Given In Incore Detector Test

Group Number	Incore Detector Number	Fuel Assembly Location	Detector Current To Average Detector Current Per Assembly							
			Level 1	Level 2	Level 3	Level 4	Level 5	Level 6	Level 7	(BG)
01	05	E-09	.815	1.041	1.036	1.185	1.234	1.101	.588	.143
	07	E-07	.835	1.075	1.040	1.159	1.236	1.071	.582	.147
	09	G-05	.834	1.063	1.038	1.177	1.228	1.089	.571	.142
	11	K-05	.815	1.076	1.030	1.166	1.256	1.082	.576	.156
	13	M-07	.814	1.044	1.049	1.178	1.232	1.087	.596	.164
	16	M-09	.820	1.051	1.033	1.176	1.250	1.083	.586	.149
	19	K-11	.827	1.048	1.012	1.171	1.267	1.088	.587	.145
	25	G-11	.835	1.070	1.037	1.184	1.247	1.073	.554	.142
02	23	F-13	1.011	1.080	.911	1.114	1.225	1.080	.579	.156
	35	F-03	.992	1.087	.904	1.111	1.228	1.078	.600	.165
	39	L-03	1.015	1.089	.895	1.115	1.244	1.062	.579	.170
	50	L-13	1.031	1.077	.909	1.136	1.207	1.075	.565	.159
	28	C-10	1.023	1.050	.919	1.160	1.249	1.046	.553	177
	32	C-06	1.008	1.104	.907	1.096	1.238	1.064	.585	.159
	43	O-06	1.002	1.070	.913	1.136	1.242	1.077	.561	.169
	47	O-10	1.012	1.092	.901	1.129	1.225	1.042	.599	.173
03	06	F-07	.852	1.081	1.087	1.159	1.207	1.049	.566	.166
	08	G-06	.866	1.071	1.049	1.171	1.218	1.050	.574	.166
04	15	N-09	.883	1.038	.971	1.172	1.260	1.085	.587	.163
	20	K-12	.859	1.029	.979	1.175	1.253	1.097	.508	.168
05	17	M-10	.889	1.037	.963	1.180	1.284	1.101	.547	.186
	18	L-11	.848	1.026	.955	1.173	1.283	1.119	.597	.171
06	22	G-13	.913	1.089	1.019	1.150	1.244	1.017	.567	.143
	29	C-09	.904	1.091	1.000	1.144	1.220	1.073	.568	.141

Table 4.7-1 (Cont'd)

Comparison Of Incore Monitoring Assemblies Flux Shapes At 40% FP
Using The Indicated Grouping Given In Incore Detector Test

Group Number	Incore Detector Number	Fuel Assembly Location	Detector Current To Average Detector Current Per Assembly							
			Level 1	Level 2	Level 3	Level 4	Level 5	Level 6	Level 7	(BG)
07	24	F-12	.959	.959	.604	1.201	1.415	1.210	.650	.148
	27	D-10	.987	.810	.629	1.262	1.415	1.242	.655	.147
08	31	B-07	.998	1.177	1.023	1.121	1.142	.990	.541	.161
	36	G-02	.996	1.171	1.023	1.109	1.139	.986	.576	.166
09	33	D-05	.900	1.038	.919	1.141	1.261	1.120	.621	.172
	34	E-04	.888	1.057	.919	1.146	1.275	1.109	.605	.160
10	38	L-02	1.547	1.216	.878	.978	1.041	.872	.468	.198
	44	P-06	1.564	1.172	.863	.997	1.043	.895	.467	.201
11	40	M-03	.911	1.101	.973	1.141	1.228	1.075	.570	.140
	42	O-05	.902	1.081	.963	1.160	1.262	1.065	.568	.157
12	01	H-08	1.473	1.158	.944	1.008	1.038	.870	.508	.220
13	02	H-09	.978	1.130	1.056	1.131	1.162	.975	.569	.177
14	03	G-09	.883	1.101	1.108	1.162	1.180	1.051	.514	.152
15	04	F-08	.824	1.087	1.094	1.186	1.189	1.042	.577	.143
16	10	H-05	.835	1.080	1.060	1.184	1.218	1.047	.576	.175
17	12	L-06	.823	1.056	1.047	1.159	1.243	1.087	.586	.149
18	14	N-08	.833	1.061	1.031	1.209	1.244	1.076	.547	.156
19	21	H-13	.877	1.106	1.068	1.154	1.194	1.050	.551	.169

Comparison Of Incore Monitoring Assemblies Flux Shapes At 40% FP
Using The Indicated Grouping Given In Incore Detector Test

Group Number	Incore Detector Number	Fuel Assembly Location	Detector Current To Average Detector Current Per Assembly							
			Level 1	Level 2	Level 3	Level 4	Level 5	Level 6	Level 7	(BG)
20	26	E-11	.879	1.026	.969	1.197	1.278	1.111	.541	.154
21	30	B-08	.908	1.158	1.090	1.145	1.162	1.066	.521	.186
22	37	H-01	.895	1.171	1.093	1.170	1.140	.991	.541	.179
23	41	N-04	.808	1.050	1.003	1.152	1.264	1.111	.612	.155
24	45	R-07	.942	1.172	1.089	1.136	1.163	.998	.500	.197
25	46	R-10	1.104	1.226	1.043	1.094	1.087	.957	.489	.167
26	48	O-12	.849	1.063	1.016	1.167	1.243	1.051	.610	.167
27	49	M-14	1.065	1.177	.991	1.136	1.170	1.007	.455	.087
28	51	D-14	.860	1.092	1.074	1.174	1.201	1.063	.538	.164
29	52	C-13	.804	1.077	1.059	1.172	1.238	1.070	.581	.182

Average = 0.163
Standard Error = 0.020

Table 4.7-1 (Cont'd)

Table 4.7-2

Comparison Of Incore Monitoring Assemblies Flux Shapes At 75% FP
Using The Indicated Grouping Given In Incore Detector Test

Group Number	Incore Detector Number	Fuel Assembly Location	Detector Current To Average Detector Current Per Assembly							
			Level 1	Level 2	Level 3	Level 4	Level 5	Level 6	Level 7	(BG)
01	05	E-09	0.664	0.899	1.139	1.325	1.270	1.131	0.572	0.159
	07	E-07	0.687	0.926	1.153	1.312	1.287	1.066	0.568	0.164
	09	G-05	0.682	0.922	1.164	1.333	1.283	1.081	0.534	0.154
	11	K-05	0.659	0.951	1.140	1.330	1.326	1.051	0.543	0.166
	13	M-07	0.654	0.911	1.174	1.333	1.272	1.074	0.582	0.192
	16	M-09	0.674	0.932	1.142	1.325	1.317	1.054	0.556	0.152
	19	K-11	0.679	0.913	1.101	1.290	1.328	1.113	0.576	0.149
	25	G-11	0.686	0.936	1.133	1.359	1.307	1.078	0.501	0.160
02	23	F-13	0.824	0.878	1.023	1.320	1.290	1.104	0.561	0.222
	35	F-03	0.811	0.883	1.046	1.327	1.311	1.075	0.547	0.185
	39	L-03	0.846	0.933	1.045	1.355	1.329	1.020	0.472	0.188
	50	L-13	0.786	0.893	1.037	1.324	1.291	1.076	0.592	0.181
	28	C-10	0.833	0.920	1.035	1.348	1.307	1.031	0.525	0.198
	32	C-06	0.787	0.883	1.066	1.325	1.316	1.090	0.532	0.026
	43	O-06	0.817	0.904	1.052	1.361	1.296	1.030	0.541	0.191
	47	O-10	0.855	0.909	1.034	1.330	1.259	1.071	0.542	0.201
03	06	F-07	0.735	0.982	1.177	1.293	1.273	1.048	0.491	0.183
	08	G-06	0.736	0.979	1.155	1.316	1.256	1.036	0.521	0.193
04	15	N-09	0.709	0.877	1.113	1.363	1.326	1.061	0.550	0.178
	20	K-12	0.699	0.870	1.086	1.360	1.304	1.055	0.596	0.173
05	17	M-10	0.746	0.894	1.129	1.437	1.408	1.106	0.280	0.224
	18	L-11	0.685	0.879	1.076	1.338	1.328	1.106	0.589	0.188
06	22	G-13	0.761	0.943	1.112	1.307	1.328	1.000	0.549	0.151
	29	C-09	0.750	0.967	1.099	1.278	1.278	1.068	0.560	0.143

Table 4.7-2 (Cont'd)

Comparison Of Incore Monitoring Assemblies Flux Shapes At 75% FP
Using The Indicated Grouping Given In Incore Detector Test

Group Number	Incore Detector Number	Fuel Assembly Location	Detector Current To Average Detector Current Per Assembly							
			Level 1	Level 2	Level 3	Level 4	Level 5	Level 6	Level 7	(BG)
07	24	F-12	0.764	0.540	0.736	1.533	1.527	1.261	0.639	0.169
	27	D-10	0.770	0.576	0.802	1.493	1.473	1.257	0.630	0.170
08	31	B-07	0.856	1.071	1.099	1.256	1.207	0.995	0.517	0.176
	36	G-02	0.841	1.073	1.117	1.224	1.171	0.981	0.594	0.190
09	33	D-05	0.705	0.820	1.058	1.378	1.344	1.100	0.596	0.189
	34	E-04	0.695	0.852	1.070	1.362	1.330	1.114	0.577	0.166
10	38	L-02	1.346	1.150	0.971	1.122	1.105	0.864	0.442	0.219
	44	P-06	1.354	1.135	0.970	1.130	1.108	0.893	0.410	0.236
11	40	M-03	0.720	0.931	1.114	1.356	1.286	1.041	0.551	0.149
	42	O-05	0.710	0.923	1.095	1.373	1.339	1.032	0.527	0.168
12	01	H-08	1.338	1.184	0.975	1.106	1.090	0.859	0.448	0.265
13	02	H-09	0.890	1.068	1.096	1.226	1.263	0.949	0.507	0.207
14	03	G-09	0.800	1.031	1.207	1.262	1.221	1.085	0.894	0.161
15	04	F-08	0.703	0.994	1.179	1.326	1.241	1.016	0.540	0.158
16	10	H-05	0.707	0.975	1.152	1.351	1.272	1.023	0.521	0.179
17	12	L-06	0.671	0.926	1.149	1.793	1.285	1.121	0.556	0.156
18	14	N-08	0.680	0.941	0.948	1.416	1.331	1.099	0.585	0.160
19	21	H-13	0.738	0.998	1.139	1.302	1.249	1.052	0.523	0.186

Table 4.7-2 (Cont'd)

Comparison Of Incore Monitoring Assemblies Flux Shapes At 75% FP
Using The Indicated Grouping Given In Incore Detector Test

Group Number	Incore Detector Number	Fuel Assembly Location	Detector Current To Average Detector Current Per Assembly							
			Level 1	Level 2	Level 3	Level 4	Level 5	Level 6	Level 7	(BG)
20	26	E-11	0.668	0.837	1.084	1.379	1.346	1.025	0.561	0.156
21	30	B-08	0.796	1.059	1.175	1.270	1.206	1.017	0.477	0.182
22	37	H-01	0.789	1.091	1.142	1.313	1.168	0.967	0.529	0.182
23	41	N-04	0.611	0.881	1.130	1.338	1.328	1.105	0.607	0.169
24	45	R-07	0.834	1.099	1.151	1.265	1.224	1.013	0.414	0.205
25	46	R-10	0.938	1.165	1.142	1.265	1.054	0.922	0.509	0.189
26	48	O-12	0.695	0.942	1.112	1.347	1.288	1.030	0.586	0.277
27	49	M-14	0.915	1.075	1.099	1.320	1.230	0.998	0.359	0.079
28	51	D-14	0.740	0.972	1.160	1.317	1.257	1.052	0.503	0.193
29	52	C-13	0.654	0.945	1.115	1.290	1.312	1.093	0.590	0.226

Average = 0.179
Standard Error = 0.038

Table 4.7-3

Deviation Between Computer And Hand Calculated Segment Powers At 40% FP

Incore Assembly (None)	Detector Level (Segment)	Detector Sense (None)	Detector Charge (Coulombs)	SPND-UC Computer (nA)	BKGC Hand (nA)	BKGC SPND Hand (nA)	DDEPC Hand (None)	SPND-BC Hand (nA)	SPND-BC Computer (nA)	Percentage Deviation (%)
H-08	1	0.990	121.152	320.80	4.94	325.74	1.0110	329.32	333.66	+1.32
	2	1.002	122.820	242.70	15.89	258.59	0.9987	258.25	262.48	+1.64
	3	0.990	123.870	183.50	24.16	207.66	1.0106	209.86	213.88	+1.92
	4	0.999	122.309	194.50	31.52	226.02	1.0015	226.36	22[illegible].45	+0.92
	5	0.986	123.328	192.00	39.05	231.05	1.0147	234.45	235.27	+0.35
	6	0.994	122.181	150.00	45.73	195.73	1.0065	197.00	197.23	+0.12
	7	0.996	122.053	64.20	49.90	114.10	1.0042	114.58	115.17	+0.51
E-07	1	1.005	123.328	310.10	2.91	313.01	0.9959	311.73	313.57	+0.59
	2	1.001	122.892	390.70	11.30	402.00	1.0001	402.04	403.6[illegible]	+0.40
	3	1.006	121.539	370.20	20.39	390.59	0.9951	388.68	390.[illegible]	[illegible]0.43
	4	0.991	120.958	400.20	29.65	429.85	1.0102	434.23	434.97	[illegible].17
	5	0.999	122.309	421.20	39.56	460.76	1.0022	461.77	464.08	[illegible]0.50
	6	0.999	122.047	351.00	48.83	399.83	1.0020	400.63	402.14	+0.38
	7	1.000	122.565	163.00	55.00	218.00	1.0004	218.09	218.51	+0.19
F-03	1	0.984	120.245	226.30	2.50	228.80	1.0169	232.67	234.61	+0.83
	2	0.985	120.373	241.20	9.04	250.24	1.0159	254.22	256.89	+1.05
	3	0.991	121.088	194.50	15.13	209.63	1.0096	211.64	213.71	+0.98
	4	0.986	121.281	237.10	21.15	258.25	1.0149	262.10	262.67	+0.22
	5	0.987	120.245	257.20	28.06	285.26	1.0139	289.23	290.36	+0.39
	6	1.001	120.023	215.80	34.62	250.42	0.9996	250.32	254.78	+1.78
	7	0.986	120.505	100.40	39.00	139.40	1.0145	141.42	141.75	+0.23
C-13	1	1.008	123.709	99.80	1.19	100.99	0.9923	100.21	101.35	+1.13
	2	1.007	121.668	130.70	4.67	135.37	0.9934	134.48	135.74	+0.94
	3	1.010	122.309	125.50	8.54	134.04	0.9904	132.75	133.54	+0.60
	4	1.006	122.437	135.20	12.48	147.68	0.9944	146.85	147.70	+0.58
	5	1.002	122.820	139.40	16.65	156.05	0.9984	155.80	156.03	+0.15
	6	1.001	122.692	114.00	20.50	134.50	0.9993	134.41	134.85	+0.33
	7	0.999	122.437	50.00	23.00	73.00	1.0011	73.08	73.24	+0.22

Corrected SPND's Signal Calculation (Detector (i) On Assembly (j))

SPND-BC = ($\text{SPNB-UC}_{i,j}$ + $\text{BCK}_{i,j}$) X ($\text{DDEPC}_{i,j}$)

Where: Sensitivity And Depletion Correction Is Given By:

$\text{DDEPC}_{i,j}$ = ($\text{Charge}_{i,j}$)/($\text{Charge}_{i,j}$ - $\text{SPND-UC}_{i,j}$ X .864E-04) X ($\text{Sense}_{i,j}$)

Where: Background Correction Is Given By:

$\text{BCK}_{i,j}$ = (BCK) X (($\int^{i}$ ø.[illegible])/($\int^{7}$ ødx))

Table 4.7-4

Deviation Between Computer And Hand Calculated Segment Powers At 75% FP

Incore Assembly (None)	Detector Level (Segment)	Detector Sense (None)	Detector Charge (Coulombs)	SPND-UC Computer (nA)	BKGC Hand (nA)	BKGC SPND Hand (nA)	DDEPC Hand (None)	SPND-BC Hand (nA)	SPND-BC Computer (nA)	Percentage Deviation (%)
H-08	1	0.990	121.152	462.50	8.77	421.27	1.0134	477.59	485.19	+1.59
	2	1.002	122.820	393.00	29.27	422.27	1.0007	422.57	429.23	+1.58
	3	0.990	123.870	298.80	45.81	344.61	1.0122	348.81	353.35	+1.30
	4	0.999	122.309	335.80	61.01	396.81	1.0034	398.16	401.07	+0.73
	5	0.986	123.328	310.50	76.54	387.04	1.0164	393.39	395.28	+0.48
	6	0.994	122.181	218.90	89.29	308.19	1.0076	310.53	311.46	+0.30
	7	0.996	122.053	65.50	96.10	161.60	1.0045	162.33	162.57	+0.15
E-07	1	1.005	123.328	421.60	4.46	426.06	0.9979	425.17	428.76	+0.84
	2	1.001	122.892	555.80	17.64	573.44	1.0029	575.10	578.59	+0.61
	3	1.006	121.539	684.50	34.38	718.88	0.9988	718.02	720.19	+0.30
	4	0.991	120.958	752.30	53.85	806.15	1.0145	817.84	819.14	+0.16
	5	0.999	122.309	724.30	73.94	798.24	1.0061	803.11	804.08	+0.12
	6	0.999	122.047	570.50	91.48	661.98	1.0050	665.29	665.82	+0.08
	7	1.000	122.565	251.50	102.60	354.10	1.0018	354.74	354.94	+0.06
F-03	1	0.984	120.245	294.70	3.65	298.35	1.0184	303.84	307.03	+1.05
	2	0.985	120.373	326.60	13.44	340.04	1.0176	346.02	349.00	+0.86
	3	0.991	121.088	374.00	24.36	398.36	1.0118	403.06	405.06	+0.50
	4	0.986	121.281	469.50	37.68	507.18	1.0176	516.11	517.28	+0.23
	5	0.987	120.245	443.50	52.04	495.54	1.0164	503.67	504.37	+0.14
	6	1.001	120.023	350.00	64.44	414.44	1.0015	415.06	420.47	+1.30
	7	0.986	120.505	155.30	72.30	227.60	1.0153	231.08	231.22	+0.06
C-13	1	1.008	123.709	137.80	139.87	139.87	0.9930	138.89	140.32	+1.03
	2	1.007	121.668	194.10	202.50	202.50	0.9944	201.37	202.70	+0.66
	3	1.010	122.309	223.80	240.16	240.16	0.9917	238.17	239.11	+0.39
	4	1.006	122.437	251.70	277.13	277.13	0.9958	275.97	276.57	+0.22
	5	1.002	122.820	246.10	281.06	281.06	0.9997	280.98	281.35	+0.13
	6	1.001	122.692	190.90	234.24	234.24	1.0003	234.31	234.47	+0.07
	7	0.999	122.437	77.80	126.30	126.30	1.0015	126.49	126.55	+0.05

Corrected SPND's Signal Calculation (Detector (i) On Assembly (j))

SPND-BC = (SPNB-UC$_{i,j}$ + BCK$_{i,j}$) X (DDEPC$_{i,j}$)

Where: Sensitivity And Depletion Correction Is Given By:

DDEPC$_{i,j}$ = (Charge$_{i,j}$)/(Charge$_{i,j}$ - SPND-UC$_{i,j}$ X .864E-04) X (Sense$_{i,j}$)

Where: Background Correction Is Given By:

BCK$_{i,j}$ = (BCK) X (($\int^{i} \phi_i dx$)/($\int^{7} \phi_i dx$))

Table 4.7-5

Enrichment, Rodded/Unrodded, And LBP Correction Factors

F Factor	Fuel Enrichment	LBP Enrichment	Factor
FA	All	All	1.000
F1	All	All	4.847×10^{-3}
F2	1.93	All	0.768
	2.54		0.943
	2.83		1.021
F7N	All	All	1.000
	1.93	0.00	0.966
	2.54	0.00	0.961
	2.83	0.00	0.965
F7R	All	All	1.000
	1.93	0.00	1.026
	2.54	0.00	1.009
	2.83	0.00	1.007
F8	All	0.00	1.000
	2.54	1.01	1.030
		1.18	1.031
		1.34	1.031
	2.83	1.18	1.021

Note: The definition of the above factors are given below:

FA = Fit Factor, assumed to be 1.000 at BOL
F1 = Megawatt Thermal to NANOAMP Conversion Factor
F2 = Fuel Enrichment Correction Factor
F7 = Non Rodded/Rodded Correction Factor
F8 = Lump Burnable Poison Correction Factor

Table 4.7-6

Deviation Between Computer And Hand Calculated Sensitivity, Depletion, And Background Corrected SPND Signals At 40% FP

Incore Assembly (None)	Detector Level (Segment)	SPND-BC Computer (nA)	Enrichment, Rodded/Unrodded, And LBP Correction Factors					SPND-AA Hand (MWt)	SPND-AA Computer (MWt)	Percentage Deviation (%)
			FA (None)	F1 (MWt/nA)	F2 (None)	F7 (None)	F8 (None)			
1	1	333.66	1.000	4.847×10^{-3}	0.943	0.961 N	1.000	1.466	1.451	-1.02
	2 *	262.48				1.009 R		1.181	1.196	+1.27
	3	213.88						0.986	0.975	-1.12
	4	228.45						1.054	1.041	-1.23
Group 7 rod	5	235.25						1.085	1.072	-1.20
2.54 % U235	6	197.23						0.910	0.899	-1.21
0.00 % B_4C	7	115.17						0.531	0.524	-1.32
7	1	313.57	1.000	4.847×10^{-3}	0.768	0.966	1.000	1.128	1.107	-1.86
	2	403.65						1.451	1.424	-1.86
	3	390.35						1.404	1.377	-1.92
	4	434.97						1.564	1.533	-1.98
Group 1 rod	5	464.08						1.669	1.634	-2.10
1.93 % U235	6	402.14						1.446	1.416	-2.07
0.00 % B_4C	7	218.58						0.786	0.769	-2.16
35	1	234.61	1.000	4.847×10^{-3}	0.943	1.000	1.031	1.106	1.081	-2.26
	2	256.89						1.211	1.183	-2.31
	3	213.71						1.007	0.984	-2.28
	4	262.67						1.237	1.209	-2.26
LBP Type 2	5	290.36						1.368	1.335	-2.41
2.54 % U235	6	254.78						1.201	1.171	-2.50
1.18 % B_4C	7	141.75						0.668	0.651	-2.54
52	1	101.35	1.000	4.847×10^{-3}	1.021	0.965	1.000	0.484	0.477	-1.45
	2	135.74						0.648	0.640	-1.23
	3	133.54						0.638	0.629	-1.41
	4	147.70						0.705	0.696	-1.28
None	5	156.03						0.745	0.735	-1.34
2.83 % U235	6	134.85						0.644	0.635	-1.40
0.00 % B_4C	7	73.24						0.350	0.344	-1.71

Note (*): This detector when group 7 is at 19% wd is 47.3 percent rodded thus the appropriate F7 value is 0.984

Note: $$\text{Deviation (\%)} = \left[\frac{\text{Computer} - \text{Hand}}{\text{Hand}}\right] \times 100$$

Deviation Between Computer And Hand Calculated Sensitivity, Depletion, And Background Corrected SPND Signals At 75% FP

Incore Assembly (None)	Detector Level (Segment)	SPND-BC Computer (nA)	Enrichment, Rodded/Unrodded, And LBP Correction Factors					SPND-AA Hand (MWt)	SPND-AA Computer (MWt)	Percentage Deviation (%)
			FA (None)	F1 (MWt/nA)	F2 (None)	F7 (None)	F8 (None)			
1	1	485.19	1.000	4.847×10^{-3}	0.943	0.961 N	1.000	2.131	2.104	-1.27
	2 *	429.23				1.009 R		1.931	1.949	+0.93
	3	353.35						1.630	1.604	-1.60
	4	401.07						1.850	1.819	-1.68
Group 7 rod	5	395.28						1.823	1.792	-1.70
2.54 % U235	6	311.46						1.436	1.411	-1.74
0.00 % B_4C	7	162.57						0.749	0.736	-1.73
7	1	428.76	1.000	4.847×10^{-3}	0.768	0.966	1.000	1.542	1.509	-2.14
	2	578.59						2.081	2.036	-2.16
	3	720.19						2.590	2.532	-2.34
	4	819.14						2.946	2.878	-2.31
Group 1 rod	5	804.03						2.891	2.822	-2.34
1.93 % U235	6	665.82						2.394	2.335	-2.46
0.00 % B_4C	7	354.94						1.276	1.243	-2.59
35	1	307.03	1.000	4.847×10^{-3}	0.943	1.000	1.031	1.447	1.408	-2.70
	2	349.00						1.645	1.599	-2.80
	3	405.06						1.909	1.855	-2.83
LBP Type 2	4	517.28						2.438	2.367	-2.91
2.54 % U235	5	504.37						2.377	2.306	-2.99
1.18 % B_4C	6	420.40						1.981	1.921	-3.03
	7	231.22						1.090	1.057	-3.03
52	1	140.32	1.000	4.847×10^{-3}	1.021	0.965	1.000	0.670	0.660	-1.49
	2	202.71						0.969	0.953	-1.65
	3	239.11						1.142	1.123	-1.66
	4	276.57						1.321	1.299	-1.67
None	5	281.35						1.344	1.321	-1.71
2.83 % U235	6	234.47						1.120	1.100	-1.79
0.00 % B_4C	7	126.55						0.604	0.594	-1.66

Note (*): This detector when group 7 is at 19% wd is 47.3 percent rodded thus the appropriate F7 value is 0.984

Note: $\text{Deviation (\%)} = \left[\frac{\text{Computer} - \text{Hand}}{\text{Hand}}\right] \times 100$

Table 4.7-7

Table 4.7-8

Comparison Of Computer And Hand Calculated Worst Case Maximum LHR's

Date	Time	Power Level (% FP)	Incore Offset (%)	Maximum Tilt (%)	Maximum P (RxA), dim		Maximum LHR, kW/ft	
					Computer *	Hand	Computer	Hand
03-01-77	0206	40.21	- 2.09	+ 0.94	1.57	1.62	4.44	4.63
03-15-77	2230	73.94	+ 1.11	+ 0.74	1.70	1.79	8.93	9.39

Note (*): The unit computer values have been reduced by their respective radial local peaking factor which was 1.05 for these two cases.

Incore Detector Core Location

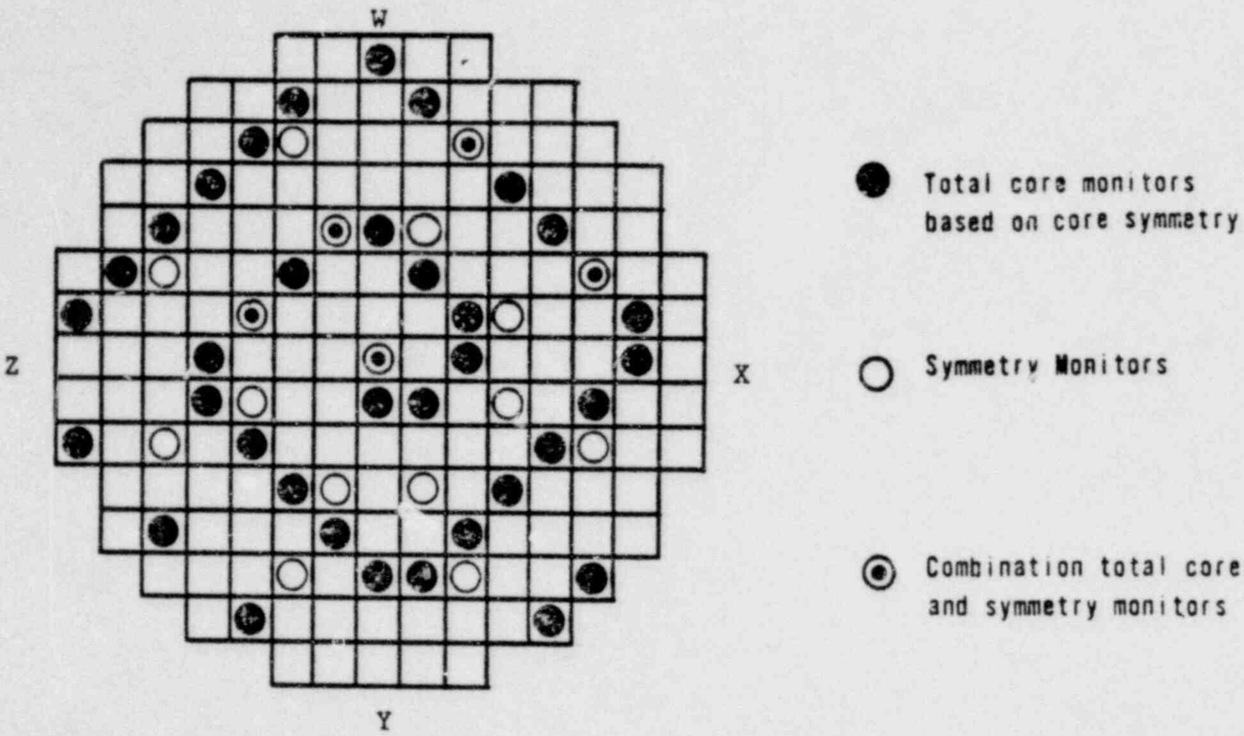

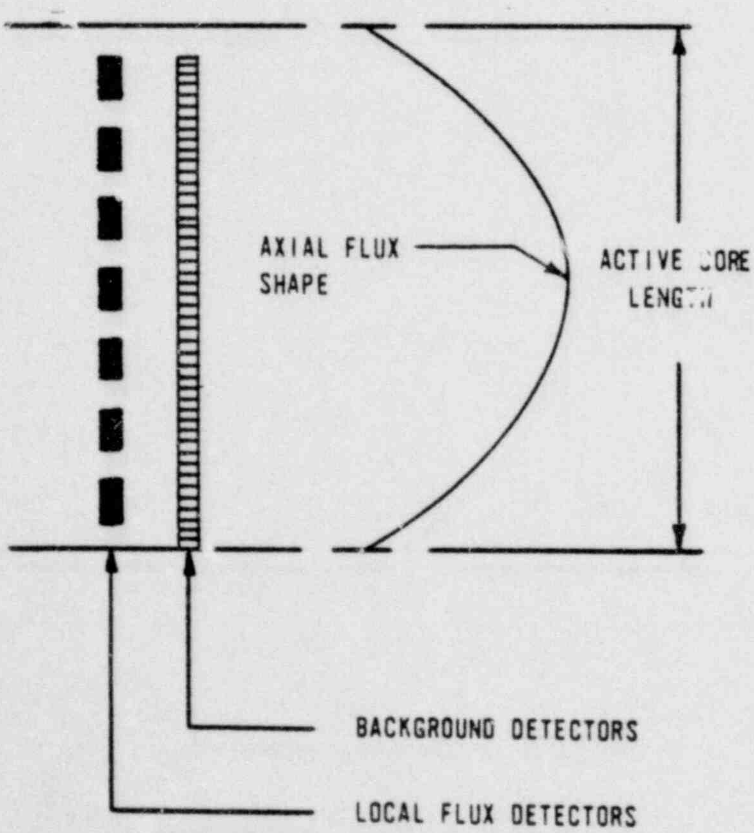

Figure 4.7-1

Comparison Between Computer And Hand Calculated Radial
Core Power Distribution At 40 And 75% Full Power

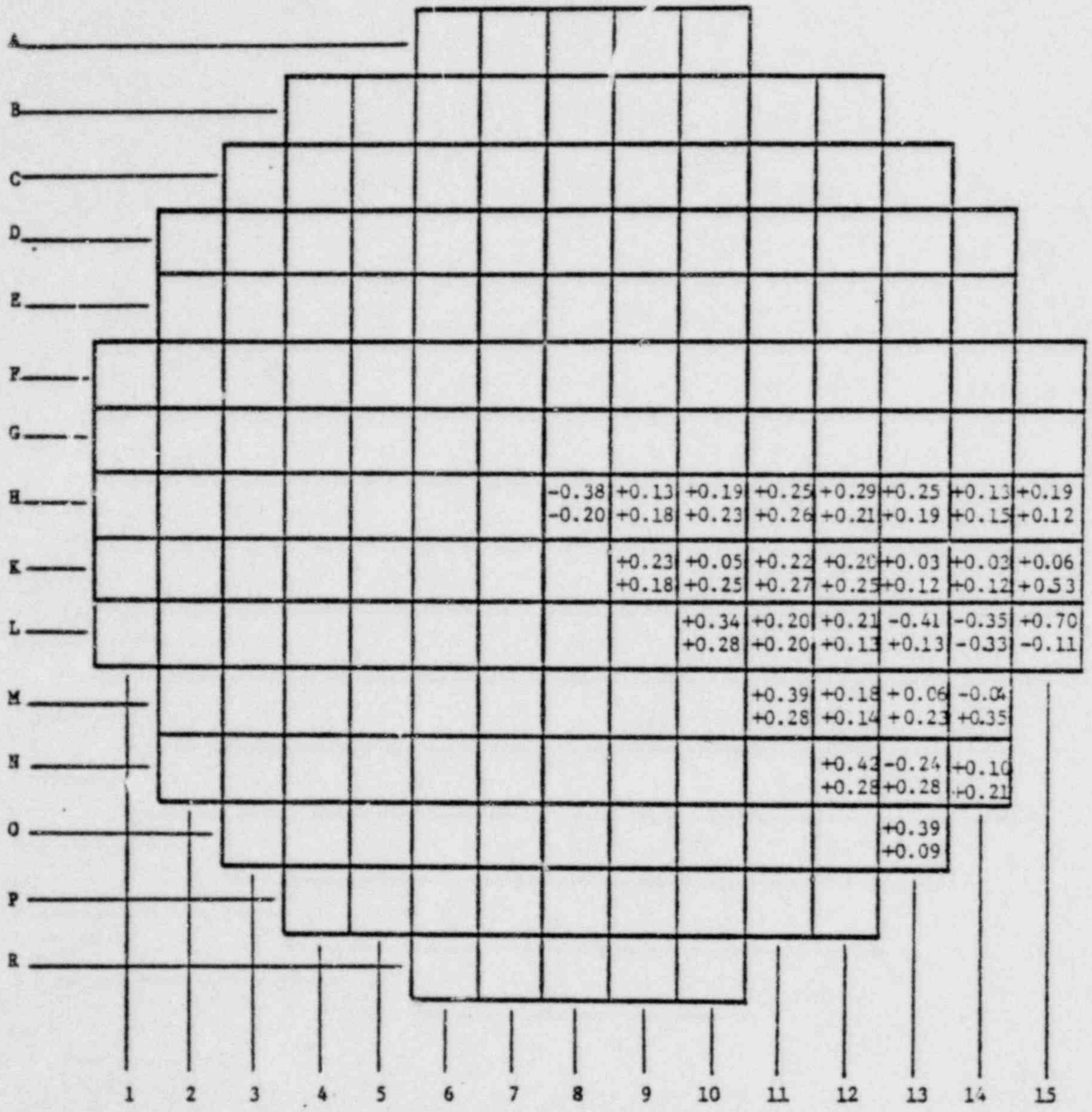

X.XX	40% Full Power
X.XX	75% Full Power

Note: Deviation (%) $= \left[\frac{\text{Computer - Hand}}{\text{Hand}}\right] \times 100$

Figure 4.7-2

Average Incore Detector Signal In Nanoamps Versus
Core Power Level In Percent Full Power

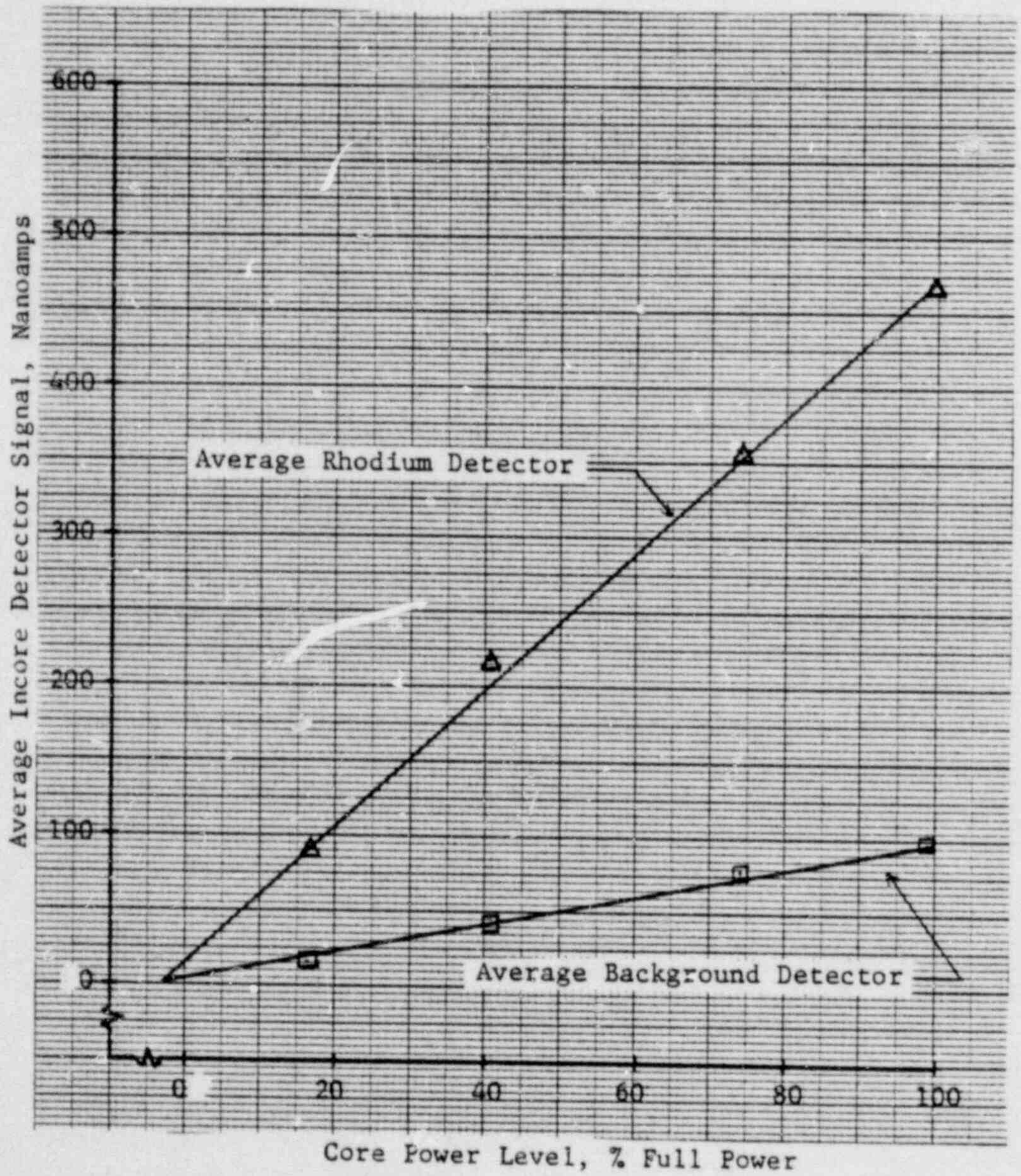

Figure 4.7-3

4.8 POWER IMBALANCE DETECTOR CORRELATION TEST

Imbalance of the neutron flux in a reactor results from temperature distributions, fuel depletion, xenon oscillations, or control rods positioned in the core. The amount of imbalance* which is allowed in the core so that DNBR or LHR limits are not exceeded is set in the reactor protection system and is a function of the power level and the reactor coolant flow. Since this imbalance is determined using input signals from the out-of-core detectors, it is essential that they are calibrated to read the true imbalance as determined from the incore detectors.

This report presents the results of incore imbalance to out-of-core imbalance induced on Crystal River Unit 3, Cycle 1 at 40 and 75 percent full power during the performance of Power Imbalance Detector Correlation Test.

4.8.1 PURPOSE

The Power Imbalance Detector Correlation Test had the following four objectives:

(a) To measure the relationship between core offset* as indicated by the out-of-core power range nuclear instrumentation detectors and as indicated by the full incore monitoring system.

(b) To provide sufficient information to adjust the NI/RPS differential amplifiers should the measured correlation indicate a need.

(c) To verify that an acceptable relationship between the backup recorder system and the full incore monitoring system indication of core offset was observed.

(d) To verify acceptable core thermal-hydraulic parameters at each imbalance condition induced.

Three acceptance criteria are specified for the Power Imbalance Detector Correlation Test and are listed below:

(1) The measured correlation between each out-of-core detector offset to full incore monitoring system offset lies within the acceptable region shown in Figure 4.8-2. The correlation slope shall be greater than or equal to 1.00 and the correlation intercept should be less than $\pm$ 3.5% offset.

(2) The measured relationship between the full incore monitoring system offset and the backup recorder offset lies within the acceptable region shown in Figure 4.8-3.

(3) The measured worst case minimum DNBR is greater than 1.30 and the measured worst case maximum LHR is less than 18.00 kW/ft.

4.8.2 TEST METHOD

During the Power Escalation Sequence at Crystal River 3, as part of the test program, imbalance measurements were made to determine the acceptability of the out-of-core detectors to detect imbalance and to establish a basis for verifying

*Imbalance = Power in top of core - power in bottom of core

$$\text{*Offset} = \frac{\text{Imbalance}}{\text{Total Core Power}}$$

that DNBR and LHR limits would not be exceeded while operating within the flux/delta flux/flow envelope set in the reactor protection system. These imbalance measurements were made at different power levels with a gain factor of 3.90 applied to the multiplier on the delta flux amplifier output.

In performing the test, APSR's were positioned to obtain the desired full incore imbalance with reactivity compensations made by control rod groups 6 and/or 7. At both test plateaus, offset as indicated by the full incore system, out-of-core system, and backup recorder system was recorded as given in Tables 4.8-1 and 4.8-2. From this data, plots of average out-of-core offset and backup recorder offset versus full incore offset were maintained as shown in Figures 4.8-4 through 4.8-7. Worst case minimum DNBR and maximum LHR data was monitored during the test. The results are plotted versus full incore offset in Figures 4.8-8 and 4.8-9.

Based upon previous startup experience, the relationship between incore offset and out-of-core offset was determined to be a linear equation of the form below:

$$OCO = M \times ICO + B \qquad \text{EQ. (4.8-1)}$$

Where: OCO = Out-of-Core Offset (Percent)
ICO = Incore Offset (Percent)
M = Slope of Relationship
B = Intercept at Zero ICO

The experimental slope and intercept could then be obtained using a linear least squares fit from the data obtained. If the measured slope of the relationship of ICO to OCO was determined to be unsatisfactory; i.e. <1.00, the gain of the out-of-core power range detector should be adjusted. The relationship of measured slope to gain factor is as follows:

$$GF = (M2/M1) \times GF_o \qquad \text{EQ. (4.8-2)}$$

Where: GF = Desired Gain Factor
M2 = Desired Slope (i.e. >1.00)
M1 = Measured Slope
GF_o = Present Gain Factor (i.e. 3.90)

Verification of the adequacy of the power imbalance system trip setpoint was performed in conjunction with worst case analysis on each minimum DNBR and maximum LHR measured. The technique used was to extrapolate each measured point to the power/imbalance/flow enverlope boundary limits given in Figure 4.8-1. In this way the adequacy of the imbalance system trip setpoints to protect the unit from exceeding thermal-hydraulic limits could be verified.

4.8.3 EVALUATION OF TEST RESULTS

The measurement of the offset correlation function between the full incore system and each out-of-core detector was determined during imbalance scans by APSR's and control rod group 6 and/or 7 at 40 and 75% full power to be a linear relationship on all power range detectors. Figures 4.8-2 and 4.8-6 show the average response in offset between the out-of-core power range detectors and the full incore system. Test data indicated that all measured offsets from the out-of-core power range detectors fell within the acceptable areas of the curve during the performance of the test. For each power range detector, a linear least squares fit was applied to the measured data points to obtain a value for the slope and intercept of the observed relationship. The results of these calculations are tabulated in Table 4.8-3. In all cases, the measured slopes were greater than the minimum allowable value of 1.00 which verified the utilization of a 3.90 gain factor for the difference amplifiers.

The ability of the backup recorder to follow full incore offset was also verified as part of this test by collecting backup recorder data and performing the necessary calculations. The results of this analysis are plotted in Figures 4.8-5 and 4.8-7 for the 40 and 75% full power cases, respectively. In all cases, the calculated offsets from the backup recorders fell within the acceptable area which satisfied the test acceptance criteria. The measurement of the slope between the backup recorders and the full incore yielded approximately 1.00.

During all phases of testing, worst case minimum DNBR and maximum LHR were recorded against incore offset and a plot maintained as shown in Figures 4.8-8 and 4.8-9. The most limiting value observed on the worst case minimum DNBR and maximum LHR was 3.81 and 12.35 kW/ft, respectively which is well within the procedural acceptance criteria. As can be seen from the plots, both worst case minimum DNBR and maximum LHR are strong functions of incore offset. It can also be concluded that the greatest thermal margins are present when an incore offset between -5 to -10 percent is present.

The measured worst case minimum DNBR and maximum LHR were then extrapolated to the power/imbalance/flow envelope limits for verification of the imbalance system trip setpoints. A summary of this analysis for the 40 and 75% full power plateaus is presented in Tables 4.8-4 and 4.8-5. The extrapoalted worst case values were then compared to the DNBR and LHR limits of 1.30 and 19.70 kW/ft, respectively. As can be seen from these tables, all worst case values were within the acceptance criteria with adequate margins.

4.8.4 CONCLUSIONS

Upon completion of power imbalance detector correlation testing at 40 and 75 percent full power, the following were concluded:

(a) The measured offset correlation function between the full incore system and each out-of-core detector was determined to be a linear relationship.

(b) A gain factor of 3.90 on each out-of-core power range detector difference amplifier will yield an acceptable slope relationship to the full incore system.

(c) The power/imbalance/flow envelope as set in the reactor protection system will protect the reactor from exceeding minimum DNBR and maximum LHR thermal limits, when a gain factor of 3.90 is utilized.

(d) The backup recorder can provide an acceptable measurement of core imbalance.

Table 4.8-1

Summary Of Test Data Obtained During The Performance Of Power Imbalance Detector Correlation Test At 40% Full Power

Date Time	Power Level (%FP)	Rod Position, %wd				Incore Offset, %		Out-Of-Core Offset, %				Worst Case Maximum LHR (kW/ft)	Worst Case Minimum DNBR (Dim)
		1-5	6	7	8	Full	Backup	NI-5	NI-6	NI-7	NI-8		
03-05-77 1311	40.20	100	90	13	1	+14.7	+17.2	+21.5	+19.9	+22.4	+19.6	5.67	8.26
03-05-77 1708	40.25	100	99	23	17	+ 7.1	+ 9.4	+ 7.7	+ 7.0	+ 9.2	+ 7.3	4.83	9.18
03-05-77 1832	41.06	100	100	25	19	- 2.0	0.0	- 3.6	- 4.0	- 1.9	- 3.1	4.50	9.97
03-05-77 1902	40.43	100	100	25	24	-13.0	-10.8	-14.8	-14.9	-12.9	-13.7	5.00	10.03
03-05-77 2156	40.35	100	100	26	20	-22.9	-20.4	-24.9	-24.9	-23.1	-23.5	5.91	8.41
03-05-77 2238	40.75	100	100	21	32	-37.7	-36.8	-39.5	-39.2	-37.2	-37.3	6.66	7.41
03-05-77 2338	40.83	100	93	16	45	-48.7	-46.1	-47.8	-48.0	-47.2	-47.1	6.64	7.37

Table 4.8-2

Summary Of Test Data Obtained During The Performance Of Power Imbalance Detector Correlation Test At 75% Full Power

Date Time	Power Level (%FP)	Rod Position, %wd				Incore Offset, %		Out-Of-Core Offset, %				Worst Case Maximum LHR (kW/ft)	Worst Case Minimum DNBR (Dim)
		1-5	6	7	8	Full	Backup	NI-5	NI-6	NI-7	NI-8		
03-28-77 0650	77.03	100	81	5	0	+ 0.2	+ 0.5	+ 3.9	+ 4.9	+ 6.4	+ 4.2	11.22	3.81
03-28-77 0814	76.94	100	89	15	18	- 1.3	- 0.2	- 1.5	- 0.0	+ 0.8	+ 0.1	9.55	4.24
03-28-77 0950	77.04	100	91	15	21	- 8.2	- 7.0	- 9.9	- 8.0	- 7.4	- 7.4	8.74	4.58
03-28-77 1050	76.69	100	91	15	21	-12.9	-11.4	-15.0	-13.0	-12.4	-12.4	9.40	4.84
03-28-77 1138	76.43	100	91	15	23	-19.9	-18.6	-22.7	-20.5	-20.1	-19.3	10.21	4.72
03-28-77 1226	76.34	100	91	15	26	-26.8	-28.7	-29.6	-27.5	-27.0	-26.1	10.97	4.39
03-28-77 1320	76.55	100	90	13	28	-34.5	-32.9	-37.9	-35.7	-35.2	-33.9	11.79	4.03
03-28-77 1405	76.67	100	90	13	29	-38.9	-37.9	-42.2	-39.9	-39.4	-38.1	12.35	3.82

Table 4.8-3

Summary Of Best Fitted Correlation Slopes And Intercepts Measured On Each Power Range Channel During The Performance Of Power Imbalance Detector Correlation Test

Power Range Channel	Gain Factor Setting	Test Data Sets	Correlation Slope, Dim			Correlation Intercept, %		
			Best Fitted	Standard Error	Acceptance Criteria	Best Fitted	Standard Error	Calibration Tolerance*
A. Power Imbalance Test At 40 Percent Full Power								
5	3.90	7	1.07	0.05	> 1.00	+1.12	1.40	±3.50
6	3.90	7	1.05	0.05	> 1.00	+0.41	1.50	±3.50
7	3.90	7	1.07	0.05	> 1.00	+2.62	1.18	±3.50
8	3.90	7	1.03	0.04	> 1.00	+0.99	1.03	±3.50
B. Power Imbalance Test At 75 Percent Full Power								
5	3.90	8	1.13	0.03	> 1.00	-0.72	0.61	±3.50
6	3.90	8	1.10	0.03	> 1.00	+2.17	0.77	±3.50
7	3.90	8	1.12	0.04	> 1.00	+3.14	0.92	±3.50
8	3.90	8	1.05	0.02	> 1.00	+2.10	0.57	±3.50

Note(*): A correlation intercept within +/- 3.5% offset is indicative of proper NI calibration during the test. A value outside this tolerance does not however invalidate the test

Table 4.8-4

Worst Case Minimum DNBR And Maximum LHR Analysis For Power Imbalance Detector Correlation Test At 40% Full Power

Data Analysis (None)	Power Level (%FP)	Incore Offset (%)	Axial Peak * (Dim)	Envelope Limits P (% FP)	Envelope Limits Δ P (% FP)	Worst Case Maximum LHR (kW/ft)	Worst Case Minimum DNBR (Dim)
Measured	40.20	+14.71	1.48 (5)			5.67	8.26
Extrapolated				100.92	+14.85	14.23	2.71
Measured	40.25	+ 7.13	1.27 (4)			4.83	9.18
Extrapolated				104.30	+ 7.44	12.52	2.89
Measured	41.06	- 1.99	1.19 (4)			4.50	9.97
Extrapolated				104.30	- 2.08	11.43	3.08
Measured	40.43	-13.00	1.30 (4)			5.00	10.03
Extrapolated				104.30	-13.56	12.90	3.33
Measured	40.35	-22.87	1.54 (3)			5.91	8.41
Extrapolated				98.30	-22.48	14.40	3.17
Measured	40.75	-37.67	1.74 (3)			6.66	7.41
Extrapolated				84.91	-31.99	13.88	3.44
Measured	40.83	-48.70	1.79 (2)			6.64	7.37
Extrapolated				72.90	-35.50	11.86	4.37

Note(*): The number in parenthesis represents the segment location of the axial peak

Table 4.8-5

Worst Case Minimum DNBR And Maximum LHR Analysis For Power Imbalance Detector Correlation Test At 75% Full Power

Data Analysis (None)	Power Level (%FP)	Incore Offset (%)	Axial Peak * (Dim)	Envelope Limits P (% FP)	Envelope Limits ΔP (% FP)	Worst Case Maximum LHR (kW/ft)	Worst Case Minimum DNBR (Dim)
Measured	77.03	+ 0.15	1.59 (4)			11.44	3.81
Extrapolated				104.30	+ 0.17	15.49	
Measured	76.94	- 1.33	1.34 (4)			9.74	4.24
Extrapolated				104.30	- 1.39	13.20	2.73
Measured	77.04	- 8.16	1.23 (4)			8.91	4.58
Extrapolated				104.30	- 8.51	12.06	2.78
Measured	76.69	-12.93	1.32 (4)			9.59	4.84
Extrapolated				104.30	-13.49	13.04	3.16
Measured	76.43	-19.90	1.44 (4)			10.41	4.72
Extrapolated				101.54	-20.21	13.83	3.47
Measured	76.34	-28.6[illegible]	1.55 (3)			11.19	4.39
Extrapolated				92.62	-26.54	13.58	3.68
Measured	76.55	-34.54	1.66 (3)			12.03	4.03
Extrapolated				87.46	-30.21	13.74	3.73
Measured	76.67	-38.88	1.75 (3)			12.60	3.82
Extrapolated				84.00	-32.66	13.80	3.96

Note(*): The number in parenthesis represents the segment location of the axial peak

Reactor Protective System Maximum Allowable Setpoints
For Four Pump Operation

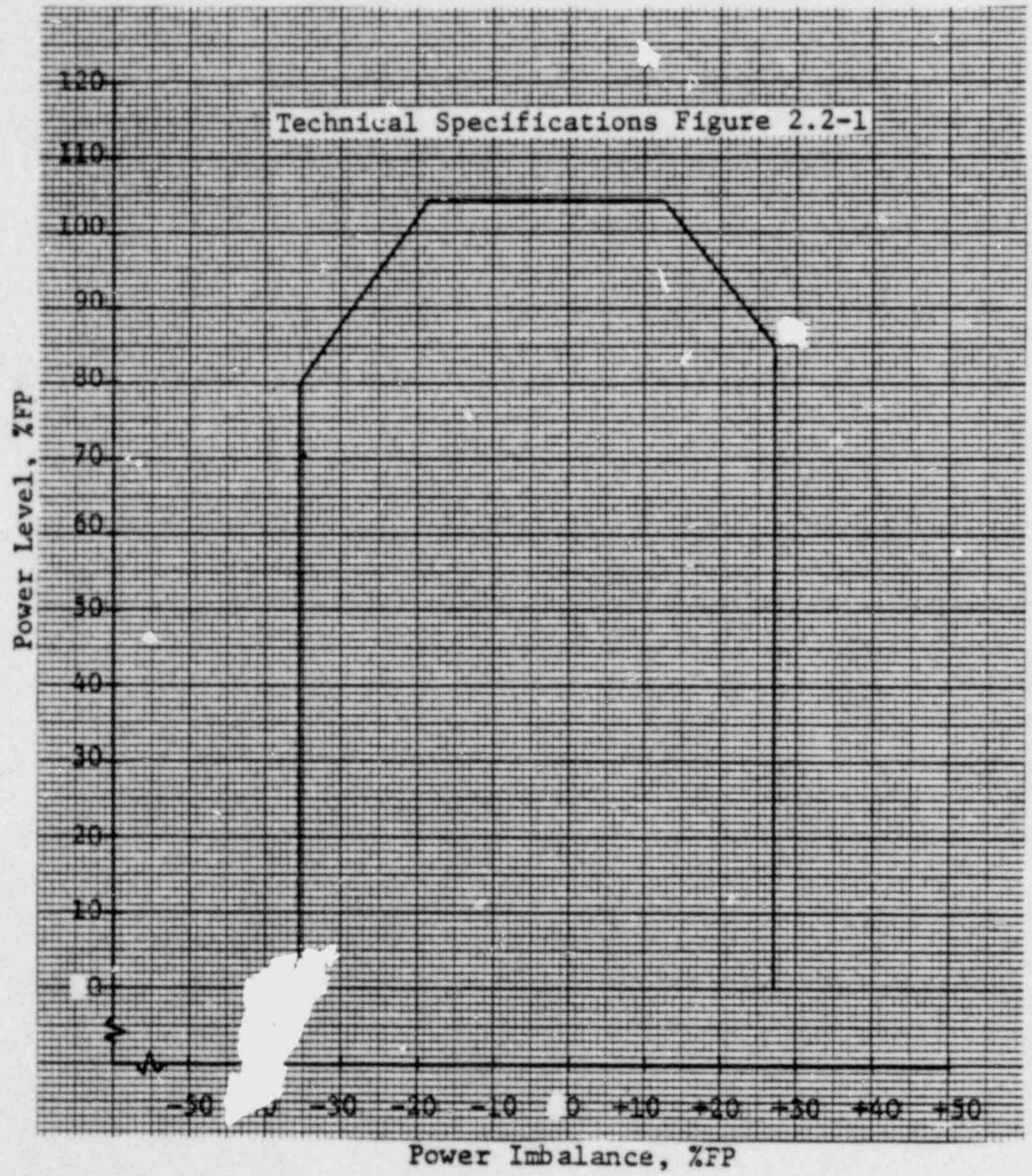

Figure 4.8-1

Acceptance Criteria Between Full Incore And Out-Of-Core Offset For Power Imbalance Detector Correlation Test

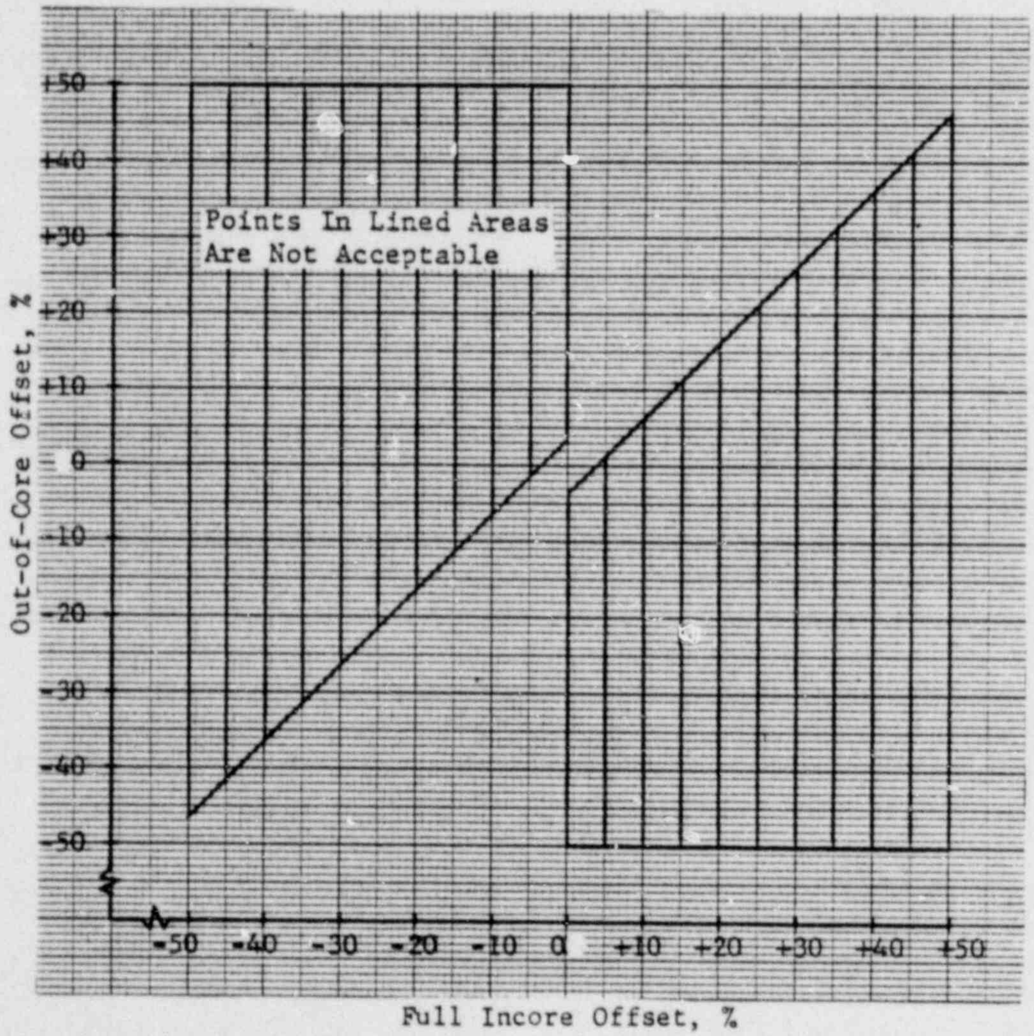

Figure 4.8-2

Acceptance Criteria Between Full Incore And Backup Recorder
Incore Offset For Power Imbalance Detector Correlation Test

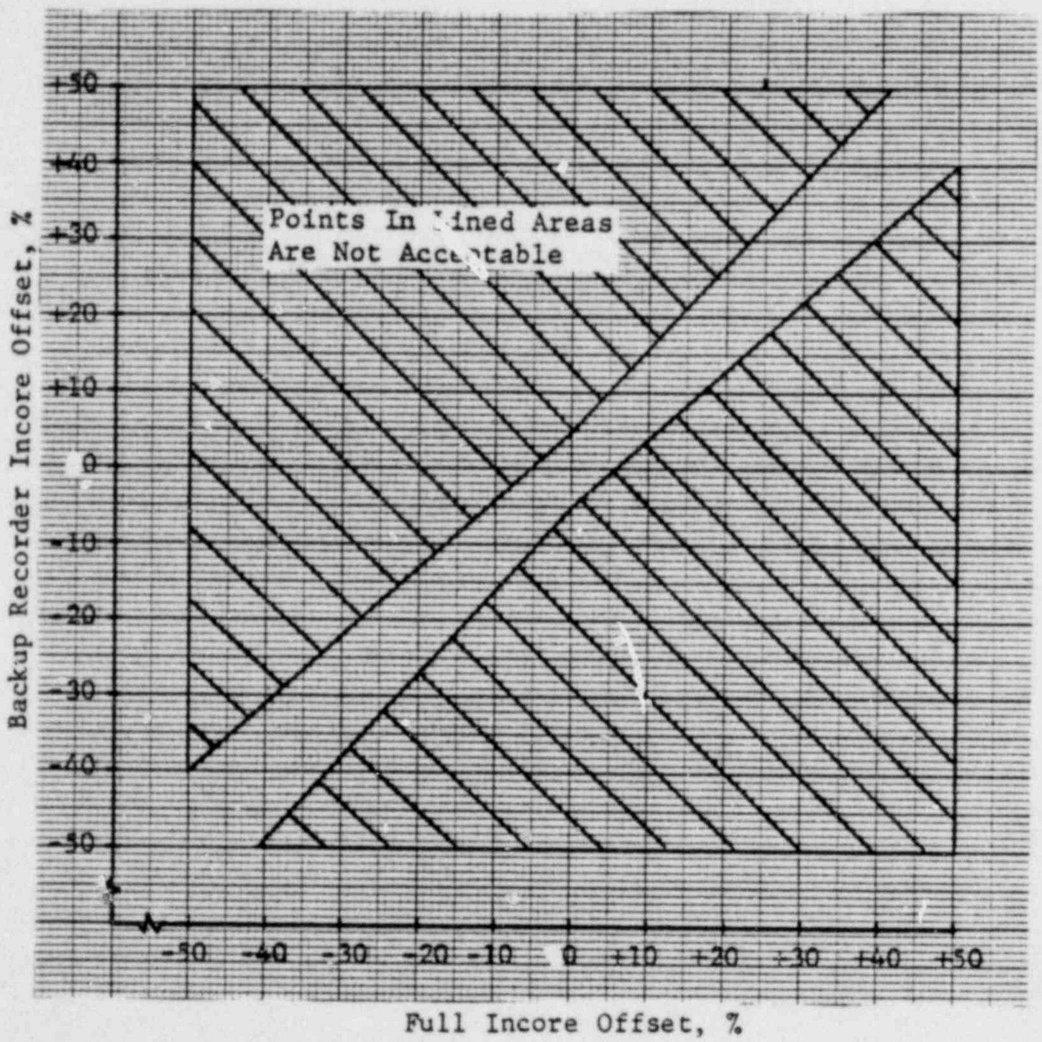

Figure 4.8-3

Average Out-Of-Core Offset Versus Full Incore Offset During The Performance Of The Power Imbalance Detector Correlation Test At 40% Full Power

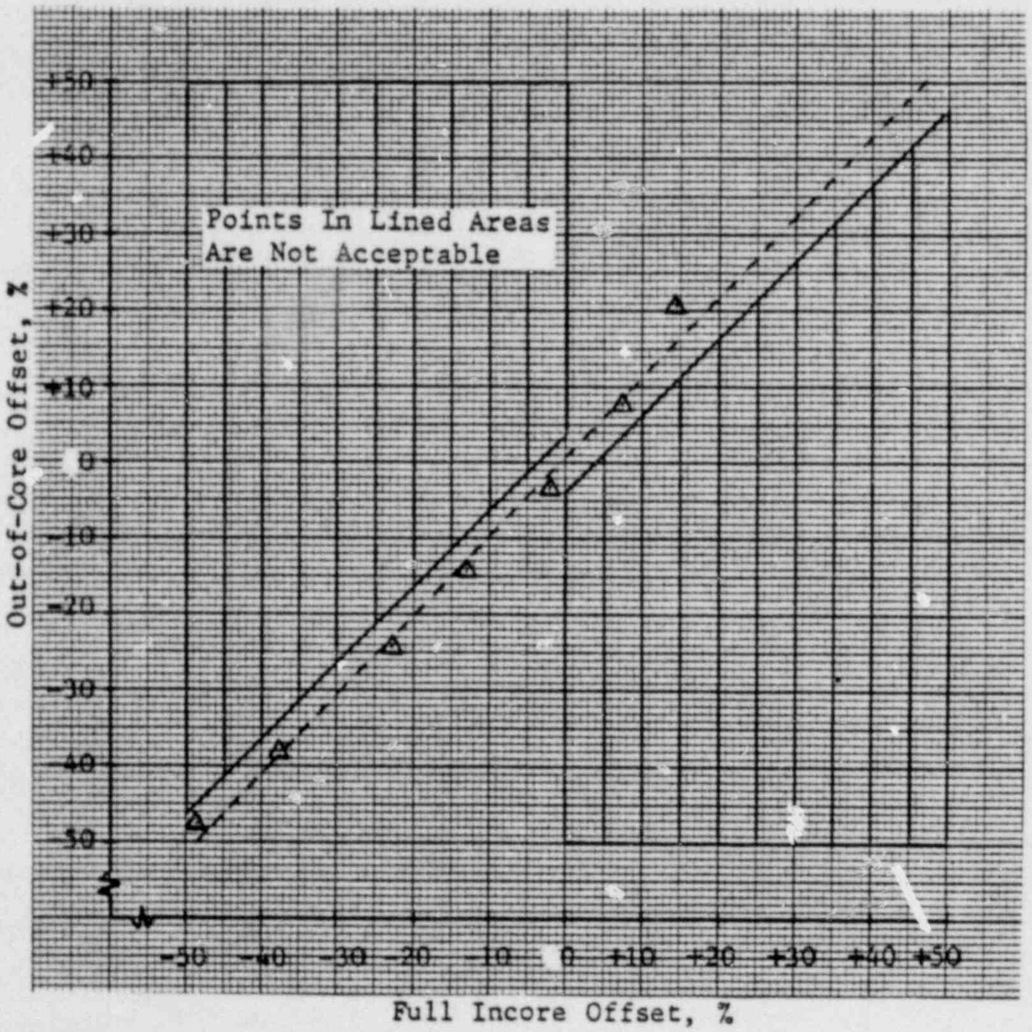

Figure 4.8-4

Average Out-Of-Core Offset Versus Full Incore Offset During The Performance Of The Power Imbalance Detector Correlation Test At 75% Full Power

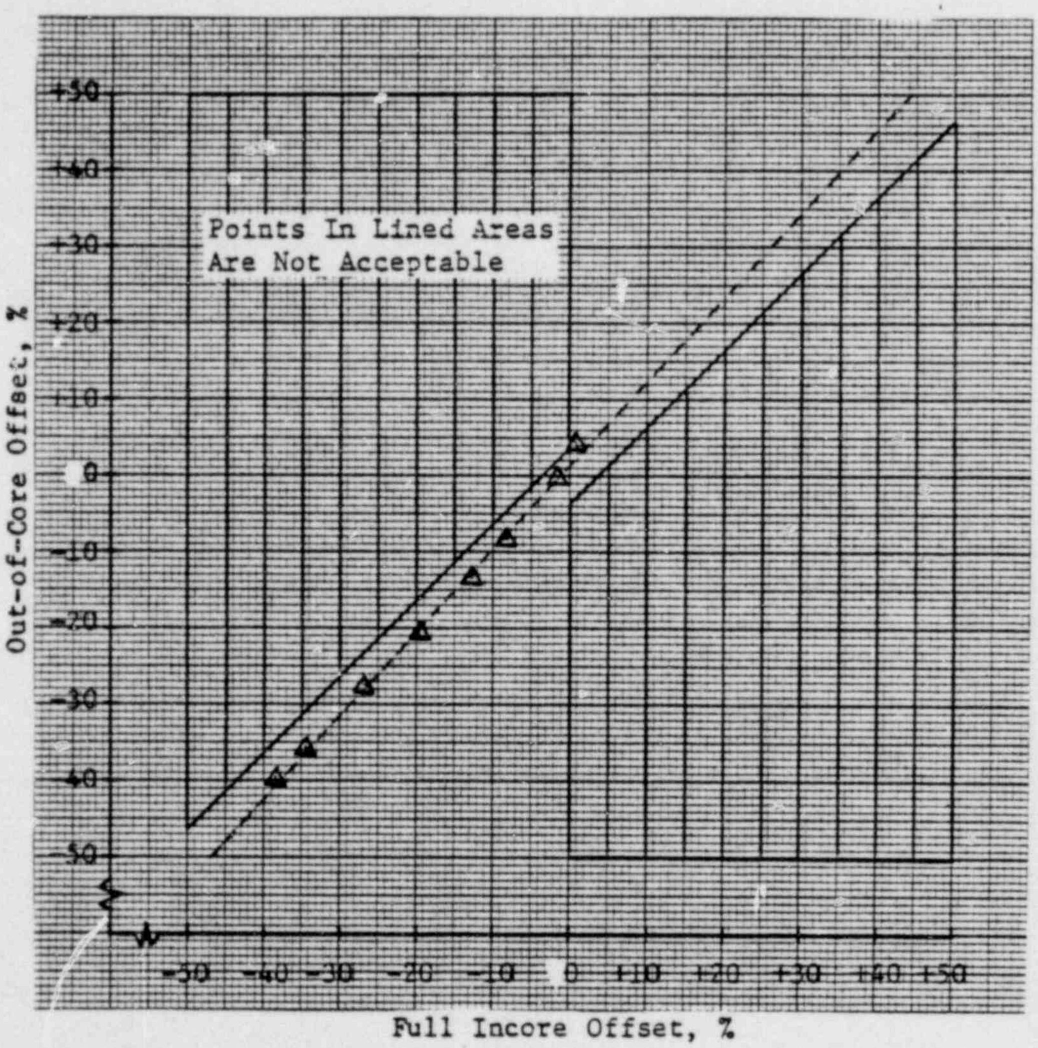

Figure 4.8-5

Backup Recorder Offset Versus Full Incore Offset During The Performance Of Power Imbalance Detector Correlation Test At 40% Full Power

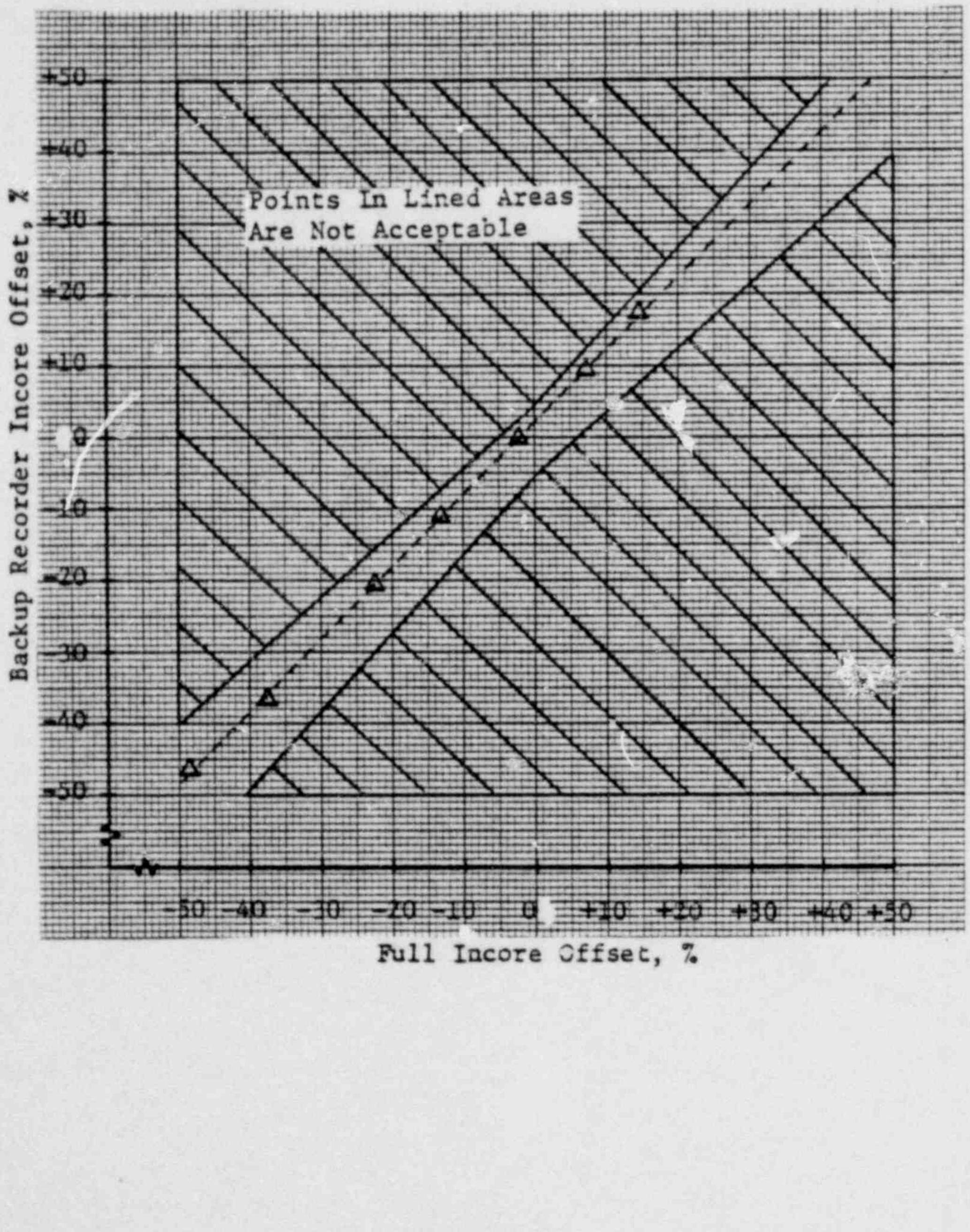

Figure 4.8-6

Backup Recorder Offset Versus Full Incore Offset During The Performance Of Power Imbalance Detector Correlation Test At 75% Full Power

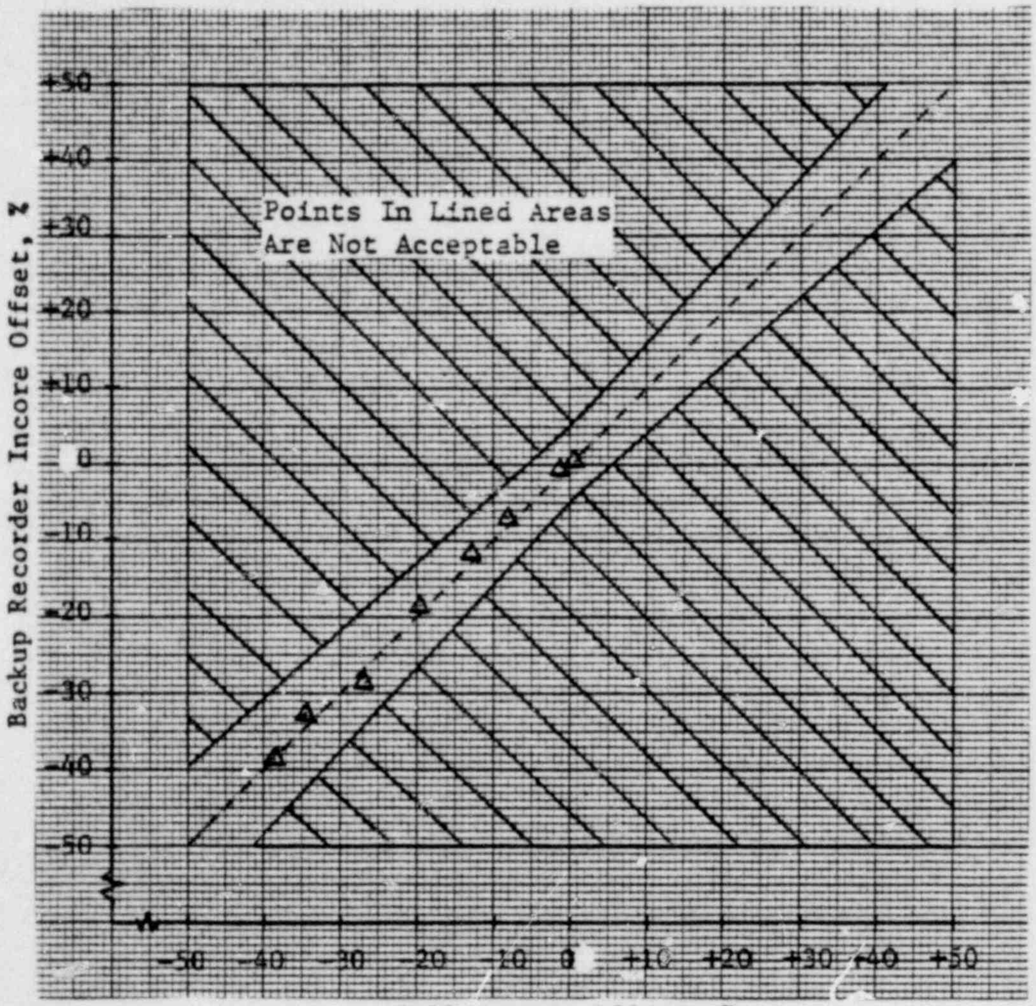

Full Incore Offset, %

Figure 4.8-7

Worst Case Minimum DNBR And Maximum LHR Versus Full Incore Offset Durir· the Perfor·ance Of Power Imbalance Detector Correlatio· ·est At 40% Full Power

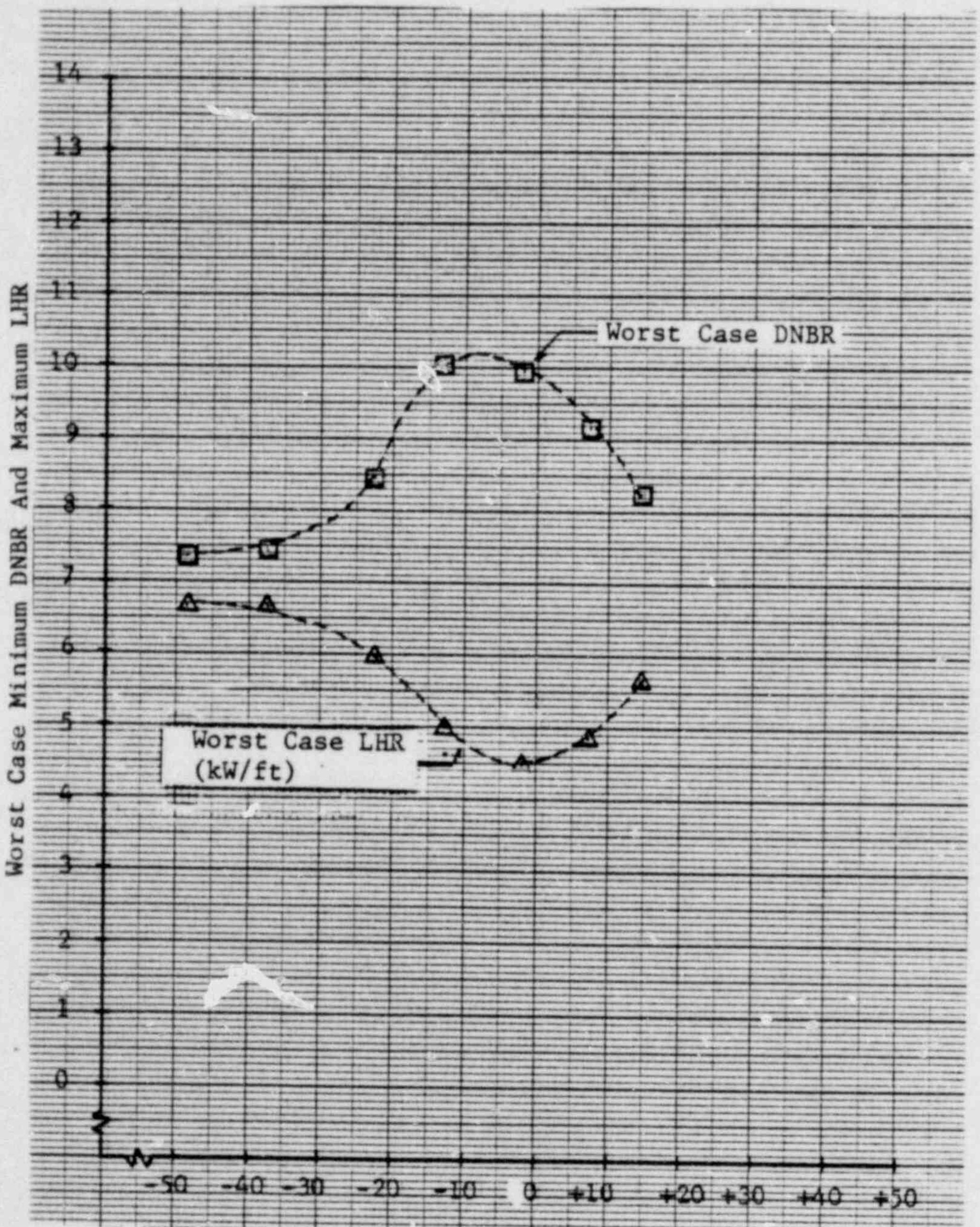

Figure 4.8-8

Worst Case Minimum DNBR And Maximum LHR Versus Full Incore Offset During The Performance Of Power Imbalance Detector Correlation Test At 75% Full Power

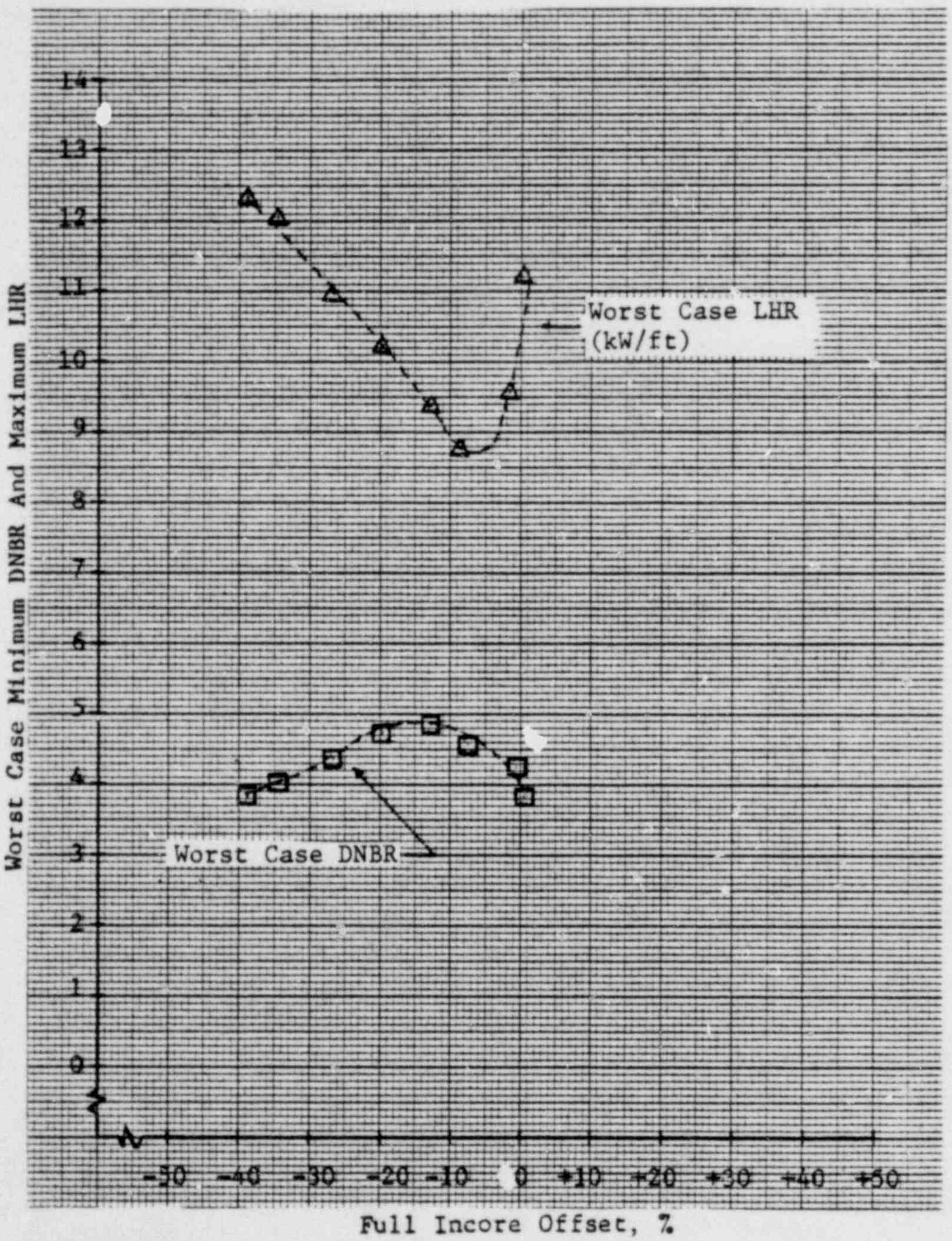

Figure 4.9-9

4.9 NSSS HEAT BALANCE TEST

The unit computer determine the core thermal power by performing both a primary and secondary heat balance. To do these calculations, the computer employs a core thermal power analysis program (CTPA). In addition, the IBM 5100 has also been programmed to calculate the core thermal power using the temperature rise across the core called the core ΔT power. The core ΔT power can be continuously displayed to the control operator. The primary heat balance and the core ΔT power both employ primary flow, which is initially normalized to the measured flow determined during the performance of Reactor Coolant Flow And Flow Coastdown Test (Section 3.1). The primary and secondary heat balance should give similar results for the reactor thermal power. If they do not, the problem is assumed to lie in this initially measured primary flow. The primary and secondary heat balance are set equal to each other and a better calculation of the primary flow is obtained. However, the primary flow determination by this heat balance method will be accurate only when there is sufficient enthalpy rise across the core, thus requiring high power to make the measurement. The test, therefore, checked out heat balance routines until after steady state 75% full power was reached. At that time, primary flow determinations were begun. Data from 75, 92, and 100% full power were used to determine primary flow. The actual adjustment to this value was made at the end of 100% full power testing.

4.9.1 PURPOSE

The purposes of this test are briefly discussed below:

(a) To verify computer calculated primary and secondary side heat balance computations.

(b) Provide baseline data for comparison with subsequent heat balance checks.

(c) To determine reactor coolant loop flow from primary and secondary heat balance calculations.

Four acceptance criteria are specified for nuclear steam supply heat balances as listed below:

(1) The primary heat balance performed by hand calculation and by the unit computer must agree to within 2% full power of each other.

(2) The secondary heat balance performed by hand calculation and by the unit computer must agree to within 2% full power of each other.

(3) The weighted average heat balance performed by hand calculation and by the unit computer must agree to within 2% full power of each other.

(4) Reactor coolant flow with four pumps operating as determined from a primary and secondary heat balance at 100% full power is between 105.0 to 115.3 percent of design flow.

4.9.2 TEST METHOD

Primary and secondary heat balances as required in the NSSS Heat Balance Test were performed at 15, 40, 75, and 100% full power. At each of the above test plateaus, steady state conditions were established as indicated below:

(a)	Turbine Header Pressure	± 9.0 Psig
(b)	Pressurizer Level	± 5.0 Inches
(c)	RCS Pressure	± 20.0 Psig
(d)	RCS T. (AVE)	± 2.0°F
(e)	Power Level	± 2.0% FP
(f)	Feedwater Flow	± 2.0%

After obtaining steady state conditions, data collection was started. This comprised of starting the unit computer to printout the unit parameters listed in Table 4.9-1 and at the same time the core thermal power analysis program (CTPA) was printed out. The unit parameters obtained were then input into the primary, secondary and weighted average heat balance equations 4.9-1, 4.9-2 and 4.9-3 in Table 4.9-2.

The reactor coolant flow measurement using the primary/secondary heat balance method was performed at various power levels above 65% full power. Once steady state conditions were established, the necessary data was collected every 10 minutes for 30 minutes. This data was then averaged and substitued into Equations 4.9-4 in Table 4.9-2 to obtain the primary flow in each loop and the total primary flow.

4.9.3 EVALUATION OF TEST RESULTS

The NSSS Heat Balance Test Procedure is the procedure used for determining the thermal output of the reactor core and the primary reactor coolant flow. There are two methods used for core thermal output: primary side heat balance and secondary side heat balance. This section covers the results of each and presents the determination of reactor coolant flow.

4.9.3.1 PRIMARY AND SECONDARY HEAT BALANCE CALCULATION

The results of the primary, secondary and weighted average heat balance measurements performed from 15 to 100% full power are presented in Table 4.9-3. Good agreement was found between the hand and computer calculated heat balances. Comparison of the hand calculated values with respective computer calculated values resulted in an average and maximum deviation of 0.97 and 1.83% full power respectively. These values are well within the procedural acceptance criteria of 2.0% full power.

Examination of the primary and secondary heat balance above 40% full power indicate the primary heat balances were consistently lower than the secondary heat balances. This difference is due mostly to the indicated reactor coolant flow being slightly less than the actual flow.

4.9.3.2 REACTOR COOLANT FLOW DETERMINATION

Crystal River Unit 3 was designed for a minimum primary coolant flow rate of 105.0 percent design flow. Even though a greater flow rate than the minimum will provide excess DNB protection, the primary flow rates should be less than the core lift limits. The core lift limit to the primary flow rate as specified by the Babcock and Wilcox Company is 115.3 percent of design flow.

The basis of the flow measurement is the application of a heat balance across the primary and secondary sides of the two steam generators. The test consisted of monitoring the thermal-hydraulics data for 30 minutes averaging the various quantities, and substituting them into Equation 4.9-4 in Table 4.9-2 to determine the primary flow.

Table 4.9-4 shows the values of the reactor coolant primary flow determined using this method for four pump operation. As can be seen, the average values of the reactor coolant primary flow measured was 109.3 percent of the design flow. Comparison of this value to the acceptance criteria in Section 4.9.1 indicates that an acceptable flow rate is present on Crystal River Unit 3.

The accuracy of the flow measurement depends on the precision of the various instruments used to measure the thermal-hydraulics data. An error analysis was performed and indicates that the error in the primary flow measurement due to the instrument tolerances and uncertainty in the flow coefficients and the ambient heat loss measurements is $\pm$ 2.0 percent of the design flow.

The primary flow measured on Crystal River Unit 3 was therefore bounded at 109.3 $\pm$ 2.0 percent of the design value. A more detailed analysis of flow was also performed by the Babcock and Wilcox Company. As a result of this investigation, the primary flow was set at 110.0 percent of the design value.

4.9.4 CONCLUSIONS

All primary and secondary heat balance calculations met their respective acceptance criteria.

The primary reactor coolant system flow rate on Crystal River Unit 3 was set at 110.0 percent of design flow, which is within the minimum and maximum allowable value as specified by the acceptance criteria.

List Of Terms Used During The Performance Of NSSS Heat Balance Test At Power

Qp	= Power using primary heat balance (BTU/hr)
Qs	= Power using secondary heat balance (BTU/hr)
Qw	= Power using weighted primary/secondary heat balance (BTU/hr)
Qpumps	= Total pump power (BTU/hr)
W_p^A	= Primary side Loop (A) flow (lbm/hr)
W_p^B	= Primary side Loop (B) flow (lbm/hr)
W_{fdw}^A	= Feedwater Loop (A) flow (lbm/hr)
W_{fdw}^B	= Feedwater Loop (B) flow (lbm/hr)
W_{Ld}	= Letdown flow from reactor coolant system (lbm/hr)
H_{out}^A	= Outlet enthalpy for Loop (A) (BTU/lbm)
H_{out}^B	= Outlet enthalpy for Loop (B) (BTU/lbm)
H_{in}^A	= Inlet enthalpy for (A) cold leg (BTU/lbm)
H_{in}^B	= Inlet enthalpy for (B) cold leg (BTU/lbm)
H_{st}^A	= Outlet steam enthalpy for OTSG (A) (BTU/lbm)
H_{st}^B	= Outlet steam enthalpy for OTSG (B) (BTU/lbm)
H_{fdw}^A	= Inlet feedwater enthalpy for OTSG (A) (BTU/lbm)
H_{fdw}^B	= Inlet feedwater enthalpy for OTSG (B) (BTU/lbm)
H_{mu}	= Enthalpy of the letdown flow from RCS reactor coolant (BTU/lbm)

Table 4.9-1

List Of Terms Used During The Performance Of NSSS Heat Balance Test At Power

P_{NI}	=	Nuclear instrumentation power level (%FP)
$P_{\Delta T}$	=	Core ΔT power level (%FP)
ΔT_C	=	Coolant temperature rise across the core (Deg. F)

Table 4.9-1 (Cont'd)

Table 4.9-2

Equations Used During The Performance Of NSSS Heat Balance Test At Power

EQ (4.9-1) Primary side heat balance for determination of core thermal power

$$Qp = W_p^A\ (H_{out}^A - H_{in}^A) + W_p^B\ (H_{out}^B - H_{in}^B) + W_{Ld}\ (H_{in}^B - H_{mu}) - Q_{pumps} + 2.300\times10^6 \text{ BTU/hr}$$

EQ (4.9-2) Secondary side heat balance for determination of core thermal power

$$Qs = W_{fdw}^A\ (H_{st}^A - H_{fdw}^A) + W_{fdw}^B\ (H_{st}^B - H_{fdw}^B) + W_{Ld}\ (H_{in}^B - H_{mu}) - Q_{pumps} + 2.484\times10^6 \text{ BTU/hr}$$

EQ (4.9-3) Weighted primary/secondary heat balance calculation

$$Qw = (100 - P_{NI})\ (Q_p/86) + P_{NI} - 15)\ (Q_s/85)$$

EQ (4.9-4) Total primary side flow calculation

$$W_p = W_p^A + W_p^B = W_{fdw}^A\ (H_{st}^A - H_{fdw}^A)/(H_{out}^A - H_{in}^A) + W_{fdw}^B\ (H_{st}^B - H_{fdw}^B)/(H_{out}^B - H_{in}^B)$$

EQ (4.9-5) Core ΔT power calculation

$P_{\Delta T} = 2.292\ (\Delta T_c - 6.912) + 15$ (Equation Used During Test Program)

Summary Of Heat Balance Performed During Power Escalation Testing

Test Plateau (%FP)	Date	Time	Core ΔT Power (% FP)	Computer And Hand Calculated Heat Balances, %FP					
				Primary		Secondary		Weighted	
				Computer	Hand	Computer	Hand	Computer	Hand
15	03-31-77	2123	16.47	16.01	16.75	14.58	14.10	16.01	16.71
40	02-27-77	2338	43.62	40.88	42.35	38.76	40.27	40.23	41.72
75	03-14-77	2100	75.65	73.98	73.84	76.71	74.88	75.98	74.47
100	04-01-77	1440	99.09	96.49	95.07	99.00	99.19	98.94	99.15

Table 4.9-3

Table 4.9-4

Determination Of Reactor Coolant System Primary Flow

Date	Time	Power Level (% FP)	Calculated Primary Flow, 1×10^6 lb/hr				Percent of Design Flow (%)	Flow Imbalance (%)
			Loop (A)	Loop (B)	Total	Design		
A. Summary Of Flow Calculations Performed At And Above 75% Full Power								
03-27-77	1536	75	69.56	72.40	141.96	129.75	109.4	4.00
03-27-77	1723	75	69.58	72.41	141.98	129.77	109.4	3.99
03-29-77	1808	92	70.33	72.78	143.11	130.33	109.8	3.45
04-01-77	1113	100	71.20	72.37	142.56	130.65	109.2	1.64
04-01-77	2025	100	69.61	72.24	141.84	130.66	108.6	3.71
						Average	109.3	3.36

4.10 UNIT LOAD STEADY STATE TEST

4.10.1 PURPOSE

The purpose of the Unit Load Steady State Test was to measure reactor coolant system and steam generator steady state parameters as a function of power to compare with design predictions, equipment, and system limits. Specific purposes are as follows:

(a) To measure RCS and OTSG parameters with four (4) reactor coolant pumps operating from 0 to 100% full power.

(b) To measure primary and secondary system operating parameters for comparison with future performance.

(c) To verify the ability of the integrated control system to meet the designed performance under steady state conditions.

(d) To verify that the adjustable steam generator downcomer restrictors are not causing flooding of the feedwater nozzles during normal operation.

Two acceptance criteria are specified for the Unit Load Steady State Test as listed below:

(1) All recorded steady state parameters, as a function of power level, are within their respective minimum and maximum limits as given in Figures 4.10-1 through 4.10-9.

(2) No indications of downcomer flooding have been observed during power escalation from zero to 100% full power.

4.10.2 TEST METHOD

This test measures the steady state behavior of the RCS and the OTSG's at various power levels. The power levels used during the performance of Power Escalation Testing were 0, 15, 25, 40, 65, 75, 92 and 100 percent full power of 2452 megawatts thermal. At each of the above power levels, steady state conditions were established and data required in Table 4.10-1 was taken for 30 minutes.

From this data the average unit parameters were calculated and plotted on Figures 4.10-1 through 4.10-9 and comparisons between the measured data and the design curves were made in order to verify the acceptance criteria. Unit parameter stability during steady state operation was measured in terms of the deviation from the average value of the parameter during the test. These comparisons were done to verify the integrated control system ability to maintain steady state conditions and to try to eliminate any oscillations.

Prior to escalation in unit power, the steady state parameters were extrapolated to the next plateau in order to estimate the acceptability of each at the next plateau. If the extrapolation indicated that a limit might be exceeded or a substantial deviation from the predicted existed, the condition was evaluated prior to escalating unit power.

At power levels of approximately 40, 75, and 100% full power, the integrated system was also operated in the turbine following and reactor/OTSG following modes of control for a period of 30 minutes and steady state data recorded. This data was then averaged and the results evaluated. Adjustments were then made to the integrated control system as necessary to improve unit steady state response.

In addition to the above data, steam generator downcomer temperature was also monitored during the escalation of core power from 0 to 100% full power, to verify that steam generator downcomer restrictors were not causing flooding. This was proven by confirming that no sudden decrease in this temperature indication was observed.

4.10.3 EVALUATION OF TEST RESULTS

Table 4.10-1 shows the unit average parameters of the primary and secondary system measured over the test period for the various power levels. Comparison between the measured data and the expected design data was performed by plotting the averaged unit parameters against the expected design curves. As can be seen in Figures 4.10-1 through 4.10-9, all measured unit average parameters fell within their respective minimum/maximum boundaries except for steam generator outlet pressure. The deficiency was found to be in the calibration of the transmitter controlling steam header pressure (i.e. nominally 885 Psig). A calibration check revealed it to be controlling at an actual pressure of approximately 20 Psig below the design setpoint.

During this test, unit stability was measured by determining the deviation of unit parameters from their respective average value. Table 4.10-2 is a listing of the standard deviation of these variables over the various test power levels. From this analysis it was concluded that flows, temperatures, and pressures were stable within the following average limits while operating in the fully integrated mode of control.

RCS Temperatures	1.3°F of an average value
RCS Pressure	15.5 Psig of an average value
Main Steam Pressure	3.5 Psig of an average value
RCS Flow	0.6% of an average value
Feedwater Flow	2.7% of an average value

The above results confirm that the integrated control system adequately controlled the unit during the startup test program. However, it should be noted that some difficulty was experienced at 75% full power due to secondary side imposed oscillations. These problems were eliminated by increasing the deadband on the turbine header pressure error from $\pm$ 5 to $\pm$ 7.5 Psig, and by slowing down the response of the feedwater pump speed controller by changing the gain and ΔP error deadband.

The results of the checkout of steam generator downcomer flooding versus power level from the 0 to 100% full power data indicates that no flooding is present.

4.10.4 CONCLUSIONS

The average of the measured unit parameters during the test period fell within their respective minimum and maximum limits, except for OTSG outlet steam pressure which was indicating 20 Psig high and therefore controlling low. This was corrected by recalibrating the pressure transmitter controlling steam header pressure.

Analysis of unit parameter stability indicates that all variables are relatively stable. The maximum variation in unit parameters was experienced around 70% full power.

Table 4.10-1

Average Unit Parameters At Various Test Plateaus For Crystal River Unit 3
During Steady State Conditions.

Unit Parameter	Units	Average Unit Parameter							
		0%FP	15%FP	25%FP	40%FP	65%FP	75%FP	92 %FP	100%FP
RC Cold Leg A1 NR Temperature	°F	532.09	573.57	573.10	569.52	564.26	562.95	559.80	558.35
RC Cold Leg A2 NR Temperature	°F	531.81	573.63	572.95	569.34	563.77	562.55	559.52	557.94
RC Cold Leg B1 NR Temperature	°F	531.36	574.08	573.04	569.36	564.07	562.74	559.61	558.18
RC Cold Leg B2 NR Temperature	°F	531.19	573.87	572.74	569.47	563.84	562.55	559.41	557.75
RC Hot Leg A NR Temperature	°F	532.90	581.37	584.17	587.27	595.53	597.53	600.55	602.63
RC Hot Leg B NR Temperature	°F	532.90	580.88	584.51	587.77	594.63	596.56	599.72	601.50
RC Average Temperature	°F	532.29	577.43	578.58	578.32	579.42	579.87	579.87	580.06
RC Loop Temperature Mismatch	°F	+0.67	-0.38	+0.14	-0.01	-0.06	-0.10	-0.15	-0.20
RC Loop A Coolant Flow	MPPH	70.01	67.78	68.30	68.68	69.10	68.98	69.52	69.76
RC Loop B Coolant Flow	MPPH	70.77	69.30	69.40	69.84	70.47	70.01	70.42	70.68
RC Pressurizer Level	Inches	111.80	127.53	134.88	134.64	134.15	134.94	134.65	134.81
RC Loop A NR Pressure	Psig	2150.17	2158.32	2139.93	2143.27	2147.44	2147.87	2139.10	2150.25
NI Power Level	% FP	0.14	14.15	25.50	40.49	67.07	74.15	90.72	97.20
FDW Loop A Flow	MPPH	0.57	0.63	1.01	1.89	3.32	3.81	4.62	5.04
FDW Loop B Flow	MPPH	0.02	0.52	1.15	1.96	3.40	3.85	4.69	5.09
FDW Loop A Temperature	°F	219.40	289.97	326.23	364.05	411.50	423.67	438.44	445.53
FDW Loop B Temperature	°F	219.18	288.70	325.69	363.38	410.20	422.27	437.36	444.86
MS Generator A S/U Level	Inches	29.58	26.36	37.71	54.98	94.28	103.70	131.11	143.76
MS Generator B S/U Level	Inches	29.61	25.82	37.13	54.42	104.29	114.52	143.09	156.38
MS Generator A OP Level	%	4.87	6.75	9.86	14.91	31.14	35.64	47.92	54.05
MS Generator B OP Level	%	6.20	8.70	11.90	16.29	28.80	34.28	46.56	52.81
MS Generator A Pressure	Psig	831.00	868.20	878.95	883.89	895.22	888.00	897.20	888.75
MS Generator B Pressure	Psig	861.10	873.30	865.25	870.64	897.89	890.62	900.80	894.00
MS Generator A Temperature	°F	100.25	580.13	584.06	No Data	592.72	593.90	594.35	593.83
MS Generator B Temperature	°F	145.30	580.04	584.66	No Data	593.01	593.94	594.38	594.15
MS Generator A D/C Temperature	°F	526.40	532.19	531.80	532.62	535.14	534.85	536.36	535.58
MS Generator B D/C Temperature	°F	530.30	530.98	530.58	531.50	534.31	534.07	535.77	535.06
Turbine Header Pressure	Psig	869.30	884.44	880.33	882.56	887.10	891.60	887.49	883.38

Note: The Above Results Are Based O- The Data Acquisition Center Output

Table 4.10-2

Maximum Deviation In Average Unit Parameters At Various Test Plateaus
For Crystal River Unit 3 During Steady State Conditions.

Unit Parameter	Units	Standard Deviation of Average Unit Parameter							
		0%FP	15%FP	25%FP	40%FP	65%FP	75%FP	92 %FP	100%FP
RC Cold Leg A1 NR Temperature	°F	0.07	0.24	0.51	0.26	0.27	0.18	0.17	0.09
RC Cold Leg A2 NR Temperature	°F	0.08	0.41	0.48	0.25	0.20	0.14	0.09	0.18
RC Cold Leg B1 NR Temperature	°F	0.06	0.41	0.43	0.25	0.34	0.16	0.11	0.07
RC Cold Leg B2 NR Temperature	°F	0.06	0.41	0.46	0.27	0.30	0.14	0.16	0.16
RC Hot Leg A NR Temperature	°F	0.08	0.40	0.44	0.28	0.13	0.18	0.11	0.09
RC Hot Leg B NR Temperature	°F	0.06	0.38	0.42	0.27	0.19	0.16	0.11	0.09
RC Average Temperature	°F	0.07	0.60	0.45	0.26	0.24	0.16	0.13	0.14
RC Loop Temperature Mismatch	°F	0.07	0.37	0.47	0.26	0.28	0.16	0.13	0.13
RC Loop A Coolant Flow	MPPH	0.32	0.17	0.19	0.13	0.20	0.21	0.19	0.11
RC Loop B Coolant Flow	MPPH	0.39	0.08	0.26	0.23	0.28	0.18	0.15	0.22
RC Pressurizer Level	Inches	0.63	0.85	0.86	0.67	0.36	0.62	0.38	0.24
RC NR Pressure	Psig	1.93	11.77	15.42	8.71	5.90	2.95	1.45	1.91
NI Power Level	% FP	0.11	0.09	0.68	0.36	0.25	0.41	0.26	0.79
FDW Loop A Flow	MPPH	0.01	0.00	0.03	0.02	0.07	0.03	0.02	0.03
FDW Loop B Flow	MPPH	0.00	0.04	0.03	0.04	0.09	0.02	0.01	0.03
FDW Loop A Temperature	°F	0.13	0.34	1.23	0.22	0.52	0.09	0.07	0.09
FDW Loop B Temperature	°F	0.11	0.44	1.25	0.21	0.36	0.15	0.15	0.21
MS Generator A S/U Level	Inches	0.17	0.30	0.88	1.04	1.91	1.58	0.46	0.18
MS Generator B S/U Level	Inches	0.05	0.25	0.62	1.04	1.84	1.49	0.13	0.36
MS Generator A OP Level	%	0.02	0.10	0.40	0.46	0.39	0.17	0.23	0.22
MS Generator B OP Level	%	0.00	0.08	0.18	0.92	0.42	0.25	0.25	0.35
MS Generator A Pressure	Psig	0.00	1.01	2.38	1.67	2.33	1.51	1.03	1.16
MS Generator B Pressure	Psig	1.18	0.94	2.50	1.65	1.76	1.51	0.92	0.93
MS Generator A Temperature	°F	0.00	0.39	0.41	No Data	0.20	0.17	0.20	0.05
MS Generator B Temperature	°F	0.20	0.32	0.19	No Data	0.18	0.15	0.12	0.16
MS Generator A D/C Temperature	°F	0.00	0.15	0.23	0.57	0.19	0.09	0.12	0.14
MS Generator B D/C Temperature	°F	0.00	0.17	0.24	0.42	0.11	0.07	0.08	0.11
Turbine Header Pressure	Psig	1.49	1.15	2.52	1.79	2.60	3.41	2.39	1.37

Note: The Above Results Are Based On The Data Acquisition Center Output

Reactor Coolant System Temperature Versus Power Level With Four Reactor Coolant Pumps Operating

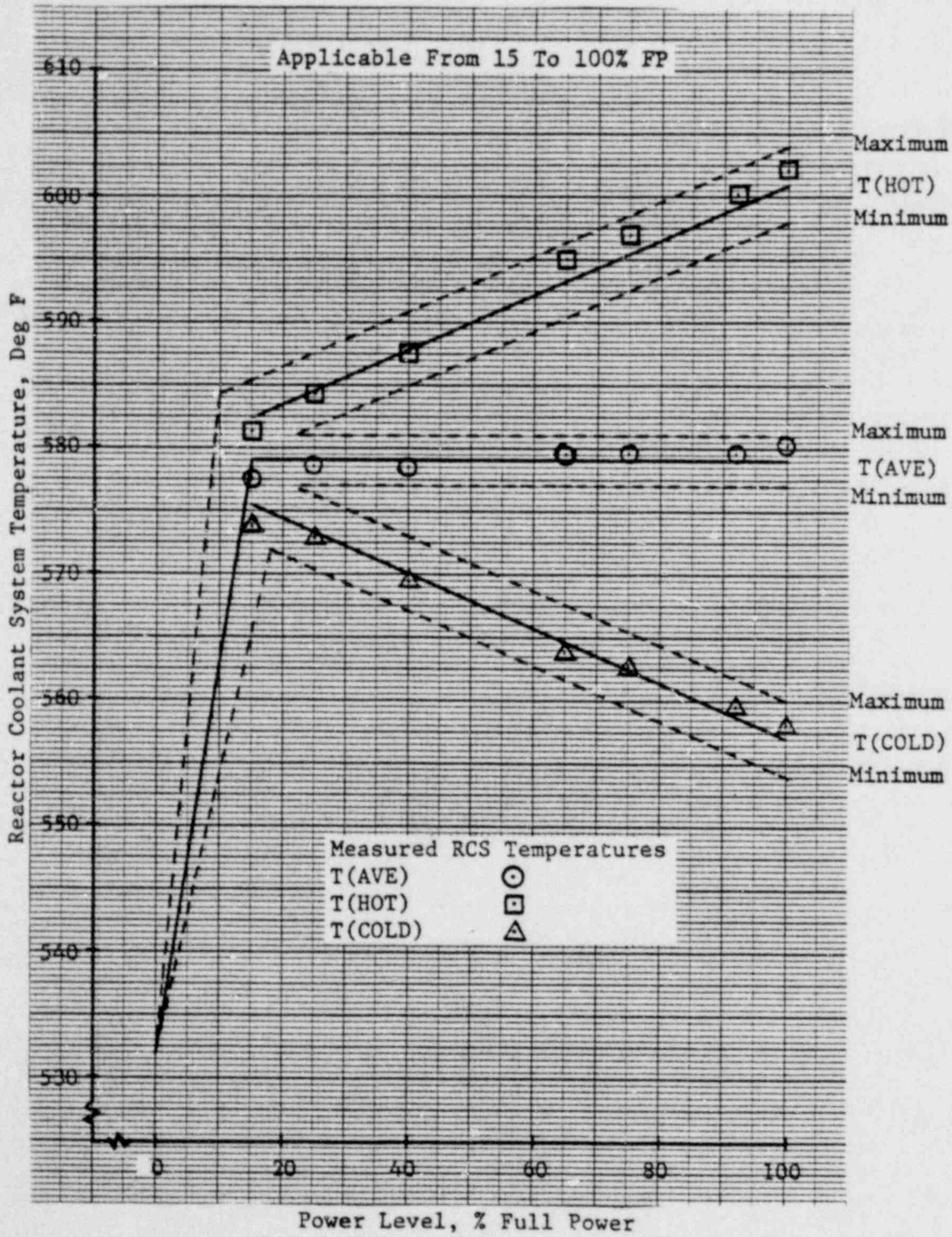

Note: The minimum and maximum curves represent design limits only.

Figure 4.10-1

Steam Generator Outlet Pressure Versus Power Level

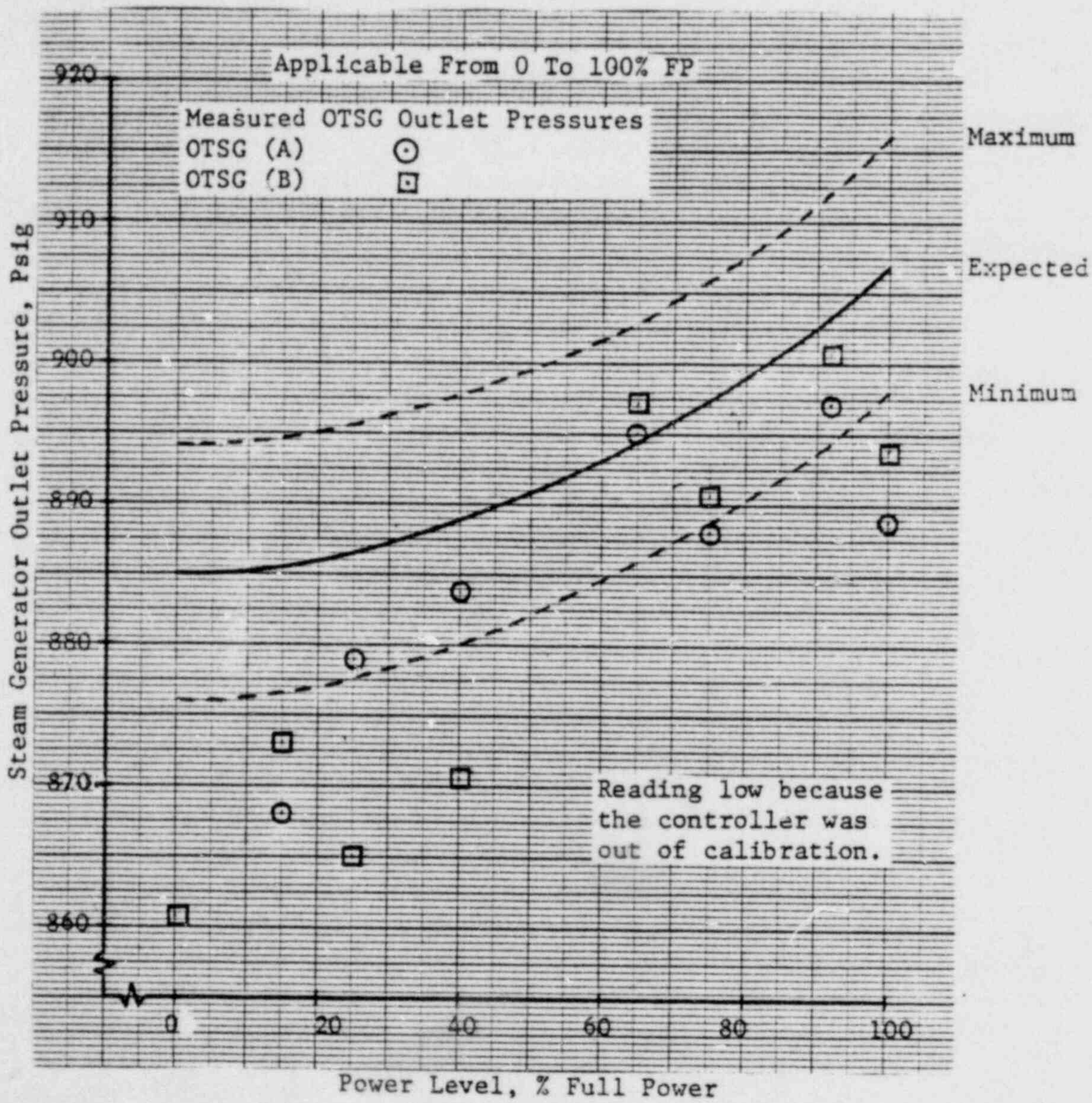

Note: At 0% full power OTSG (A) steam pressure was off scale at 831 Psig.

Note: The minimum and maximum curves represent design limits only.

Figure 4.10-2

Steam Generator Startup Level Versus Power Level

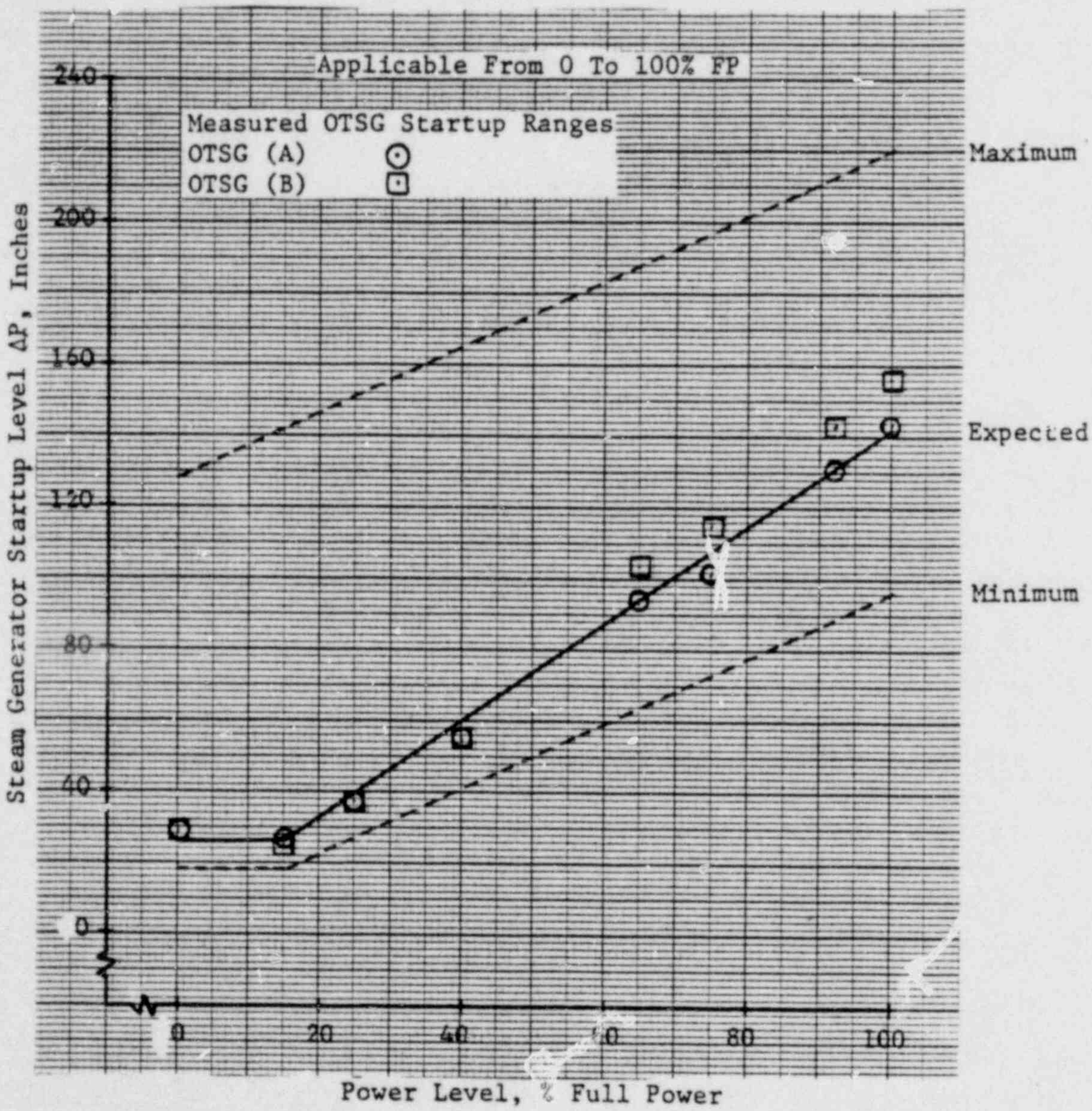

Note: The minimum and maximum curves represent design limits only.

Figure 4.10-3

Steam Generator Operating Range Versus Power Level

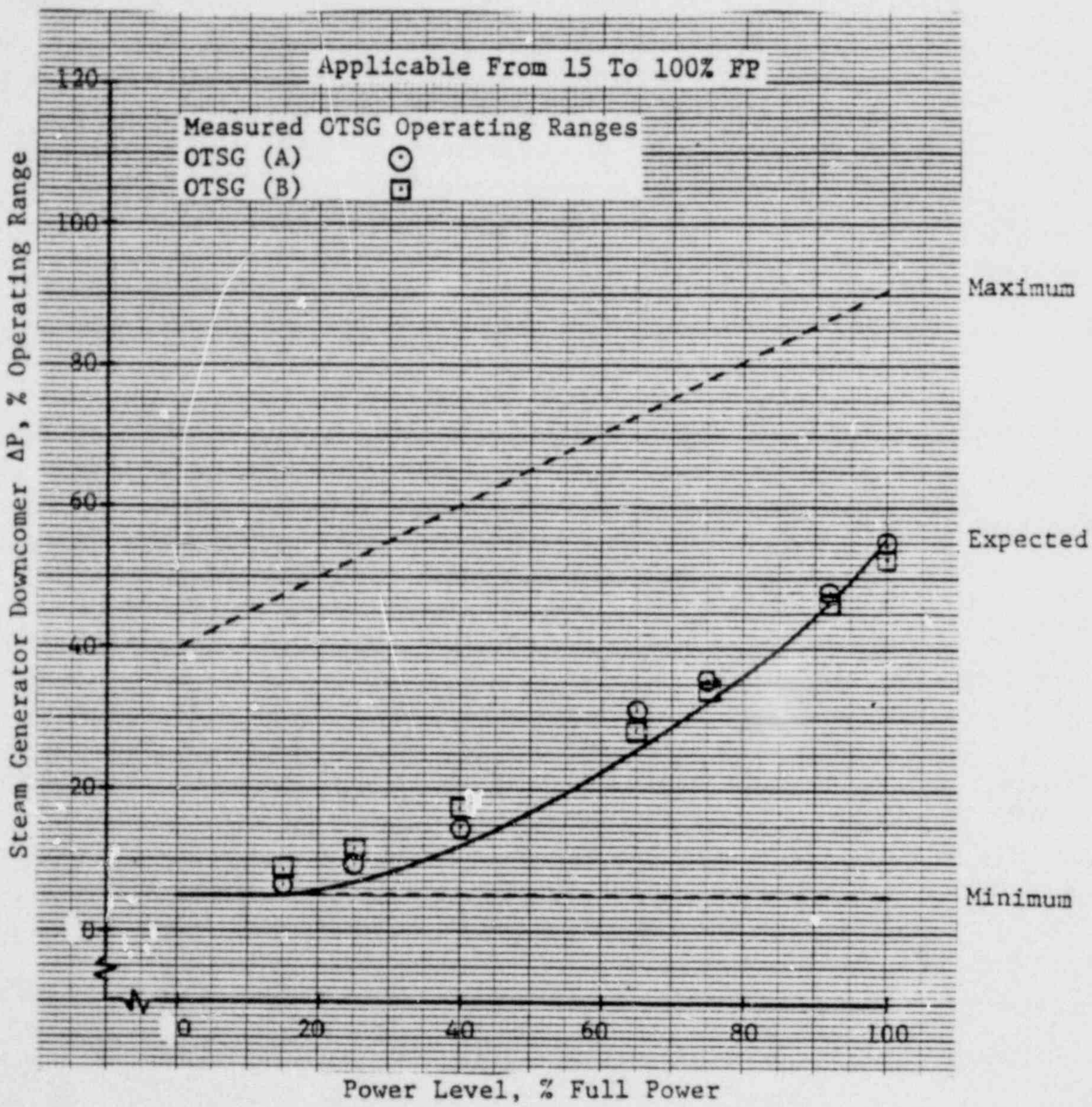

Note: The minimum and maximum curves represent design limits only.

Figure 4.10-4

Steam Generator Steam Temperature Versus Power Level

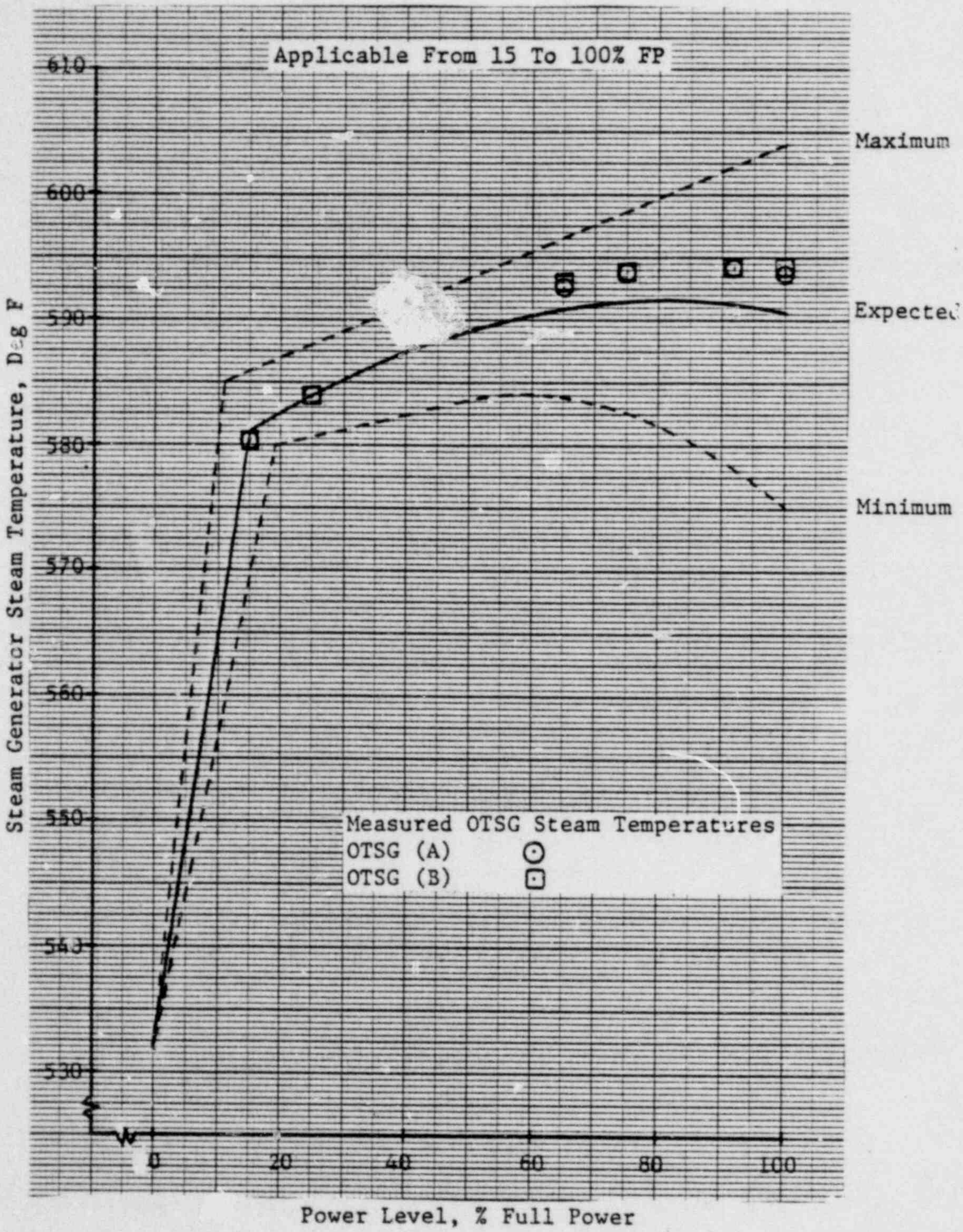

Note: The minimum and maximum curves represent design limits only.

Figure 4.10-5

Feedwater Temperature Versus Power Level

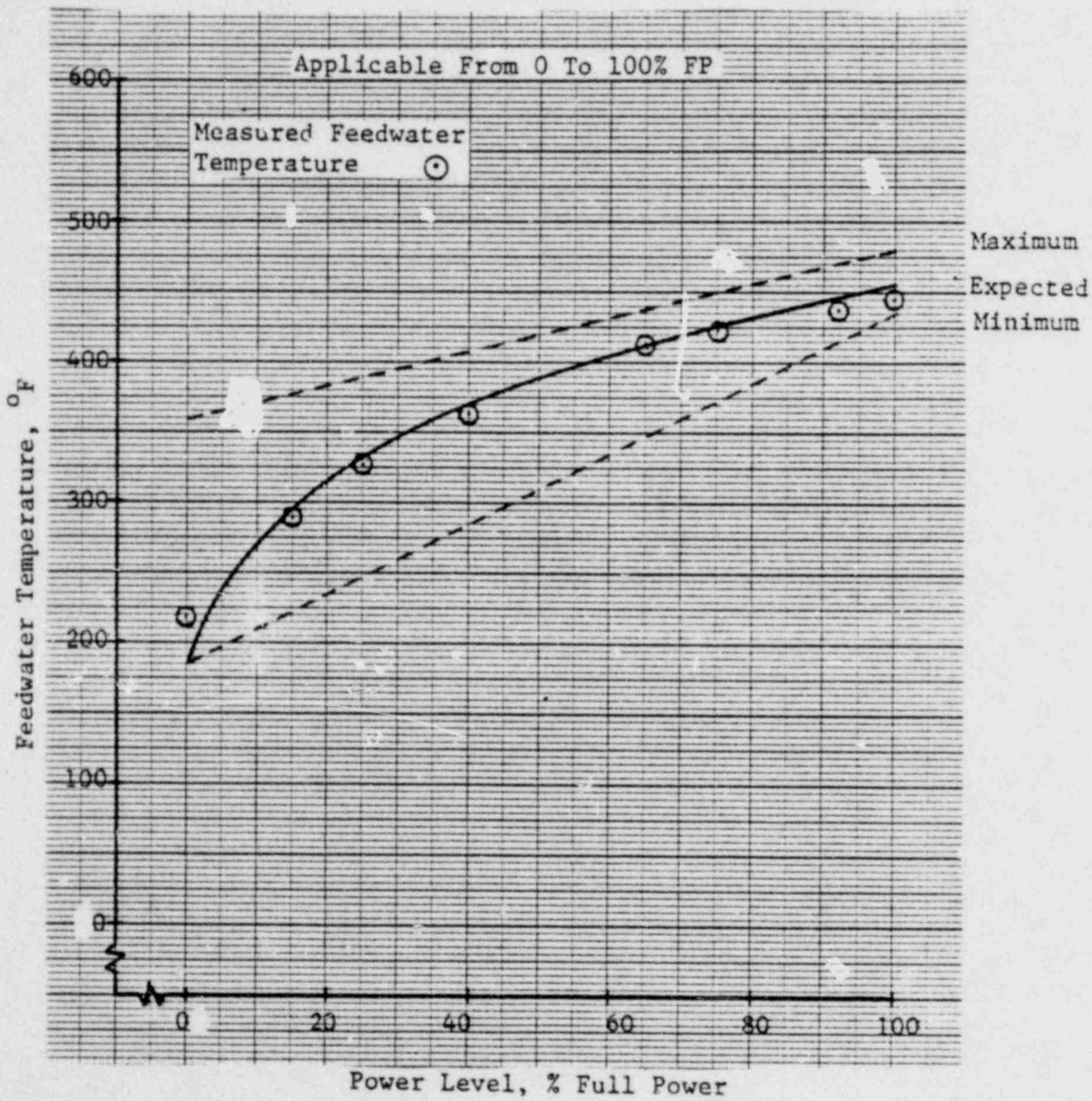

Note: The minimum and maximum curves represent design limits only.

Figure 4.10-6

Total Feedwater Flow Versus Power Level

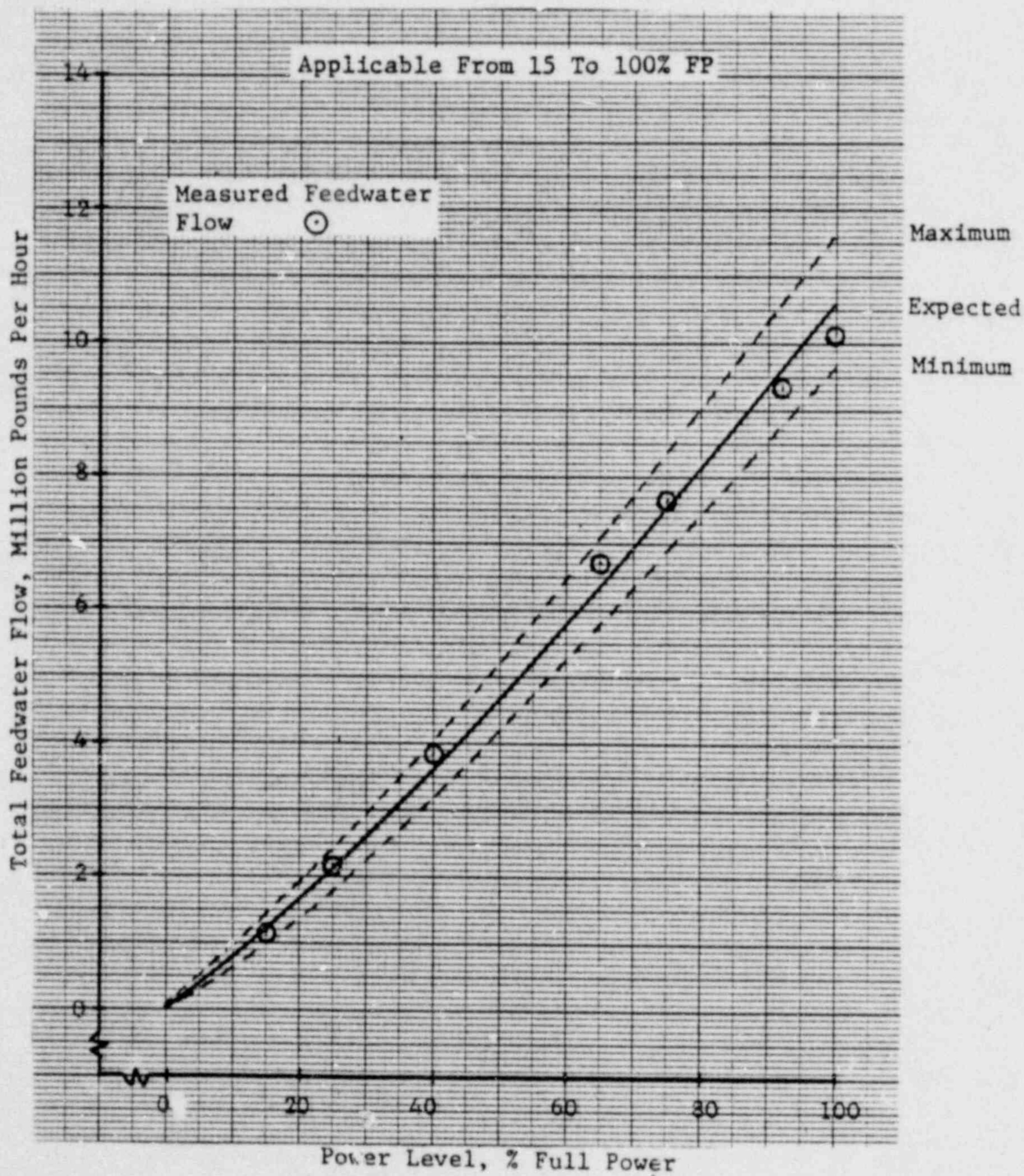

Note: The minimum and maximum curves represent design limits only.

Figure 4.10-7

Turbine Header Pressure Versus Power Level

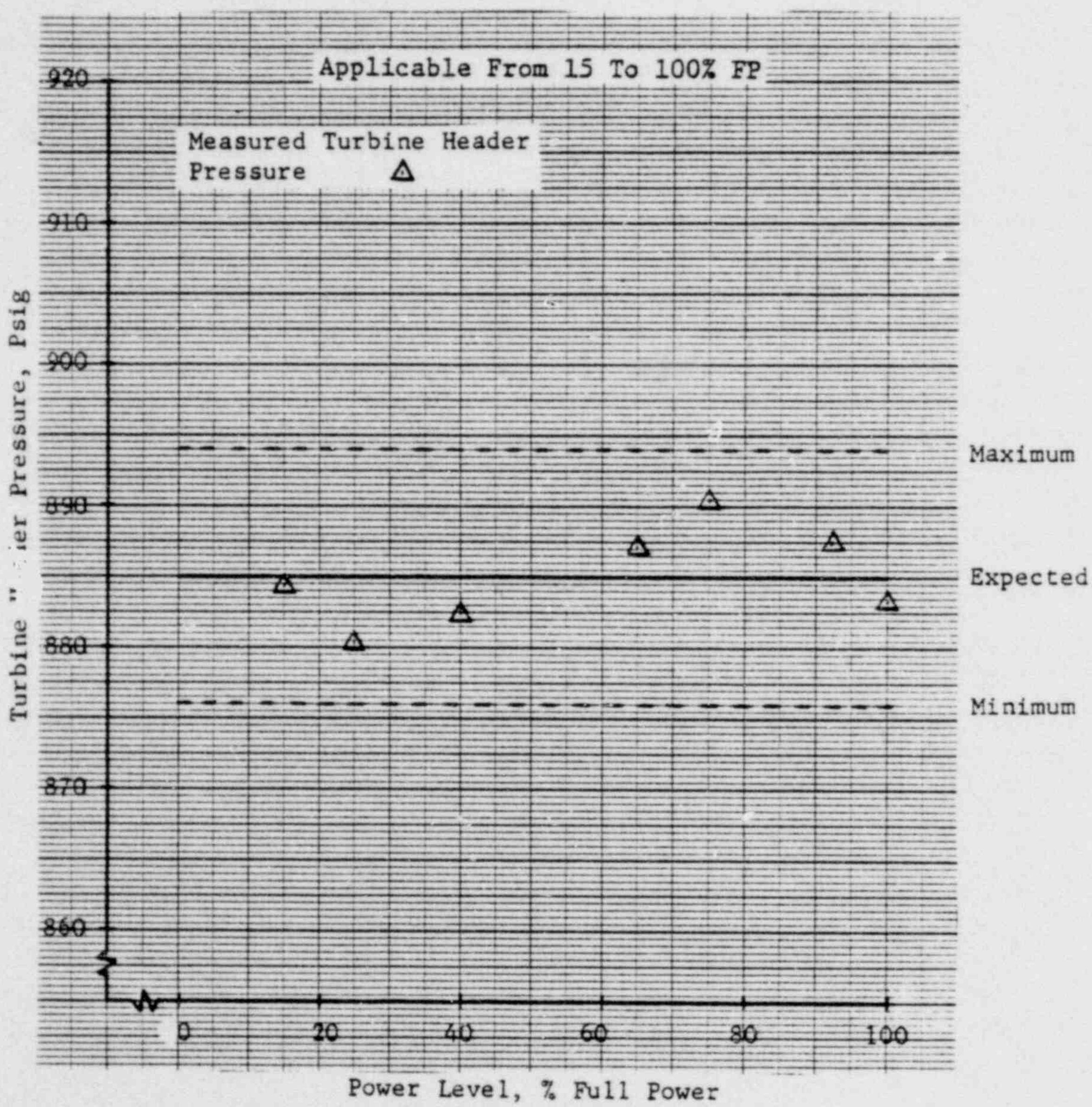

Note: The minimum and maximum curves represent design limits only.

Figure 4.10-8

Reactor Coolant System Loop Temperature Mismatch Versus
Power Level With Four Reactor Coolant Pumps Operating

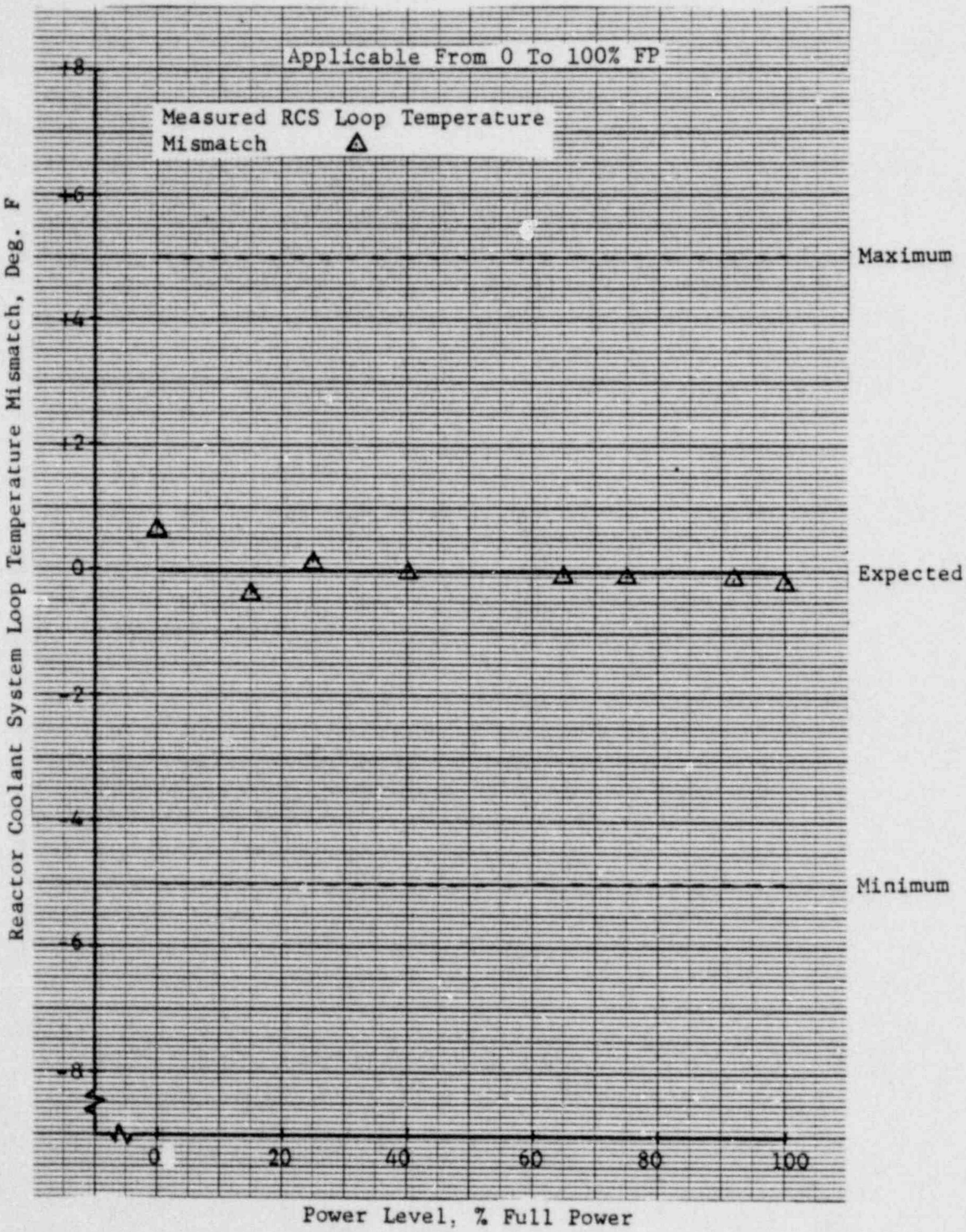

Note: The minimum and maximum curves represent design limits only.

Figure 4.10-9

4.11 UNIT LOAD TRANSIENT TEST

The integrated control system at Crystal River Unit 3 is designed to produce the best megawatt response to megawatt demand consistent with the capabilities and limitations of the entire unit. The control philosophy is developed recognizing that each of the control variables has independent requirements that must be considered separately and that all variables must be coordinated into one system to produce automatic control. Figure 4.11-1 displays the conceptual organization of the integrated control system designed to operate the unit with minimum operator involvement. This complex control system can be thought of as having five levels of unit or system control, ranging from local closed loop control of components to complete system control whose purpose is to generate the megawatts being requested.

The ICS incorporates the following different normal modes of operation, (Figure 4.11-2):

(a) Reactor/OTSG-following control mode defined as the turbine controlling electrical megawatts with the reactor/steam generator maintaining the required steam conditions and following an index of the unit load to maintain the required steam conditions.

(b) Turbine-following control mode defined as the reactor/steam generator controlling thermal megawatt generation and the turbine following this steam production to maintain the required steam pressure.

(c) Fully integrated mode or the integrated reactor/steam generator/turbine generator control mode for once-through steam generators designed to combine both of these basic control schemes in such a way that the advantages of both are accented and their disadvantages are minimized.

The ICS takes advantage of the rapid, accurate steam pressure control available with the turbine-following approach. At the same time, the ICS achieves the rapid response to load changes available from the reactor-following scheme by programmed borrowing and depositing of energy in the steam generator during transient conditions. The ICS thus provides improved unit stability by allowing a limited change in the energy stored in both steam generators during a transient and ensuring that normal steam pressure and temperature are restored at the desired megawatt generation after the transient has occurred. The basic requirement of the reactor/steam generator/turbine unit control is matching megawatt generation to unit load demand. The integrated reactor/steam generator/turbine control does this by coordinating steam flow to the turbine with the rate of steam generation.

The ICS also has the capability to automatically run back and/or limit the unit output (and thereby reactor power) when certain unit conditions would prevent operation at the desired power level.

When the ICS is operating in the fully integrated mode, it utilizes feed forward control signals developed from a megawatt demand signal to control both feedwater flow and reactor power simultaneously with changes to the turbine control valves to produce the megawatts desired. If an imbalance exists between the flow of steam to the turbine and the steam production rate, the signals to the feedwater and reactor power systems are modified to shorten the interval of time required to re-establish equal steam flow/steam production conditions. The ICS is therefore characterized by fast response and stable operation of the unit as a whole.

4.11.1 PURPOSE

The purposes of the Unit Load Transient Test are listed below:

(a) To demonstrate the ability of the ICS to maintain control of the unit during power changes up to the design ramp rates after tuning and optimization.

(b) To demonstrate proper ICS response to tripping one reactor coolant pump at 40% full power and restarting it at 20% full power.

(c) To demonstrate the proper ICS response during a runback initiated by tripping one main feedwater pump at 75% full power.

Three acceptance criteria are specified for Unit Load Transient Test as listed below:

(1) Reactor power can be varied at the design ramp rates without exceeding the limits stated in Technical Specifications and Sections 1 and 2 of Plant Limits And Precautions.

(2) Each transient must be completed without causing the reactor protective system to actuate.

(3) The tripped reactor coolant pump will not restart until reactor power is less than 30% full power.

4.11.2 TEST METHOD

During the Power Escalation Sequence at Crystal River Unit 3, the Unit Load Transient Test was performed at three different power plateaus: 40, 75, and 100% of rated full power. Table 4.11-1 gives a general summary of all transients required by the Unit Load Transient Test. The transients were performed with the ICS in four separate modes of control:

(a) The fully integrated control mode

(b) The turbine-following control mode

(c) The reactor/OTSG - following control mode

(d) The turbine/OTSG - following control mode

The turbine/OTSG-following control mode is not normally employed for changing power during unit operation. However, application of this mode does help in tuning the ICS since it tends to isolate the response of various modules.

Transient testing at the 40% and the 75% full power plateaus was performed in accordance with the test procedure and as specified in Table 4.11-1. Transients in each mode of ICS control were performed at ramp rates of approximately 5% FP per minute to assist in verification of the acceptance criteria. Additional transients to check unit response to a reactor coolant pump trip at 40% full power and a feedwater pump trip at 75% full power were performed.

Transient testing at the 100% full power plateau was also performed as specified in Table 4.11-1. Transients in each mode of ICS control were performed at ramp rates of approximately 5% FP per minute between 90 to 100% full power and at ramp rates of approximately 10% FP per minute between 45 to 85% full power. These transients were then used to assist in verification of the acceptance criteria.

The desired transient response of the unit was that reactor power could be varied at the design ramp rates of 5% FP per minute at 40 and 75 percent full power and of 10% FP per minute at 100 percent full power and return to steady state operation without exceeding the unit parameters deviations given below:

TRANSIENT STATE	Turbine Header Pressure	+/- 50 Psig
	Reactor Coolant Average Temperature	+/- 5 deg F
	Loop Temperature Mismatch	+/- 5 deg F
STEADY STATE	Turbine Header Pressure	+/- 9 Psig
	Reactor Coolant Average Temperature	+/- 1 deg F
	Loop Temperature Mismatch	+/- 1 deg F
	Reactor Power Error	+/- 1% FP

Throughout this test, ICS tuning was performed when the above unit parameters indicated that tuning was necessary in order to optimize the transient response of the ICS.

The technique of inducing each transient was to decrease reactor power from the test plateau to a predetermined lower power level, then after establishing steady state conditions, reactor power was re-escalated to the test plateau. During all transients, the variation of pertinent primary and secondary system parameters during negative and positive power ramps was monitored and recorded on Brush recorders and the Reactimeter.

4.11.3 EVALUATION OF TEST RESULTS

The Unit Load Transient Test was conducted at 40%, 75% and 100% full power to evaluate the ability of the Integrated Control System to accomplish smooth negative and positive changes in power level while operating in the fully integrated, turbine-following, reactor/OTSG-following, and turbine/OTSG-following modes of control. It was also done to observe the transient response of the unit to the loss of a reactor coolant pump and a main feedwater pump.

The data taken during each transient (i.e. power, unit average temperature, loop temperature mismatch, and turbine header pressure) were then analyzed. This analyses included verifying that the transient response fell within the desired limits stated in 4.11.2.

The evaluation of the results of the Unit Load Transient Test has been subdivided into three sections, one for each test plateau.

4.11.3.1 ICS TRANSIENT TEST AT THE 40% POWER LEVEL

The behavior of the unit during the negative and positive ramps in power level is presented in Figures 4.11-3 through 4.11-7 and summarized in Table 4.11-2. In every case, the desired transient response was observed, thus no ICS tuning was required.

The reactor coolant pump trip portion was performed after the completion of the above ICS transient. It was initiated from a steady state condition of approximately 45% full power. Figure 4.11-8 shows the behavior of various unit parameters versus time. From this Figure, it can be concluded that the $\Delta T(c)$, controller smoothly accomplished the four pump to three pump transient. Verification of the reactor coolant pumps inhibit was then demonstrated by trying to start the pump at 32% full power. Reactor power was then reduced to 20% full power and the pump re-started.

In conclusion, all required transients were performed at 40% full power with the acceptance criteria on each met.

4.11.3.2 ICS TRANSIENT TEST AT THE 75% POWER LEVEL

The behavior of the unit during the negative and positive ramps in power level is presented in Figures 4.11-9 through 4.11-13 and summarized in Table 4.11-3. In every case, the desired transient response was observed, thus no ICS tuning was required.

The feedwater pump portion was performed after the completion of the above ICS transient. The test method was to trip one of the two main feedwater pumps and record the transient response of the unit. Figure 4.11-14 shows the behavior of various unit parameters versus time. Even though this resulted in a rapid runback in reactor power to 56% full power, the ICS adequately corrected the various error signals that developed and returned the unit to a steady state condition in approximately 3 minutes.

In conclusion, all required transients were performed at 75% full power with the acceptance criteria on each met.

4.11.3.3 ICS TRANSIENT TEST AT THE 100% POWER LEVEL

The behavior of the unit during the negative and positive ramps in power levels is presented in Figures 4.11-15 through 4.11-21 and summarized in Table 4.11-4. In every case, the desired transient response was observed, thus no ICS tuning was required.

In conclusion, all required transients were performed at 100% full power with the acceptance criteria on each met.

4.11.4 CONCLUSIONS

From analyses of all the test data, the following conclusions may be made for the 40, 75, and 100% full power plateau sections of the Unit Load Transient Test.

(a) All transients were performed without exceeding the limits of the Crystal River Unit 3 Technical Specifications and Sections 1 and 2 of Plant Limits And Precautions.

(b) All transients were completed without causing the reactor protective system to actuate.

(c) The ability of the Integrated Control System to control unit parameters (i.e. power, unit average temperature, loop temperature mismatch, and turbine header pressure) during the transient was excellent and within the limits stated in 4.11.2.

General Summary Of Transients Required By Unit Load Transient Test

Transient Group (Dim)	ICS Mode of Operation (Dim)	General Comment (Dim)	Power Decrease (%FP)	Power Increase (%FP)	Test Ramp Rate (%/min)
A. Unit Load Transient Test at 40% Full Power					
1.1	Fully Integrated		40 to 30	30 to 40	5
1.2	Turbine Following		40 to 30	30 to 40	5
1.3	Reactor/OTSG Following		40 to 30	30 to 40	5
1.4	Turbine/OTSG Following	(3 cases)	40 to 30	30 to 40	5
1.5	Fully Integrated		40 to 15	15 to 40	5
1.6	Fully Integrated	(RCP Trip)	(Reduce Power/Start RCP)		
1.7	Fully Integrated			15 to 40	5
B. Unit Load Transient Test at 75% Full Power					
2.1	Fully Integrated		75 to 65	65 to 75	5
2.2	Turbine Following		75 to 65	65 to 75	5
2.3	Reactor/OTSG Following		75 to 65	65 to 75	5
2.4	Turbine/OTSG Following	(3Cases)	75 to 65	65 to 75	5
2.5	Fully Integrated		75 to 30	30 to 75	5
2.6	Fully Integrated	(FWP Trip)	75 to 55		
2.7	Fully Integrated			55 to 75	10
C. Unit Load Transient Test at 100% Full Power					
3.1	Fully Integrated		100 to 90	90 to 100	5
3.2	Turbine Following		100 to 90	90 to 100	5
3.3	Reactor/OTSG Following		100 to 90	90 to 100	5
3.4	Turbine/OTSG Following	(3 Cases)	100 to 90	90 to 100	5
	Fully Integrated		100 to 85		NA
3.5	Fully Integrated		85 to 45	45 to 85	10
3.6	Turbine Following		85 to 45	45 to 85	10
3.7	Reactor/OTSG Following		85 to 45	45 to 85	10

Table 4.11-1

Table 4-11-2

ICS Transient Data Obtained During The Performance Of Unit Load Transient Test At 40% Full Power

Transient Number	ICS Mode of Operation	Power (%FP)	Unit Transient Response								Unit Steady State Return							
			Rate, %/min		ΔT(AVE), F		ΔT(C), F		ΔTHP, PSI		ΔP, % FP		ΔT(Ave), F		ΔT(C), F		ΔTHP, PSI	
			Ave	Max	Min	Max	Min	Max	Min	Max	Min	Max	Min	Max	Min	Max	Min	Max
1.1	Fully Integrated	40 to 29	-2.6	-4.7	-1.8	+0.0	-0.1	+0.4	+0.0	+32.6	-0.2	+0.1	-0.2	+0.3	-0.1	+0.1	-1.3	+2.0
		29 to 39	+2.8	+4.8	+0.0	+0.9	-0.4	+0.0	-35.4	+0.0	-0.2	+0.1	-0.1	+0.1	-0.1	+0.1	-0.7	+0.8
1.2	Turbine Following	40 to 30	-2.5	-3.1	-0.7	+0.5	+0.0	+0.4	-1.8	+4.8	-0.1	+0.1	+0.0	+0.1	-0.1	+0.1	-0.8	+1.6
		30 to 40	+1.6	+3.0	-0.2	+0.5	-0.2	+0.0	-1.5	+4.8	-0.1	+0.0	-0.2	0.0	-0.1	+0.1	-1.5	+0.0
1.3	Reactor/OTSG Following	40 to 30	-2.3	-3.5	-0.4	+0.1	+0.0	+0.3	+0.0	+45.3	-0.6	+0.6	-0.4	+0.2	-0.1	+0.1	-2.7	+2.7
		30 to 39	+2.0	+3.5	+0.0	+0.2	-0.6	+0.0	-44.1	+0.0	-0.6	+0.4	-0.2	+0.1	-0.1	+0.1	-5.6	+5.2
1.4 (1)	Turbine/OTSG Following (Rods In Hand)	41 to [illegible]	-2.2	-2.5	-2.3	+0.0	-0.2	+0.1	-4.8	+0.0	-0.1	+0.1	-0.6	+0.4	-0.1	+0.1	-4.0	+4.0
		29 to 39	+2.2	+2.5	+0.0	+2.1	-0.2	+0.1	+0.0	+8.7	-0.6	+0.3	-0.3	+0.6	-0.2	+0.2	-3.1	+3.5
1.4 (2)	Turbine/OTSG Following (Reactor Demand In Hand)	40 to 29	-3.4	-3.6	-5.4	+0.0	-0.2	+0.5	-12.9	+3.3	-0.3	+0.1	-0.1	+0.2	-0.1	+0.1	-3.8	+3.4
		29 to 39	+3.2	+4.1	+0.0	+4.7	-0.4	+0.0	-2.1	+7.8	-0.1	+0.0	-0.2	+0.4	-0.2	+0.2	-0.9	+1.2
1.4 (3)	Turbine/OTSG Following (Rods & Reactor In Hand)	40 to 29	-2.3	-3.7	-2.4	+0.2	+0.0	+0.8	-8.1	+0.0	-0.4	+0.4	-0.2	+0.1	-0.1	+0.1	-2.2	+2.0
1.5	Fully Integrated	42 to 15	-4.5	-7.1	-0.8	-0.1	0.0	+0.6	+0.0	+32.0	-0.9	+0.6	-0.3	+0.4	-0.2	+0.6	-2.5	+2.5
			+4.3	+6.2	+0.0	+1.5	-0.9	+0.3	-27.8	+0.0	-0.6	+0.3	-0.1	+0.0	-0.7	+0.5	-8.0	+4.3
1.6	Fully Integrated (RCP Trip)	45 to 32	-5.1	-5.5	-1.4	+0.[illegible]	-0.6	+0.0	-4.3	+18.5	-1.8	+2.3	-0.8	+0.5	-0.1	+0.1	-5.2	+12.0
1.7	Fully Integrated	32 to 41	+6.3	+8.4	-0.9	+1.1	-5.6	-1.4	-38.4	-10.6	-0.1	+0.1	-0.2	+0.3	-0.5	+0.5	-5.7	+1.7

Table 4.11-3

ICS Transient Data Obtained During The Performance Of Unit
Load Transient Test At 75% Full Power

Transient Number	ICS Mode of Operation	Power (%FP)	Unit Transient Response								Unit Steady State Return							
			Rate, %/min		ΔT(AVE), F		ΔT(C), F		ΔTHP, PSI		ΔP, % FP		ΔT(Ave), F		ΔT(C), F		ΔTHP, PSI	
			Ave	Max	Min	Max	Min	Max	Min	Max	Min	Max	Min	Max	Min	Max	Min	Max
2.1	Fully Integrated	77 to 67	-3.4	-4.9	-0.2	+0.3	-0.1	+0.2	0.0	+16.5	-0.1	+0.2	-0.1	+0.2	-0.1	+0.2	-6.9	+5.7
		67 to 76	-2.4	-4.9	-0.3	+0.5	-0.3	+0.4	0.0	-18.4	-0.1	+0.1	-0.1	+0.2	-0.2	+0.2	-3.9	+4.2
2.2	Turbine Following	77 to 66	-2.4	-3.5	-0.9	+0.2	-0.1	+0.4	+9.2	+1.3	-0.3	+0.4	-0.1	+0.0	-0.1	+0.0	-1.6	+1.2
		66 to 78	+2.9	+4.5	-0.4	+0.7	-0.1	+0.1	0.0	+15.4	-0.3	+0.2	-0.2	+0.2	-0.2	+0.0	-1.3	+2.4
2.3	Reactor/OTSG Following	78 to 67	-2.7	-4.8	-0.4	+0.7	-0.4	+0.3	+0.0	+24.8	-0.3	+0.3	-0.2	+0.2	-0.2	+0.2	-5.5	+2.8
		67 to 77	+2.2	+3.5	+0.0	+1.6	-0.1	+0.5	-1.9	+9.3	-0.4	+0.4	-0.1	+0.0	0.0	+0.2	-6.5	+7.8
2.4 (1)	Turbine/OTSG Following (Rods In Hand)	78 to 66	-2.2	-2.7	-2.4	+0.0	-0.3	+0.6	-8.1	+8.8	-0.3	+0.3	-0.1	+0.0	-0.2	+0.1	-2.4	+3.2
		66 to 77	+2.2	+3.5	+0.0	+1.6	-0.1	+0.5	-1.9	+9.3	-0.4	+0.4	-0.1	+0.0	0.0	+0.2	-6.5	+7.8
2.4 (2)	Turbine/OTSG Following (Reactor Demand In Hand)	79 to 67	-2.3	-3.6	-3.2	+0.0	+0.0	+0.3	-15.4	0.0	-0.2	+0.3	-0.5	+0.5	-0.1	+0.2	-2.9	+3.9
		67 to 77	+2.4	+3.2	+0.0	+2.7	+0.0	+0.4	-0.9	+5.0	-0.2	+0.2	-0.2	+0.2	-0.1	+0.1	-1.8	+2.1
2.4 (3)	Turbine/OTSG Following (Rods & Reactor In Hand)	77 to 66	-2.0	-2.8	-2.1	+0.0	-0.3	+0.1	-9.6	+0.0	-0.2	+0.2	-0.2	+0.2	-0.2	+0.2	-0.7	+1.1
		66 to 77	+2.5	+3.2	+0.0	+2.5	+0.0	+0.2	+0.0	+10.8	-0.4	+0.6	-0.2	+0.2	-0.1	+0.1	-4.6	+5.7
2.5	Fully Integrated	78 to 31	-4.2	-7.7	-0.4	+2.6	-1.6	+1.3	-22.9	+22.4	-0.7	+0.4	-0.5	+0.3	-0.8	+0.6	-9.8	+10.6
		31 to 75	+5.6	+11.7	-3.5	+0.5	-1.2	+1.1	-17.2	+0.0	-0.9	+0.9	-0.2	+0.1	-0.7	+0.7	-5.9	+5.3
2.6	Fully Integrated (FDW Pump Trip)	77 to 56	-16.6	-20.4	-3.9	+3.5	-0.5	+4.1	-3.3	+12.8	-0.2	+0.1	-0.3	+0.2	-0.2	+0.1	-2.7	+3.5
2.7	Fully Integrated	50 to 76	+8.6	+10.8	-2.5	+0.0	-0.3	+0.7	-8.1	+0.0	-0.4	+0.5	-0.1	+0.2	-0.3	+0.3	-7.0	+4.9

ICS Transient Data Obtained During The Performance Of Unit Load Transient Test At 100% Full Power

Transient Number	ICS Mode of Operation	Power (%FP)	Unit Transient Response								Unit Steady State Return							
			Rate, %/min		ΔT(AVE), F		ΔT(C), F		ΔTHP, PSI		ΔP, % FP		ΔT(Avc), F		ΔT(C), F		ΔTHP, PSI	
			Ave	Max	Min	Max	Min	Max	Min	Max	Min	Max	Min	Max	Min	Max	Min	Max
3.1	Fully Integrated	97 to 85	-2.5	-5.3	-0.1	+0.7	-0.2	+0.4	-3.5	+16.4	-0.4	+0.3	-0.4	+0.2	-0.1	+0.3	-2.3	+4.2
		85 to 97	+2.4	+4.6	+0.0	+0.6	-0.4	+0.3	-18.1	+0.0	-0.5	+0.2	-0.1	+0.2	-0.4	+0.2	-2.3	+2.3
3.2	Turbine Following	98 to 85	-2.5	-3.4	-0.6	+0.5	-0.1	+0.4	-10.8	+0.0	-0.4	+0.2	-0.1	+0.1	-0.1	+0.3	-1.0	+0.8
		85 to 97	+2.0	+3.7	-0.7	+0.5	-0.2	+0.5	-5.5	+0.5	-0.4	+0.2	-0.1	+0.1	-0.2	+0.1	-2.0	+3.3
3.3	Reactor/OTSG Following	97 to 85	-2.4	-6.7	-0.1	+0.6	-0.2	+0.4	0.0	+36.6	-0.1	+0.1	-0.3	+0.2	-0.1	+0.1	-3.7	+2.9
		85 to 96	+2.8	+4.6	-0.7	+0.0	-0.4	+0.0	-12.5	+4.8	-0.4	+0.3	-0.2	+0.1	-0.2	+0.0	-1.8	+0.8
3.4 (1)	Turbine/OTSG Following (Rods In Hand)	96 to 87	-1.7	-2.9	-3.2	+0.0	-0.3	+1.3	-7.2	+0.0	-0.5	+0.4	-0.5	+0.6	-0.2	+0.4	-4.7	+2.0
		87 to 95	+2.0	+2.9	-0.3	+2.0	-0.4	+0.1	+0.0	+11.5	-0.2	+0.3	-0.1	+0.3	-0.2	+0.3	-3.7	+2.0
3.4 (2)	Turbine/OTSG Following (Reactor Demand In Hand)	95 to 87	-1.7	-2.5	-3.5	+0.0	+0.0	+0.9	-7.6	+0.0	-0.4	+0.1	-0.5	+0.3	-0.1	+0.0	-5.7	+3.8
		87 to 96	+1.8	+2.6	+0.8	+3.3	-0.1	+0.3	+4.0	+9.5	-0.1	+0.2	-0.2	+0.2	-0.2	+0.2	-2.3	+1.6
3.4 (3)	Turbine/OTSG Following (Rods & Reactor In Hand)	96 to 88	-1.4	-2.1	-3.4	+0.0	-0.2	+1.2	-8.8	+0.0	-0.2	+0.3	-0.5	+0.5	-0.4	+0.3	-2.2	+1.5
		88 to 95	+1.5	+2.9	+0.0	+3.4	+0.0	+0.5	0.0	+15.8	-0.1	+0.2	-0.1	+0.2	-0.2	+0.1	-1.5	+2.1
3.5	Fully Integrated	86 to 44	-7.1	-14.9	-0.9	[illegible]	-1.6	+0.4	-3.1	+19.0	-0.2	+0.1	-0.1	+0.1	-0.2	+0.1	-1.8	+2.8
		44 to 86	+8.0	+10.8	-1.3	-0.2	-0.4	+0.8	-29.7	0.0	-0.7	+0.4	-0.2	+0.3	-0.4	+0.2	-2.2	+1.2
3.6	Turbine Following	87 to 41	-3.4	-10.0	-0.4	+2.3	-2.6	+0.5	-12.2	+7.2	-0.1	+0.1	+0.0	+0.0	+0.0	+0.1	-0.1	+0.1
		41 to 85	+3.7	+8.3	-1.9	+0.4	-0.3	+1.0	-7.2	+3.0	-0.4	+0.2	-0.1	+0.1	-0.4	+0.4	-4.4	+3.2
3.7	Reactor/OTSG Following	85 to 44	-2.2	-5.6	+0.0	+1.6	-0.7	+0.6	+0.0	+34.2	-0.5	+0.1	-0.2	+0.2	-0.1	+0.1	-3.4	+7.3
		42 to 82	+3.2	+6.6	-1.6	+0.5	-0.3	+1.7	-35.1	+5.9	-1.1	+1.7	-0.8	+0.6	-0.1	+0.1	-5.6	+5.7

Table 4.ii-4

Integrated Control System Organization

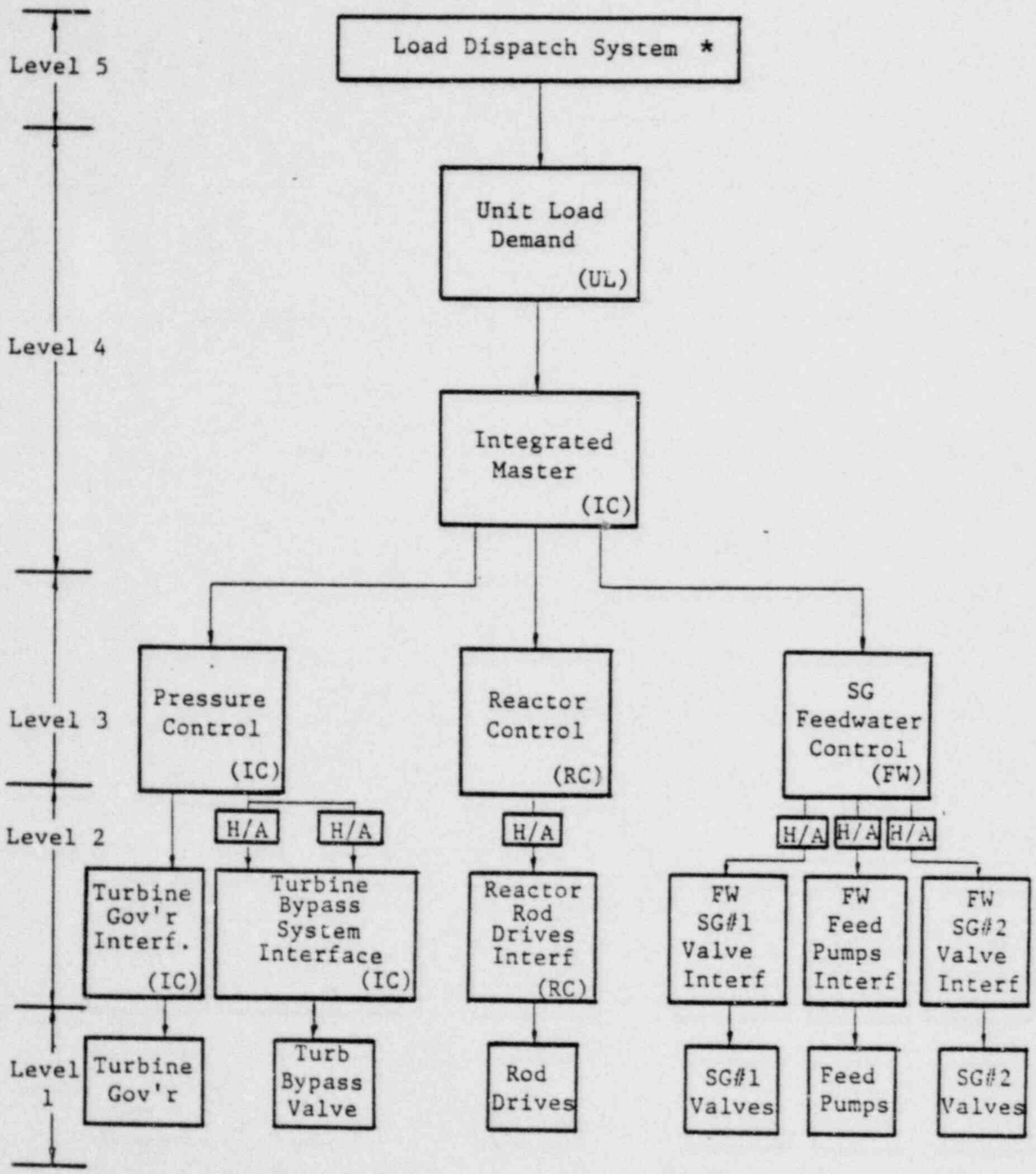

NOTE (*): Not used at Crystal River Unit 3

Figure 4.11-1

Integrated Control System

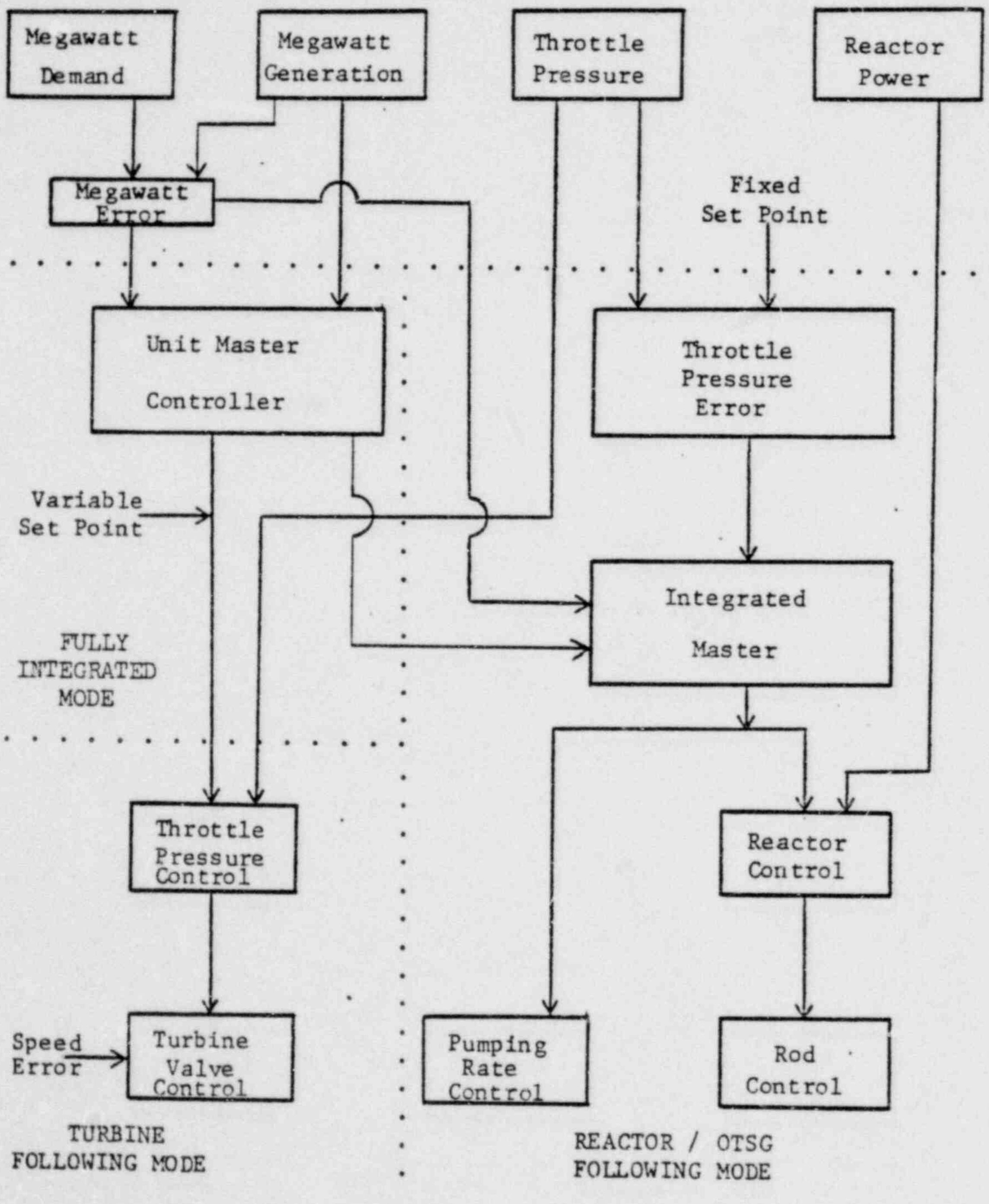

Figure 4.11-2

UNIT LOAD TRANSIENT TEST AT 40 PERCENT FULL POWER

Maximum Power Increase Rate: +4.8 %/Minute
Maximum Power Decrease Rate: -4.7 %/Minute

Transient Number: 1.1
ICS Mode: Fully Integrated

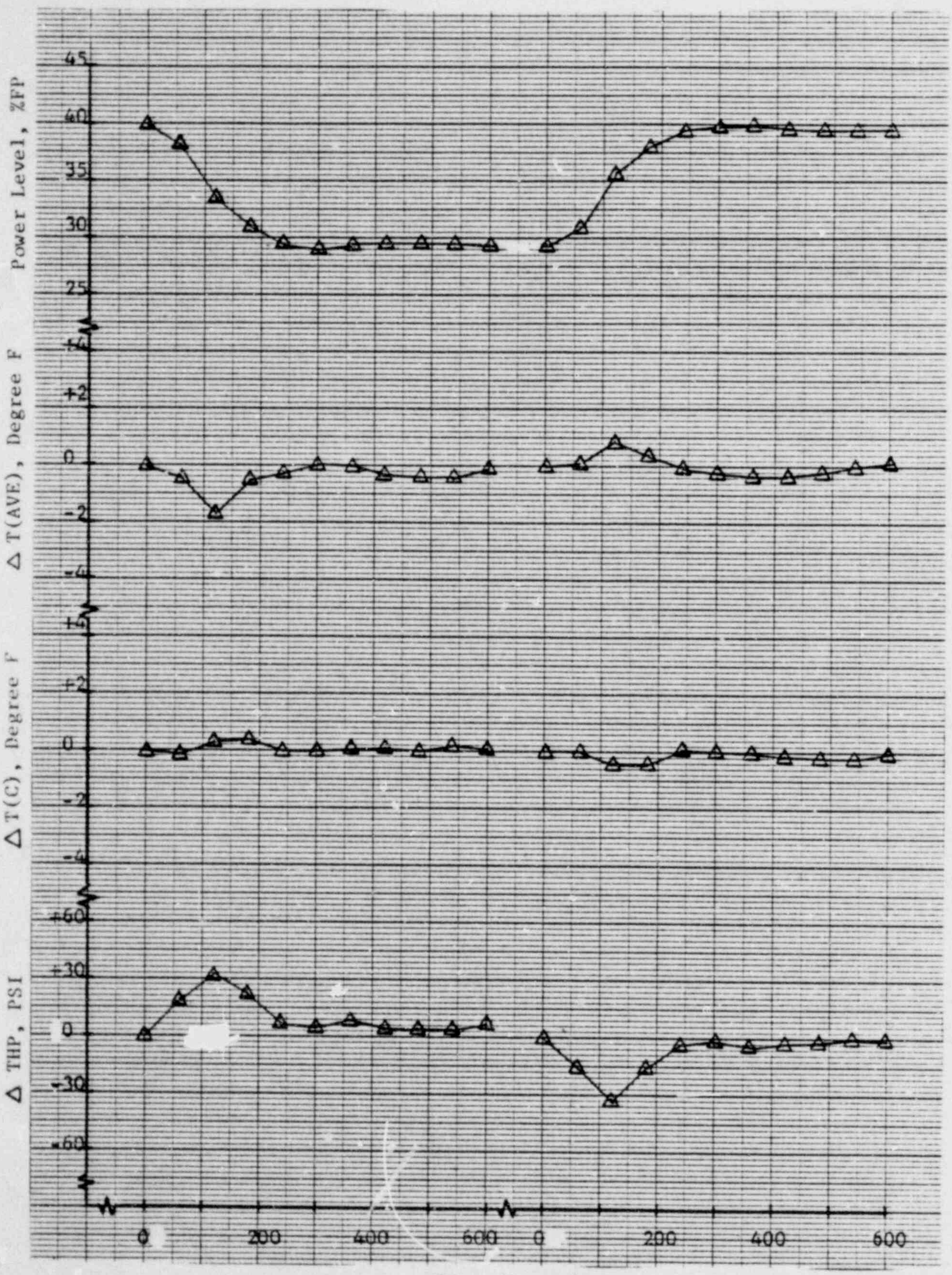

Figure 4.11-3

UNIT LOAD TRANSIENT TEST AT 40 PERCENT FULL POWER

Maximum Power Increase Rate: +3.0 %/Minute
Maximum Power Decrease Rate: -3.1 %/Minute

Transient Number: 1.2
ICS Mode: Turbine Following

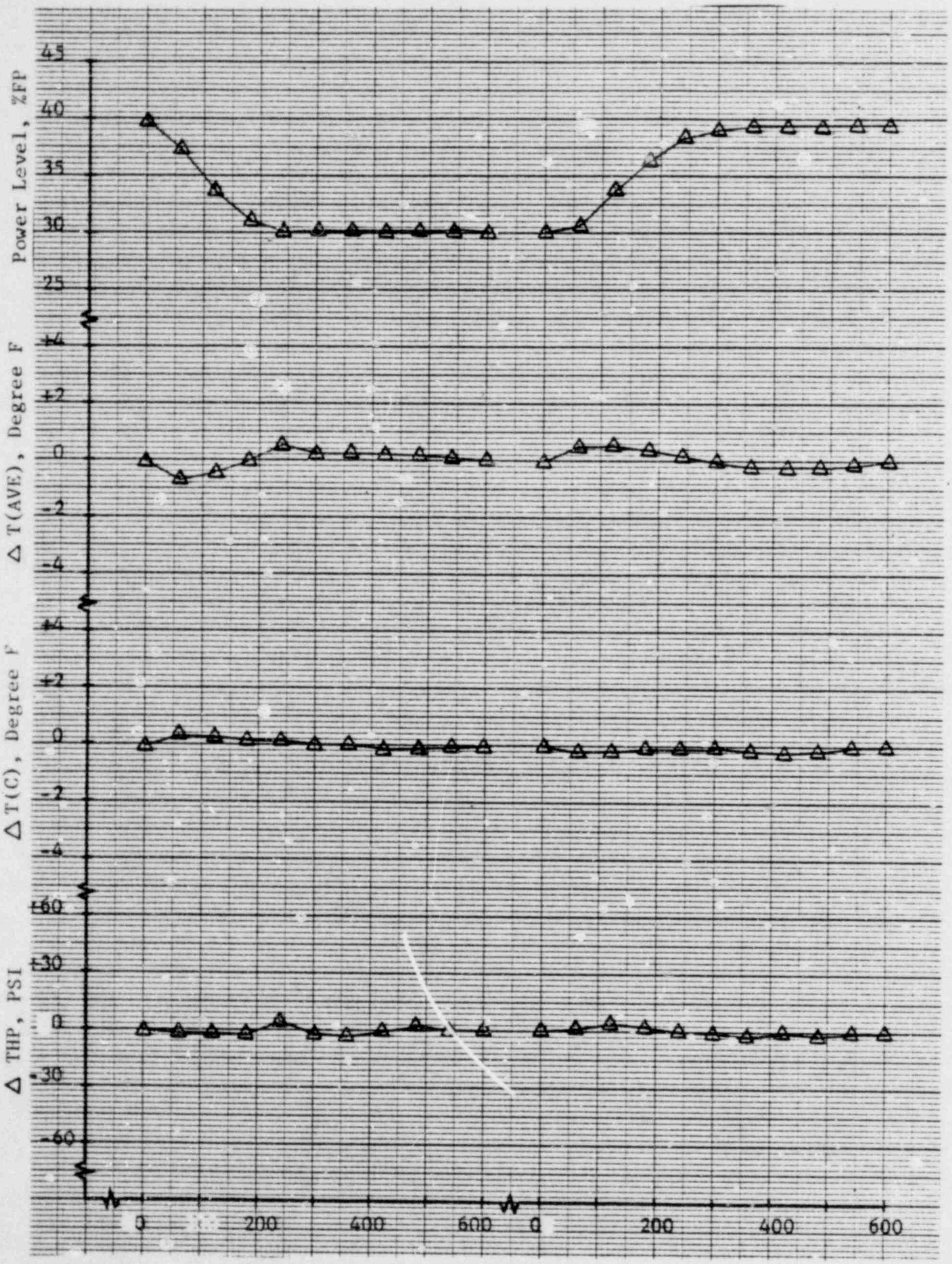

Figure 4.11-4

UNIT LOAD TRANSIENT TEST AT 40 PERCENT FULL POWER

Maximum Power Increase Rate: +3.5%/Minute
Maximum Power Decrease Rate: -3.5%/Minute

Transient Number: 1.3
ICS Mode: Reactor/OTSG Following

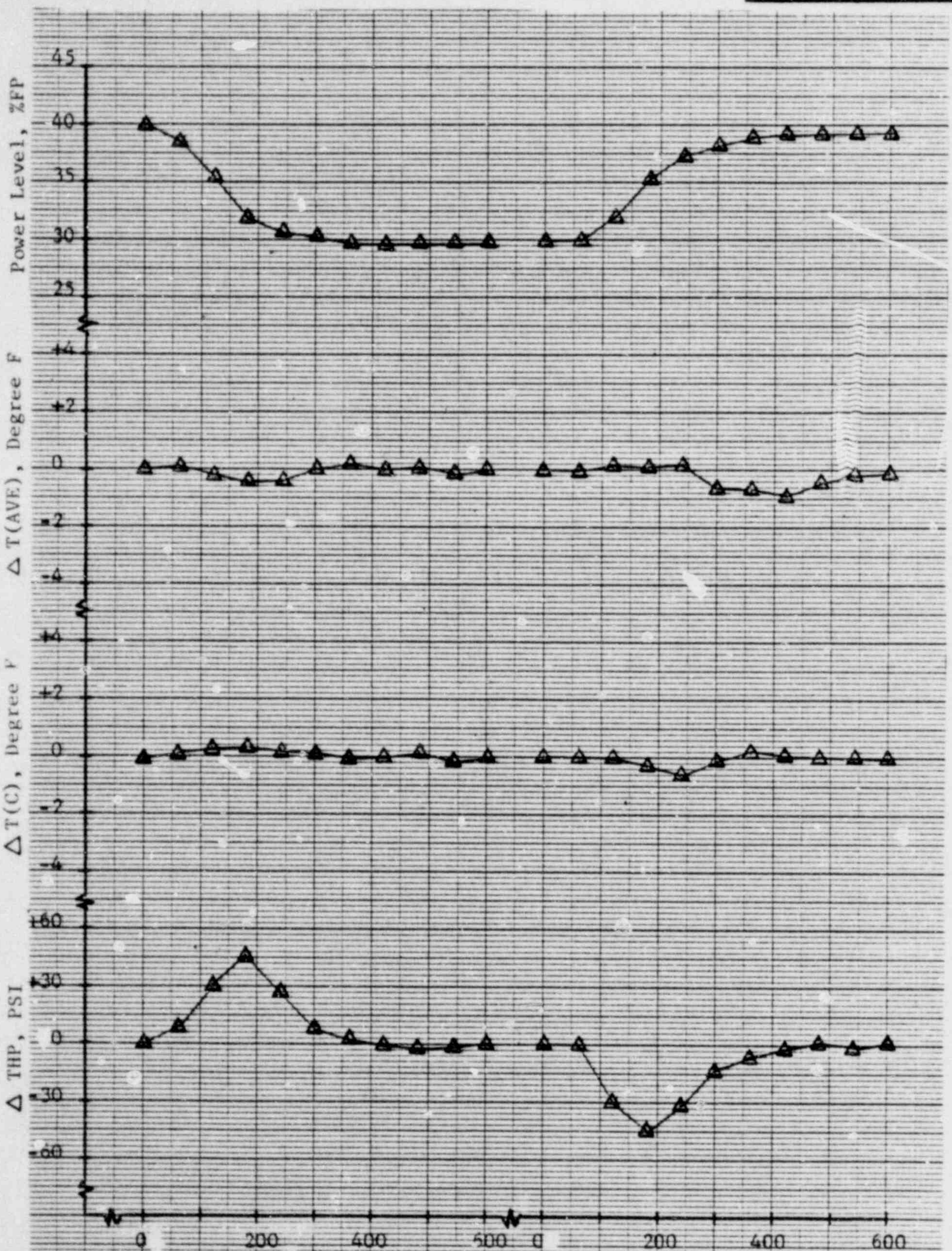

Time, Seconds

Figure 4.11-5

UNIT LOAD TRA'SIENT TEST AT 40 PERCENT FULL POWER

Maximum Power Increase Rate: +2.5 %/Minute
Maximum Power Decrease Rate: -2.5 %/Minute

Transient Number: 1.4
ICS Mode: Turbine/OTSG Following

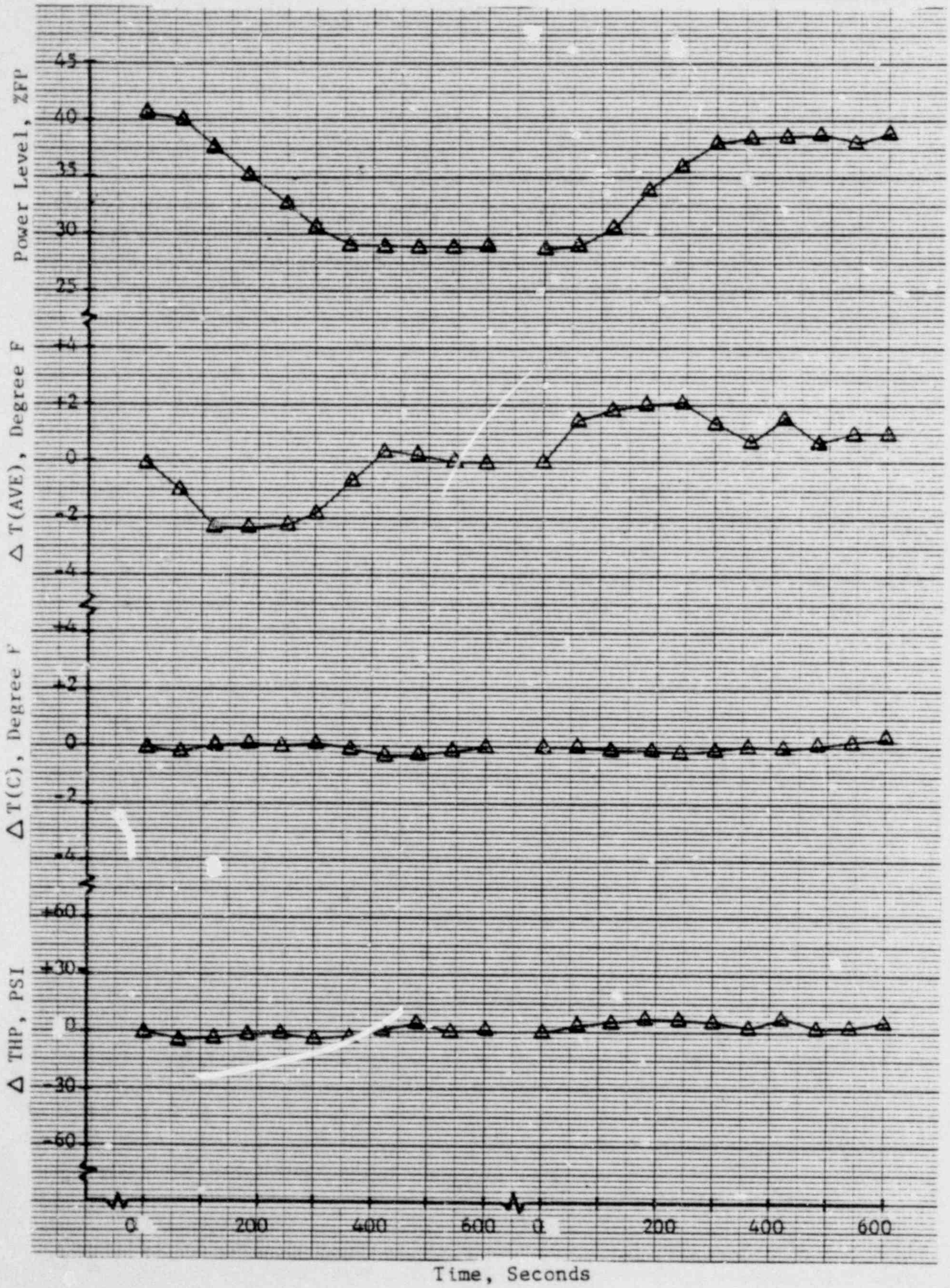

Figure 4.11-6

UNIT LOAD TRANSIENT TEST AT 40 PERCENT FULL POWER

Maximum Power Increase Rate: +6.2 %/Minute
Maximum Power Decrease Rate: -7.1 %/Minute

Transient Number: 1.5
ICS Mode: Fully Integrated

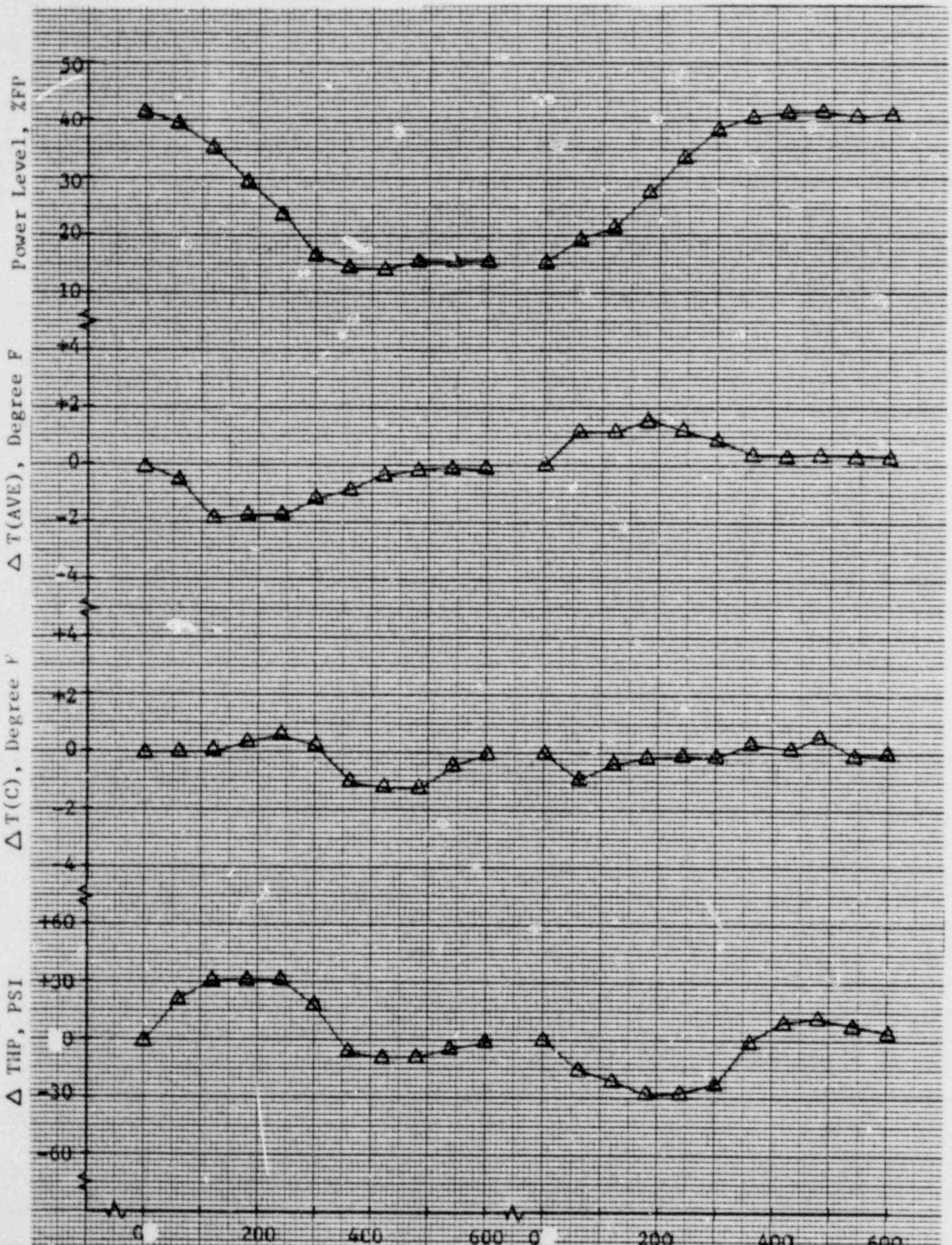

Figure 4.11-7

UNIT LOAD TRANSIENT TEST AT 40 PERCENT FULL POWER

Maximum Power Increase Rate: NA %/Minute
Maximum Power Decrease Rate: -5.5 %/Minute

Transient Number: 1.6
ICS Mode: Fully Integrated

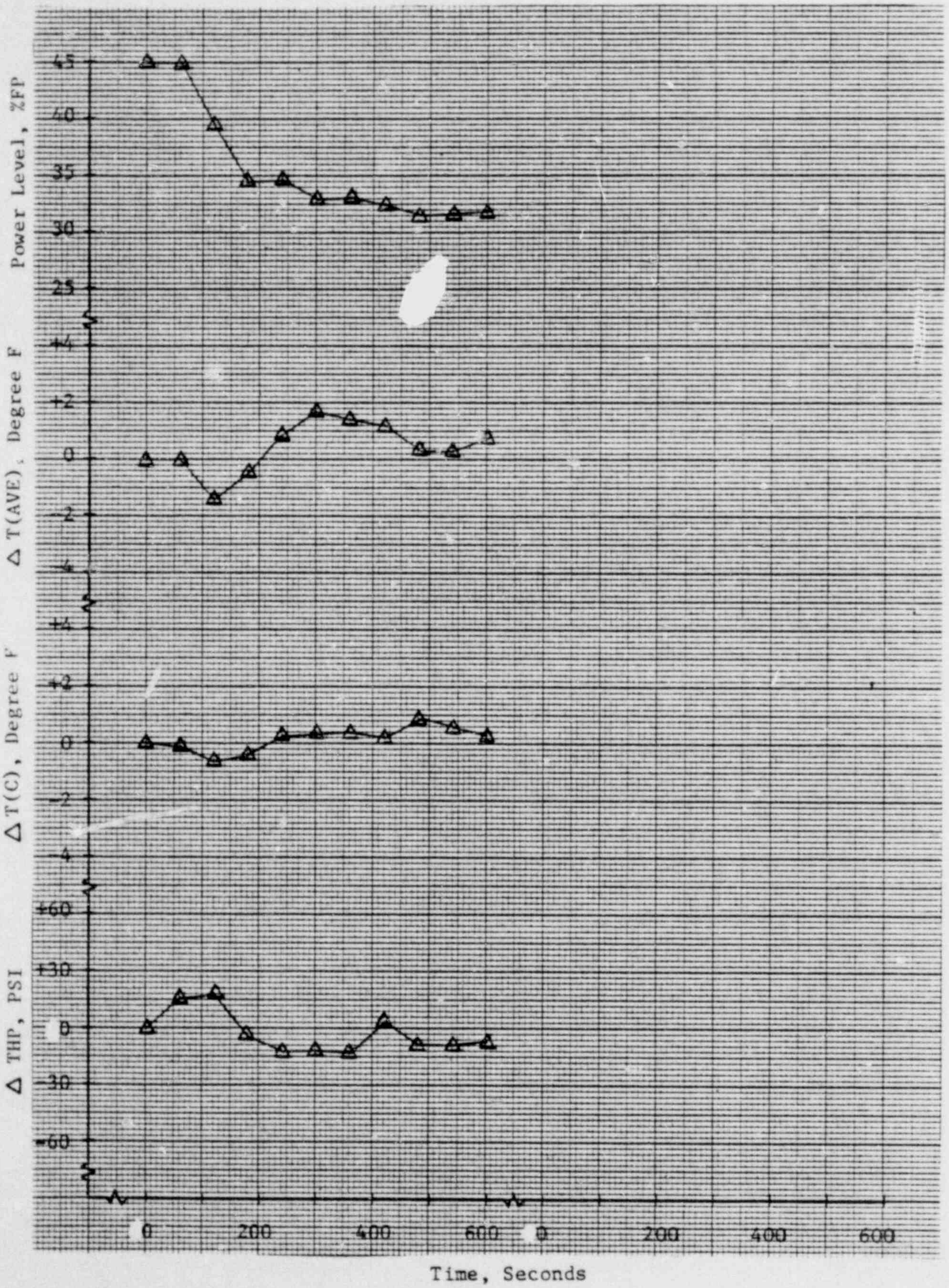

Figure 4.11-8

UNIT LOAD TRANSIENT TEST AT 75 PERCENT FULL POWER

Maximum Power Increase Rate: +4.9 %/Minute   Transient Number: 2.1
Maximum Power Decrease Rate: -4.9 %/Minute   ICS Mode: Fully Integrated

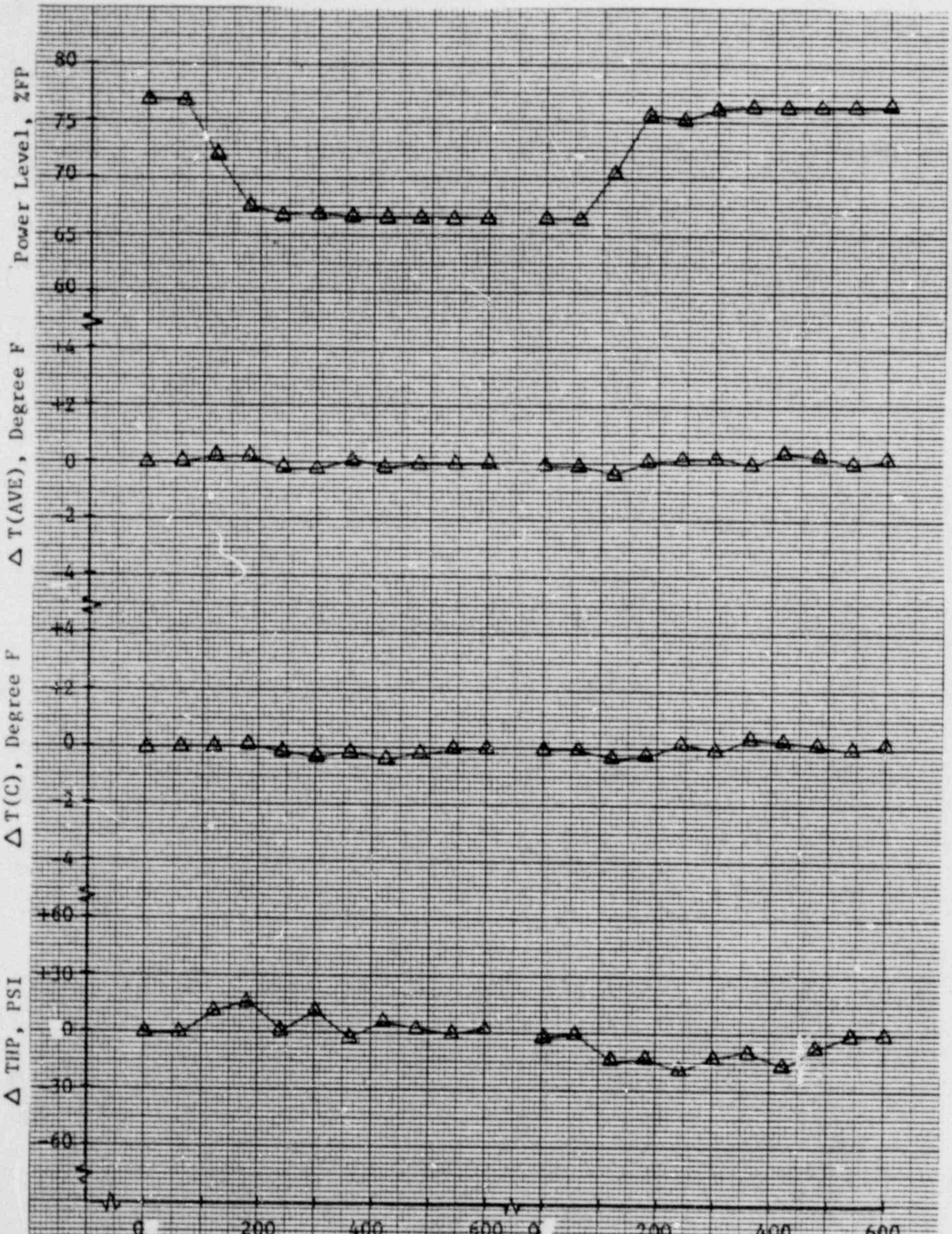

Time, Seconds

Figure 4.11-9

UNIT LOAD TRANSIENT TEST AT 75 PERCENT FULL POWER

Maximum Power Increase Rate: +4.5 %/Minute
Maximum Power Decrease Rate: -3.5 %/Minute

Transient Number: 2.2
ICS Mode: Turbine Following

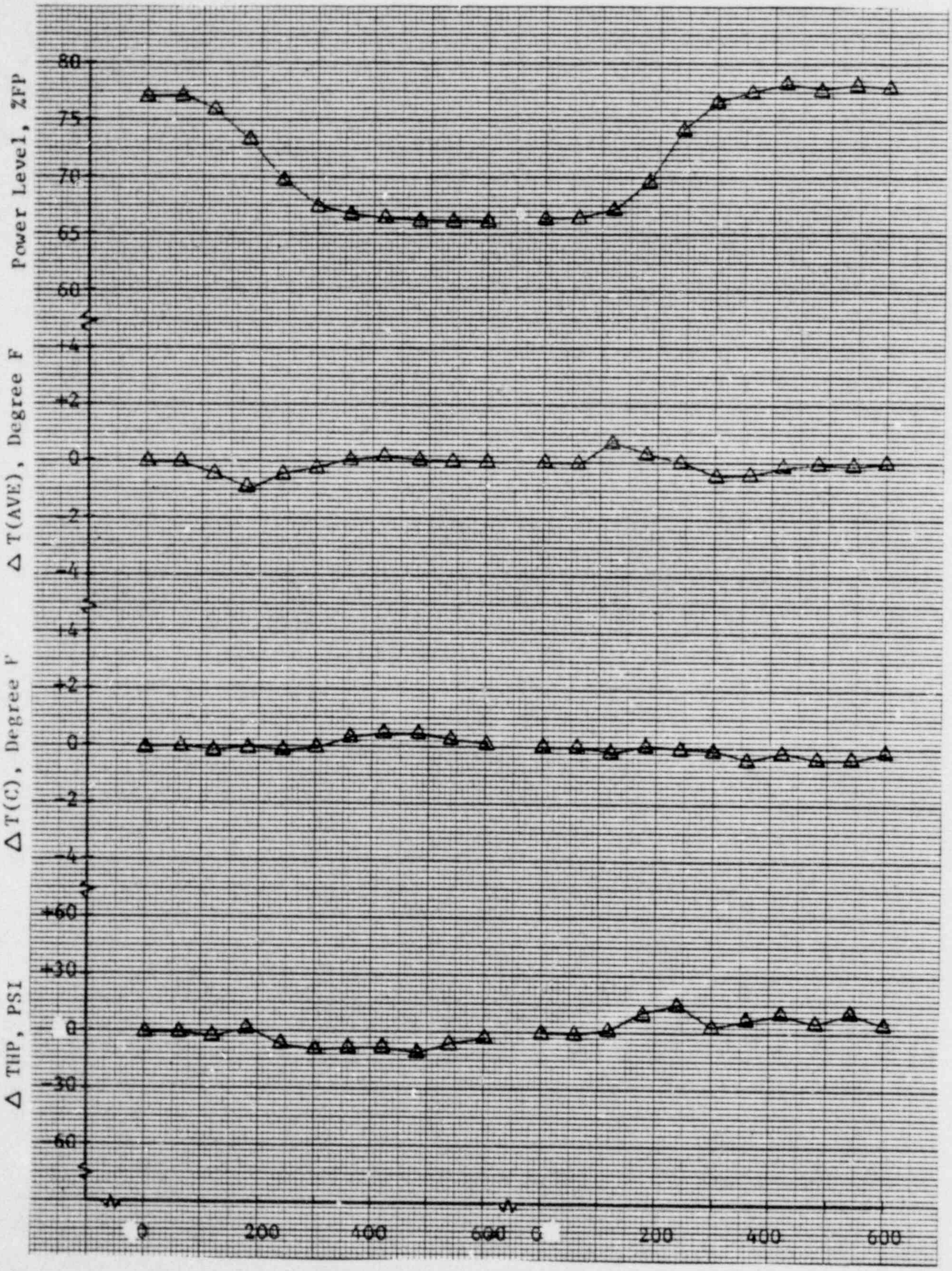

Figure 4.11-10

UNIT LOAD TRANSIENT TEST AT 75 PERCENT FULL POWER

Maximum Power Increase Rate: +5.8 %/Minute
Maximum Power Decrease Rate: -4.8 %/Minute

Transient Number: 2.3
ICS Mode: Reactor/OTSG Following

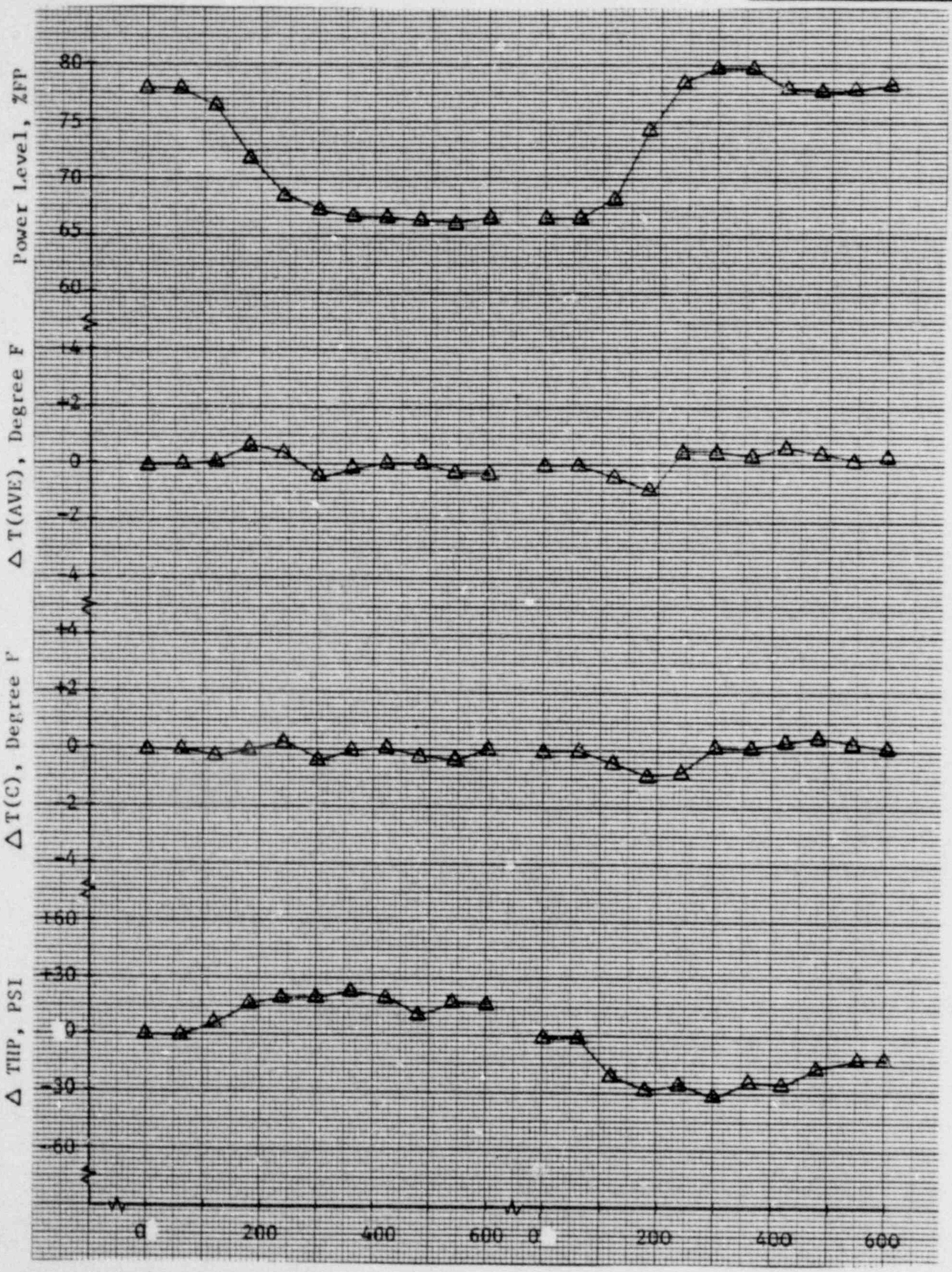

Time, Seconds

Figure 4.11-11

UNIT LOAD TRANSIENT TEST AT 75 PERCENT FULL POWER

Maximum Power Increase Rate: +3.5 %/Minute
Maximum Power Decrease Rate: -2.7 %/Minute

Transient Number: 2.4
ICS Mode: Turbine/OTSG Following

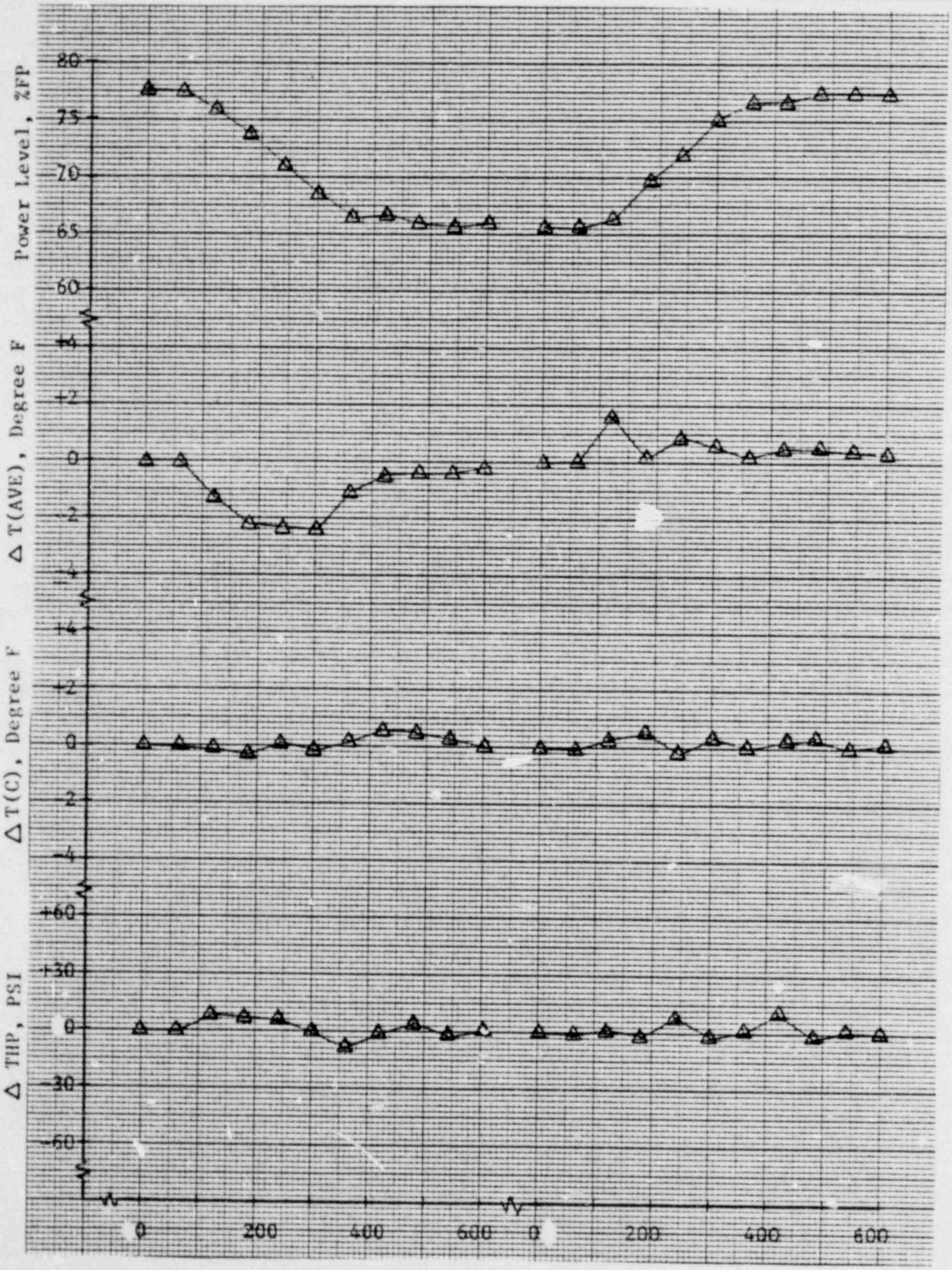

Figure 4.11-12

UNIT LOAD TRANSIENT TEST AT 75 PERCENT FULL POWER

Maximum Power Increase Rate:+11.7 %/Minute
Maximum Power Decrease Rate:- 7.7 %/Minute

Transient Number: 2.5
ICS Mode: Fully Integrated

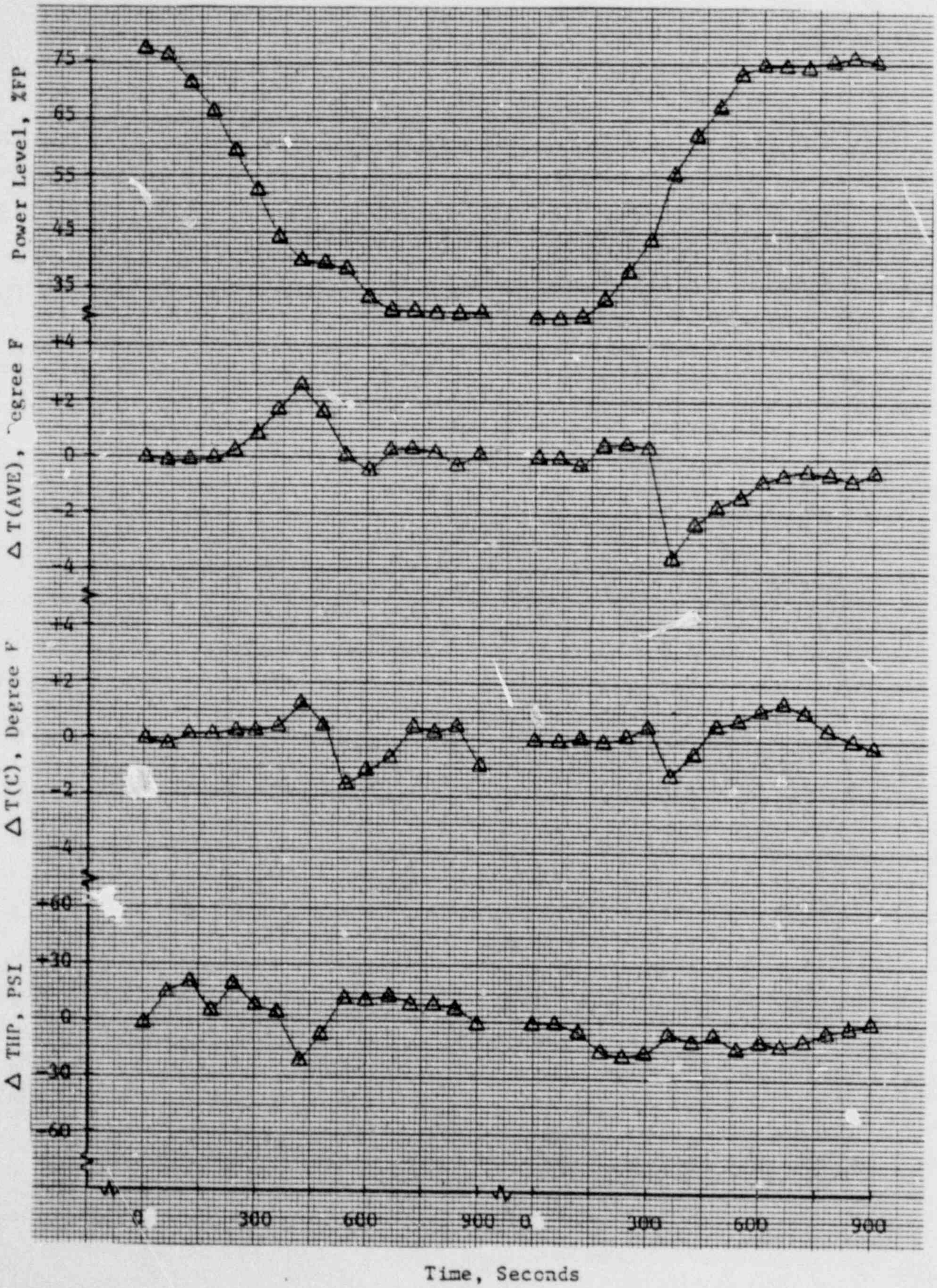

Figure 4.11-13

UNIT LOAD TRANSIENT TEST AT 75 PERCENT FULL POWER

Maximum Power Increase Rate: NA %/Minute
Maximum Power Decrease Rate: -20.4 %/Minute

Transient Number: 2.6
ICS Mode: Fully Integrated

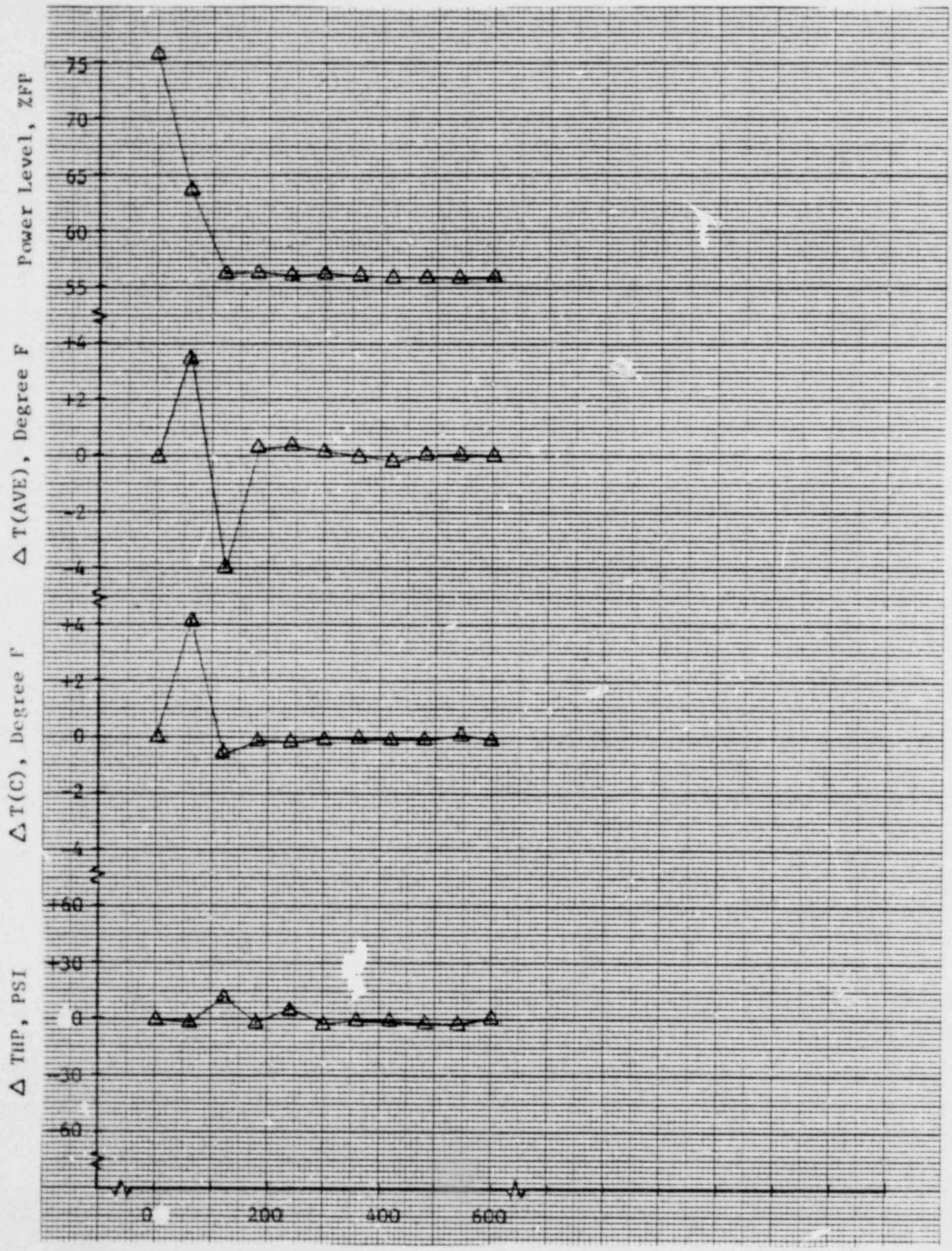

Time, Seconds

Figure 4.11-14

UNIT LOAD TRANSIENT TEST AT 100 PERCENT FULL POWER

Maximum Power Increase Rate: +4.6 %/Minute
Maximum Power Decrease Rate: -5.3 %/Minute

Transient Number: 3.1
ICS Mode: Fully Integrated

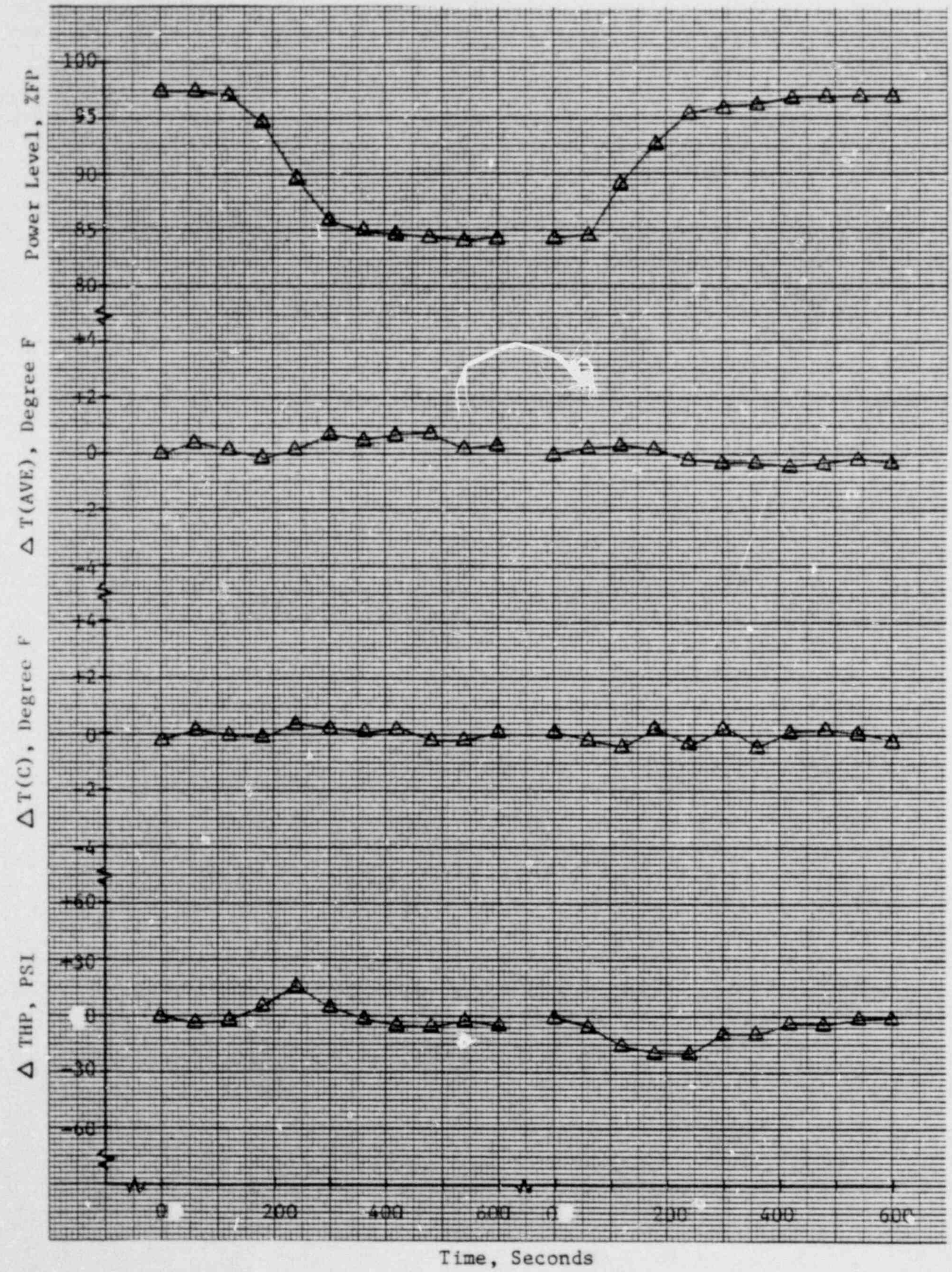

Figure 4.11-15

UNIT LOAD TRANSIENT TEST AT 100 PERCENT FULL POWER

Maximum Power Increase Rate: +3.7 %/Minute
Maximum Power Decrease Rate: -3.4 %/Minute

Transient Number: 3.2
ICS Mode: Turbine Following

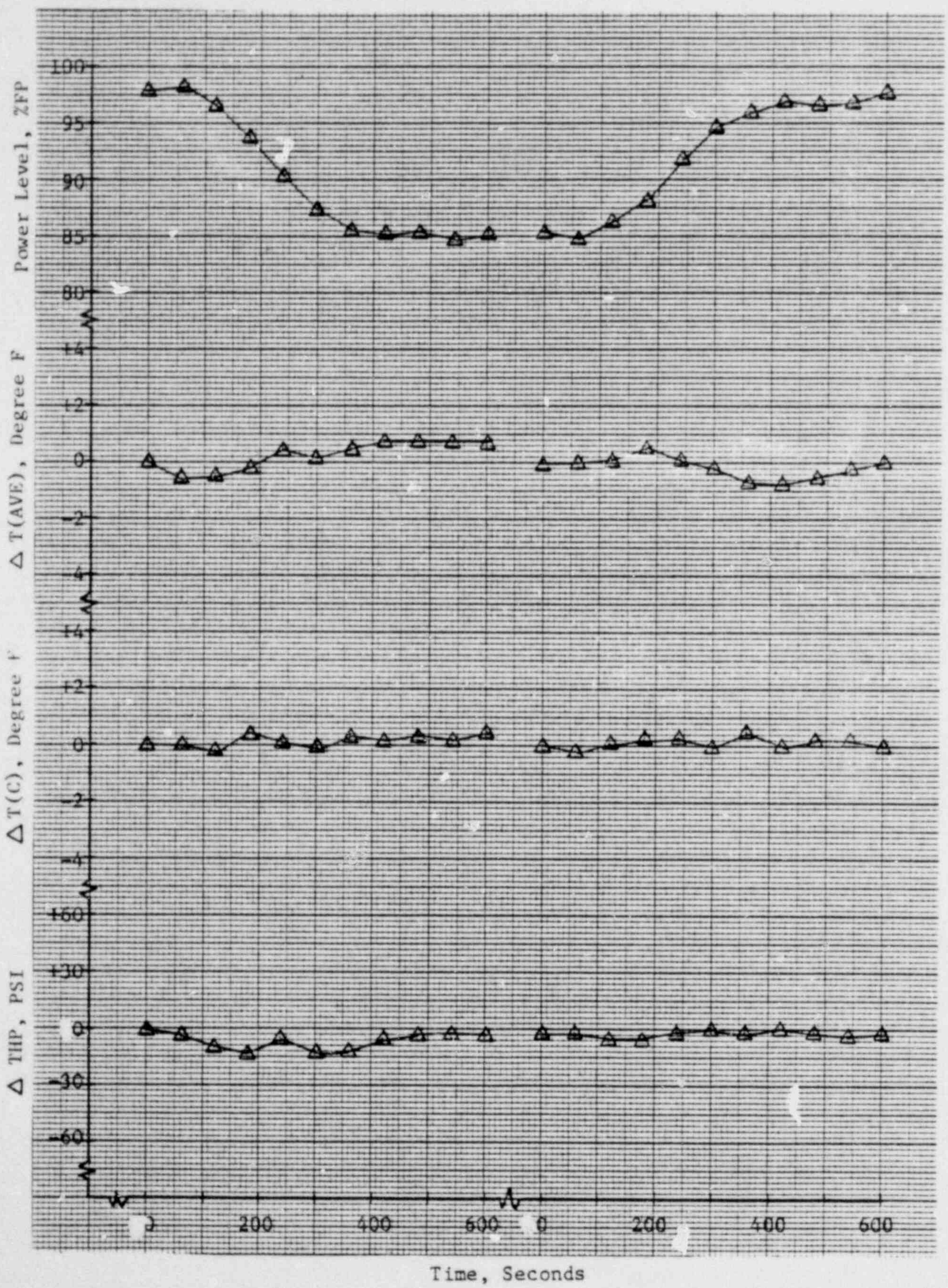

Figure 4.11-16

UNIT LOAD TRANSIENT TEST AT 100 PERCENT FULL POWER

Maximum Power Increase Rate: +4.6 %/Minute
Maximum Power Decrease Rate: -6.7 %/Minute

Transient Number: 3.3
ICS Mode: Reactor/OTSG Following

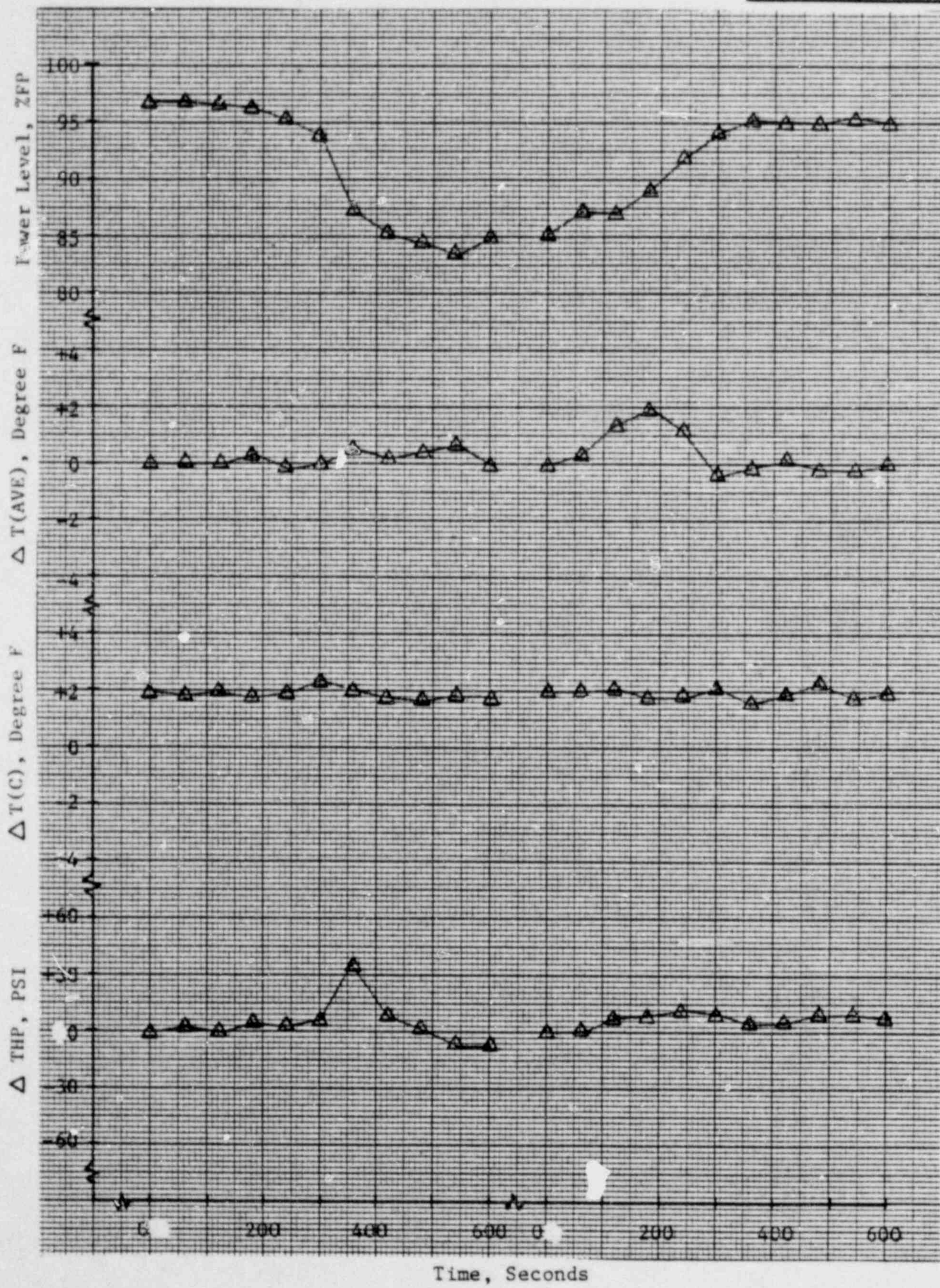

Figure 4.11-17

UNIT LOAD TRANSIENT TEST AT 100 PERCENT FULL POWER

Maximum Power Increase Rate: +2.9 %/Minute
Maximum Power Decrease Rate: -2.9 %/Minute

Transient Number: 3.4
ICS Mode: Turbine/OTSG Following

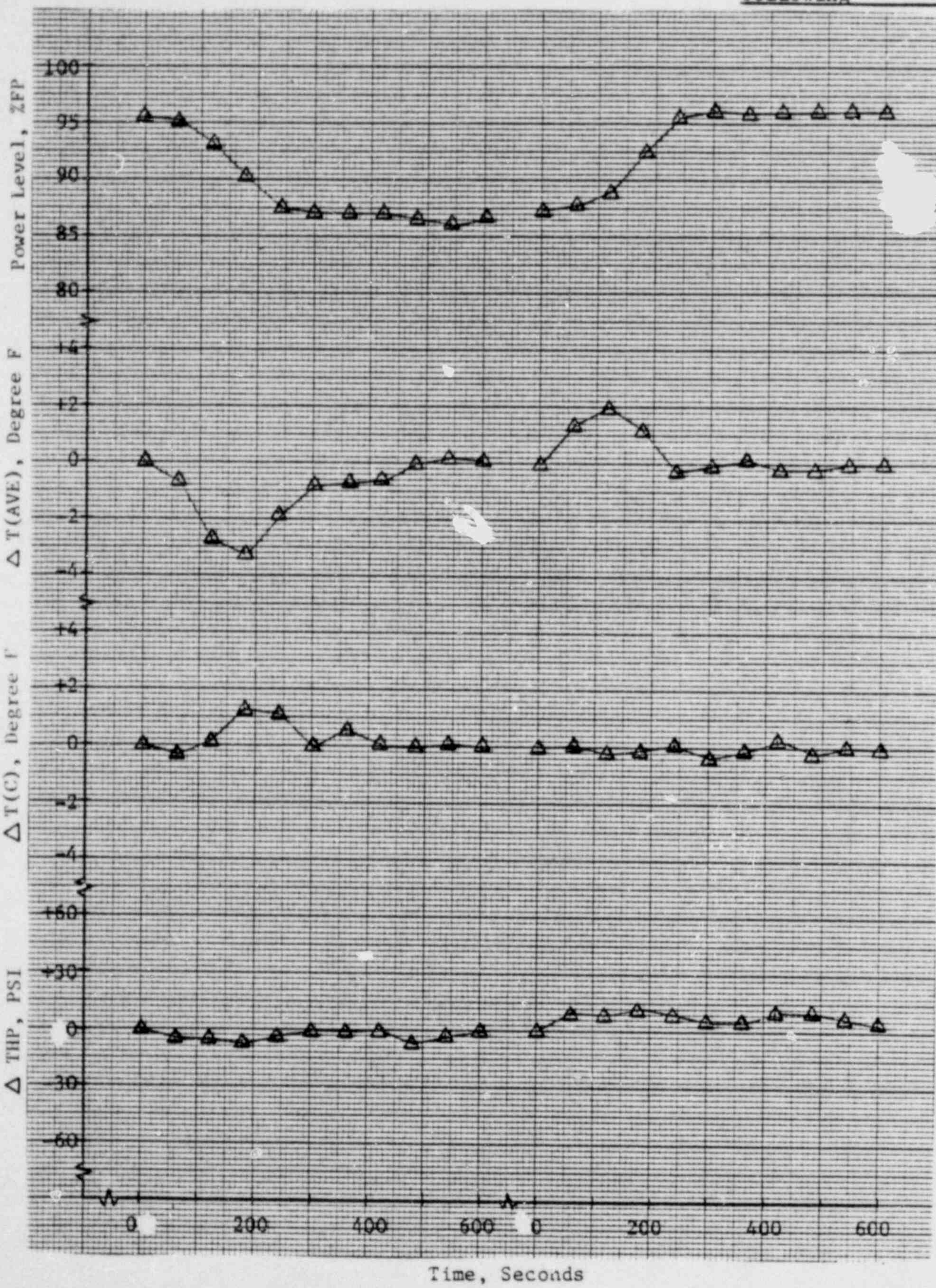

Figure 4.11-18

UNIT LOAD TRANSIENT TEST AT 100 PERCENT FULL POWER

Maximum Power Increase Rate: +10.8%/Minute
Maximum Power Decrease Rate: -14.9%/Minute

Transient Number: 3.5
ICS Mode: Fully Integrated

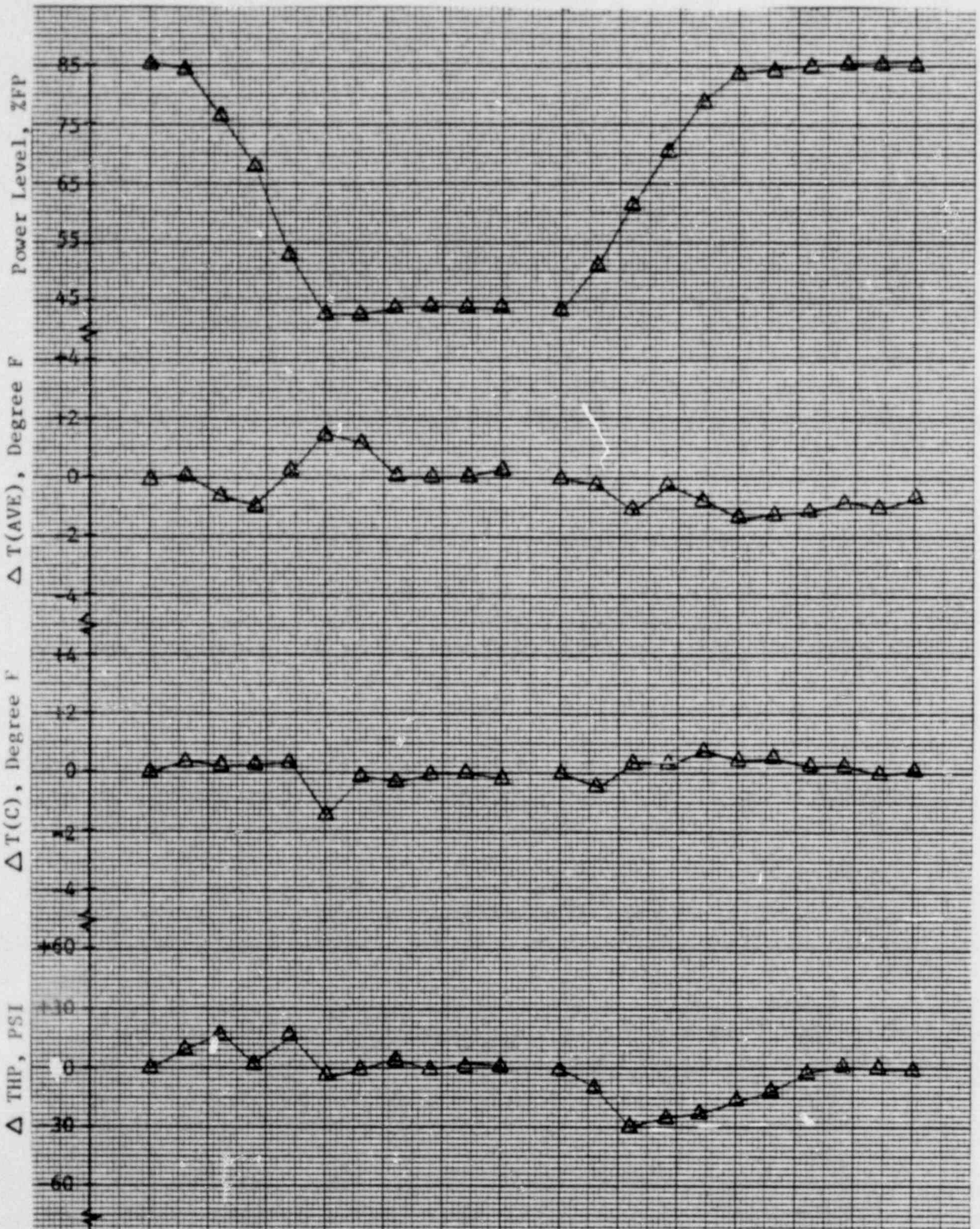

Figure 4.11-19

UNIT LOAD TRANSIENT TEST AT 100 PERCENT FULL POWER

Maximum Power Increase Rate: +8.3 %/Minute

Maximum Power Decrease Rate: -10.0 %/Minute

Transient Number: 3.6

ICS Mode: Turbine Following

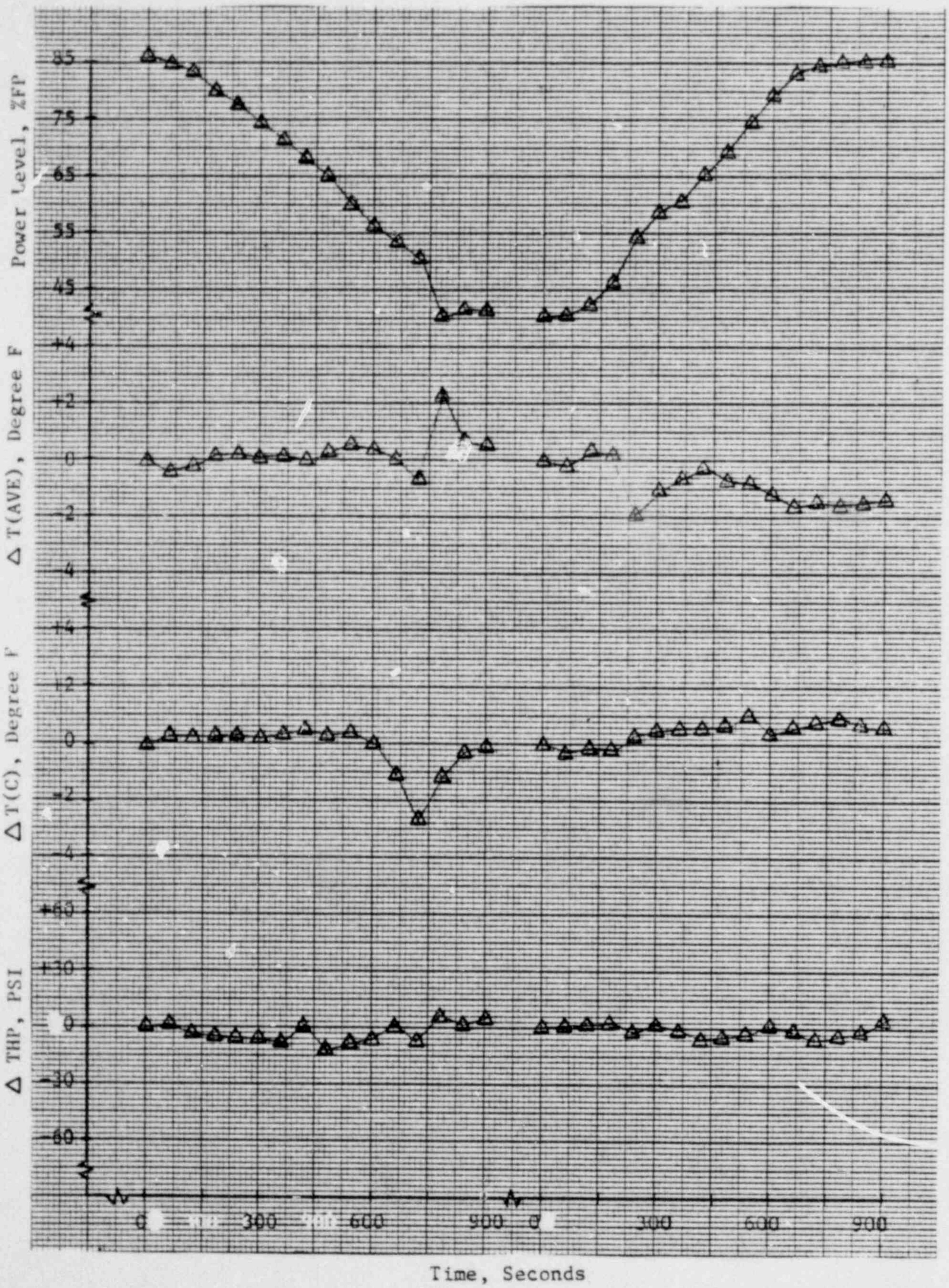

Figure 4.11-20

UNIT LOAD TRANSIENT TEST AT 100 PERCENT FULL POWER

Maximum Power Increase Rate: +6.6 %/Minute
Maximum Power Decrease Rate: -5.6 %/Minute

Transient Number: 3.7
ICS Mode: Reactor/OTSG Following

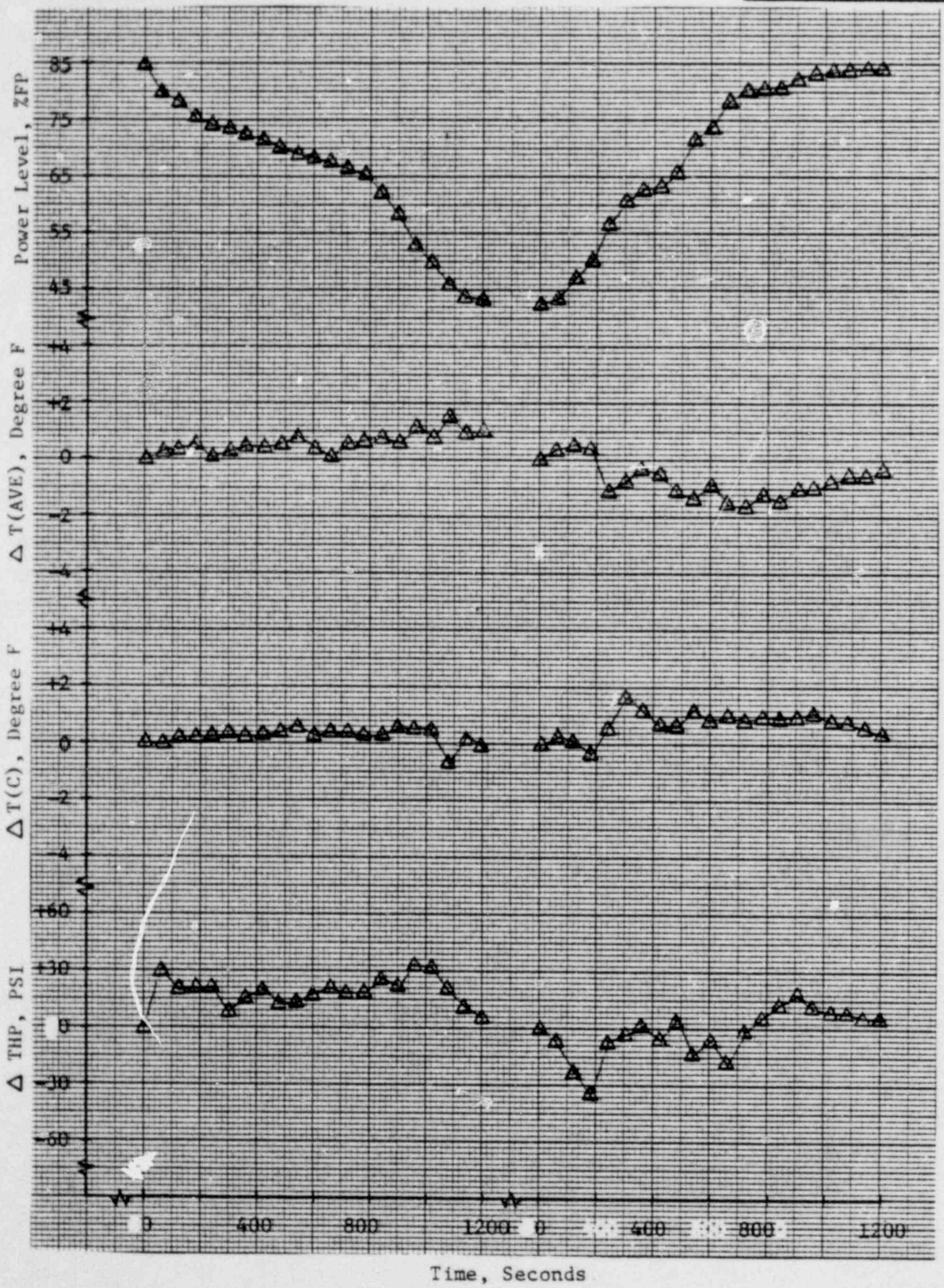

Figure 4.11-21

4.12 SHUTDOWN FROM OUTSIDE CONTROL ROOM TEST

The shutdown from outside the control room test simulates an emergency situation requiring evacuation of the control room. All plant controls are left in automatic unless remote indication requires taking them into manual modes of operation.

4.12.1 PURPOSE

The purpose of this test is to demonstrate that the unit can safely be brought to hot standby conditions from outside the control room.

4.12.2 TEST METHOD

The test was started from 15% power. Letdown flow was stopped and the control room evacuated by the normal shift complement of operators. The operators manned their stations as shown in Table 4.12-1. A complete second set of operators was left in the control room to assume plant control if the test failed. The reactor was tripped remotely and the plant allowed to come to hot standby automatically. The operators outside the control room were to take control of various equipment if it was not performing adequately in automatic.

4.12.3 EVALUATION OF TEST RESULTS

On April 16, 1977, the first run at shutdown from outside the control room was attempted and aborted after approximately 18 minutes due to feedpump ΔP oscillations. Main feedwater pump speed control had been shifted to hand by the operators in the control room early in the test. After the reactor trip high leakage through the startup valves resulted in overfeeding both steam generators. The test was terminated due to loss of steam generator level control and greater than desired cooldown of the primary plant. As a result of this experience, the plant emergency procedure for shutdown from outside the control room was changed to require tripping the main feedpump remotely. This would allow the steam driven emergency feedwater pump to start and take over steam generator feed requirements.

On April 22, 1977, the test was repeated with the above modifications. This run was stopped after approximately 9 minutes due to low levels in both steam generators. Subsequent investigation revealed that initial conditions for steam pressure to the steam driven emergency feedwater pump were not met. This resulted in both steam generators being dry* until flow was established by the electrical driven emergency feedpump. The plant emergency procedure was modified to require the operator to check the steam driven pump and, if it is not operating properly, start the electrical driven pump.

On April 23, 1977, the test was run successfully. The control room was evacuated with the plant at 15% power. The running main feedpump was tripped remotely (which trips the main turbine). The reactor, however, was not tripped until at least one minute later, resulting in low steam generator levels. The operators

* The steam generators were designed for 20 allowable thermal cycles equivalent to being boiled dry.

started the electric driven feedwater pump, took manual control of both feedwater startup valves and restored level in both steam generators. Twenty minutes into the test, an operator remotely added water to the makeup tank, otherwise the plant remained in a fully automatic mode of operation and came to a hot standby condition. The test was allowed to run for thirty minutes to verify that the operators outside the control room had complete control of the plant. At this time, plant parameters were at or near their final steady state values (see Figure 4.12-1) and the test was ended.

Although level and feedflow indication do not show zero, post test analysis indicates that the steam generators were dry about seven minutes. (See Figure 4.12-1). This occurred because of a combination of problems with reference legs, flows, and/or calibration errors. This can be verified by noting that during the dry period, main steam pressure was below the saturation pressure and recovered as soon as feedflow was re-established.

4.12.4 CONCLUSIONS

The test proved that the reactor can be brought to and maintained in a safe hot standby condition from locations outside the control room by the normal shift complement of operators.

Table 4.12-1

Individual Personnel Responsibilities During The Performance Of Shutdown From Outside The Control Room Test

Assignment Number	Personnel Title	Individual Personnel Responsibilities
1	Nuclear Operator	1. Coordinate the shutdown of the unit at the remote shutdown panel by directing operators to perform specific functions at various stations around the unit. Start electrically driven emergency FW pump, if required.
2	Chief Nuclear Operator	1. Control RCS pressure through pressurizer spray valve RCV-14. 2. Trip main feed pump(s) and main turbine locally.
3	Assistant Nuclear Operator (Plant)	1. Check that the steam driven emergency feedwater pump is on line with adequate discharge pressure. 2. Cycle MUV-30 or MUV-73 as necessary to maintain makeup tank level.
4.	Assistant Nuclear Operator	1. Maintain steam generator level with FWV-39 and FWV-40. 2. Control RCS outlet temperature with MSV-25 and MSV-26.
5	Nuclear Auxiliary Operator	1. Verify that power to the 6900 V and 4160V unit buses has transferred to the S/U transformers. 2. Assist any member of the operating crew as requested.
6	Shift Supervisor	1. To ensure that the unit shutdown is proceeding properly as observed from the remote control shutdown area. 2. Trip the reactor by tripping the CRD breakers.

Unit Parameters VS Time Shutdown
From Outside Control Room Test

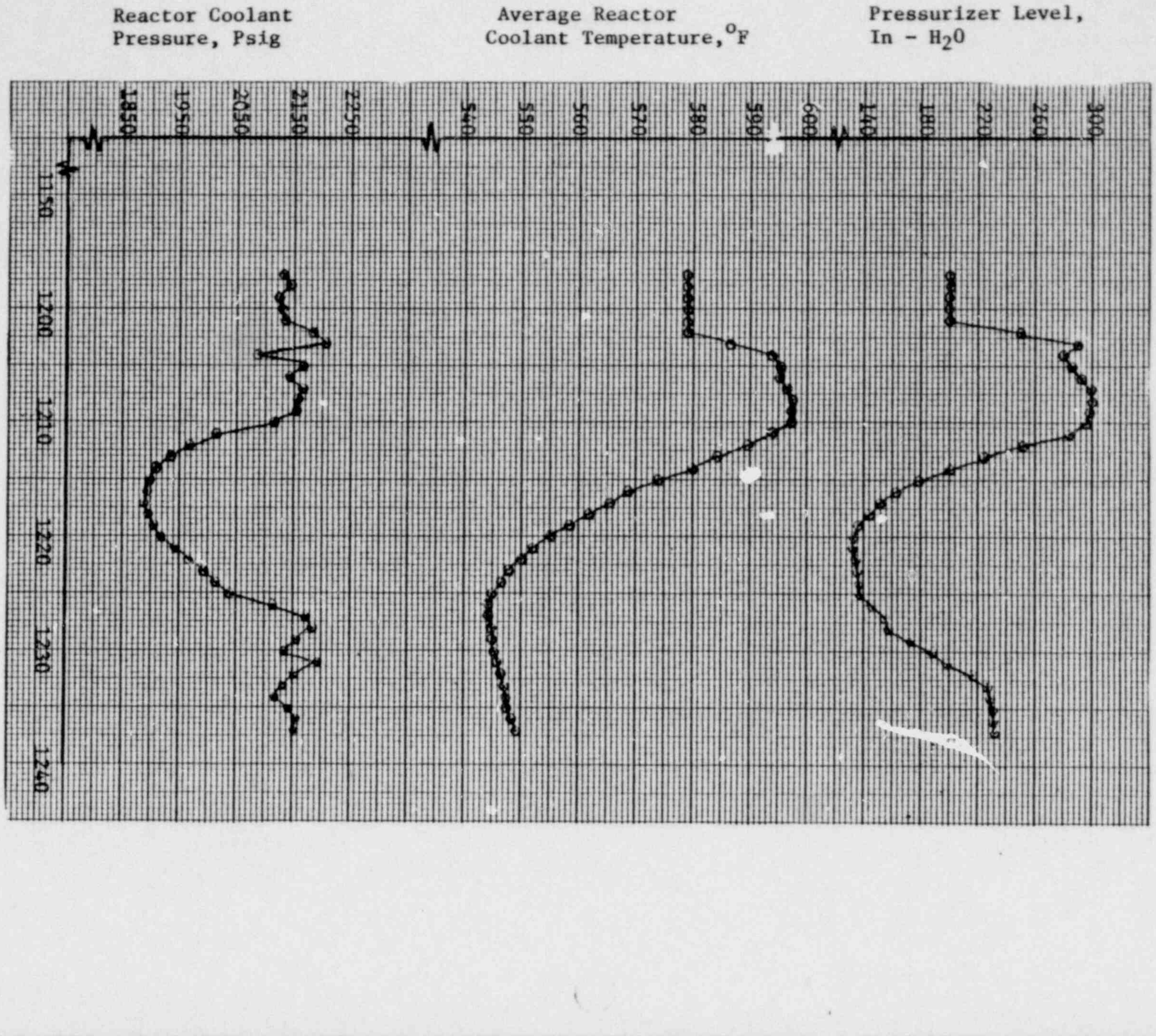

Figure 4.12.1

Unit Parameters VS Time Shutdown
From Outside Control Room Test

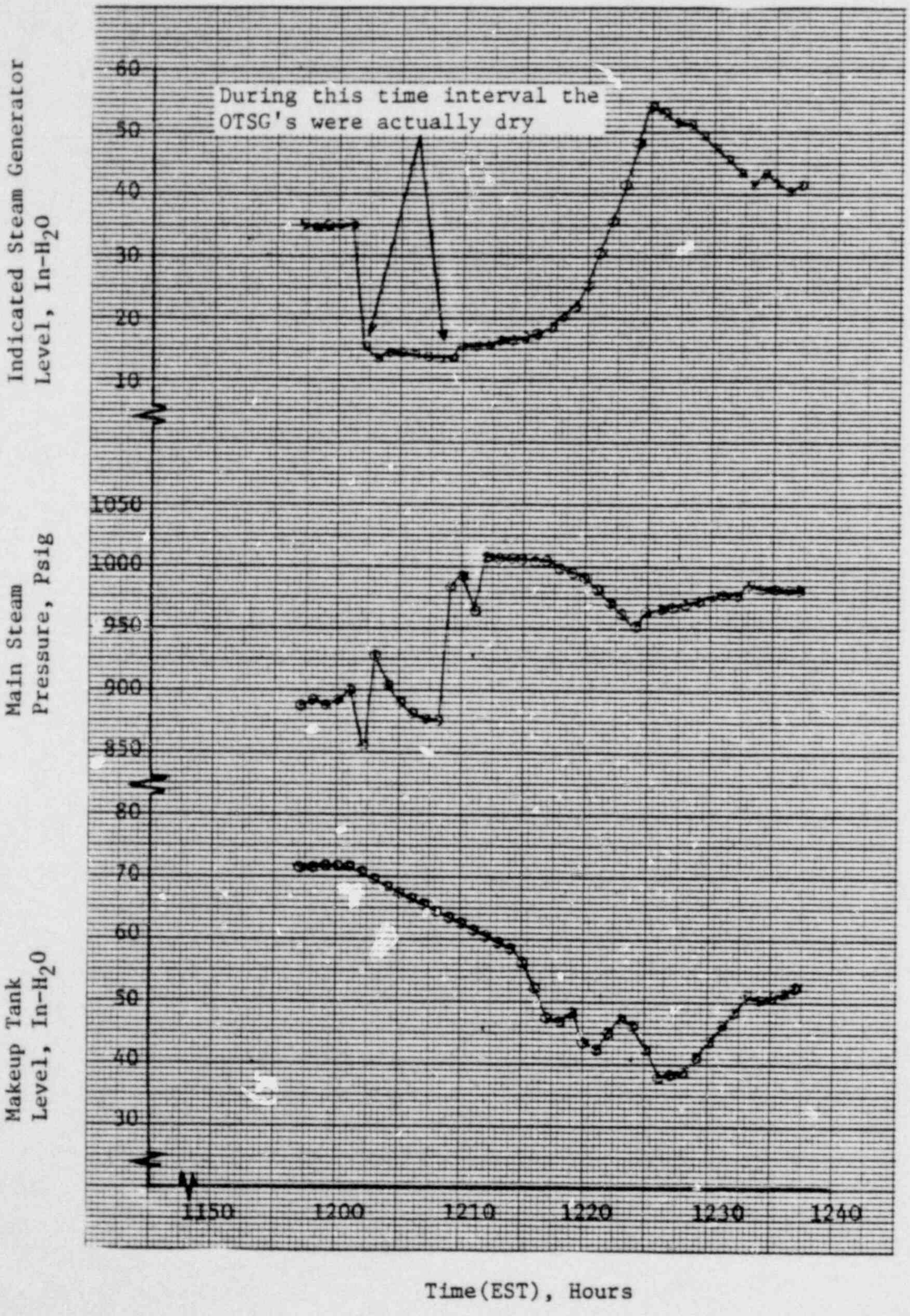

Figure 4.12.1 (Cont'd)

4.13 PSEUDO CONTROL ROD EJECTION TEST

During normal full power operation, a control rod assembly could only be ejected from the core if a physical failure of a pressure barrier component in the control rod drive assembly occurred. Such a failure would cause a pressure differential to act on a control rod assembly and rapidly eject the assembly from the core region. The resulting power excursion due to the rapid increase in reactivity is ultimately limited by the Doppler Effect and terminated by reactor protection system trip. The severity of the rod ejection accident is dependent upon the worth of the ejected control rod assembly, the reactor power level, and the core power distribution. For these reasons, the maximum allowable control rod assembly worth at power is set at $0.65\%\Delta k/k$. The only control rod group fully inserted during full power operation is group 7, which is used for load control. Other rod groups are maintained out of the core for rapid shutdown. Thus, the maximum worth of an ejected rod at power is limited to the most reactive rod of control rod group 7 which is rod 7-1 at core location H-08. This selection was based on calculations presented in the FSAR, Section 3.2.2. Figure 4.13-1 shows the location of this control rod and its location relative to each core quadrant.

4.13.1 PURPOSE

The purpose of this test was to verify the safety analysis relating to the accidental ejection of a control rod which is normally inserted in the core during full power operation. In the Pseudo Ejected Control Rod Test, this was accomplished by determining the worth of the most reactive control rod which is inserted in the core during full power operation.

The acceptance criterion specified for the Pseudo Control Rod Ejection Test is that the most reactive control rod worth does not exceed $0.65\%\Delta k/k$.

4.13.2 TEST METHOD

The pseudo control rod ejection worth measurement was performed by static techniques, in which the reactor is maintained in an approximate critical state through control rod 7-1 and group 6 exchange. During this exchange, differential rod worth measurements were done on group 6 for each 20% withdrawal of control rod 7-1 by the fast insertion/withdrawal method. The above data obtained was then used to determine the average differential worth of rod 7-1 as a function of rod position as shown in Figure 4.13-2. The integral worth of rod 7-1 was then obtained by integration of the differential rod worth curve using the trapezoidal method.

The effect of the power distortion produced by the withdrawal of control rod 7-1 was measured using the unit computer performance data output program which printed out core power distribution and thermal hydraulics data at 22% and 100% withdrawn. Since control rod 7-1 is the center control rod as shown in Figure 4.13-1, 1/8 core symmetry was present throughout the test. A comparison of the radial and total core power distributions measured before and after the pseudo ejection of control rod 7-1 is presented in Figure 4.13-3 and 4.13-4.

4.13.3 EVALUATION OF TEST RESULTS

The test results at 40 percent full power in terms of reactivity were calculated by integrating the differential worth curve measured on rod 7-1 as it was withdrawn as shown in Figure 4.13-2. An integration of the measured differential worth curve gives an ejected control rod worth of $0.20\%\Delta k/k$ as compared to the predicted value of $0.49\%\Delta k/k$. This value is well below the acceptance criterion of $0.65\%\Delta k/k$.

The effect of withdrawing control rod 7-1 on the core power distribution was determined by recording Core Power Distribution and Thermal Hydraulic data at 22% and 100% withdrawn as shown in Table 4.13-1. The graphical representation of radial peaking factors as a function of radial position along the X-Z plane at Level 08 is presented in Figure 4.13-5. This exemplifies the marked deviation in the radial peaking factor in the proximity of H-08 due to the pseudo ejection of control rod 7-1. The worst case maximum linear heat rate LHR (kW/ft), the worst case minimum DNBR (dim) and the maximum total peaking factor (dim) measured with rod 7-1 at 100% withdrawn were 9.18, 4.87, and 2.89, respectively. These values were measured in core location H-08, the fuel assembly containing the ejected rod. The effects on quadrant power tilt was small, since control rod 7-1 was located in the center of the core. Maximum positive quadrant power tilts of +0.94 and +1.13 percent were measured in quadrant WX before and after ejection of control rod 7-1 respectively. The shift of the power to the bottom of the core as indicated by the incore offset was the result of the insertion of control rod group 6 from 94.2 to 64.8% withdrawn and by the withdrawal of control rod 7-1 from 22 to 100% withdrawn. Thus, the large change of offset did not totally result from the ejection of control rod 7-1.

4.13.4 CONCLUSIONS

The measured worth of the most reactive control rod was found to be $0.20\%\Delta k/k$ which is less than the acceptance criterion of $0.65\%\Delta k/k$.

Analyzed core power distribution and thermal hydraulic data indicated a large perturbation to the steady state core power distribution, as was expected.

Table 4.13-1

Summary Of Core Power Distributions And Thermal Hydraulics Data
Taken During The Performance Of Pseudo Rod Ejection Test

Rod 7-1 Position (% wd)	Power Level (% FP)	Incore Offset (%)	Quadrant Tilt, %				Maximum Peaking, Dim		Worst Case Maximum LHR (kW/ft)	Worst Case Minimum DNBR (Dim)
			WX	XY	WZ	ZY	Radial	Total		
22	40.21	- 0.82	+0.94	-0.93	+0.54	-0.60	1.40	1.62	4.44	10.13
100	46.61	-31.14	+1.13	-0.85	+0.64	-0.92	2.07	2.89	9.18	4.87

Ejected Rod Worth And Location At 40% FP Plateau

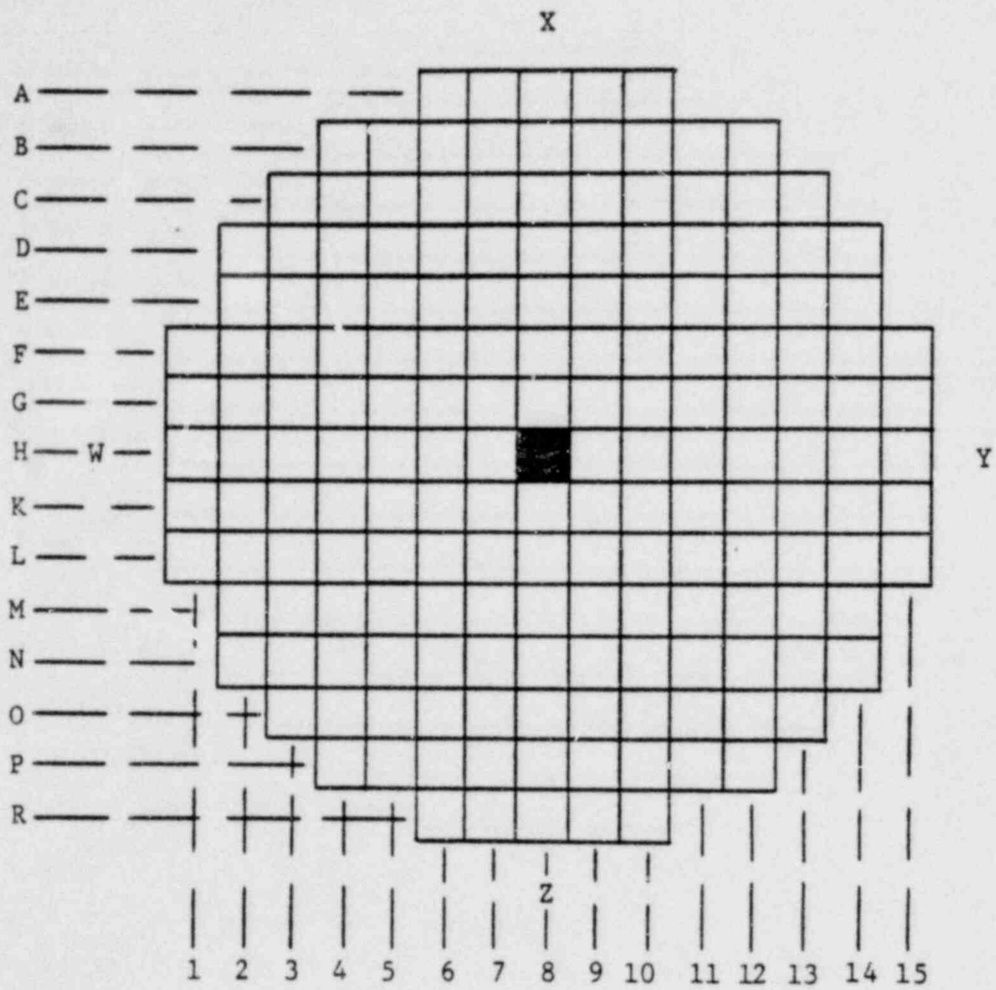

CONTROL ROD	CORE POSITION	CONTROL ROD WORTH, % $\Delta k/k$ CALCULATED	MEASURED
7-1	H-08	0.49	0.20

Figure 4.13-1

Differential And Integral Worth Of Rod 7-1 Versus Rod Position During The Performance Of Pseudo Rod Ejection Test At 40 Percent Full Power

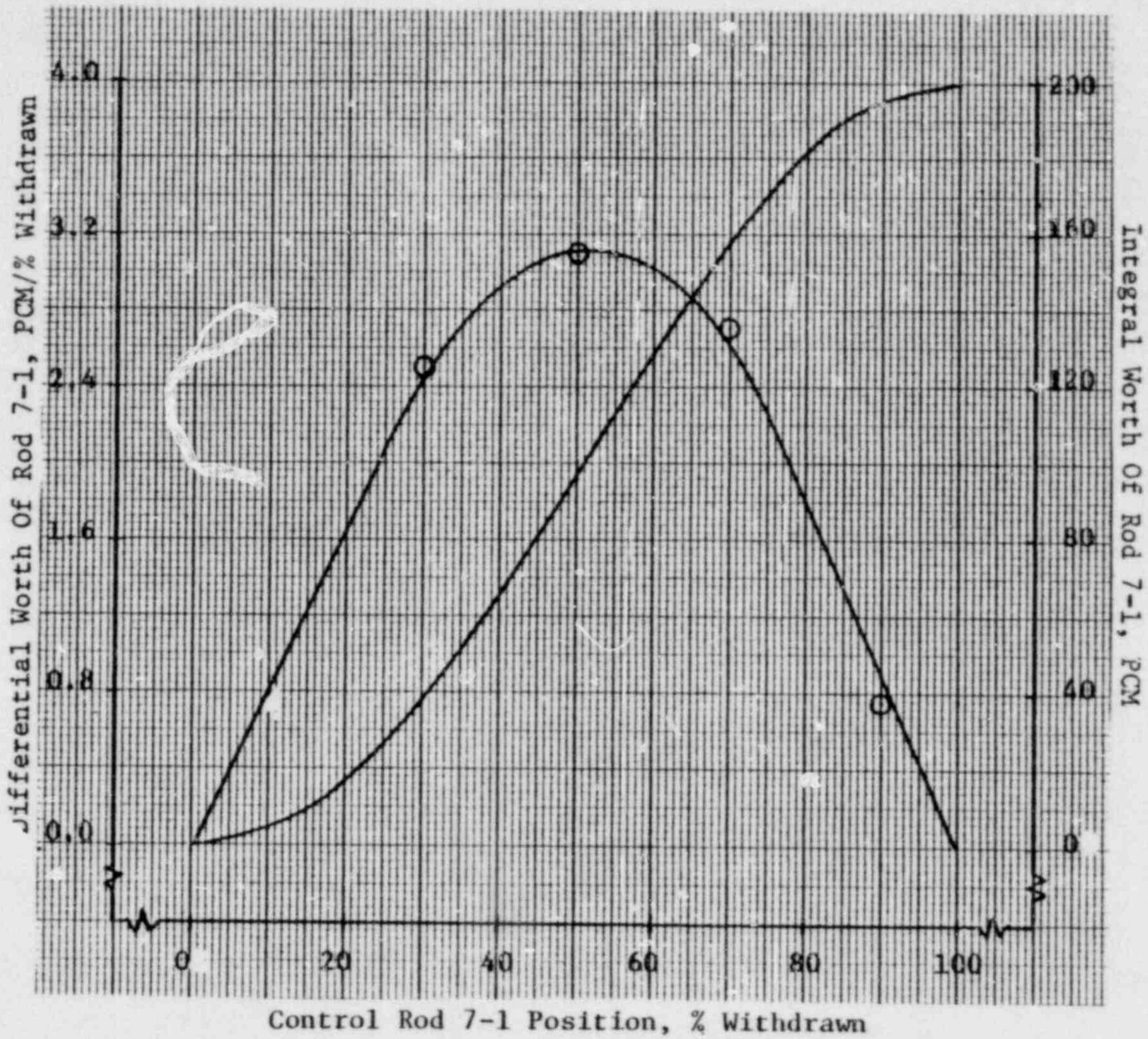

Figure 4.13-2

Comparison Of Measured Radial Core Power Distributions Before And After Ejection Of Control Rod 7-1 At 40 Percent Full Power

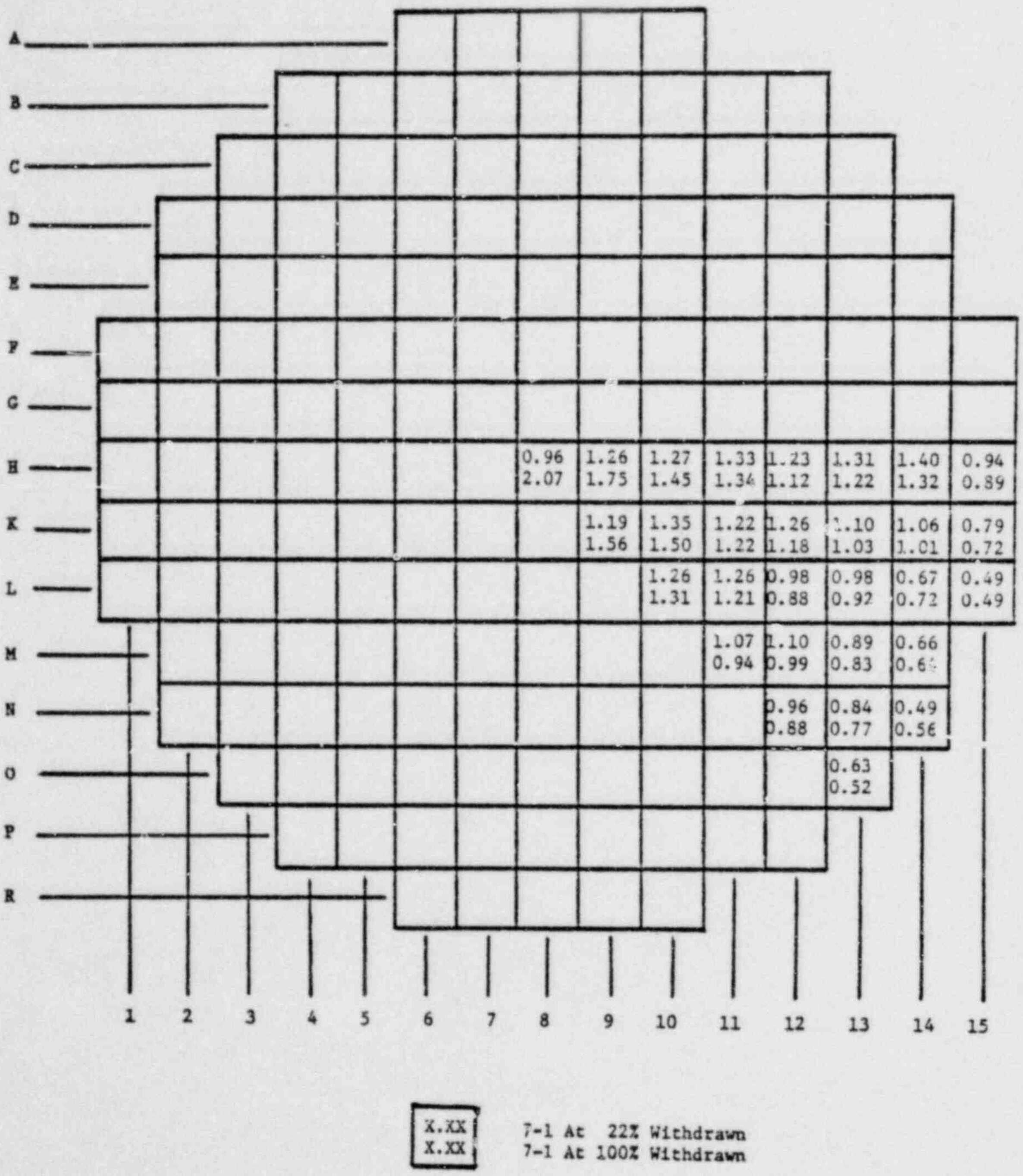

Figure 4.13-3

Comparison Of Measured Total Peaking Core Power Distribution Before And After Ejection Of Control Rod 7-1 At 40 Percent Full Power

	1	2	3	4	5	6	7	8	9	10	11	12	13	14	15
A															
B															
C															
D															
E															
F															
G															
H								1.36 2.89	1.46 2.44	1.50 2.04	1.61 1.93	1.53 1.70	1.56 1.86	1.62 2.08	1.10 1.41
K									1.46 2.23	1.62 2.09	1.50 1.70	1.59 1.70	1.34 1.57	1.21 1.66	0.92 1.23
L										1.56 1.81	1.62 1.71	1.36 1.23	1.22 1.39	1.01 1.42	0.60 0.86
M											1.37 1.42	1.39 1.45	1.12 1.25	0.78 1.08	
N												1.22 1.28	1.04 1.08	0.59 0.70	
O													0.69 0.76		
P															
R															

X.XX	7-1 At 22% Withdrawn
X.XX	7-1 At 100% Withdrawn

Figure 4.13-4

Radial Peaking Factor Versus Radial Position Along The X-Z Plane
At Level 08 Both Before And After The Ejection Of Control Rod 7-1

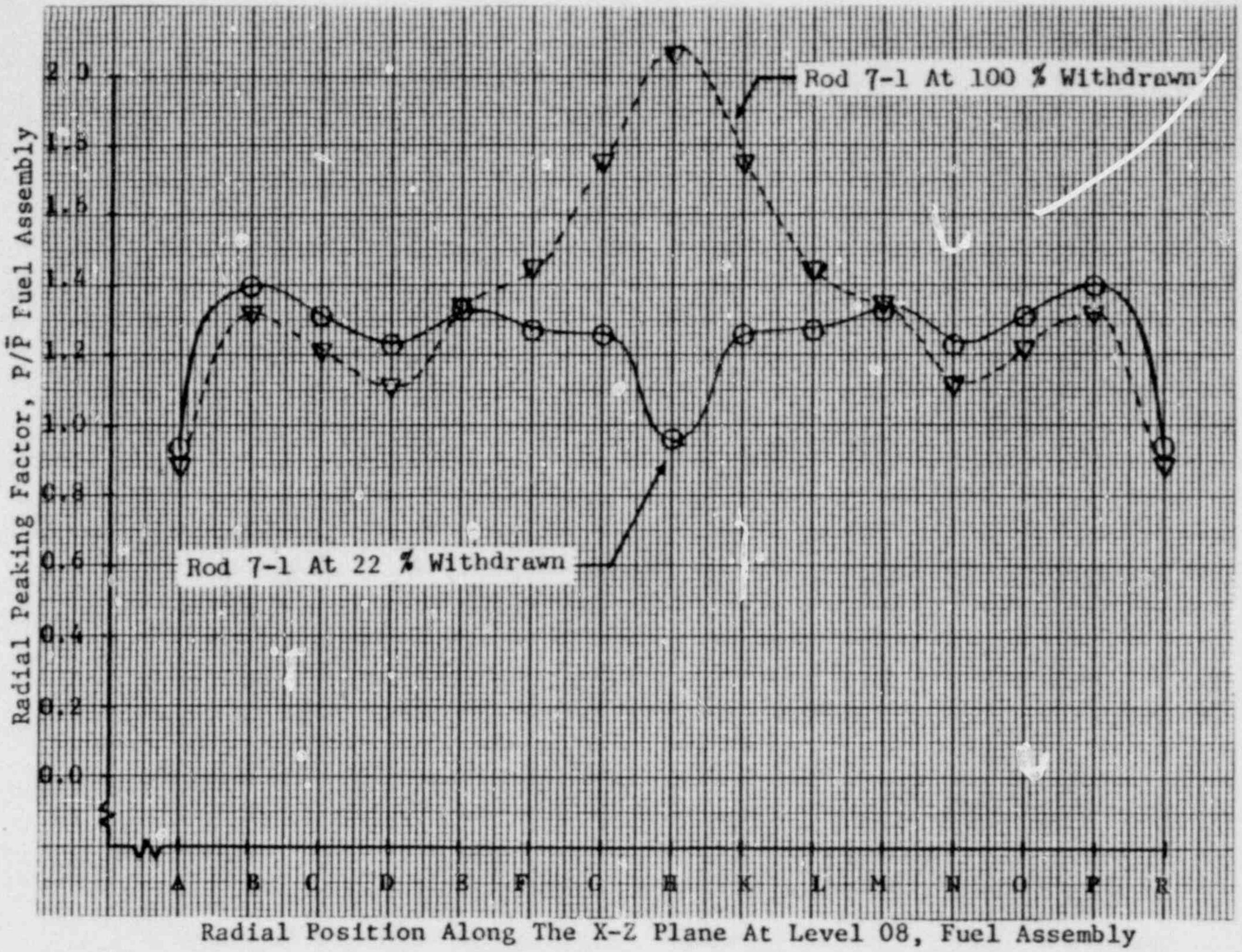

Figure 4.13-5

4.14 DROPPED CONTROL ROD TEST

In performing the Dropped Control Rod Test, the control rod which produces the most adverse thermal effects in the case of an inadvertent rod drop at full power is selected for analysis. Based upon results of PDQ-7 calculations performed by the Babcock and Wilcox Company, control rod 6-5 in core locations N-08 was selected for this purpose. Figure 4.14-1 shows the location of this control rod and its relative location to each core quadrant.

4.14.1 PURPOSE

The purpose of this test was to verify the safety analysis relating to the accidental dropping of a control rod which is normally withdrawn from the core at full power. The control rod chosen was one which was calculated to produce the most adverse thermal effects on the core. During the test, the individual objectives were as follows:

(a) To measure the core power distribution with an asymmetric control rod at 50% and 0% withdrawn.

(b) To demonstrate that the position indicator alarm and asymmetric rod alarm indicated an asymmetric control rod.

(c) To demonstrate that control rod withdrawal is inhibited at 60% full power or above when a control rod is asymmetric

(d) To demonstrate that reactor power is automatically reduced below 60% full power when a control rod is asymmetric (9 inches from group average).

Four acceptance criteria are specified for the Dropped Control Rod Test and are listed below:

(1) The measured worst case maximum LHR and minimum DNBR when extrapolated to 100% FP is less than their respective limits of 19.70 kW/ft and 1.30 or falls outside the power imbalance trip envelope --- see Figure 4.4-1.

(2) The asymmetry alarm lamp at the control rod position panel and the asymmetry rod fault lamp at the Diamond rod control station both indicate the asymmetric control rod condition at their appropriate setpoints of 7 and 9 inches, respectively.

(3) The power level is automatically reduced to below 60% full power when a control rod is asymmetric.

(4) Control rod withdrawal is inhibited when a control rod is asymmetric with reactor power at 60% full power or above.

4.14.2 TEST METHOD

The Dropped Control Rod Test was performed by static techniques in which the reactor is maintained in an approximate critical state through control rod 6-5 and group 6 exchange. During this exchange, the power and thermal distortion produced by the insertion of control rod 6-5 was measured at 91, 50 and 0 percent withdrawn using the unit computer performance data output program which prints out core power distribution and thermal hydraulics data. The effects of the dropped control rod on axial and radial core power distributions were analyzed using full core analysis since 1/8 core symmetry did not exist due to the fact that control rod 6-5 was not located at the center of the core. Quadrant power tilt for each core quadrant during the measurement was calculated using the signals from the sixteen symmetric radial incore monitoring assemblies. The thermal distortion was measured in terms of the worst case minimum DNBR and the maximum LHR as calculated by the unit computer.

As part of the above measurement, verification of proper detection of an asymmetric control rod was also performed. The technique was to take this control rod out of group average by first 7 inches and then 9 inches and verify that the asymmetry rod alarm lamp and the asymmetry rod fault lamp came on at their respective setpoints.

The remaining objectives (c and d) were performed at 75 percent full power by simulating an asymmetric rod condition on rod 6-5. This was done by placing a test signal on the absolute position indication module for this rod. After verification that the reactor power was automatically runback to less than 60 percent full power was checked, the control rod withdrawal inhibit during this asymmetric rod condition was verified.

4.14.3 EVALUATION OF TEST RESULTS

The effects of the droppped control rod relative to the core power distribution were determined by measuring the incore axial offset, the quadrant power tilt, and the radial and total peaking factors at the 91, 50, and 0 percent withdrawn positions of control rod 6-5. As was expected, the quadrant power tilts increased as rod 6-5 was further inserted into the core. The results of this trend is plotted in Figure 4.14-2 and tabulated in Table 4.14-1. Calculation of the quadrant power tilts using the sixteen symmetric incore monitoring assemblies indicated a maximum positive power tilt of +13.48 percent when control rod 6-5 was fully inserted. Core peaking analysis was also performed as control rod 6-5 was inserted. The results of this analysis is shown in Figures 4.14-3 and 4.14-4. Examination of the radial power peaking trend at different core locations as a function of control rod 6-5 position clearly indicates that, as control rod 6-5 is inserted into the core, a radial flux perturbation in the quadrants containing the dropped rod was observed, with the maximum measured radial and total peaking factor occurring in fuel assembly B-08 at 1.64 and 2.25, respectively.

Thermal analysis of the core was done using the thermal hydraulics data at 91, 50 and 0 percent withdrawn position of control rod 6-5. The worst case minimum DNBR and maximum LHR were normalized to a reference test power of 40% full power in order that only the rod insertion effects would be observed. Figure 4.14-2 shows the effects of rod insertion on normalized worst case minimum DNBR and maximum LHR. As can be seen, the normalized worst case minimum DNBR decreases and the normalized worst case maximum LHR increases as control rod 6-5 was inserted into the core. The measured thermal data was then subjected to extrapolation to 100 percent full power to ensure that acceptable margins were present at rated power. The results yielded a worst case minimum DNBR margin of 122.3 percent and a worst case maximum LHR margin of 25.3 percent when control rod 6-5 was 0% withdrawn from the core -- see Table 4.14-2. These results indicate that the thermal limit will not be exceeded even if the worst control rod were to drop into the core, go undetected, and the integrated control system maintained power at 100% full power.

An approximation of the worth of control rod 6-5 was also performed by the rod swap method during the insertion of rod 6-5 from its group average position to 0% withdrawn. Control rod group 7 was withdrawn 8% to compensate for reactivity effects of the dropped rod. The initial and final positions of group 7 were 15 and 23% withdrawn, respectively. From rod worth available at power, this change is equivalent to a dropped rod worth of -0.12%Δk/k.

The integrated control system ability to detect the asymmetric control rod with the appropriate alarms and to initiate a reactor runback to below 60% full power was performed in two distinct parts. The first part was performed in conjunction with the 40% full power testing during the withdrawal of rod 6-5 back to group average position. During this withdrawal, the setpoints on the asymmetry alarm lamp and asymmetry fault lamp were verified to go out at their respective setpoints of 7 and 9 inches from group average. The second part, a reactor runback due to an asymmetric rod indication was performed at 75% full power by simulating an asymmetric rod condition on rod 6-5. Upon receiving the asymmetric rod signal, the reactor automatically ran back from an initial power of 75.4% full power to a power level less than 60.0% full power in 36.7 seconds with an average ramp rate of 25.8% FP/min. The test of the control rod withdrawal inhibit was then successfully conducted by proving that the unit would not go beyond 60.0% full power.

4.14.4 CONCLUSIONS

Upon analysis of the Dropped Control Rod Test data, the following conclusions are deduced:

(a) Analyzed core power distribution and thermal hydraulic data provided results indicating sufficient margin to minimum DNBR and maximum linear heat rate limiting criteria. The perturbation to the steady state power distribution was as expected with a maximum quadrant power tilt of +13.48%.

(b) The measured worth of the control rod which is calculated to produce the most adverse thermal effects in the core, if it is inadvertently dropped, was found to be -0.12%Δk/k.

(c) The integrated control system accurately detected the asymmetric control rod with appropriate alarms and initiated reactor runback to a power level below 60.0% full power in 36.7 seconds.

(d) The control rod withdrawal inhibit was shown to limit power to less than 60.0% full power when an asymmetric control rod condition exists.

Therefore, all acceptance criteria were met.

Table 4.14-1

Summary Of Core Power Distributions And Thermal Hydraulics Data
Taken During The Performance Of Dropped Control Rod Test

Rod 6-5 Position (% wd)	Power Level (% FP)	Incore Offset (%)	Quadrant Power Tilt, %				Maximum Peaking, Dim		Worst Case Maximum LHR (kW/ft)	Worst Case Minimum DNBR (Dim)
			WX	XY	WZ	ZY	Radial	Total		
91 *	40.28	+ 2.5	+1.51	+0.18	-1.61	-0.09	1.41	1.74	4.81	9.12
50	42.23	-22.66	+8.89	+7.22	-8.83	-7.29	1.57	2.20	6.53	7.56
0	41.06	-10.94	+13.48	+11.84	-13.16	-12.16	1.64	2.25	6.19	8.09

Note(*): This position on rod 6-5 represents a normal configuration.

Table 4.14-2

Minimum DNBR and Maximum LHR Analysis For The Dropped Control Rod Test

Rod 6-5 Position (% wd)	Data Analysis (none)	Power Level (% FP)	Incore Offset (%)	Axial Peaking (Dim)	Assembly Location (Dim)	Worst Case Maximum LHR (kW/ft)	Worst Case Minimum DNBR (Dim)
91 *	Measured	40.28	+02.50	1.23 (5)	B-08	4.81	9.12
	Normalized	40.00				4.78	9.18
	Extrapolated	100.00				11.94	2.76
50	Measured	42.23	-22.66	1.40 (2)	B-08	6.53	7.56
	Normalized	40.00				6.18	7.99
	Extrapolated	100.00				15.47	2.78
0	Measured	41.06	-10.94	1.37 (2)	B-08	6.19	8.09
	Normalized	40.00				6.03	8.30
	Extrapolated	100.00				15.08	2.89

Note(*): This position on rod 6-5 represents a normal configu[illegible]on.

Dropped Rod Worth And Location At 40% FP Plateau

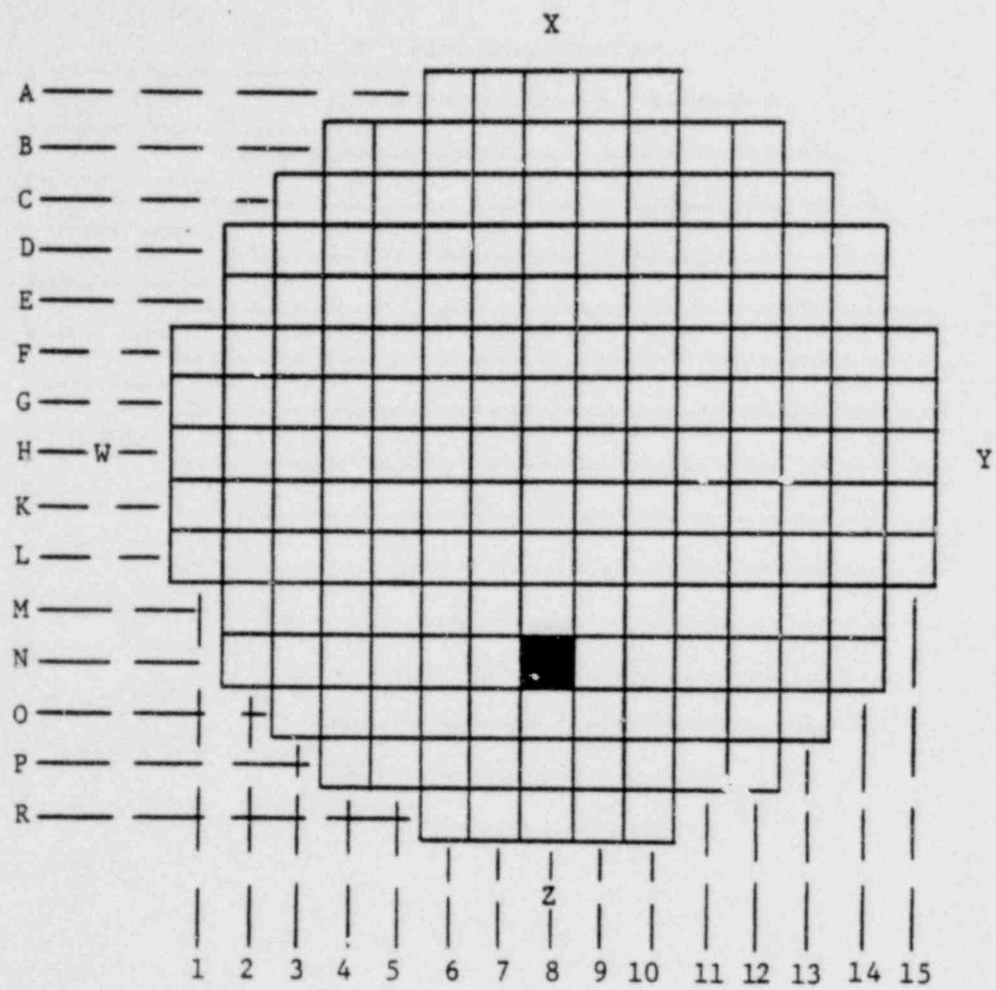

CONTROL ROD	CORE POSITION	MEASURED CONTROL ROD WORTH, %Δk/k
6-5	N-08	-0.12

Figure 4.14-1

Quadrant Power Tilt, Incore Axial Offset, Worst Case Minimum DNBR And Maximum LHR Versus Control Rod 6-5 Position During The Performance Of Dropped Control Rod Test

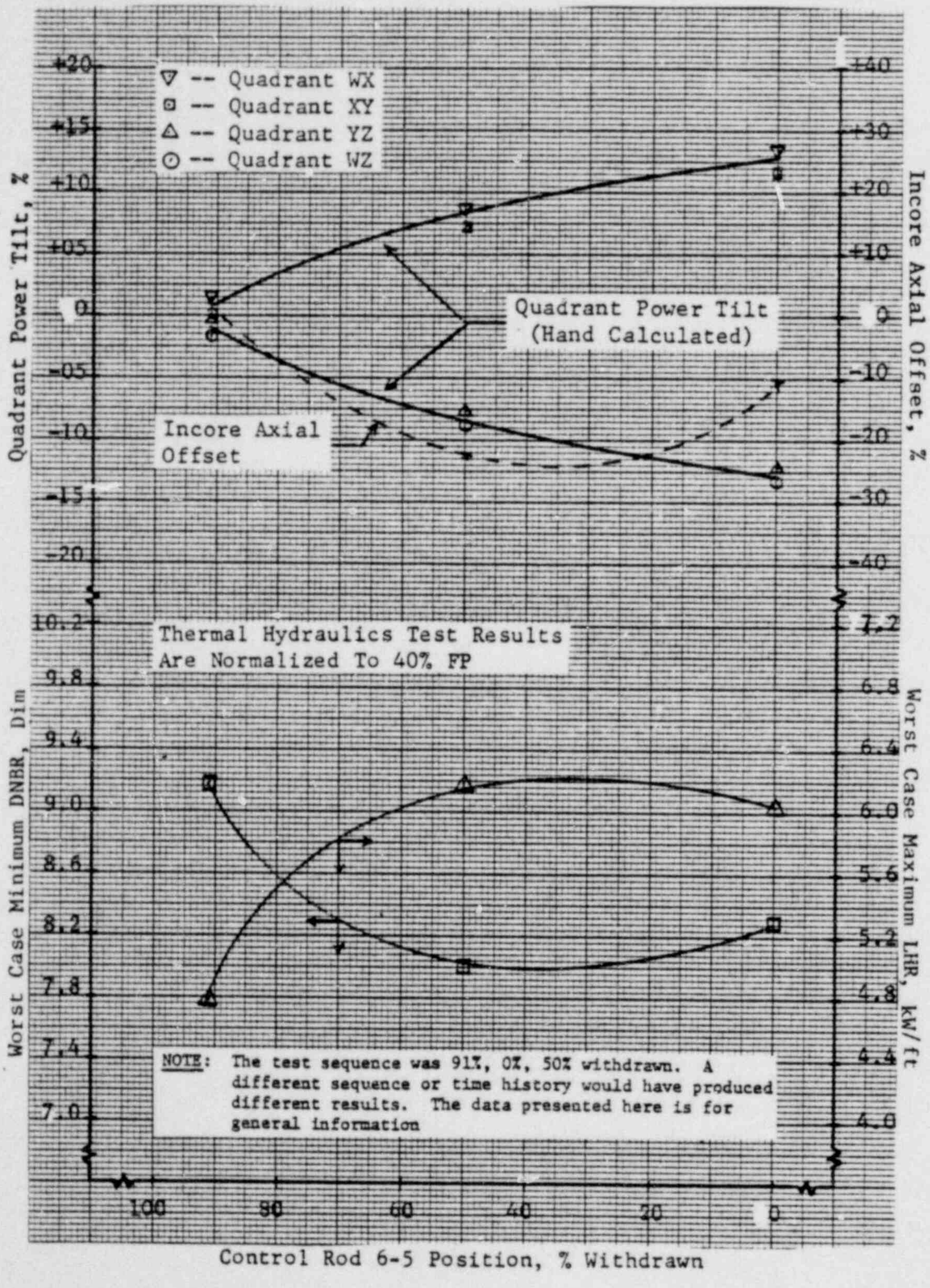

Figure 4.14-2

Comparison Of Measured Radial Peaking Factors With Dropped Control Rod 6-5 At 91, 50 And 0% Withdrawn From The Core At 40% Full Power During Dropped Control Rod Test

	1	2	3	4	5	6	7	8	9	10	11	12	13	14	15
A						0.49 0.64 0.69	0.78 0.89 0.92	0.98 1.06 1.07	0.78 0.88 0.91	0.49 0.63 0.69					
B				0.51 0.56 0.57	0.69 0.81 0.85	0.64 0.89 0.96	1.07 1.20 1.26	1.41 1.57 1.64	1.37 1.20 1.26	0.63 0.88 0.95	0.69 0.80 0.84	0.51 0.55 0.56			
C			0.58 0.63 0.66	0.85 0.97 1.05	0.90 1.04 1.14	1.06 1.18 1.24	1.12 1.23 1.29	1.37 1.48 1.54	1.12 1.22 1.29	1.01 1.12 1.17	0.89 1.03 1.13	0.85 0.95 1.04	0.58 0.62 0.65		
D		0.50 0.54 0.57	0.84 0.96 1.05	1.00 1.12 1.22	1.09 1.17 1.23	0.98 1.05 1.11	1.26 1.27 1.24	1.25 1.13 0.93	1.26 1.27 1.24	0.98 1.04 1.10	1.09 1.16 1.22	0.99 1.10 1.21	0.84 0.94 1.03	0.49 0.53 0.56	
E		0.67 0.78 0.84	0.90 1.01 1.11	1.10 1.16 1.22	1.09 1.16 1.23	1.25 1.32 1.38	1.26 1.32 1.37	1.32 1.39 1.45	1.23 1.29 1.34	1.25 1.31 1.38	1.09 1.14 1.22	1.10 1.15 1.21	0.89 1.00 1.09	0.66 0.77 0.83	
F	0.46 0.60 0.68	0.65 0.84 0.91	1.02 1.10 1.15	0.98 1.02 1.07	1.31 1.37 1.45	1.28 1.31 1.38	1.34 1.38 1.43	1.27 1.30 1.35	1.34 1.38 1.43	1.27 1.31 1.37	1.31 1.36 1.44	0.97 1.01 1.06	1.03 1.11 1.16	0.64 0.83 0.90	0.46 0.59 0.68
G	0.75 0.84 0.89	1.04 1.12 1.16	1.10 1.16 1.20	1.31 1.36 1.43	1.23 1.25 1.28	1.30 1.31 1.35	1.23 1.26 1.28	1.25 1.29 1.32	1.23 1.25 1.28	1.29 1.30 1.34	1.23 1.25 1.29	1.30 1.35 1.42	1.09 1.15 1.19	1.04 1.11 1.16	0.74 0.83 0.89
H	0.94 0.99 1.03	1.37 1.48 1.56	1.34 1.38 1.43	1.22 1.02 0.80	1.30 1.29 1.32	1.26 1.23 1.24	1.25 1.25 1.26	0.91 1.02 1.02	1.24 1.25 1.26	1.25 1.23 1.24	1.29 1.28 1.32	1.21 1.01 0.80	1.33 1.37 1.42	1.36 1.47 1.56	0.93 0.99 1.03
K	0.74 0.81 0.85	1.04 1.07 1.09	1.10 1.10 1.11	1.31 1.29 1.32	1.23 1.20 1.21	1.30 1.23 1.21	1.23 1.17 1.14	1.24 1.20 1.18	1.23 1.16 1.13	1.29 1.22 1.21	1.24 1.19 1.21	1.29 1.28 1.31	1.09 1.09 1.10	1.03 1.07 1.09	0.74 0.81 0.85
L	0.46 0.55 0.61	0.64 0.76 0.78	0.95 0.96 0.98	0.97 0.89 0.85	1.31 1.22 1.21	1.27 1.15 1.11	1.34 1.21 1.16	1.26 1.13 1.07	1.33 1.21 1.16	1.26 1.14 1.11	1.30 1.21 1.20	0.96 0.88 0.85	0.96 0.97 0.99	0.63 0.75 0.78	0.45 0.55 0.61
M		0.66 0.68 0.68	0.89 0.87 0.87	1.09 0.98 0.93	1.08 0.95 0.89	1.25 1.09 1.01	1.27 1.06 0.93	1.31 1.14 1.06	1.26 1.04 0.92	1.24 1.09 1.01	1.07 0.94 0.89	1.09 0.98 0.93	0.88 0.86 0.87	0.63 0.67 0.68	
N		0.49 0.44 0.41	0.84 0.79 0.79	0.99 0.91 0.88	1.08 0.92 0.83	0.97 0.78 0.67	1.25 0.98 0.78	1.23 0.83 0.46	1.24 0.98 0.78	0.96 0.78 0.67	1.07 0.92 0.83	0.98 0.90 0.88	0.82 0.79 0.79	0.48 0.44 0.41	
O			0.57 0.49 0.43	0.84 0.76 0.72	0.88 0.79 0.73	1.03 0.89 0.78	1.10 0.92 0.80	1.36 1.17 1.04	1.10 0.92 0.80	0.97 0.85 0.74	0.87 0.79 0.73	0.83 0.75 0.72	0.56 0.48 0.43		
P				0.50 0.40 0.31	0.68 0.59 0.50	0.62 0.63 0.53	1.05 0.91 0.80	1.40 1.27 1.17	1.05 0.91 0.80	0.62 0.63 0.54	0.67 0.59 0.49	0.49 0.39 0.30			
R						0.48 0.45 0.38	0.77 0.66 0.55	0.97 0.82 0.70	0.77 0.66 0.55	0.48 0.44 0.37					

6-5 At 91% Withdrawn
6-5 At 50% Withdrawn
6-5 At 0% Withdrawn

Figure 4.14-3

Comparison Of Measured Total Peaking Factors With Dropped Control Rod 6-5 At 91, 50, And 0% Withdrawn From The Core At 40% Full Power During Dropped Control Rod Test

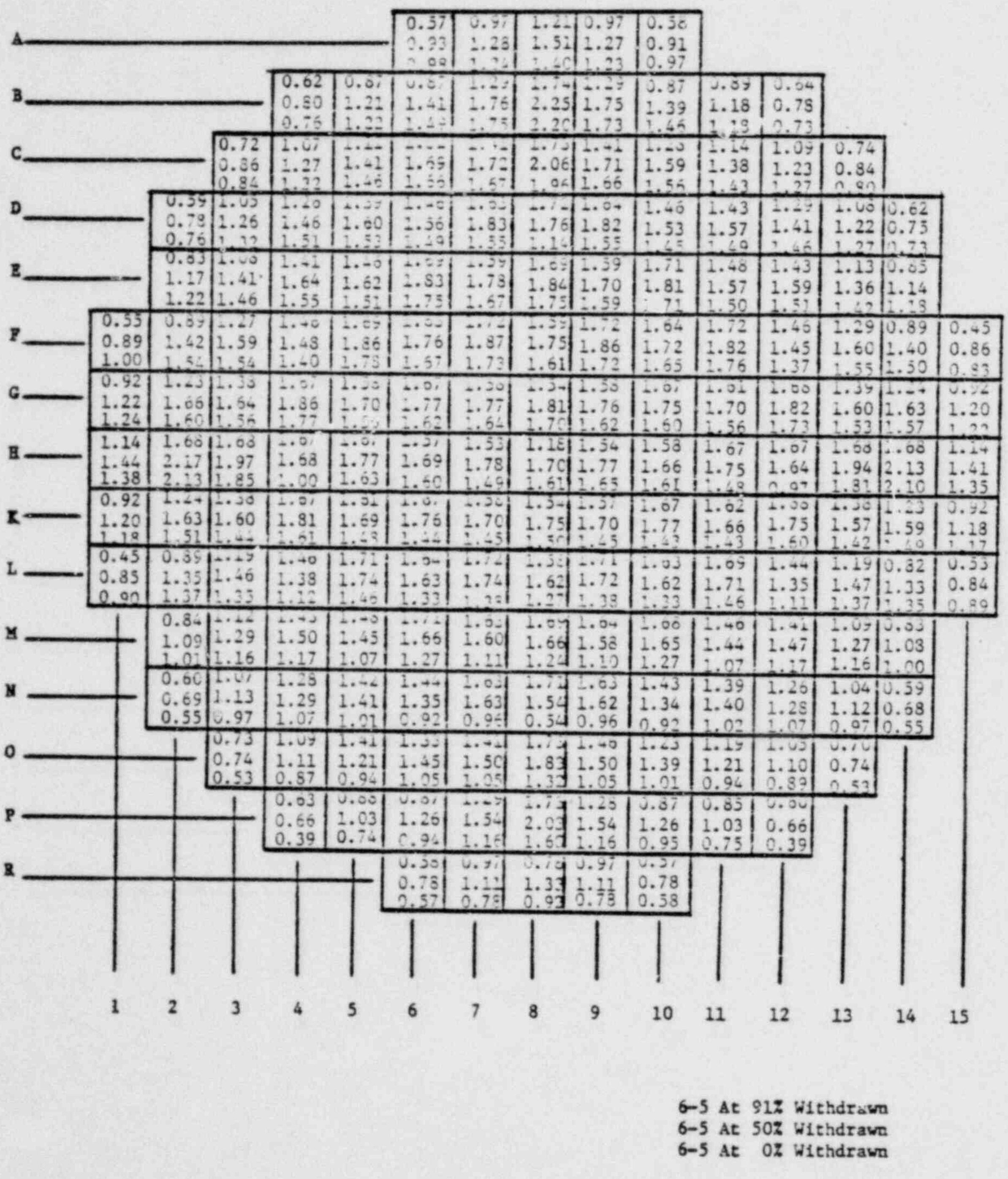

Figure 4.14-4

4.15 LOSS OF OFFSITE POWER TEST

The Loss Of Offsite Power Test consisted of two (2) parts. The first part approximated a total plant blackout from 15% reactor power; the second part was performed from a shutdown condition and verified a diesel generator's ability to start and pick up certain vital loads.

4.15.1 PURPOSE

The purpose of this test was to verify the ability of the plant to sustain a loss of offsite power.

4.15.2 TEST METHOD

The most comprehensive test would be to trip all sources of electrical power to the plant at once, except emergency battery powered equipment, and allow the two diesel generators to start and pick up vital equipment necessary for reactor safety and plant protection. However, this approach presents too great a risk for possible damage to equipment, such as reactor coolant pump seals. Therefore, the test was modified and run as follows: The plant electrical system lineup was normal with the exception of emergency diesel generator 3B which was running, and carrying the following loads (considered necessary to allow plant equipment to survive the test): a makeup pump, a nuclear services closed cycle cooling water sea water pump, a nuclear services closed cycle cooling water pump, a control rod drive cooling water booster pump, an instrument air compressor and two groups of pressurizer heaters. (Additional minor loads were left energized for convenience, but were of no importance to the test).

With the plant at 15% power, the reactor and startup transformer were simultaneously tripped. This immediately reduced total plant power to the emergency batteries and the above mentioned diesel generator. The 3A diesel generator was timed as it started, came up to speed and picked up certain predetermined loads on its ES Bus. After allowing the plant to operate in this condition for fifteen minutes, the startup transformer was re-energized. Loads considered necessary to allow plant equipment to survive the test were shifted from the 3B to 3A diesel generator. The 3B diesel was then stopped and the startup transformer again tripped. This allowed the timing of the 3B diesel as it came up to speed and picked up its pre-selected loads. At that point, the test was complete and normal plant operations resumed.

4.15.3 EVALUATION OF TEST RESULTS

Both emergency diesel generators received an undervoltage signal, started and block loaded in less than the required sixteen seconds. This was the only formal acceptance criteria for the test. However, it was observed that there was a large imbalance in feedflow. Subsequent investigation and evaluation revealed the following sequence of events (refer to Figure 4.15-1):

APPROXIMATE TIME (Minutes)	EVENT
0	Tripped power, both feedwater pumps stopped, and all feedwater flow was lost.

APPROXIMATE TIME (Minutes)	EVENTS
1	Steam driven emergency feedwater (EFW) pump automatically up to speed and feeding both steam generators.
2	Operator started electric driven emergency feedwater pump. "A" steam generator is being preferentially fed, but both are getting water.
3	Operator stopped steam driven EFW pump. "A" steam generator is being filled (startup level indication), "B" steam generator startup and operating range level indicators are both apparently at the bottom of their range. This can be verified by noting that loop "B" hot and cold leg temperatures indicate that little or no heat transfer is occurring through "B" loop. (Figure 4.15-1)
4	"B" loop startup feedwater flow indication is at the bottom of its range. (This was confirmed by a zero calibration check of the instrument made on 5/11/77. This check showed the zero had shifted to 1.5 x 10^5 Lbm/Hr. A similar check of "B" startup flow made on 5/11/77 showed its zero shifted to .95 x 10^5 Lbm/Hr.)
9½	Operator restarted steam driven EFW pump, started feeding "B" steam generator again.
10	Operator opened parallel valve (EFV-162) in the feedwater train to "A" steam generator by mistake.
12½	Operator shut EFV-162 and opened a parallel valve (EFV-161) in the feedwater train to "B" steam generator
14	"B" steam generator filling, on its way to recovery

The plant should have responded automatically by starting the steam driven emergency feedwater pump within 1 minute and filling each steam generators to 50% on the operating range. However, with one pump feeding both steam generators any imbalance in steam pressure will result in one generator getting more feedwater than the other. After primary flow has coasted down (approximately two minutes) the cold feedwater cools the primary water in the steam generator. This results in a continuing lowering of the pressure in the steam generator already being fed, thus increasing its feedflow. This feedback effect allows one steam generator to be underfed until the other one reaches a level of 50% at which point its feed valve will shut.

4.15.4 CONCLUSIONS

The test proved the plant's ability to sustain a loss of offsite power and all acceptance criteria were met. The problem of steam generator level control during the transient is still under study. The emergency procedure for loss of offsite power has been changed to require the operator to monitor levels and keep the feedflow shared between steam generators.

Various Plant Parameters VS Time
Loss Of Offsite Power Test

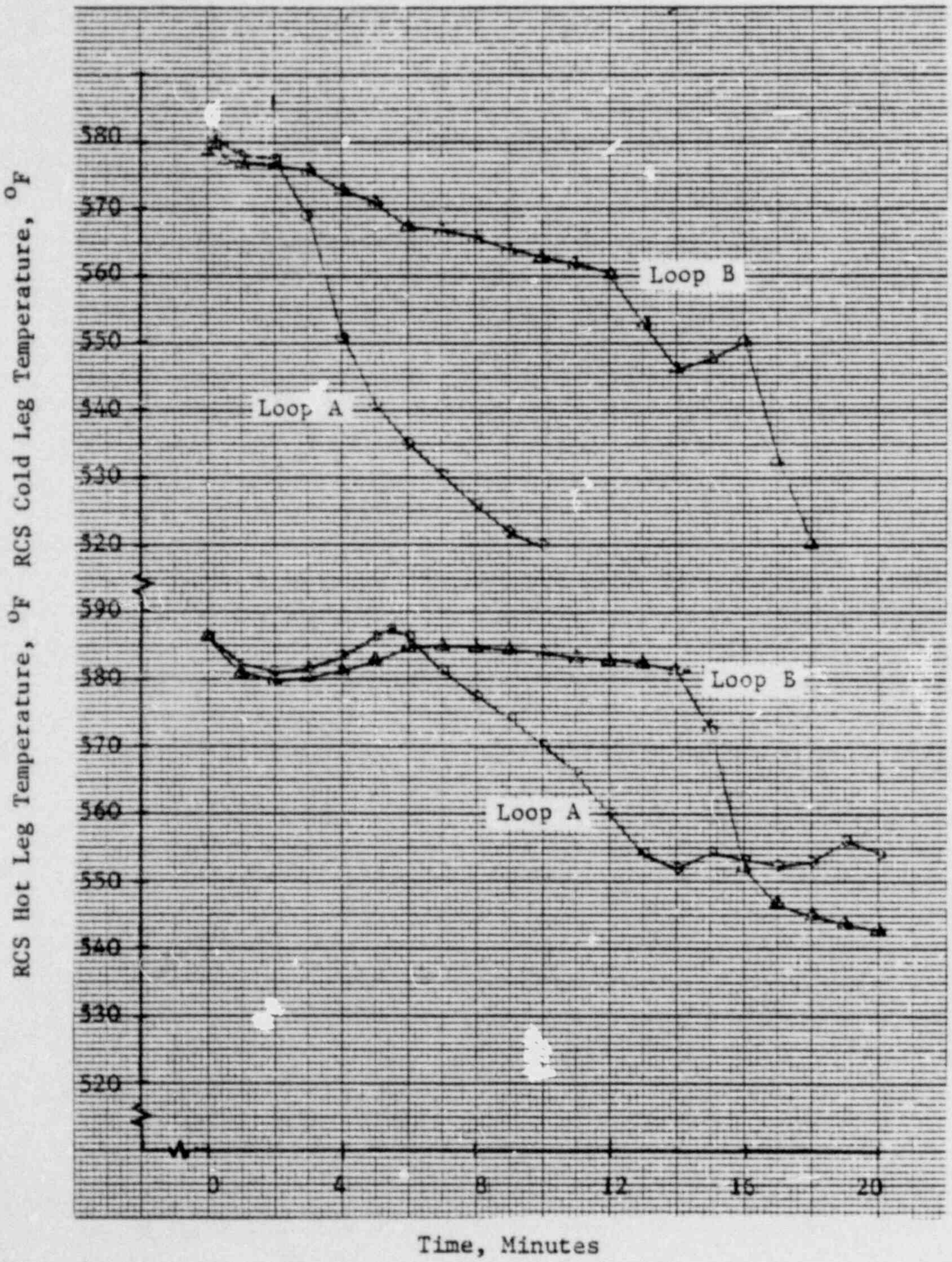

Figure 4.15.1

Various Plant Parameters VS Time
Loss Of Offsite Power Test

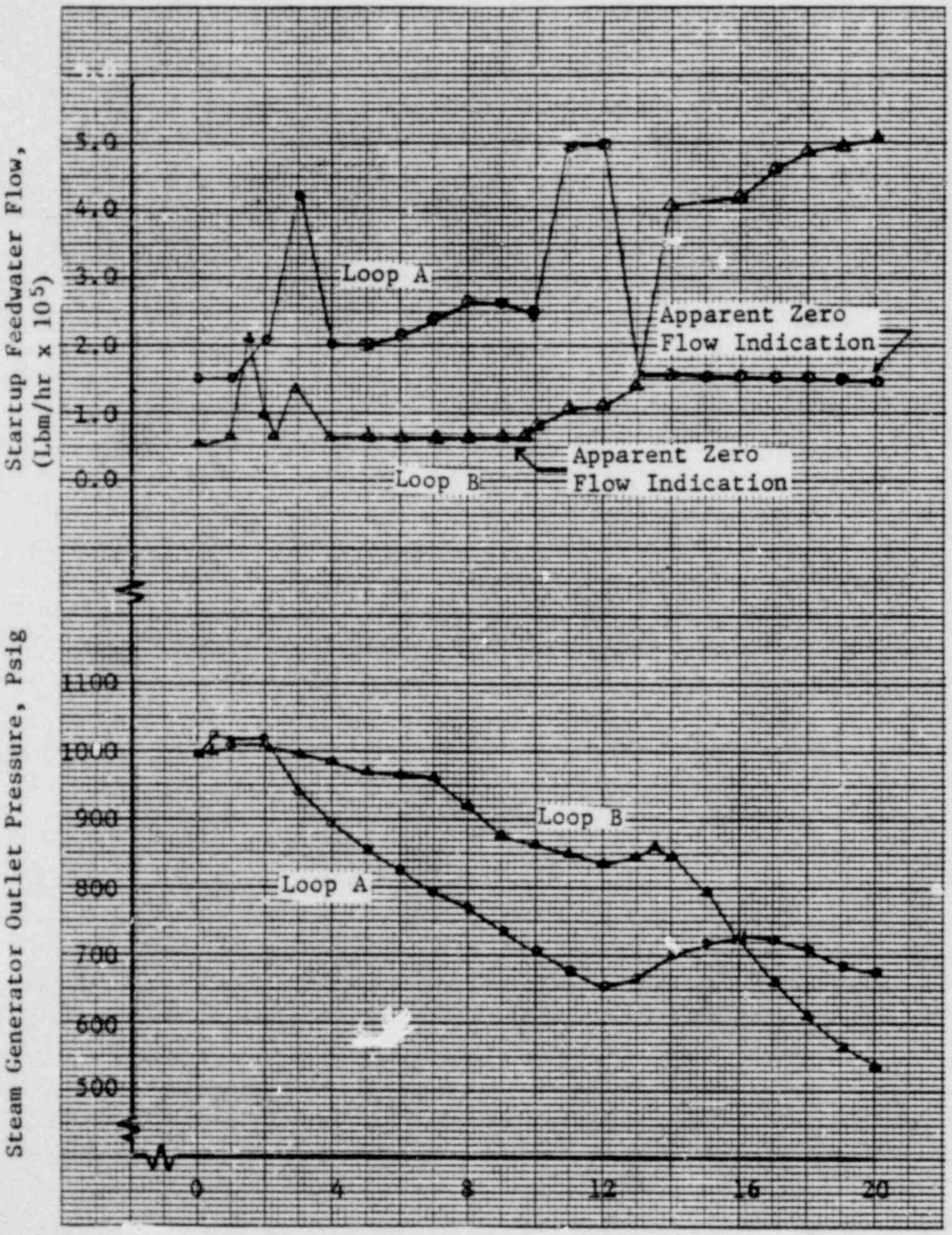

Time, Minutes

Figure 4.15.1 (Cont'd)

Various Plant Parameters VS Time
Loss Of Offsite Power Test

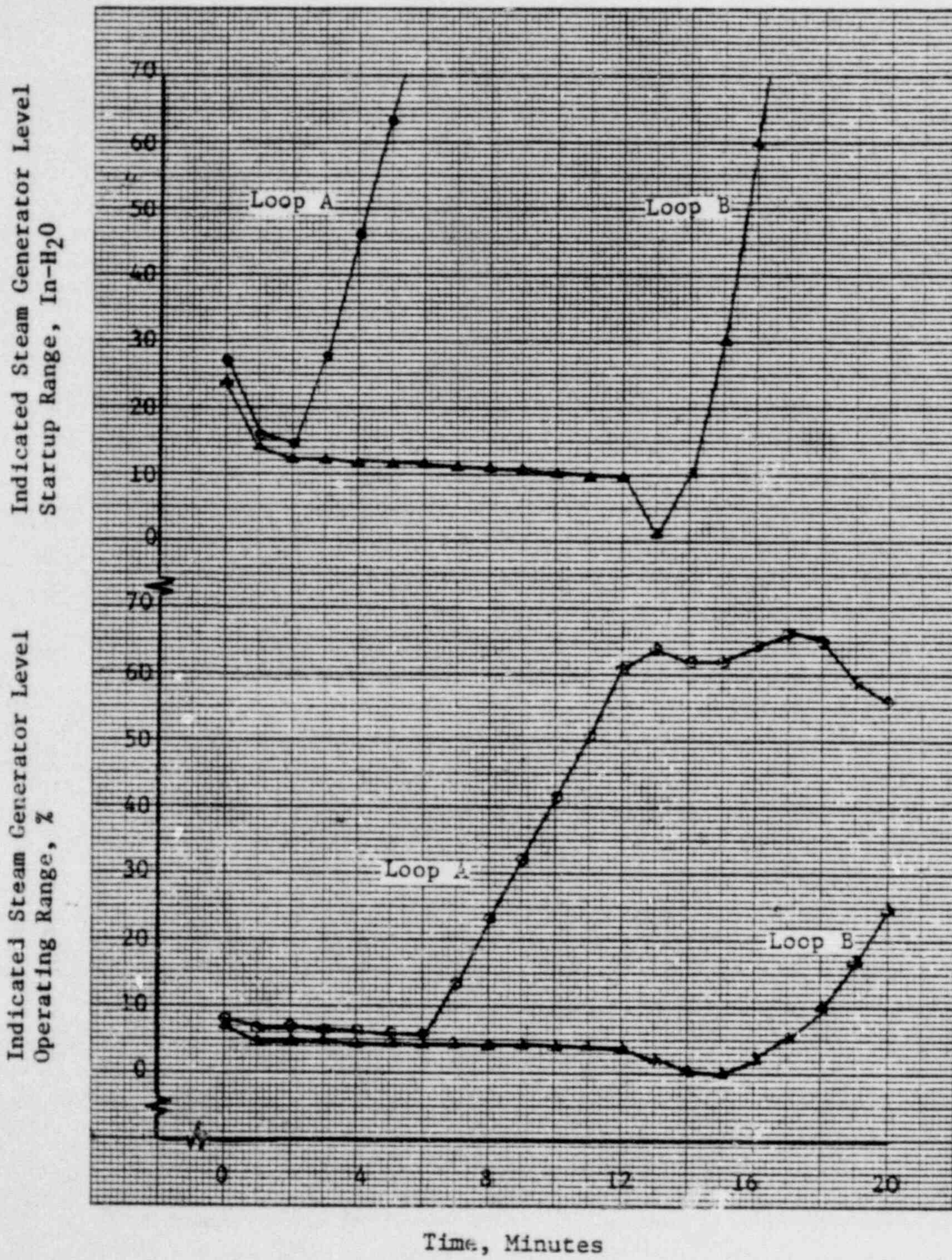

Figure 4.15.1 (Cont'd)